THE INFRARED BAND INTENSITIES OF 1,4-DIOXAN AND RELATED COMPOUNDS

BY

TIMOTHY RICHARD HOGAN (ROYAL HOLLOWAY COLLEGE)

PH.D. THESIS

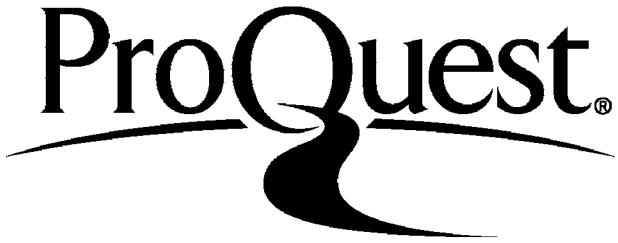

DEDICATION

THIS THESIS IS DEDICATED TO MY MUM AND DAD

ABSTRACT

This thesis describes an investigation of the redistribution of electronic charge that occurs during the molecular vibrations of 1,4-dioxan and related compounds. The infrared band intensities of dioxan-d_0, dioxan-d_8, cyclohexane-d_0, cyclohexane-d_{12} and tetrahydropyran were measured in both solution and gas phases. In the solution phase, overlapping band systems were split into their components by assuming Lorentzian band contours and producing the absorbance maximum, band halfwidth and peak frequency from a least squares procedure. The individual gas phase intensities in such spectral regions were then derived by assuming that the distribution of intensity across the region was the same in both phases. Normal coordinate calculations were performed and extended to reduce the dioxan and cyclohexane experimental intensities to parameters known as atomic polar tensors (APTs). Each element of the APT for an atom represents the change in a component (x, y or z) of the molecular dipole moment on moving the atom along one of the molecule-fixed Cartesian axes. The sign ambiguity of the experimental dipole derivatives was satisfactorily resolved using constraints provided by the intensities of the deuterated compounds: APTs were calculated from each possible choice of signs and these were used in turn to predict the intensity of the deuterated molecule - the APT was rejected if the agreement was unsatisfactory (as measured by a "fit factor"). The Gaussian 76 package for MO calculations was used to calculate ab initio APTs, and also, for dioxan, to derive a general valence force field. The latter, after least-squares refinement to the frequencies, proved more appropriate for the analysis of the dioxan intensities than a field derived from the Snyder-Zerbi generalized ether force field alone. A reasonable correspondence exists between the APTs derived from experiment and those

from the Gaussian 76 package, and certain trends are apparent along the series of molecules that hopefully will aid future studies and will provide a route to the prediction of spectra of related molecules.

CONTENTS.

CHAPTER 6.

CHAPTER 7.

TABLES.

Chapter 1 - INTRODUCTION.

Section 1.1 Infra-Red Band Intensities.

Vibrational spectroscopy is a source of information on a number of different aspects of molecular dynamics. Band frequencies may be related, through a normal coordinate calculation, to the form and amplitude of each molecular vibration. The band shape is determined by the relaxation processes of the transition dipole undertaken by the molecules as well as by the direction of the transition moment. The band intensities, with which this thesis will be primarily concerned, are related to the resulting fluctuation in the charge distribution in the molecule.

Historically it is the frequency that has been the subject of most investigation. It is the most easily measured parameter, and has the most direct analytical application. It may be understood theoretically using the classical mechanics of vibrating systems as a starting point, and the development of this understanding has proceeded smoothly through the construction of generalised model force fields, and the acquisition and processing of expanding quantities of diverse experimental data. The study of band intensities however, has followed a more hesitant approach.

There are two definitions of band intensity currently in use.

$$\Gamma_k = \frac{1}{c\ell} \int \ln \left(\frac{I_o}{I}\right)_\nu \, d\ln\nu$$

c is the concentration of the absorbing material. ℓ is the path length of the cell. $(I_o)_\nu$ is the initial beam intensity at frequency ν. $(I)_\nu$ is the intensity of the beam having passed through the sample. An alternative expression is:

$$A_i = \frac{1}{c\ell} \int \ln \left(\frac{I_o}{I}\right)_\nu \, d\nu$$

Here the integration is performed with respect to the frequency (yielding simply the area under the absorption curve), rather than the natural logarithm of the frequency.

As will be seen below, Γ can be directly related to the transition moment, the fundamental quantity which describes the change in electronic configuration in terms of wavefunctions of the initial and final vibrational states. Various rules can be formulated for the sum of Γ for a molecule, which are exact within the harmonic approximation, for the comparison of spectra of isotopically substituted molecules[1], and also for resonance interaction between energy states[2].

Although no such rules exist for 'A', these are the values most frequently reported in the literature. Since $A_i \simeq \Gamma_i \nu_i$ within the accuracy of most experiments, the two quantities may be readily interconverted.

Section 1.2 Experimental Determination of Band Intensities.

Experimentally, the absolute intensity of an infra red absorption band is a difficult quantity to obtain. Data should be obtained from gas phase spectra since in liquid and solution the molecules of the sample are subject to perturbation due to intermolecular interactions. The effective field acting on the absorbing molecule may also be modified by dielectric phenomena that are difficult to quantify, and by fluctuating intermolecular interactions; the resulting spectrum is not a completely reliable record of the intramolecular events taking place.

Except for all but the smallest of polyatomic molecules, a spectrum will consist not of well defined individual absorption bands, but sets of band complexes with overlapping components. In solution-phase spectra, each band may be assumed to be described by a Lorentzian or near Lorentzian - type function, and the components 'resolved' by the application of educated guesswork, simulation techniques, or least squares methods. In the gas phase, however, each band has an inherently complex structure, since the rotational fine structure remains intact, this information being lost in the liquid phase as intermolecular collisions and interactions destroy the separate identity of the rotational states.

From the point of view of assigning each band in a spectrum as arising from a transition of specified symmetry, this

superposition of information is extremely valuable, since the actual band contour is determined by the direction of change of dipole moment during the molecular vibration. Without this insight into the character of the transition yielding each band, it would be extremely difficult to unravel the frequency data from a spectrum, this being a necessity for force constant calculations.

From the point of view of acquiring total band intensity data, however, this information is not only superfluous, but it greatly increases the magnitude of the difficulty of data analysis due to the overlapping of bands. Although success has been achieved through simulation techniques, requiring the capability to perform asymmetric rotor calculations, such an approach requires an amount of effort to be expended which is prohibitive as far as routine investigations are concerned.

The procedure adopted in this study is to attempt to determine the individual gas phase band intensities by comparison of gas with solution phase data. Although this has been performed quite successfully, such approximations increase the magnitude of error in the results to a degree that is perhaps difficult to estimate.

Even considering a well defined, distinct absorption band in a spectrum, the question arises - is this a true representation of the physical processes occuring at the molecule? To what extent is the spectrum degraded by instrumental distortion? In a conventional spectrometer, the beam of light travelling from the sample passes through a slit and onto the detector. The fact that this slit is of finite width means that an interval of frequencies is actually being monitored at a given frequency setting. The resulting plot of transmission versus frequency does not then correspond to the true spectrum, but is actually a convolution of it with the slit function, which is often approximated as triangular in form.

$$T(\nu') = \int_0^\infty I(\nu)g(\nu,\nu')d\nu$$

$T(\nu')$ is the apparent intensity at frequency ν'. $I(\nu)$ is the true intensity at ν. $g(\nu,\nu')$ is the slit function, which is

zero except in a range close to ν'. This is the factor which determines the resolution of the spectrometer.

The spectrum is distorted so as to yield an absorbance which is too low, and consequently the apparent band intensity is low. There is also a loss of information on the band contour, which is broadened by the effect. The magnitude of this distortion is determined by the ratio of the slit width to the band half-width - generally if this is maintained at a value less than 0.2, errors in the band intensity arising from this source should be less than ~2%.

Early studies on band intensities, in the late 1920's, brought attention to this problem of having adequate instrumental resolution. The fundamental of HCl was measured both by Bourgin[3] and Bartholomé[4] but for the above mentioned reason, their results differed by a factor of four.

A decade later, Wilson and Wells[5] showed that as 'cl' reaches zero, then the observed intensity becomes the true intensity. Thus by making a series of measurements at different values of 'cl' the true value may be obtained by extrapolation.

If (observed intensity x cl) is plotted against cl, the slope of the tangent at the origin gives the desired value. Alternatively if B/cl is plotted versus cl, the intercept at cl=0 gives the true intensity. Care should be taken with such an approach, since the results obtained will rely heavily on data corresponding to low absorption which are subject to the largest experimental error.

Gas phase spectra often contain a number of exceptionally sharp features, i.e. strong Q branches, and these are especially prone to distortion due to inadequate resolution. It is then desirable to smear out the peak by adding to the cell a high pressure of inert gas, such as nitrogen. If the measured absorbance is roughly constant over the range of the slit function, direct integration over the band will yield the correct intensity. Again, some caution is necessary, when dealing with weak bands, since a molecule undergoing excessive collisional perturbations may show induced absorption. This may occur for both normally inactive fundamentals, e.g. the a_{1g} mode of methane[6], and for simultaneous transitions where absorption may occur at a frequency $\nu_a \pm \nu_b$ where ν_a and ν_b refer to the

fundamentals of the two different molecules[7].

Solution and liquid phase studies are not hindered to such a large extent by the slit effect, but nevertheless it is still not negligible. Correction factors have been calculated and tabulated for e.g. a triangular slit and a Lorentzian band[10], and for a gaussian slit function with either Lorentzian or gaussian bandshapes[11].

A source of error unique to solution/liquid phase measurements is that the wings of a band may spread out to distances far from the band centre, and the point at which these merge with the baseline is difficult to determine. A way to circumvent this problem is to assume that the band may be represented analytically, and then integrate this function over all space.

With very high resolution the slit width problem is no longer relevant. As the resolution is increased, however, the spectrum will exhibit a higher level of noise unless the scan speed is slowed accordingly. Alternatively the noise level can be reduced at the stage of data analysis. One of the simplest ways to smooth fluctuating data is by applying to it a moving average such as a triangular or exponential type function. This process in itself leads to degradation of peak intensity.

This method of treating data is equivalent to convoluting it with the appropriate set of integers, these being fixed by the type of averaging function being employed. More sophisticated numerical analysis furnishes coefficients which yield a curve representing a least squares fit to the observed points[12].

There are various methods which seek to derive the true from the observed spectrum. The relationship between the latter may be restated:

$$f(\nu') = \int_{-\infty}^{+\infty} a(\nu-\nu')\ \phi(\nu)d\nu$$

$a(\nu-\nu')$ is the fraction of radiation of frequency ν transmitted to the recorder set at ν'.

There are three groups of methods by which $\phi(\nu)$ can be deduced from $f(\nu')$, having gained one experimental scan only.

(1) $F(t) = \Phi(t).A(t)$ where F, Φ, and A are Fourier transforms of f, ϕ, and a. Inverse Fourier transformation of $\Phi(t)$ will yield $\phi(\nu)$.

(2) The true spectrum may be recovered by adding a correction to the observed spectrum, based on the second derivative:

$$\phi(\nu) = f(\nu) - \frac{s^2}{12} \frac{\partial^2 f(\nu)}{\partial \nu^2} + \text{higher derivatives.}$$

This example is appropriate for a symmetric monochromator with a triangular instrument function.

(3) Pseudo-deconvolution. This involves convoluting the observed spectrum with the slit function. The true curve may be derived by analysis of the ordinate differences resulting from this operation[15].

So it can be seen that experimentally there is often far more to obtaining the intensity of a band than running the spectrum and directly measuring the area under the curves. Certainly, before the spread of computer technology, the acquisition of reliable data had proved one of the main stumbling blocks in the field. Accurate work should now be capable of yielding band intensities correct to within 5%.

Section 1.3 The Origin of the Band Intensity.

In a quantitative investigation of the phenomena occuring at the initiation of the absorption process, quantum mechanics may be used to describe the material body whilst the radiation field is satisfactorily formulated using classical electo-magnetic theory. First order perturbation theory is employed to determine how a molecule can interact with radiation, and shows that the probability of a transition between two states described by the wavefunctions ψ^n and ψ^m is proportional to the square of the 'transition moment' '$\underline{\mu}_{nm}$'

$$\underline{\mu}_{nm} = \langle \psi^n | \underline{p} | \psi^m \rangle \qquad \underline{p} = \text{molecular dipole moment}$$

According to classical electrodynamics, a system may absorb and emit radiation if its dipole moment is fluctuating in a periodic manner, and here the transition moment is in fact analogous to the classical amplitude of the oscillation.

If it is assumed that each molecular vibration is a simple harmonic motion, then the wavefunctions for the vibrational states are derived by solving the Schrödinger equation for the system, and they take the form

$$\psi_v^k = N_v \exp(-\tfrac{1}{2}Y_k Q_k^2)\ H_v\ (Y_k^{\frac{1}{2}} Q_k)$$

Q_k is the normal coordinate for the k^{th} vibration.
$Y_k = \frac{4\pi^2}{h}(\nu_{cl})_k$, ν_{cl} = classical frequency. H_v is a Hermite polynomial, the order 'v' being given by the quantum number v. N_i is a normalising factor.

The corresponding eigenvalue is given by $\varepsilon_v = (v+\frac{1}{2})h\nu_{cl}$. Hence the frequencies at which radiation is absorbed can be identified with the classical mechanical frequencies.

The magnitudes of the components of the molecular dipole moment depend on the atomic configurations, and thus are functions of all vibrational coordinates, and capable of expansion as a Taylor series:

$$\underline{p} = \underline{p}_o + \sum_k \left[\left(\frac{\partial \underline{p}}{\partial Q_k}\right)_o Q_k\right] + \ldots.$$

'o' signifies correspondence to the equilibrium position.

So for the molecular dipole to vary, $\frac{\partial \underline{p}}{\partial Q_k}$ must have at least one non-zero component. This actually corresponds to a 'selection rule', but it is 'restricted', in that its validity depends on two assumptions:

(1) That each vibration is simple harmonic. Otherwise the separability of the total vibrational motion into the individual normal modes is not possible.
(2) That higher terms in the Taylor expansion are negligible.

Further insight into the conditions necessary for absorption may be obtained by substituting the expansion for $\underline{p}$ into the definition of the transition moment.

$$\underline{\mu}_{nm} = \underline{p}_o \int \psi^{n*}\psi^m d\tau + \sum_k \left[\left(\frac{\partial \underline{p}}{\partial Q_k}\right)_o \int \psi^{n*} Q_k \psi^m d\tau\right]$$

The first term on the right hand side vanishes unless n=m, due to the mutual orthogonality of the wavefunctions, and since

this corresponds to no absorption, the term may be disregarded.

Consider the k^{th} term of the remaining summation. The total vibrational wavefunction describing the state 'n' is a product of wavefuntions, one for each normal mode.

$$\psi^n = \Pi_k \psi_k^n$$

$$\therefore \mu_{nm} = \int \psi_1^{n*} \psi_1^m dQ_1 \int \psi_2^{n*} \psi_2^m dQ_2 \ldots \int \psi_k^{n*} Q_k \psi_k^m dQ_k$$

There are two conditions that determine whether the RHS will be non-zero:

(1) For all modes except the k^{th}, the two states must be identical, from the orthogonality restrictions on the wavefunctions.

(2) The properties of the Hermite polynomials dictate that the vibrational quantum number must only change by unity during a transition.

The correctness of all these assumptions is brought into perspective by the fact that overtone and combination bands do have intrinsic intensity and are generally very common in infra red spectra. The fundamental bands remain as the dominant feature, however, and it is usual to treat mechanical and electrical anharmonicity as a perturbation to the simple harmonic description of the vibrational motion.

All the above 'selection rules' have been restricted in that their validity retains certain assumptions. Ultimately it is molecular symmetry that determines whether the dipole change is non-zero for a given motion. The rules obtained from these considerations are rooted mathematically in Group Theory, and are completely general in their application to both harmonic and anharmonic forms of motion.

So the criterion for the activity of a fundamental ultimately rests with the symmetry properties of the transition moment. In fact, group theory shows that this must belong to a representation whose structure contains the totally symmetric species, and for this to be true, the species of the vibration must be the same as that of one of the components of the dipole moment,

i.e. as one of the translations in the x, y, and z directions. Since the ordinary character tables list this information for each point group, the symmetry of the vibrations that are infra red active may be readily ascertained.

The discussion so far has presented the conclusions which determine only whether or not to expect a given fundamental to feature in an infra red spectrum. This only represents a superficial analysis of the transition moment, and does not indicate the precise nature of the phenomena which contribute to its value.

Section 1.4 Analysis of Intensity Data.

The primary task of intensity theory is to use the experimental data, the set of fundamental band intensities, to derive a set of parameters which describe the physical processes that occur as a molecule changes its configuration. Since it is the change in dipole moment that is all important, we are actually describing the way the charge distribution is distorted as the atomic centres are displaced.

The way in which we examine these processes depends on the coordinate system employed in the calculations, i.e. the way in which we describe the form of each vibration and the flow of charge.

The experimentally derived quantity is the derivative of the molecular dipole moment with respect to the normal coordinate for the vibration.

$$A_i = \frac{N\pi g_i}{3c^2} (\partial \underline{p}/\partial Q_i)^2$$

N is Avogadro's number, c is the velocity of light, and g_i is the degeneracy of the vibration.

This derivative is a quantity that is difficult to physically visualise and is of little use in itself in rationalising the flow of charge. The first step in the analysis is to decompose the $\partial \underline{p}/\partial Q$ into parameters which are chemically more meaningful, such as functions of bond lengths and interbond angles.

The transformation between internal coordinates and normal coordinates is given, in matrix notation, by

$$R = LQ, \quad \text{where } L_{ij} = dR_i/dQ_j.$$

Thus,

$$d\underline{p}/dQ_i = \sum_j (\partial \underline{p}/\partial R_j)(\partial R_j/\partial Q_i)$$

$$= \sum_j (\partial \underline{p}/\partial R_j)L_{ji}$$

and $$d\underline{p}/\partial R_j = \sum_i (\partial \underline{p}/\partial Q_i)(\partial Q_i/\partial R_j)$$

$$= \sum_i (\partial \underline{p}/\partial Q_i)L_{ij}^{-1}$$

Thus in order to deduce a set of $\partial \underline{p}/\partial R_j$ it is necessary to measure the intensities of all the fundamentals, and to have determined the L matrix. The latter is only available if the molecular force field has been determined, and this fact contributes a major stumbling block. Although much effort and progress has been made in the area of normal coordinate/force constant calculations, force fields have been completely determined for only the smallest of polyatomic molecules.

First, the reverse computation will be considered, i.e. the calculation of vibrational frequencies employing a predetermined or assumed force field. The secular equation which must be solved takes the following form:

$$GFL = L\Lambda$$

The G matrix is the kinetic energy term, and its elements are functions of the nuclear masses and geometry (so the latter must be known by electron diffraction, or other means),

$$G = BM^{-1}B^t$$

M^{-1} is a $3N \times 3N$ diagonal matrix, of the inverse atomic masses (N = number of atoms). The B matrix relates the internal and Cartesian coordinate systems:

$$R = BX, \quad B_{ij} = \frac{\partial R_i}{\partial X_j}$$

Setting up the G matrix is a straightforward computational matter.

The potential energy is defined by the F matrix in the secular equation. It is a function of the internal displacement coordinates, and may be expanded as a Taylor series in these.

$$V(R_1,R_2,\ldots) = V_o + (\frac{\partial V}{\partial R_1})_o R_1 + (\frac{\partial V}{\partial R_2})_o R_2 + \ldots$$

$$+ \tfrac{1}{2}(\frac{\partial^2 V}{\partial R_1^{\,2}})_o R_1^{\,2} + \tfrac{1}{2}(\frac{\partial^2 V}{\partial R_2^{\,2}})_o R_2^{\,2} + \ldots$$

$$+ (\frac{\partial^2 V}{\partial R_1 \partial R_2})_o R_1 R_2 + (\frac{\partial^2 V}{\partial R_2 \partial R_3}) R_2 R_3 + \ldots$$

V_o is the potential energy corresponding to the equilibrium geometry and it may arbitrarily be taken as zero, and the energies measured relative to it. The 'o' subscript signifies the equilibrium position, and hence the first derivatives in the expansion are zero. The second derivatives that remain are the 'force constants'.

$$F_{11} = (\frac{\partial^2 V}{\partial R_1^{\,2}})_o, \quad F_{12} = (\frac{\partial^2 V}{\partial R_1 \partial R_2})_o \quad \text{etc.}$$

Higher derivatives in the expansion would correspond to the anharmonic components of the force field.

Finally, the L matrix defines the form of each vibrational mode, and is the transformation matrix between internal and normal coordinates.

$$R = LQ \quad \text{i.e.} \quad L_{ij} = \partial R_i / \partial Q_j .$$

The secular equation takes the form of an eigenvector/eigenvalue problem. The frequencies are the elements of the diagonal matrix Λ, and are the eigenvalues of the product GF. Each row of L is the corresponding eigenvector. Such

computations are routine, and thus there is no inherent difficulty in calculating the frequencies starting from a known nuclear geometry and force field.

However, it is the vibrational frequencies which are the experimental observables, and therefore the principal source of data from which the molecular parameters, the force constants, have to be derived. Unfortunately the latter, in the general valence force field described above, are far greater in number than the independent pieces of data.

The most important source of extra information is the sets of new frequencies obtained by isotopic substitution. Here, the molecular force field remains unchanged, but the different atomic masses produce a new G matrix and hence furnish a different set of eigenvalues for GF. In this way, constraints are imposed on the possible values of the force constants. The sets of frequencies are, however, related:

$$\frac{\Pi\lambda}{\Pi\lambda'} = \frac{|G|}{|G'|}$$

One such expansion exists for each symmetry block, and thus limits the new information available.

Previous experience may enable various assumptions regarding the numerical values of the force constants to be made. For instance, it is often reasonable to assume that the only interaction constants to take non-zero values should be those corresponding to internal coordinates with two atoms in common. Or certain force constants might be transferred from smaller, chemically related molecules which have already been studied in detail.

There is actually no straightforward way to reverse the normal coordinate calculation to yield force constants from frequencies. The usual procedure is to employ an iterative method. A guessed set of force constants is used to generate a set of frequencies which is compared with those observed, and the force field is then modified so as to reduce to a minimum the sum of the squares of the differences. Such a procedure may be 'badly behaved', in that the fit between postulated and experimental frequencies may oscillate during the cycle of

iteration or even get progressively worse. The convergence depends on a reasonable initial guess, and if this is not provided the assumption on which the process is mathematically based will not be obeyed. There may be some doubt concerning the acual assignment of the frequencies, and this may constitute a serious source of error in the calculation.

Even if the above is carried out successfully, the force field finally obtained will to some extent reflect the constraints and type of parametrization enforced by the investigator. And similarly, there will be some question as to how accurately the L matrix then calculated will describe the form of each vibration. Thus immediately a veil of uncertainty is drawn across the parameters obtainable from the experimental dp/dQ.

And yet an equally important problem must be considered at this initial stage. Experiment yields the square of dp/dQ, and hence only its magnitude, not its sign. There are 2^n possible sets of dp/dQ where 'n' is the number of infra red active bands. Symmetry reduces this to being true for each individual symmetry species. Each different set will yield a different set of dp/dR, so the problem is to decide which one is correct.

Again, isotopic substitution can be of great benefit. The parameters that characterise the way in which the charge is redistributed are independent of the actual atomic masses, being functions only of the electronic wavefunctions. Thus the dp/dR obtained from a set of dp/dQ, for say the undeuterated compound, should reproduce the intensities observed for the fully deuterated compound. The $(dp/dQ)_{d0}$ which produce the dp/dR which best adhere to this constraint are then considered to be the 'correct' sign choice. This procedure is subject to errors both from the experimental intensities and the force field being employed.

Supposing that a satisfactory set of dp/dR has been obtained - how does the analysis now proceed?

Section 1.5 Models for the flow of Charge.

There are essentially two different routes of analysis which offer contrasting views of the charge redistribution. Historically the first was to regard each chemical bond as a separate molecular building block, a fragment whose electronic distribution acts in an independent manner. This 'zeroth bond moment hypothesis', rests on three simplifying assumptions:

(1) The stretching of a bond by dr produces a change of dipole moment along the bond of $(\partial\underline{\mu}/\partial r)dr$.

(2) The deformation of a bond through an angle $d\theta$ produces a dipole change $(\partial\underline{\mu}/\partial\theta)d\theta$ perpendicular to the bond and in the plane of movement.

(3) Changes in one bond do not result in changes in another bond except when geometrically necessary.

In the above, '$\underline{\mu}$' stands for the 'bond moment', and is equal to $q.\underline{r}$, $\underline{r}$ being the unit vector along the bond and q the charge apportioned to each atom of the bond.

The usefulness of such a model may be measured by how the parameters obtained transfer between chemically similar molecules, and how resulting discrepencies can be rationalized. In fact the above model proves to be unsatisfactory[16], and the more sophisticated treatment required must employ a greater number of parameters to describe the contribution to the total dipole moment and individual bond moments from electron flow in regions actually removed from the atomic displacements.

Such a model is found in the Gribov formulation[17]

$$d\vec{M}/dQ_i = [(\vec{e}^{\,o})`(\partial\underline{\underline{\mu}}/\partial R) + (\underline{\mu}^{o})`(\partial\underline{\underline{\vec{e}}}/\partial R)]\ L_i$$

As previously, the total molecular dipole moment is given by the vector sum of the bond moments.

$$\vec{M} = \sum_k \mu^k \vec{e}^k$$

These bond moments include the dipole contributions from lone pair eletrons and off-axis moments.

$\underline{\mu}^k$ is the k^{th} bond moment.
$\underline{\underline{e}}^o$ is the matrix defining the direction of each bond.
$\partial\underline{\mu}/\partial R$ is the rectangular matrix of derivatives of the bond moments with respect to the internal coordinates - including cross terms of the type $\partial\underline{\mu}_i/\partial R_j$. These are the molecular 'electrooptical parameters'. L_i is the i^{th} column of the L matrix.

The above approach provides a method of examining the charge flow through a configuration space based on the system of internal coordinates. An alternative viewpoint is gained by considering the flow as the nuclear centres are displaced along each of the three Cartesian axes. It is assumed that the change in dipole moment depends linearly on small displacements of the atom, and that simultaneous displacements of several nuclei have an additive effect.

$$P_Q = P_x A L$$

P_Q is the 'polar tensor in normal coordinate space', a direct representation of the experimental intensities. It is a $3\times 3N-6$ matrix:

$$P_Q = \begin{bmatrix} dp_x/dQ_1 & dp_x/dQ_2 & \cdots & dp_x/dQ_n \\ dp_y/dQ_1 & & \cdots & dp_y/dQ_n \\ dp_z/dQ_1 & & \cdots & dp_z/dQ_n \end{bmatrix}$$

P_x is the polar tensor in cartesian coordinate space

$$P_x = \begin{bmatrix} dp_x/dx_1 & dp_x/dy_1 & \cdots & dp_x/dz_n \\ dp_y/dx_1 & & \cdots & dp_y/dz_n \\ dp_z/dx_1 & & \cdots & dp_z/dz_n \end{bmatrix}$$

'A' is the matrix that effects the transformation from internal coordinates to space fixed coordinates.

$X = AR$, and $BA = E$

P_x is actually written as a juxtaposition of 'atomic polar tensors' (APT's), P_x^{α}, one for each atom α.

$$P_x = [P_x^{1} : P_x^{2} : \ldots . P_x^{n}]$$

$$P_x^{\alpha} = \begin{bmatrix} dp_x/dx_\alpha & dp_x/dy_\alpha & dp_x/dz_\alpha \\ dp_y/dx_\alpha & dp_y/dy_\alpha & dp_y/dz_\alpha \\ dp_z/dx_\alpha & dp_z/dy_\alpha & dp_z/dz_\alpha \end{bmatrix}$$

These atomic polar tensors are the quantities sought from the experimental intensities. The first column gives the x, y, and z components of the dipole change due to a unit displacement of atom α in the x-direction.

The reverse transformation, required to derive P_x from P_Q is given by

$$P_x = P_Q L^{-1} B + P_\rho \beta$$

'$P_\rho \beta$' is a 'rotational correction' term which is required because of the apparent rotation of a permanent dipole moment in exchanging internal and cartesian coordinate systems. The β matrix is defined by the Eckart conditions, the constraints that are imposed on the B matrix to ensure zero angular momentum and translational kinetic energy. The elements of P_ρ are functions of the permanent dipole moment and moments of inertia.

The P_Q matrix will reflect the molecular symmetry - molecules with a sufficient degree of symmetry that $d\underline{p}/dQ_i$ is directed along only one of the x, y and z axes will only have entries along the single appropriate row, all other entries being zero. The number of independent elements in the P_x matrix is similarly restricted. For instance, if an atom lies on an axis with 3-fold symmetry or greater, the APT must necessarily

be diagonal in form. Atoms which are classed as belonging to an 'equivalent set', have APT's which are related by the same similarity transformation that rotates one atom into another.

The actual numerical values of the APT elements depend on the arbitrary choice of direction for the molecular cartesian axes. For comparing the trends of atoms in different molecules, a useful convention is to direct the z axis along the bond in question.

Section 1.6 The Scope of this Project.

Up to this stage some of the tools and methods that may be employed in attempting to understand vibrational intensities have been introduced. Much of the above will be discussed further in later sections of this report, including the acquisition of experimental data and its subsequent interpretation.

In the field of intensity studies, most work has so far been centered on only small polyatomic molecules, such as simple hydrocarbons, and the halomethanes. This project represents an attempt to extend these studies to larger molecules with spectra that are correspondingly more complex. Two cyclic compounds, 1,4-dioxan and cyclohexane are examined and the results obtained are then used to predict the spectrum of the compound intermediate between the two, tetrahydropyran.

Chapter 2 - EXPERIMENTAL SECTION.

Section 2.1 Acquisition of Intensity Data.

The experimental procedure which is described in the following pages is directed towards the goal of obtaining gas phase band intensities for the infrared active fundamentals of the molecules under consideration - 1,4-dioxan, cyclohexane and tetrahydropyran. As discussed in the introduction, a gas phase spectrum typically consists of a series of overlapping bands, which themselves possess complex and ill-defined contours. This results in it being necessary to make measurements of the corresponding solution phase spectra in an attempt to determine the intensity contribution of each individual band in the gas phase.

Each band in the solution spectrum may be satisfactorily described as near-Lorentzian in shape; a simplification that enables overlapping band systems to be broken down into their components using least squares analysis. The extrapolation from solution to gas phase results is then made by making the assumption that the distribution of intensity across these band profiles is the same in both phases.

Before the advent of computer technology, a far higher degree of error was inherent to the measurement of the area under a spectral curve, methods often relying on the use of a planimeter or even counting squares on the chart paper. Now the spectral information may be recorded via a microcomputer onto tape or disc, and is thus in a form more amenable to analysis or any desired numerical manipulation.

At the beginning of this study, spectra were recorded using a Perkin-Elmer 325 spectrometer, interfaced to a Tektronix minicomputer. A computer program was developed, in BASIC, which enabled the spectroscopic transmittance data to enter the memory, and which after a given run provided various options that constitute the initial stages of the data analysis. [Program is listed in the appendix.]

These operations include:

(1) Acquisition of spectral data.
(2) Plotting of spectrum on the terminal screen.

(3) Storage of data on magnetic tape (cassette).
(4) Ratioing of sample and background as required.
(5) Conversion into absorbance.
(6) Correction of absorbances for solvent effects.
(7) Integration of absorbance, yielding the total band area for a desired spectral range.

A typical 'sample run' consists of obtaining the spectrum of a solution of known molarity (a gas of known pressure), in a cell of known pathlength placed in the sample beam of the spectrometer, with a matching cell containing solvent alone in the reference beam (left blank for gas phase measurements). The 'background run' then consists of replacing the sample solution by pure solvent (or evacuating the gas phase sample and refilling one cell with the pressure-broadening gas).

The interface converts the signals from the spectrometer into ASCII Form. There are five pieces of information - three digits defining the transmittance value i.e. units, tens and hundreds of units (A$, B$, and C$), '983' corresponding to zero radiation reaching the detector. Frequency increments are represented through a two digit number (D$ and E$). Knowledge of the separation of each point enables the frequency axis to be reconstructed to match the transmittance data.

The Tektronix minicomputer possesses an extensive graphics capability, which renders the programming of the plotting routine a straightforward matter. The WINDOW and VIEWPORT commands combine to define a grid on the terminal screen, and the MOVE command allows a chosen symbol to be placed anywhere on this grid. Axes may also be drawn to any given specification. A hand copy of the graphical or numerical information present on the screen may be obtained from a graph plotter, which may also be brought under direct program control.

More recently, this research group has acquired a Perkin-Elmer 983 spectrometer, and accompanying data station. A far larger range of commands for spectral acquisition and data manipulation are available as part of the fundamental operations of the instrument and data station. Now spectra are recorded on disc, which proves to be a more economical method of storage.

One of the main problems associated with the solution measurements is that the solvent employed may itself show absorbance in a region of interest, and for accurate intensity results there is a need to remove this source of distortion from the actual sample spectrum. For weak solvent absorption it is sufficient to simply subtract the background absorbance spectrum from that of the sample. However, the change from pure solvent to sample solution (say 95% solvent by volume) is of course accompanied by a drop in 'solvent concentration' - as the molarity of sample solution increases the absorption due to solvent will diminish in proportion. This means that it is possible to over-compensate for solvent absorption on subtraction of the pure solvent spectrum, in the worst instance leading to the appearance of a negative absorbance peak.

The absorption resulting from the sum of these effects may be represented by:

$$\frac{I(\nu)\text{bgrd}}{I(\nu)\text{ sample}} = \exp\left[\varepsilon^{\nu}\ell(1-x) - \varepsilon^{\nu}_{CCl_4}\ell(1-x)\right]$$

ℓ = path length of the cell containing sample solution (a pure solvent for 'background' run).
x = fractional concentration of solvent in sample solution.
ε^{ν} = extinction coefficient at frequency ν.

$\varepsilon^{\nu}_{CCl_4}$ may be obtained from measurements of solvent spectra at different cell path lengths, and on adding the correction factor, '$\varepsilon^{\nu}_{CCl_4}\ell(1-x)$' to the absorbance points in the sample spectrum, the above described error is counteracted.

Another potential source of error to be aware of is background drift. During a given run this is negligible (except in the case of evaporation of liquid from either of the cells leading to bubble formation, when the run should simply be discontinued). However, comparison of background runs obtained at the beginning and end of the day will often show a shift in the 100% transmission points. Ideally there will be an area present in the sample spectrum corresponding to zero absorbance, and the background absorbance spectrum raised or lowered to ensure that this condition is met. Otherwise the absorbance at a given frequency (of constant or slowly changing absorption) may be fixed at a predetermined value (obtained from variable path-length measurements), the background transmittance spectrum being multiplied by the appropriate scaling factor.

The above operation may be programmed into the micro-computer, but the calculations required to analyse overlapping band systems into their individual components need a far larger amount of memory than is available. Thus there is a need to transfer the spectral data from tape or disc to a mainframe computer. For this purpose, the Tektronix was put into 'terminal mode' and linked to the London University CDC 7600, the data being sent over to previously created files. This process was effected by setting the tape at the beginning of the data file and pressing the 'SEND OVER' key. Latterly, the new Perkin-Elmer data station was linked to the VAX computer at Royal Holloway College, a small program being constructed to shift data from the datastation memory to the VAX via the auxilliary port.

The solutions employed were of strengths in the region 0.1 molar - 0.5 molar for 1,4-dioxan, 0.1 molar - 1.5 molar for cyclohexane, and 0.1 - 0.6 M for tetrahydropyran, spectroscopic grade carbon tetrachloride and carbon disulphide being the solvents. The path lengths of the cells used were determined from an analysis of the diffraction patterns obtained from the spectrum of the empty cell alone.

Gas phase spectra were obtained using a variable path length gas cell (1.25 to 10 metres) and the pressure measured with a Baratron gauge. Pressures of sample (room temperature) employed fell in the range 0.1 - 5 mm Hg of 1,4-dioxan (1.25 metres) 0.5 - 10 mm cyclohexane (5 metres) and 0.2 - 3 mm tetrahydropyran (up to 5 metres path length). The introduction stressed the problems associated with spectral distortion due to the finite resolving power of the spectrometer, this being especially relevant to the gas phase spectra, where such sharp features as Q-branches are common. An attempt has been made to negate these errors, by introducing into the cell 500mm pressure of an inert gas, nitrogen. The experimental results listed show no obvious pressure dependence, and hence it is justified in simply taking the mean as the best figure. In order to perform a more thorough numerical analysis, more time should be spent carrying out further experimental runs to provide a larger number of points on which to base any curve fitting.

Section 2.2 Solution Spectra - Bandfitting.

A solution phase absorption band possesses a contour that is well described by a Lorentzian function, except for the wings of the band, which would then be required to spread out to infinity. This behaviour may be suppressed by the inclusion of an exponential damping factor, leading to the following expression:

$$I(\nu) = I_{max} \cdot \frac{\Delta\nu_{\frac{1}{4}}^2}{\Delta\nu_{\frac{1}{4}}^2+(\nu-\nu_o)^2} \exp(-a|\nu-\nu_o|^b)$$

$I(\nu)$ is the absorbance at frequency ν.
ν_o is the frequency of the band centre.
$\Delta\nu_{\frac{1}{4}}$ is half the band half-width - the difference in frequency (cm^{-1}) separating the band centre and the frequency corresponding to an absorbance of $I_{max}/2$.
'a' and 'b' are parameters which have been empirically found to take values of 0.002 and 1.5 respectively to provide adequate damping.

A set of overlapping bands would then have a contour described by:

$$I(\nu) = I^1(\nu) + I^2(\nu) + I^3(\nu) + \ldots$$

where $I^n(\nu)$ contains the parameters specific to the n'th band. Application of least squares theory (presented in the appendix) furnishes the parameters that represent the best fit to the overall observed band structure. The theory gives:

$$\Delta\hat{p} = (J^t\omega J)^{-1} J^t\omega\hat{\varepsilon}$$

J is the Jacobian matrix:

$$\frac{\partial(I(\nu))}{\partial I_{max}} = \frac{\Delta\nu_{\frac{1}{4}}^2}{\Delta\nu_{\frac{1}{4}}^2+(\nu-\nu_o)^2} \cdot \exp[-a|\nu-\nu_o|^b]$$

$$\frac{\partial I(\nu)}{\partial \Delta\nu_{\frac{1}{4}}} = 2I_{max}\,\Delta\nu_{\frac{1}{4}}\,\frac{(\nu-\nu_o)^2}{[\Delta\nu_{\frac{1}{4}}^2+(\nu-\nu_o)^2]^2}\cdot\exp[-a|\nu-\nu_o|^b]$$

$$\frac{\partial I(\nu)}{\partial \nu_o} = 2I_{max}(\nu-\nu_o)\,\frac{\Delta\nu_{\frac{1}{4}}^2}{(\Delta\nu_{\frac{1}{4}}^2+(\nu-\nu_o)^2)^2}\cdot\exp[-a|\nu-\nu_o|^b]$$

'$\hat{\varepsilon}$' is the error vector; the difference between $I(\nu)$ calculated from a guessed set of parameters and the actual absorbance observed.
'ω' is the weighting matrix - each element in the error vector is weighted by the observed absorbance.
$\Delta\hat{p}$ is the desired correction to each band parameter that improves the fit.

Generally it was found that four or five cycles of iteration were required before the optimum fit was achieved.

EXPERIMENTAL DATA.

Section 2.3 1,4-Dioxan.

In the following pages, the experimental data is presented from which the individual, gas phase band intensities are derived. Table 1 lists the gas phase results for dioxan-d_o and Table 2 the corresponding data from the solution phase. Similarly, Tables 3 and 4 give the results for dioxan-d_8.

In Tables 5 and 6 this information is summarised, the solution band intensities and the gas region intensities having been averaged, and the standard error of the mean determined. The solution/gas phase intensity ratio is obtained by comparing the total intensity for a given gas phase region with the sum of the solution intensities for bands contained within that region. This is the parameter which scales the solution band intensities to yield the final absolute gas phase band intensities

For instance, take the 1300-1070 cm^{-1} region in the spectrum of completely deuterated dioxan. In the solution phase, four bands exist whose individual intensities have been determined, but in the gas phase they overlap substantially, and only their sum may be determined experimentally. The ratio of this sum of four bands for solution and gas is 1.013, and this is the figure by which the solution band intensities are divided to

yield the corresponding 'experimental' gas phase results. Or in a completely analogous fashion, the total gas phase intensity in this region is divided amongst the constituent bands in exactly the same manner as found in the solution results. The final intensities derived are given in Tables 7 and 8 for the d_o and d_8 compounds respectively.

TABLE 1.

Dioxan d_o : Gas Phase Data.

Frequency Range(cm^{-1})	Pressure (mm, 298°K)	Intensity (km mol^{-1})
3050-2800	.373	331.2
	.376	330.0
	.410	327.2
	.424	339.5
	.670	322.0
1520-1410	0.77	16.4
	1.02	16.9
	1.75	15.4
	2.97	16.1
1410-1335	0.53	12.7
	0.96	14.0
	1.47	13.3
	2.05	13.6
1335-1200	0.53	46.2
	0.96	48.6
	1.47	52.6
	2.05	46.9
1200-1000	0.13	179.4
	0.19	176.2
	0.22	177.6
	0.34	174.6
	0.48	174.5
960-800	0.15	88.0
	0.31	95.8
	0.45	83.9
	0.59	99.8
	0.70	96.1
660-540	0.83	15.5
	1.44	14.9
	2.95	13.9
	4.49	14.2
320-220	0.49	21.4
	0.85	20.6
	1.03	20.2
	1.08	19.1
	1.52	19.8
	1.56	19.8
	1.97	20.6

TABLE 2.

d_o Dioxan Solution Data.

Frequency (cm^{-1})	Concentration (molar)	$I_{max}^{log_e}$	$\Delta\nu_{\frac{1}{2}}(cm^{-1})$	$A_i(km\ mol^{-1})$
2967	.0921	.893	20.3	112.2
	.1077	1.020	20.5	110.6
	.2793	2.605	21.3	112.4
2917†	.0921	.515	15.4	51.4
	.1077	.590	15.1	49.7
	.2793	1.508	16.7	53.1
2893†	.0921	.421	9.8	28.6
	.1077	.490	9.8	27.9
	.2793	1.243	10.6	29.4
2859	.0921	1.062	16.8	114.5
	.1077	1.215	16.8	111.4
	.2793	3.106	17.4	113.4
1453	.1735	.417	6.8	10.6
	.1122	.252	6.6	9.5
	.2503	.586	6.8	10.4
	.3595	.786	6.7	9.55
	.1630	.374	6.9	10.4
1445	.1735	.285	11.3	11.5
	.1122	.179	11.6	11.4
	.2503	.414	11.3	11.55
	.3595	.564	12.4	11.9
	.1630	.260	12.2	12.0
1376	.1773	.063	5.12	1.23
	.1114	.0359	4.26	0.91
	.2484	.096	11.28	2.67
	.0379	.009	16.44	2.31
	.5451	.182	10.2	2.13
	.2406	.084	9.9	2.15
	.3561	.123	7.9	1.72
	.0919	.048	8.0	2.17
	.1617	.065	6.4	1.66
1366	.1773	.318	8.9	10.34
	.1114	.206	8.7	10.17
	.2484	.465	8.1	9.66
	.0379	.068	9.0	10.20
	.5451	.954	8.7	9.59
	.2406	.429	9.6	10.70
	.3561	.619	8.9	9.76
	.0919	.180	8.0	9.97
	.1617	.295	9.0	10.36

continued...

TABLE 2 - continued...

1320†	.1735	.046	34.1	4.61
	.1122	.029	14.6	2.31
	.2503	.062	31.2	4.02
	.0379	.010	34.2	4.44
1290	.1735	.410	9.4	14.05
	.1122	.257	9.4	13.93
	.2503	.606	9.3	14.27
	.0379	.082	10.0	13.52
1255	.1735	2.140	4.7	38.4
	.1122	1.403	4.7	38.6
	.2503	2.923	4.9	37.4
	.0379	.489	4.3	36.7
1126	.0599	1.357	14.2	193.9
	.0379	.875	13.8	194.2
	.1122	2.512	14.6	195.6
	.1350	2.974	14.4	191.7
1085	.0599	.211	5.2	12.2
	.0379	.132	5.4	12.45
	.1122	.422	5.3	13.1
	.1350	.500	5.3	13.0
1050	.0599	.131	6.6	9.45
	.0379	.086	6.5	9.60
	.1122	.252	7.1	10.34
	.1350	.301	7.0	10.11
887	.1735	1.026	6.0	22.44
	.0596	.330	5.3	19.31
	.0379	.200	5.4	18.93
	.1122	.653	5.4	20.85
	.1350	.800	5.5	21.48
	.2406	1.342	5.6	20.40
	.0919	.543	5.3	20.53
	.1617	.916	5.5	20.43
876	.1735	3.823	6.4	88.6
	.0596	1.275	6.7	92.3
	.0379	.798	6.4	88.3
	.1122	2.387	6.6	91.9
	.1350	2.892	6.6	91.6
	.2406	4.369	7.1	82.5
	.0919	1.954	6.4	87.9
	.1617	3.126	6.7	83.2
612	.3569	1.485	6.7	18.0
	.0919	.427	7.1	21.2
	.1617	.722	6.7	19.5
	.1735			22.5
	.1122			20.0
	.2503			18.9
273††	.2529			23.6

† Not a fundamental

†† A_i obtained directly from area under spectral curve

TABLE 3.

Dioxan d_8 Gas Phase Data.

Frequency Range(cm^{-1})	Pressure (mm, 298°K)	Intensity (km mol^{-1})
2315-2150	0.52	89.2
	0.59	87.8
	0.59	90.8
	0.70	83.2
	0.75	85.4
2150-1900	0.36	107.6
	0.45	105.2
	0.59	94.3
	0.75	99.2
	0.81	100.5
1300-1070	0.37	244.1
	0.52	245.8
	0.53	219.3
	0.595	239.6
	0.70	234.8
	0.71	223.5
	0.97	215.1
1070-1000	0.37	43.1
	0.52	43.9
	0.53	38.7
	0.595	43.4
	0.70	40.4
	0.71	39.4
	0.97	38.0
1000-840	0.53	17.8
	1.26	17.5
	1.40	17.2
	1.56	17.7
	1.60	16.7
840-700	0.53	42.2
	0.71	45.9
	0.97	43.6
	1.56	45.4
560-440	1.32	10.2
	2.04	10.8
	3.00	10.6
	3.88	10.7
270-200	1.30	13.6
	2.51	13.4
	2.93	13.6
	3.46	15.3
	2.46	12.6
	3.00	12.2

TABLE 4.

Dioxan d_8 Solution Data.

Frequency (cm^{-1})	Concentration (molar)	I_{max}	$\Delta\nu_{\frac{1}{2}}(cm^{-1})$	$A_i(km\ mol^{-1})$
2315-2150	.1438			83.2
	.2143			80.2
	.0923			80.8
2150-1900	.1438			104.6
	.2143			100.7
	.0923			101.3
1183	.2143	3.608	8.3	89.6
	.1438	2.800	7.6	95.3
	.0923	1.721	7.8	93.4
1145	.2143	1.319	7.4	29.3
	.1438	.963	7.0	30.2
	.0923	.590	7.2	29.85
1109	.2143	4.170	7.5	94.1
	.1438	3.410	6.7	103.3
	.0923	2.118	6.7	99.9
1089	.2143	.641	6.6	12.9
	.1438	.460	6.2	12.9
	.0923	.275	7.1	13.6
1039	.2143	2.330	4.5	32.3
	.1438	1.751	4.3	34.6
	.0923	1.046	4.4	33.4
1028	.2143	.808	6.6	16.1
	.1438	.572	5.5	14.5
	.0923	.348	6.5	16.0
1000-840 = 896	.2143	.987	6.2	18.8
	.1438	.572	5.5	19.4
	.0923	.425	6.3	18.9
758	.1251*	1.892	5.3	52.7
731	.1251*	.198	6.8	6.98
492	.2143	.665	6.4	12.9
	.1438	.472	6.2	13.4
	.0923	.288	6.4	13.1
270-200	.2143			20.4
	.1438			18.3
	.0923			21.7

* in CS_2.

TABLE 5.

Frequency (cm^{-1})	Solution Phase A_i (km mol^{-1})	Gas Phase Region (cm^{-1})	A_i	Solution/Gas Ratio for Region.
2967	111.7± 2	3050-2800	330.0	.924±.011
2917	51.4± 2			
2893	28.6±.8			
2859	113.1±1.5			
1453	10.1±.2	1520-1410	16.19±.35	1.355±.034
1445	11.88±.19			
1376	1.78±.51	1410-1335	13.39±.33	.894±.028
1365	10.09±.18			
1320	3.84±.63	1335-1200	48.6±1.6	1.144±.043
1290	13.94±.19			
1255	37.77±.55			
1126	193.9±1.0	1200-1000	176.5±1.1	1.226±.0095
1085	12.69±.25			
1050	9.87±.26			
887	20.55±.43	960-800	84.9±3.0	1.281±.048
876	88.3±1.5			
612	19.92±.63	660-540	14.64±.43	1.361±.059
273	23.6	320-220	20.22±.36	1.167

Dioxan d_o.

Summary of Experimental Intensity Measurements.

TABLE 6.

Frequency (cm^{-1})	Solution Phase A_i (km mol^{-1})	Gas Phase Region (cm^{-1})	A_i	Solution/Gas Ratio for Region
2315-2150	81.0±1.2	2315-2150	87.3±1.5	.928±.025
2150-1900	102.2±1.6	2150-1900	101.4±2.6	1.008±.030
1183	92.8±2.2	1300-1070	231.7±5.0	1.013±.028
1145	29.8±3.4			
1109	99.1±3.4			
1039	33.4±1.2	1070-1000	40.97±.99	1.195±.039
1089	13.16±.31			
1028	15.5±.5			
894	19.01±.23	1000-840	17.40±.21	1.093±.022
758	35.9	840-700	59.7	1.47
731	47.5			
492	13.11±.17	560-440	9.56±.17	1.371±.03
270-200	20.1±.15	270-200	13.94±.9	1.44

Dioxan d_8.

Summary of experimental intensity measurements.

TABLE 7.

1,4-Dioxan Individual Gas Phase Band Intensities.

d_0 Dioxan.

Frequency (cm^{-1})	A_i (km mol^{-1})
2970 au, 2970 bu, 2863 au, 2863 bu	330±3.2
1457 bu, 1449 au	16.19±.35
1378 bu	2.11±.23
1369 au	11.28±.39
1291 bu	12.19±.48
1256 au	33.00±1.3
1136 au	158.1±1.5
1086 au	10.35±.22
1052 bu	8.05±.22
889 bu	17.51±.76
881 au	75.2±3.1
610 bu	14.64±.43
288 au	~0
274 bu	20.22±1.1

TABLE 8.

1,4-Dioxan Individual Gas Phase Band Intensities.

d_8 Dioxan.

Frequency (cm^{-1})	A_i (km mol^{-1})
2235 au, 2232 bu, 2098 bu, 2086 au	188.7±3.1
1191 au	91.5±3.3
1153 bu	29.41±.89
1117 au	97.8±4.4
1087 bu	12.99±.47
1042 bu	28.0±1.2
1030 au	12.99±.70
922 au	~0
896 bu	17.40±.23
809 au	~0
762 au	39.14±2.0
732 bu	5.19±0.10
490 bu	9.56±.17
254 au	~0
238 bu	13.94±.9

Section 2.4 F Sum Rule.

As was indicated in the Introduction, the following expression transforms $d\underline{p}/dQ_i$ to derivatives with respect to the internal coordinates:

$$\frac{d\underline{p}}{dQ_i} = \sum_j L_{ji} \frac{d\underline{p}}{dR_j}$$

This leads to the following expression for the i^{th} band intensity:

$$\Gamma_i = \frac{N\pi}{3c^2} \frac{1}{\omega_i} \sum_{j,k} L_{ji} L_{ki} \frac{d\underline{p}}{dR_j} \frac{d\underline{p}}{dR_k}$$

On dividing this equation by the frequency ω_i and summing over i,

$$\sum_i \frac{\Gamma i}{\omega_i} = \frac{N\pi}{3c^2} \sum_{j,k} \sum_i \frac{L_{ji} L_{ki}}{\omega_i^2} \frac{d\underline{p}}{dR_i} \frac{d\underline{p}}{dR_k}$$

$$= \frac{N\pi}{3c^2} \sum_{j,k} F_{jk}^{-1} \frac{d\underline{p}}{dR_i} \frac{d\underline{p}}{dR_k}$$

Since the right hand side is invariant to isotopic substitution as long as the isotopically related molecules belong to the same molecular point group, then so is $\sum_i \Gamma_i/\omega_i$. As $\Gamma_i \simeq A_i/\nu_i$, then $\sum_i A_i/\nu_i^2$ is an invariant - this is known as the F sum rule, which may be used to check the consistency of the data from undeuterated and completely deuterated compounds.

Tables 9 and 10 show the application of the F sum rule, which should hold for the bands in the au and bu species separately, as well as the total summation of band intensity divided by the square of the frequency.

It is seen that the total sums agree very well, but that comparing the d_o au and d_o bu figures with those for the d_8 compound, the former appear too high and the latter too low. A possible answer for this discrepency could be found in the bandsplitting suggested for the d_o 889 cm^{-1} (bu) and 881 cm^{-1} (au) bands. A comparison of the solution and gas phase spectra show that there appears to be a change in the relative intensities of the bands on the change of phase. In solution, the

au band possesses the greater proportion of intensity (75 as opposed to 17.5 km mol^{-1}), but in the gas phase the intensity seems to be far more equally shared between the two components. It would therefore be reasonable to transfer some of the intensity attributed to the au band to the bu in order to yield better agreement in the sum rule for the individual symmetry species.

Thus, if the two band intensities were actually constrained to be equal, 46.4 km mol^{-1} each,

$$A_{889}/\nu^2 = 5.879 \times 10^{-15} \text{ km}^3 \text{ mol}^{-1}$$

$$A_{881}/\nu^2 = 5.978 \times 10^{-15} \text{ km}^3 \text{ mol}^{-1}$$

and then

$$\text{au sum} = 24.119 \times 10^{-15} \text{ l}$$
$$\text{bu sum} = 40.634 \times 10^{-15} \text{ l}$$

and the agreement with the d_8 figures would then be excellent.

TABLE 9.

d_o Dioxan Intensity Sums.

Frequency(cm^{-1})	A_i(km mol^{-1})	A_i/ν_i^2(km^3 mol^{-1})
2970 au, 2970 bu	176.6	2.00×10^{-15}
2863 au, 2863 bu	153.4	1.87
1457 bu, 1449 au	16.19	.767
1378 bu	2.11	.111
1369 au	11.28	.602
1291 bu	12.19	.731
1256 au	33.00	2.092
1136 au	158.1	12.251
1086 au	10.35	.878
1052 bu	8.05	.727
889 bu	17.51	2.216
881 au	75.2	9.689
610 bu	14.64	3.934
288 au	0	0
274 bu	20.22	26.933

Total (au+bu) = 64.801×10^{-15} km^3 mol^{-1}

au = 27.830×10^{-15}

bu = 36.971×10^{-15}

TABLE 10.

d_8 Dioxan Intensity Sums.

Frequency(cm^{-1})	A_i(km mol^{-1})	A_i/ν_i^2(km^3 mol^{-1})
2235 au 2232 bu 2098 bu 2086 au	188.7	4.0×10^{-15}
1191 au	91.5	6.450
1153 bu	29.41	2.212
1117 au	97.80	7.838
1087 bu	12.99	1.099
1042 bu	28.0	2.579
1030 au	12.99	1.224
922 au	0	0
896 bu	17.40	2.167
809 au	0	0
762 au	39.14	6.740
732 bu	5.186	.968
490 bu	9.56	3.982
254 au	0	0
238 bu	13.94	24.610

Total (au+bu) = 63.869×10^{-15}

au = 24.252×10^{-15}

bu = 39.617×10^{-15}

Section 2.5 Effective atomic charges - 1,4-Dioxan.

The 'effective charge' of an atom is an invariant of its atomic polar tensor - its numerical value does not change upon rotation from one axis system to another.

$$\chi_\alpha^2 = (1/3) \text{ Trace } [P_x^\alpha (P_x^\alpha)^t]$$

In fact, this parameter is related to the sum of infra red band intensities for a molecule[18]

$$K \sum_i A_i + \Omega = \sum_\alpha (1/m_\alpha)\xi_\alpha^2$$

ξ_α is a former definition of effective charge, $\frac{1}{3}\xi_\alpha^2 = \chi_\alpha^2$. Ω is a 'rotational correction' required for polar molecules. $K = 1.0255 \times 10^{-3}$ for A_i in km mol^{-1}, m_α in amu and ξ in e.

Thus, if experimental data is available for say the undeuterated and completely deuterated molecules, the hydrogen effective charges may be computed by simply solving the two resulting simultaneous equations.

From the dioxan measurements,

$$\sum_i A_i(d_o) = 708.8 \text{ km mol}^{-1}$$

$$\sum_i A_i(d_8) = 546.6 \text{ km mol}^{-1}$$

This leads to $\chi_H = 0.118$.

Section 2.6 Experimental Data for Cyclohexane.

The absolute gas phase band intensities have been determined for cyclohexane d_o and d_{12} using the same techniques as described above for 1,4-dioxan. The experimental data is presented in the following set of tables.

Tables 11 and 12 give the d_o and d_{12} gas phase data and Tables 13 and 14 give the corresponding solution phase data. In Tables 15 and 16 the final averages are listed, together with the solution/gas ratios. Tables 17 and 18 show the final derived band intensities for cyclohexane d_o and d_{12}.

TABLE 11.

d_o Cyclohexane - Gas Phase.

Frequency Range(cm^{-1})	Pressure (mm,298°K)	Intensity(km mol^{-1})
3030-2894	.195	385.00
(1.25m path length)	.257	356.4
	.267	375.7
2894-2830	.195	105.9
(1.25m)	.257	102.7
	.267	99.6
1500-1400	.537	24.42
(5m)	.598	25.00
	.763	23.80
	1.009	24.26
	1.220	24.79
	1.52	23.20
	2.08	22.90
	2.49	20.85
1380-1330	7.28	0.25
(5m)	9.30	0.23
	20.11	0.24
	29.85	0.23
1310-1190	3.06	3.06
(5m)	3.56	3.61
	3.82	3.61
	4.21	3.61
1100-970	5.08	2.02
(5m)	6.31	1.87
	6.85	2.02
	7.65	2.04
970-800	2.078	6.56
(5m)	2.585	6.62
	3.140	6.71
	3.530	6.58
560-480	7.17	0.48
(5m)	9.85	0.47
	14.53	0.46
	14.53	0.46
	19.70	0.44

TABLE 12.

d_{12} Cyclohexane - Gas Phase.

Frequency Range (cm^{-1})	Pressure (mm, 298°K)	Intensity(km mol^{-1})
2300-2000	.464	240.3
(1.25m)	.485	250.4
	.497	253.6
	.580	250.9
1240-1130	1.269	6.46
(5m)	1.578	6.24
	1.845	6.44
	2.083	6.36
1130-1045	1.269	6.63
(5m)	1.578	6.34
	1.845	6.48
	2.083	6.40
1045-950	1.269	5.84
(5m)	1.578	6.36
	1.845	6.04
	2.083	5.53
950-880	.699	3.64
(5m)	1.035	3.43
	1.276	3.57
	1.515	3.42
770-600	2.976	3.35
(5m)	4.047	3.44
	4.36	3.61
	4.710	3.55
450-350	13.92	0.43
(5m)		

TABLE 13.

d_o Cyclohexane - Solution Data.

Frequency (cm^{-1})	Concentration (molar) [ℓ=.0224cm]	$I_{max}^{(\log_e)}$	$\Delta\nu_{\frac{1}{2}}^{(cm^{-1})}$	A_i (km mol^{-1})
2928	.1882	4.543	30.58	386.0
	.1513	4.108	27.68	402.5
	.1263[1]	4.085	30.40	372.0
	.1263[2]	3.020	27.40	374.8
	.1263[3]	1.600	26.06	364.9
2854	.1882	2.628	12.82	109.4
	.1513	2.248	12.62	114.8
	.1263[1]	2.334	12.78	104.3
	.1263[2]	1.591	13.10	107.3
	.1263[3]	.821	13.14	106.0
1449	.1513	1.066	6.94	31.69
	.1882	1.270	6.94	30.35
	.3481	2.227	7.08	29.31
	.5961	3.808	7.04	29.11
	.6709	4.124	7.22	28.68
1257	.1882	.0936	10.86	3.37
	.4735	.2428	8.62	2.815
	.4846	.2507	8.58	2.83
	.5961	.2884	10.26	3.11
	.6709	.3290	8.66	2.99
	.9607	.4849	8.56	2.76
	1.0829	.5193	9.30	2.82
1038	1.4098*	.411	12.62	2.25
1015	1.4098	.280	18.04	2.08
904	.4735	.512	5.32	3.11
	.4846	.524	4.42	3.18
	.9607	1.044	4.30	3.11
862	.4735	.402	7.64	4.17
	.4846	.412	7.72	4.24
	.9607	.825	7.60	4.20

continued...

TABLE 13 - continued...

524	.4735	.104	7.60	1.05
	.4846	.109	7.54	1.09
	.9607	.209	7.52	1.05

[1] = 0.31cm
[2] = .020cm
[3] = .011cm

} Variable path length cell employed.

* CS_2 solvent

TABLE 14.

d_{12} Cyclohexane - Solution Data.

Frequency (cm^{-1})	Concentration [ℓ=.0224cm]	$I_{max}^{(\log_e)}$	$\Delta\nu_{\frac{1}{2}}^{(cm^{-1})}$	A_i (km mol^{-1})
2300-2000	.3367			262.7
1160	.3367	.282	8.66	4.61
	.3757	.321	8.36	4.56
	.7260	.613	8.58	4.61
1085	.3367	.625	5.84	7.11
	.3757	.713	5.90	7.09
	.7260	1.352	5.92	7.20
1068	.3367	.118	6.88	1.57
	.3757	.133	6.78	1.60
	.7260	.260	6.81	1.58
988	.3367	.298	9.66	5.38
	.3757	.338	9.59	5.39
	.7260	.651	9.58	5.39
915	.3367	.500	4.54	4.66
	.3757	.563	4.68	4.71
	.7260	1.088	4.62	4.59
719	.4895*			2.24
685	.4895*			3.34

* CS_2 is solvent

TABLE 15.

d_0-Cyclohexane - Summary of Experimental Intensity Measurements.

Solution		Gas		Solution/gas ratio
Frequency	A_i (km mol^{-1})	Region	A_i (km mol^{-1})	for region
2829	380.1±7.6	3030-2894	370±15	1.027±.031
2854	108.4±2.1	2894-2830	103±3	1.052±.028
1449	28.72±.81	1500-1400 1380-1330	23.65±.51 .238±.010	1.214±.043
1257	2.956±.093	1310-1190	3.60±.003	0.820±.026
1038	2.25	1100-970	1.99±.11	2.18
1015	2.08			
904	3.135±.035	970-800	6.611±.040	1.110±.009
862	4.204±.035			
524	1.074±.014	560-480	.463±.006	2.320±.043

TABLE 16.

d_{12}-Cyclohexane - Summary of Experimental Intensity Measurements.

2300-2000	262.7	2300-2000	248.8±.3	1.06
1160	4.59±.03	1240-1130	6.375±.057	.720±.007
1085	7.135±.045	1130-1045	6.460±.072	1.349±.017
1068	1.580±.040	1045-950	5.940±.020	.906±.030
988	5.387±.001			
915	4.65±.05	950-880	3.517±.062	1.323±.026
719	2.24	770-600	3.49±.10	1.60
685	3.34			
394	0.84	450-350	.426	1.979

TABLE 17.

d_o-Cyclohexane Individual Gas Phase Band Intensities.

Frequency (cm^{-1})	A_i ($km\ mol^{-1}$)
2933 eu 2914 a_{2u}	370±15
2863 eu 2863 a_{2u}	103±3
1449 eu 1449 a_{2u}	23.65±.51
1346 eu	0.24±.01
1257 eu	3.6±.003
1033 a_{2u} 1015 *	2.0
904 eu	2.824±.035
862 eu	3.787±.039
524 a_{2u}	.463±.006
241 eu	~0

* Combination band

TABLE 18.

d_{12}-Cyclohexane Individual Gas Phase Band Intensities.

Frequency (cm^{-1})	A_i(km mol^{-1})
2221 eu	
2206 a_{2u}	248.8±5.0
2111 eu	
2104 a_{2u}	
1160 eu	6.375±.057
1085 a_{2u}	5.288±.073
1068 eu	1.171±.016
988 eu	5.940±.20
915 a_{2u}	3.517±.062
719 eu	1.397±.05
685 eu	2.089±.07
394 a_{2u}	0.43
190 eu	~0

Section 2.7 F Sum Rule - Cyclohexane.

As for 1,4-dioxan, the consistency of the d_0 and d_{12} cyclohexane experimental band intensities is checked using the F sum rule - i.e. by comparing the values obtained for $\sum_i A_i/\nu_i^2$. The results are shown in tables 19 and 20.

It is seen that there is very good agreement not only for the total sums, but also for the separate sums for the a_{2u} and e_u symmetry species.

TABLE 19.

d_0 Cyclohexane - Intensity Sums.

$\nu/km^{-1}\times10^{-15}$	$A_i/km\ mol^{-1}$	A_i/ν_i^2, $km^3\ mol^{-1}$
2933 eu	79	0.9183×10^{-15}
2933	79	0.9183
2914 a_{2u}	212	2.4966
2863 eu	26	0.3172
2863	26	0.3172
2863 a_{2u}	51	0.6222
1449 eu	4.9	0.2334
1449	4.9	0.2334
1449 a_{2u}	13.9	0.6620
1346 eu	0.12	0.0066
1346	0.12	0.0066
1257 eu	1.8	0.1139
1257	1.8	0.1139
1038 a_{2u}	1.99	0.1847
904 eu	1.41	0.1725
904	1.41	0.1725
862 eu	1.9	0.2557
862	1.9	0.2557
524 a_{2u}	0.46	0.1675
241 eu	0	0

a_{2u} total = 4.133×10^{-15} $km^3\ mol^{-1}$

eu total = 4.035×10^{-15} $km^3\ mol^{-1}$

a_{2u} + eu = 8.168×10^{-15} $km^3\ mol^{-1}$

TABLE 20.

d_{12} - Cyclohexane - Intensity Sums.

$\nu/km^{-1} \times 10^{-15}$	A_i/km mol^{-1}	A_i/ν_i^2, $km^3\ mol^{-1} \times 10^{15}$
2221 eu	38.3	0.7764
2221	38.3	0.7764
2206 a_{2u}	108.3	2.2254
2111 eu	14.9	0.3344
2111	14.9	0.3344
2104 a_{2u}	35.2	0.7952
1160 eu	3.2	0.2378
1160	3.2	0.2378
1085 a_{2u}	5.3	0.4502
1068 eu	0.6	0.0526
1068	0.6	0.0526
988 eu	2.97	0.3042
988	2.97	0.3042
915 a_{2u}	3.52	0.4204
719 eu	0.7	0.1354
719	0.7	0.1354
685 eu	1.04	0.2216
685	1.04	0.2216
394 a_{2u}	0.43	0.2770
190 eu	0	0

a_{2u} total = 4.168×10^{-15} $km^3\ mol^{-1}$

eu total = 4.1248×10^{-15} $km^3\ mol^{-1}$

a_{2u} + eu = 8.293×10^{-15} $km^3\ mol^{-1}$

Section 2.8 Cyclohexane - Effective Atomic Charges.

$$\sum A_i(d_0) = 509.6 \text{ km mol}^{-1}$$

$$\sum A_i(d_{12}) = 276.1 \text{ km mol}^{-1}$$

This pair of results yields the following value for the hydrogen atomic charge:

$$\chi_H = 0.115$$

This represents quite a high value if it is considered that χ_H for most hydrocarbons has a value of ~.100. The figure presented, however, should be considered accurate since there is excellent adherence to the F sum rule by the d_0 and d_{12} intensities.

The effective atomic charge for the carbon atoms may be obtained by substituting the value for hydrogen back into the intensity sum equation. This yields:

$$\chi_C = 0.175$$

Section 2.9.

TETRAHYDROPYRAN - EXPERIMENTAL RESULTS.

Gas and solution phase intensity measurements were made for tetrahydropyran, following the same procedure employed for 1,4-dioxan and cyclohexane. In this study, the resulting derived band intensities are not used to generate a set of atomic polar tensors, but are used to investigate the applicability of tensors calculated using quantum mechanical methods, and also the transferability of tensors acquired for dioxan and cyclohexane.

The experimental data is presented below.

TETRAHYDROPYRAN-GAS PHASE DATA. - TABLE 21.

Freq. Range	Pressure(mm)	A_i(km mol^{-1})
3100 - 2780	.258	319.3
	.268	302.1
	.291	336.2
	.345	336.9
	.383	355.0
	.420	346.8
	.495	331.2
1550 - 1415	1.952	19.3
	2.495	20.2
	2.590	19.8
	3.073	20.1
	3.575	20.1
1415 - 1325	1.952	10.95
	2.495	11.9
	2.590	11.7
	3.073	11.8
	3.575	12.2
1325 - 1235	2.815	14.8
	4.050	14.5
	4.250	15.0
	5.050	15.3
1235 - 1165	.591	38.9
	.845	41.1
	1.005	43.3
	1.218	45.3
	1.520	37.4
1165 - 1140	.591	2.65
	.845	2.31
	1.005	2.19
	1.218	2.23
	1.520	2.10

continued...

1140 - 977	.591	103.9
	.845	105.8
	1.005	102.3
	1.218	103.6
	1.520	103.7
977 - 930	2.540	2.38
	3.025	2.42
	3.48	2.44
925 - 832	1.495	26.6
	2.007	28.4
	2.195	28.4
	2.510	28.1
832 - 780	1.495	3.69
	2.007	3.97
	2.195	4.24
	2.510	4.27
620 - 520	1.435	3.65
	2.45	3.85
	3.025	3.55
	3.48	3.84
450 - 340	2.065	7.29
	2.735	6.95
	2.370	7.28
290 - 200	1.856	4.23
	1.910	4.30
	2.234	4.39
	2.535	4.295

TABLE 22.

TETRAHYDROPYRAN - SOLUTION DATA.

Frequency	Mol. Conc.	I_{max}	$\Delta\nu_{\frac{1}{2}}$	A_i
3100-2780	0.1107			402.0
	0.2083			384.8
	(0.5742)			(344.7)
1440	.1107	.193	15.80	16.23
	.1628	.275	16.06	15.95
	.2083	.350	16.52	16.27
	.5742	.965	15.65	15.53
1454	.1107	.209	4.88	6.05
	.1628	.299	4.88	5.89
	.2083	.387	4.86	5.95
	.5742	1.028	4.92	5.80
1468	.1107	.198	4.84	5.69
	.1628	.281	4.88	5.56
	.2083	.365	4.96	5.72
	.5742	.9785	4.85	5.44
1384	.1107	.187	5.62	6.18
	.1628	.265	5.70	6.04
	.2083	.341	5.82	6.20
	.5742	.920	5.72	5.97
1362	.1107	.041	4.78	1.17
	.1628	.060	4.50	1.10
	.2083	.077	5.12	1.25
	.5742	.219	4.52	1.14
1349	.1107	.064	14.60	5.03
	.1628	.092	15.36	5.14
	.2083	.123	14.68	5.15
	.5742	.319	13.36	4.48
1300	.1107	.194	6.22	7.08
	.1628	.276	6.30	6.92
	.2083	.355	6.46	7.12
	.5742	.981	6.11	6.78
1273	.1107	.164	7.81	7.37
	.1628	.234	7.92	7.20
	.2083	.298	8.17	7.43
	.5742	.827	7.64	7.04
1257	.1107	.135	5.44	4.33
	.1628	.198	5.34	4.25
	.2083	.257	5.50	4.44
	.5742	.679	5.34	4.14
1197	.1107	.852	6.88	34.13
	.1628	1.214	6.90	33.10
	.2083	1.510	7.16	33.34
	.5742	3.710	7.80	32.09

continued...

1157	.1107	.099	6.62	3.81
	.1628	.137	7.92	3.76
	.2083	.181	7.26	4.06
	.5742	.503	5.90	3.36
1092	.1107	1.293	9.96	72.62
	.1628	1.828	10.02	70.23
	.2083	2.317	10.22	70.79
	.5742	5.071	12.48	67.13
1048	.1107	.896	5.04	26.82
	.1628	1.258	5.08	25.74
	.2083	1.588	5.14	25.74
	.5742	3.735	5.74	24.33
1032	.1107	.310	6.54	11.86
	.1628	.442	6.52	11.46
	.2083	.566	6.80	11.89
	.5742	1.526	6.58	11.28
1011	.1107	.297	5.68	9.94
	.1628	.422	5.58	9.45
	.2083	.542	5.64	9.94
	.5742	1.437	5.50	8.98
969	.1107	.171	4.56	4.65
	.1628	.244	4.66	4.59
	.2083	.304	4.48	4.32
	.5742	.816	4.16	3.92
872	.3188	2.284	6.76	31.21
	.5108	3.388	7.22	30.69
854	.3188	.385	7.28	5.62
	.5108	.611	7.42	5.67
816	.3188	.432	6.40	5.61
	.5108	.712	7.36	6.56
565	.1107	.161	6.70	6.29
	.2083	.285	6.66	5.87
	.5742	.761	6.46	5.55
520-350	.3187			11.02
	.5106			11.42
290-200	.3187			4.79
	.5106			4.96

TABLE 23.

TETRAHYDROPYRAN - SUMMARY OF SOLUTION AND GAS PHASE RESULTS.

Solution Phase		Gas Phase		Sol/Gas
Band(cm^{-1})	A_i ($km\ mol^{-1}$)	Region (cm^{-1})	A_i ($km\ mol^{-1}$)	Ratio
3100-2780	393.0(10)	3100-2780	332.5(7.1)	1.18(.07)
1468	5.60(.08)	1550-1415	19.89(1.90)	1.38(.02)
1454	5.92(.06)			
1440	16.0(.2)			
1384	6.10(.07)	1415-1325	11.72(.24)	1.04(.03)
1362	15.64(.04)			
1349	4.95(.02)			
1300	6.97(.09)	1325-1235	14.90(.19)	1.24(.02)
1273	7.26(.11)			
1257	4.29(.08)			
1197	33.16(.51)	1235-1165	41.2(1.6)	.80(.03)
1157	3.75(.17)	1165-1140	2.30(.11)	1.63(.11)
1092	70.2(1.4)	1140-977	103.84(.62)	1.13(.02)
1048	25.66(.62)			
1032	11.62(.18)			
1011	9.48(.24)			
969	4.37(.20)	977-930	2.41(.02)	1.81(0.8)
872	30.95(.39)	925-832	27.9(.50)	1.31(.03)
854	5.65(.04)			
816	6.08(.71)	832-780	4.04(.56)	1.51(.18)
565	5.90(.28)	620-520	3.72(.08)	1.59(.08)
520-350	11.2(.2)	450-340	7.2(.1)	1.56
290-200	4.87	290-200	4.30	1.13

TABLE 24.

TETRAHYDROPYRAN - FINAL DERIVED BAND INTENSITIES.

ν_i cm^{-1}	A_i (km mol^{-1})
2958a`	
2958a``	
2942a`	114.4 ± 2.4
2933a`	
2924a``	
2860a`	
2860a``	
2849a`	218.1 ± 4.7
2849a``	
2842a`	
1468a`	4.05 ± .08
1454a`	4.28 ± .07
1441a``	11.56 ± .21
1434a`	~0
1420a``	~0
1384a`	5.85 ± .17
1360a``	1.12 ± .05
1347a``	4.75 ± .08
1338a``	~0
1297a`	5.61 ± .12
1271a`	5.84 ± .12
1254a`	3.45 ± .08
1242a``	~0
1195a``	41.2 ± 1.6
1170a`	~0
1155a`	2.30 ± .11
1090a``	70.2 ± 1.4
1046a``	25.7 ± .6
1030a`	11.62 ± .18
1009a`	9.48 ± .24

continued...

969a``	2.41 ± .16
880a``	~0
875a`	23.6 ± .6
856a`	4.30 ± .09
818a`	4.04 ± .56
811a``	~0
565a`	3.72 ± .08
458a``	
432a`	7.2
400a`	
252a`	4.3
252a``	

Chapter 3.

Section 3.1 The Role of Quantum Mechanics in IR Spectroscopy.

All theoretical treatments in which it is desired to calculate the physical characteristics of a molecular system from simply a knowledge of its atomic constituents rely on the derivation of the molecular wave function. This is the function that satisfies the Schrödinger equation for the system and contains all information regarding its dynamical properties.

Exact solution of the Schrödinger equation is not feasible except in the simplest of cases such as the hydrogen atom, and hence results will in general only represent an approximation. An important simplifying assumption is to constrain the nuclei to remain fixed during electronic motion, due to the vast differences in their masses (Born Oppenheimer approximation).

The formation of a molecule may be visualised as a transfer of charge between its constituent atoms, or a pairing of their electrons. The latter now 'inhabit' 'molecular' rather than atomic orbitals. In the LCAO method (Linear Combination of Atomic Orbitals) each molecular orbital is assumed to appear from a 'mixing' of the original atomic orbitals.

$$\psi_i = \sum_r c_{ir} \eta_r$$

ψ_i = wavefunction describing the i^{th} electronic state.
η_r = the r^{th} atomic orbital.
c_{ir} = coefficient of the r^{th} AO in the i^{th} MO.

The Variational Principle dictates that as the ψ_i become more accurately defined by such an expansion, the corresponding orbital energy reaches a minimum. Thus the coefficients c_{ir} must be chosen so as to minimize the energy of the system. The level of approximation that can be achieved is raised on increasing the number of η_r employed - as this number reaches infinity, the 'Hartree-Fock' Limit is said to be approached. The actual number and type of such functions defines the 'basis set' for the calculation.

The coefficients c_{ir}, and hence the molecular wavefunctions, are determined through the self-consistent field method (SCF)[19]. The equation that is to be solved takes the following form:

$$FC = SCE$$

F is the 'Fock' matrix.
C is the matrix of LCAO coefficients.
S is the overlap matrix
E is the diagonal matrix of MO eigenvalues.

To describe how the elements of these matrices are obtained, it is instructive to briefly examine the origin of the equation. Consider the form of the electronic Hamiltonian for the hydrogen molecule:

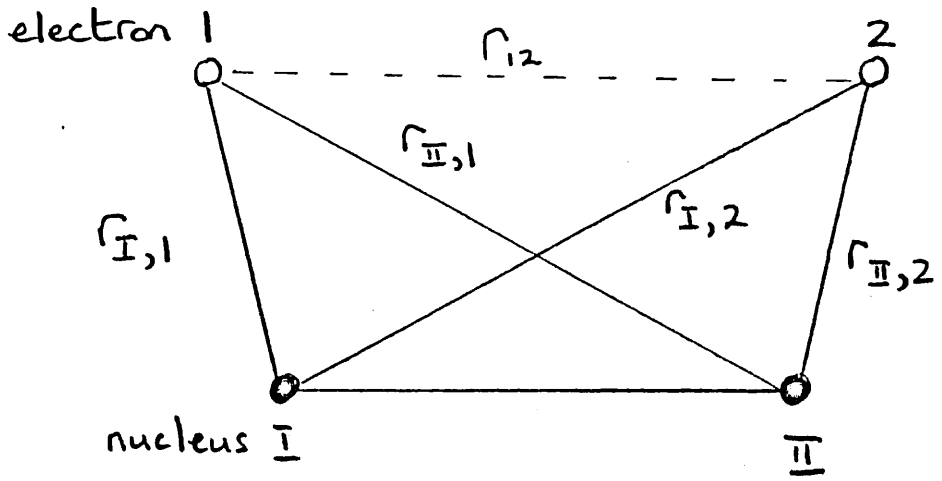

$$H^e_{1,2} = -\tfrac{1}{2}\nabla_1^2 - \frac{1}{r_{I,1}} - \frac{1}{r_{II,1}} \qquad [\equiv \hat{h}_1]$$

$$-\tfrac{1}{2}\nabla_2^2 - \frac{1}{r_{I,2}} - \frac{1}{r_{II,2}} \qquad [\equiv \hat{h}_2]$$

$$+ \frac{1}{r_{12}} \qquad [\equiv \hat{g}_{12}]$$

i.e. $H^e_{1,2} = \hat{h}_1 + \hat{h}_2 + \hat{g}_{12}$

The terms that contribute to the Hamiltonian are thus separated into the 1-electron operators '$\hat{h}$' and the 2-electron electron-electron interaction '$\hat{g}$'. Similarly for a 2M electron system,

$$H(1,2,\ldots) = \sum_{\mu=1}^{2M} \hat{h}_\mu + \sum_{\mu<\nu}^{M(2M-1)} g_{\mu\nu}$$

The expectation value of the energy is $\langle\psi|\hat{H}|\psi\rangle$. Thus:

$$E = 2\sum_{p}^{M} \langle\phi p(1)|\hat{h}_1|\phi p(1)\rangle + \sum_{p}^{M}\sum_{q}^{M} [2\langle\phi p(1)\phi q(2)|\hat{g}_{12}|\phi p(1)\phi q(2)\rangle - \langle\phi p(1)\phi p(2)|\hat{g}_{12}|\phi q(1)\phi q(2)\rangle]$$

$$\text{or} \quad E = 2\sum_{p}^{M} h^{\phi}_{pp} + \sum_{p}^{M}\sum_{q}^{M} (2J^{\phi}_{pq} - K^{\phi}_{pq})$$

J_{pq} and K_{pq} symbolize the Coulomb and Exchange integrals respectively.

In this way it is seen that the energy is the sum of the one-electron energies (kinetic energy and electron nuclear attractions) and interactions between the charge clouds of all pairs of electrons.

J_{pq} and K_{pq} may be related to pseudo-one-electron operators:

$$J_{pq} = \langle\phi p|\hat{J}_q|\phi p\rangle, \quad K_{pq} = \langle\phi p|\hat{K}_q|\phi_p\rangle$$

and the Schrödinger equation, $H\psi=E\psi$, may be written in the form:

$$[\hat{h} + \sum_{q}^{M} (2\hat{J}_q - \hat{K}_q)]\ \phi_p = \phi_p \varepsilon_{pp}$$

$$\text{or} \quad \hat{F}\phi p = \phi p\ \varepsilon pp$$

where $\hat{F}$ is the Fock operator. The elements of the diagonal matrix ε are the molecular orbital energies. For the computation the matrix representative of the Fock operator must be generated over the MO basis:

$$F^{\phi}_{st} \equiv \langle \phi_s | F | \phi_t \rangle$$

and then, $\underline{\underline{F}}^{\phi} = \underline{\underline{\varepsilon}}$, since $S^{\phi}_{st} = \delta_{st}$

The unknown ϕ are expressed in terms of the atomic orbitals, η

$$\phi = \eta \underline{\underline{c}} \; ; \; \phi^{+} = \underline{\underline{c}}^{+} \eta^{+}$$

It is required to transform the Fock matrix from the AO to the MO basis by an orthogonal transformation, which is equivalent to a rotation of the AO vector space via the appropriate similarity transformation:

$$\underline{\underline{c}} \; \underline{\underline{F}}^{\eta} \; \underline{\underline{c}} = \underline{\underline{c}} \; \underline{\underline{S}}^{\eta} \; \underline{\underline{c}} \; \underline{\underline{\varepsilon}}$$

where $\underline{\underline{F}}^{\eta} = \underline{\underline{h}}^{\eta} + 2\underline{\underline{J}}^{\eta} - \underline{\underline{k}}^{\eta}$

and $S^{\eta}_{ij} = \langle \eta_i | \eta_j \rangle$

And thus the equation on which the SCF method is based has been reached. An initial guess is used to compute the Fock matrix, and the equation solved for $\underline{\underline{c}}$ and $\underline{\underline{E}}$. This $\underline{\underline{c}}$ is then used to calculate the Fock matrix for the next cycle of iteration which should result in a lower molecular energy. The procedure is repeated until convergence is achieved.

The quality and character of such a MO calculation is determined by the number and nature of the basis functions employed in constructing the molecular orbitals. Historically, these functions were chosen to bear a close resemblance to atomic orbitals. Prior to the 1960's most calculations were carried out using Slater Type Orbitals (STO), which are analogous to the actual solution of the Schrödinger equation for the hydrogen atom, but possess different nodal properties:

$$n_{n\ell m}(r,\Theta,\phi) = A_n \; r^{n-1} \; e^{-\xi r} \; Y_{\ell,m}(\Theta,\phi)$$

Recently, Gaussian type functions(GTF) have been used. The difference lies in their radial dependence:

$$\eta = r^{\eta_e} - \alpha r^2$$

The advantage of these is that they facilitate the rapid computation of the molecular integrals, and thus render practicable the extension of the method to large polyatomic molecules - the importance of this point is seen on noting that as the number of basis functions (N) increases, the number of two-electron integrals increases as N^4 e.g. if 50 basis functions are required for a NH_4 MO calculation, there are $\sim 10^6$ such integrals.

A 'minimal' basis set corresponds to one which provides one function for every atomic orbital occupied in the isolated atom. The orbital exponents ($\xi \equiv$ zeta) which are usually chosen are those variationally optimized for the free atoms.

As already stated, the basis set fundamentally determines the reliability of a calculation, though it is often difficult to fully estimate the value of the resulting quantum mechanical interpretation that can be given to an experimentally determined physical property. It should be expected that the larger the number of functions included, the better will the outcome of a computation correspond to experiment. Some conclusions may be drawn from trends observed from calculations using different basis sets.

It was not until the early 1970's that such MO calculations made an impact on infra-red spectroscopic studies[20]. Before then, the wavefunctions obtained were not generally of sufficient quality to yield satisfactory force constants and dipole derivatives that could aid significantly the interpretation of experimental data. The expense of computations was often prohibitive, but the simplifications provided by semi-empirical methods made it possible for a larger number of investigators to pursue such studies.

In the CNDO method (Complete neglect of differential overlap), $S_{ij} \equiv \langle \eta_i | \eta_j \rangle = \delta_{ij}$ resulting in a massive reduction in the number of integrations to be performed. Calculations

using this method showed an encouraging degree of success in predicting equilibrium dipole moments[21] that lead to their application to the calculation of dipole moment derivatives.[22]

More recently, much effort has been expended in calculating spectroscopic data using the Gaussian packages developed by Pople and co-workers.[23] Structural parameters obtained have been found to mirror accurately those determined by experiment (e.g. by electron diffraction). Blom et al.[24] examined the usefulness of the 4-31G basis set (for definition, see ab initio section) using Gaussian 70 - for unstrained saturated hydrocarbons they could reproduce bond distances to within .003Å, and 0.4° for bond angles.

Such calculations have been employed in attempting to predict force constants, using a number of possible different approaches. Garrett and Mills[25] derived expressions for force constants and dipole derivatives in terms of Hartree Fock wavefunctions. In the Pulay method,[26] the nuclear geometry is determined by relaxing the nuclear coordinates until the forces acting on the atoms vanish. The force constants are then calculated by differentiating the forces numerically.

Alternatively, having assumed a given functional dependence of the potential energy on the internal displacement coordinates, the parameters that define the potential surface may be determined by their least-squares fit to the series of energies corresponding to a number of different molecular configurations. Such a method can provide a pathway to the prediction of anharmonic force constants,[27] since it appears surprisingly that these may be predicted more reliably than quadratic constants when using simple basis sets.

Dipole derivatives/atomic polar tensor elements can be deduced from the dipole moment calculated at different molecular configurations. One of the principal applications of the parameters thus obtained is to help resolve the sign ambiguity of the dp/dQ obtained by experiment. As mentioned previously, comparison of results from isotopically substituted molecules may limit the number of possible sign choices. The one which then corresponds best to that derived from the quantum-mechanically calculated parameters may be reasonably designated as the 'correct' choice.

Section 3.2 Gaussian 76.

As has been mentioned above, there has been recent success in applying the results derived from quantum mechanical calculations to the interpretation of spectroscopic data. In this section it will be shown how a readily available quantum mechanical package, Gaussian 76, has been employed to obtain parameters that will hopefully provide both a meaningful set of constraints for the perturbation treatment used to derive the force constants of 1,4-dioxan, and a guide to the correct sign choice for the experimental dipole derivatives.

Gaussian 76 is a computer program that performs ab initio Hartree-Fock molecular orbital calculations.[28] The one- and two-electron integrals are calculated using basis sets of s,p or d cartesian gaussian functions, and the wavefunctions and energies are determined through the Self Consistent Field method. The following input data is required for the execution of the program:

(1) System control card. This determines the route for the calculation (i.e. which of the various options are desired) and the type of basis set. The size of this basis is limited by the maximum permissable number of basis functions (90), number of shells (80), and degree of contraction (i.e. the number of terms in the linear combination of primitive gaussians that defines the atomic orbital, =6). This means that for 1,4-dioxan the largest allowable basis set is 4-31G, corresponding to 70 basis functions.

(2) The title for the run.

(3) The net charge and spin multiplicity - the latter specifying the number of electrons of either α or β spin.

(4) The nuclear geometry. This may be defined in one of two ways.

a) In terms of internuclear bond lengths and angles.
b) From the Cartesian coordinates of the atoms.

The former method is the approach relevant to obtaining force constants, which are functions of the internal coordinates, whilst the latter is appropriate to the derivation of the ab initio atomic polar tensors.

Section 3.3 Force Constant Determination.

The potential energy may be calculated for a series of configurations that correspond to different values of the molecular symmetry coordinates. The zero point energy, equilibrium geometry and symmetrized force constants are then obtained by the least squares fitting of these parameters to the resulting potential surface.

The required specification of geometry is in many cases a non-trivial matter, since as will become apparent below, care must be exercised to maintain the correct conditions for ring closure. Examine the input for a typical fully symmetric (Ag) configuration.

The position of a nucleus is given by a bond length, bond angle and dihedral angle. Alternatively, the dihedral angle may be replaced by a second angle and a ±1 which indicates the direction in which the bond points. For instance, atom 4- a carbon atom, so the first entry in '6' the atomic number. Atom 4 is joined to atom 3 (the mid-point of the C-C band), by a line of length $R_{cc}/2 = .75814\text{Å}$. The subsequent entry of '1' and '90°' indicates that the angle $\hat{431}$ is 90°. Then '2' and '90' indicates that the magnitude of the internuclear dihedral angle 4,3,1,2 to 90°.

Now examine card 7 for atom 7. This is similar to the above until the third atom is specified. The '1' after the second angle shows that rather than being a dihedral angle, 109.421° refers to the value of the angle $\hat{846}$.

It is seen that the atoms 1,2,3,5,9 and 14 have the 'atomic number' of -1. This shows that they are 'dummy' atoms. These are strategically placed at convenient reference points in the molecular skeleton, and facilitate the definition of the other atomic positions.

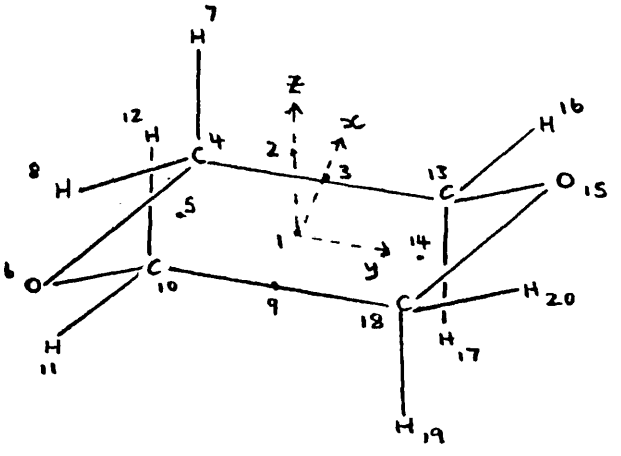


```
NETWORK(UHCA104,RUN=ULCC)
JOB(UHCA104,J12,T500,M7600)
ATTACH(OVG,GAUSSIAN76,ID=PUBLIC)
OVG.
**EOR**
$  1 1    1 4
 OLD EQN
 0 1
 -1
 -1     1 1.0
 -1     11.1994      2   90.0
  6     3.75814      1   90.0000       2    90.0
 -1     1.75814      3   90.0          4    0.0
  8     50.7864      1   126.841       2   180.0
  1     41.08418     3  109.736        6  109.421        1
  1     41.07769     3  111.2697       6  106.63        -1
 -1     11.1994      2   90.0          3   180.0         1
  6     9 .75814     1   90.0000       2   270.0
  1   101.07769      9  111.2697       6  106.63         1
  1   101.08418      9  109.736        6  109.421       -1
  6     3 .75814     1   90.0000       2   270.0
 -1     1.75814      3   90.0          4   180.0
  8   14.7864        1  126.841        2     0.0
  1   131.07769     15  106.63         3   111.2697      1
  1   131.08418     15  109.421        3   109.736      -1
  6     9 .75814     1    90.0        10    180.0
  1   181.08418     15   109.421       9    109.736       1
  1   181.07769     15   106.63        9    111.2697     -1

 -1
**EOF**
```

FULLY SYMMETRIC MOLECULAR DISTORTIONS.

At equilibrium, and in distortions that preserve the full symmetry of the molecule (Ag), the CO, COC and OCC internal coordinates are defined by:

$$r_{45} = CO \sin(\frac{\hat{COC}}{2}) \qquad (3\text{-}1)$$

$$r_{65} = CO \cos(\frac{\hat{COC}}{2}) \qquad (3\text{-}2)$$

and by the angles $6,\hat{5},14$ and $15,\hat{14},5$ that introduce $\hat{OCC}$, as indicated by the following algebra:

$$\vec{R}_{6,4} = a\,\vec{e}_x + b\,\vec{e}_y + c\,\vec{e}_z$$

$$(\vec{R}_{6,10} = -a\,\vec{e}_x + b\,\vec{e}_y + c\,\vec{e}_z)$$

Since $\vec{R}_{4,13} = \vec{e}_y$, then $\cos \hat{OCC} = b$.
Now, $y_6 - y_4 = y_6 - y_5 = br_{64}$ and $\cos(6,\hat{5},14) = \vec{R}_{6,5} \cdot \vec{R}_{14,5}$

$$\therefore \quad \cos(6,\hat{5},14) = (y_6 - y_5)/r_{65}$$

$$= \frac{br_{64}}{r_{64} \cos(\frac{\hat{COC}}{2})}$$

$$\therefore \quad \cos(6,\hat{5},14) = \frac{\cos \hat{OCC}}{\cos(\frac{\hat{COC}}{2})} \qquad (3\text{-}3)$$

The CH bond distances and angles are inputted directly, and their distortion conforming to any of the symmetry species may be performed without disturbing the other ring angles and bonds.

Bu SYMMETRY COORDINATES.

Consider the distortions required to construct the CO symmetry coordinate:

$$S_{CO}(bu) = \tfrac{1}{2}(\Delta r_{46} + \Delta r_{10,6} - \Delta r_{13,15} - \Delta r_{18,15})$$

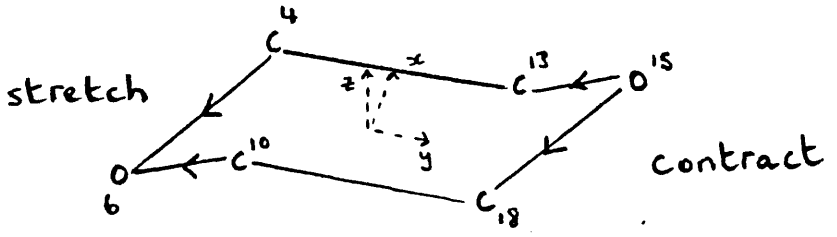

As one section of the ring expands and the other contracts, the two CC bonds move in the xy plane so that they are no longer parallel:

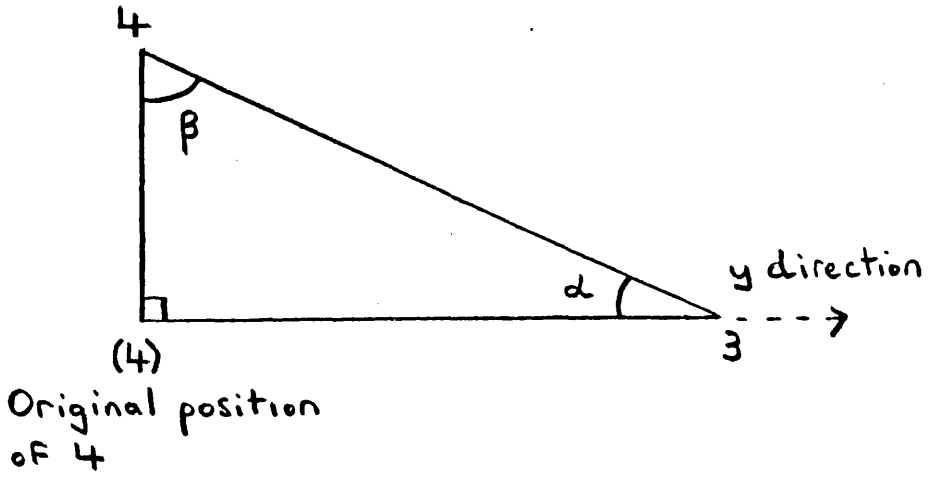

Thus, instead of being parallel with the y axis, this CC bond points in the negative x direction, and is described by:

$$\vec{R}_{4,13} = -\cos\beta.\vec{e}_x + \sin\beta.\vec{e}_y.$$

If the CO bonds are defined by the following expressions:

$$\vec{R}_{4,6} = a\,\vec{e}_x + b\,\vec{e}_y + c\,\vec{e}_z$$

$$\vec{R}_{10,6} = -a\,\vec{e}_x + b\,\vec{e}_y + c\,\vec{e}_z$$

the magnitude of the $\hat{COC}$ angle is determined by taking the dot product.

$$\cos(4,\hat{6},10) = \cos\hat{COC} = \vec{R}_{4,6}.\vec{R}_{10,6}$$

$$= -a^2 + b^2 + c^2.$$

Normalisation gives: $a^2 + b^2 + c^2 = 1$

$$\therefore \quad a = [\tfrac{1}{2}(1-\cos\hat{COC})]^{\frac{1}{2}} \qquad (3\text{-}4)$$

(a is negative).

Again taking dot products:

$$\cos(6,\hat{4},13) = \cos\hat{OCC} = \vec{R}_{6,4}.\vec{R}_{13,4}$$

$$= -a.\cos\beta + b\sin\beta$$

$$\therefore \quad b = (\cos\hat{OCC} + a.\cos\beta)/\sin\beta \qquad (3\text{-}5)$$

The expression for $6,\hat{5},14$ derived in the Ag section is still applicable:

$$\cos(6,5,14) = \frac{b}{\cos(\frac{\hat{COC}}{2})} \qquad (3\text{-}6)$$

except that b no longer corresponds to $\cos\hat{OCC}$ alone.

A similar analysis can be made for the other half of the ring, where:

$$\vec{R}_{18,10} = -\vec{e}_x.\cos\beta - \vec{e}_y.\sin\beta$$

$$\vec{R}_{13,15} = f\,\vec{e}_x + g\,e_y + h\,e_z$$

$$\vec{R}_{18,15} = -f\,\vec{e}_x + g\,\vec{e}_y + h\,\vec{e}_z$$

This provides the expressions:

$$f = [\tfrac{1}{2}(1-\cos\hat{COC})]^{\frac{1}{2}} \qquad (3\text{-}7)$$

(f is positive)
and,

$$g = (\cos\hat{OCC} + f\cos\beta)/\sin\beta \qquad (3\text{-}8)$$

$$\cos(15,\hat{14},5) = \frac{g}{\cos(\frac{\hat{COC}}{2})} \qquad (3\text{-}9)$$

Note that as ΔCO becomes smaller in magnitude, $\beta \to 90^\circ$, and the expressions given for 'b' and 'g' approach those appropriate to the equilibrium structure.

It is now possible to construct the molecular geometry input required for Gaussian 76. The distances 1-3 and 1-9 retain their equilibrium values, $[CO^{eq}\sin(\hat{COC}/2)]$, since the mid-points of the CC bonds do not move, being the pivots for their motion. The distances 5-6 and 14-15 take the value $[CO\cos(\hat{COC}/2)]$, but are in this case of different magnitudes due to the different lengths of the CO bonds on opposite parts of the ring. And finally, the above vector algebra gives the expressions for the angles $6,\hat{5},14$ and $15,\hat{14},5$.

One such run actually performed employed the following values:

$$\Delta CO = \pm.02\text{Å}, \quad \hat{COC} = 113.5^\circ, \quad \hat{OCC} = 109.198^\circ,$$
$$CC = 1.51628\text{Å}, \quad CO^{eq} = 1.4342\text{Å}$$

Substituting these figures gives:

$\cos\beta = (2 \times .02 \sin 56.75^\circ)/1.51628 = .02206$

$\therefore \quad \beta = 88.7359^\circ$

and, $a = -f = -[\frac{1}{2}(1-\cos 113.5^\circ)]^{\frac{1}{2}} = -.83629$

The expressions for b and g now become

$b = [\cos 109.193^\circ + (-.83629 \times .02206)]/.99976$

$= -.34728$ (using equation 3-5)

$g = [\cos 109.193^\circ + (+ .83629 \times .02206)]/.99976$

$= -.31038$ (using equation 3-7)

Thus, $\cos 6,\hat{5},14 = (-.34728)/\cos 56.75^\circ$

$\cos 15,\hat{14},5 = -.31038/\cos 56.75^\circ$

$\therefore \quad 6,\hat{5},14 = 129.301^\circ; \quad 15,\hat{14},5 = 124.478^\circ$

Finally,

$CO^{eq}\sin(COC/2) = 1.19940$, corresponding to distance 1-3
$CO^{+} \cos(COC/2) = 0.79733$, corresponding to distance 6-5
$CO^{-} \cos(COC/2) = 0.77540$, corresponding to distance 15-14

This treatment may be extended to investigate the effect that a bu $\hat{COC}$ angle distortion has on the rest of the molecular geometry. Take $\Delta(4,\hat{6},10) = + 2^\circ$; $\Delta(13,\hat{15},18) = -2^\circ$. Equation (3-4) becomes:

$a = [\frac{1}{2}(1-\cos 115.5)]^{\frac{1}{2}} = -.84573.$

Now define the direction of the CC bond:

$$\vec{R}_{4,13} = m\,\vec{e}_x + n\,\vec{e}_y; \quad m^2 + n^2 = 1$$

and $\cos \hat{OCC} = \vec{R}_{6,4} \cdot \vec{R}_{13,4} = ma + nb$

Knowing the CC bond length and the difference in the x coordinates of atoms 4 and 13, the angle θ may be obtained :

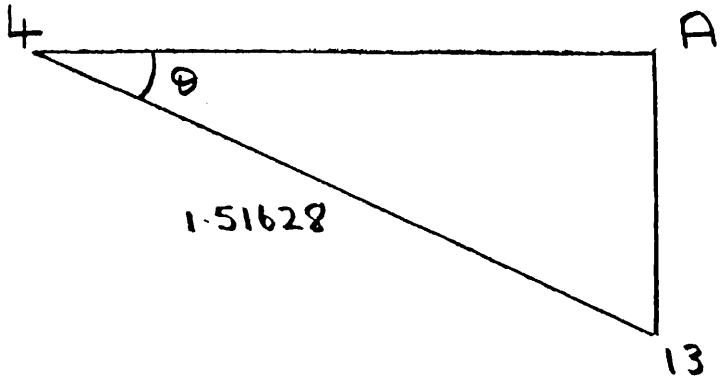

The x coordinate of A is CO $\sin(\hat{COC}^+/2)$ = 1.4342 sin (115.5/2) = 1.21294
The x coordinate of '13' is CO $\sin(\hat{COC}^-/2)$ = 1.4342 × sin (111.5/2) = 1.18550 .
So the difference in x coordinates is .02744

$\therefore$ $\sin\theta$ = .02744/1.51628 and θ = 1.03693°

Now, m = $-\sin\theta$ = -.01810 and n = $\cos\theta$ = .99984
Substituting in expressions (3-5) and (3-6)

$$b = [-.32875 + .0181(-.84573)]/.99984 = -.34411$$

and

$$\hat{6,5,14} = \text{acos}\left[\frac{-.34411}{\cos(\frac{115.5}{2})}\right] = 130.156^\circ$$

Using the same logic for the other side of the ring, where $\hat{COC}^-$ = 111.50°, $\hat{15,14,5}$ = 123.850°. Thus these angles which are required as input have now been evaluated. For this run, CO remains at its equilibrium value and it is $\hat{COC}$ that produces the difference between distances 6-5 and 15-14:

$CO^{eq}\sin(COC^{eq}/2)$ = 1.19940, corresponding to distance 1-3

$CO^{eq}\cos(COC^{+}/2)$ = 0.76531, corresponding to distance 6-5

$CO^{eq}\cos(COC^{-}/2)$ = 0.80717, corresponding to distance 15-14

The bu $\hat{OCC}$ deformations are straightforward, since they are defined through the values of the angles $6,\hat{5},14$ and $15,\hat{14},5$, whilst all other input remains the same as for the equilibrium geometry.

Au SYMMETRY COORDINATES.

Ring distortions of a_u symmetry prove rather more difficult to simulate, since out of the CO, CC and $\hat{OCC}$ coordinates it is only possible to vary two independently.

Consider the CO symmetry coordinate:

$$S_{CO}(a_u) = \tfrac{1}{2}(\Delta r_{46} - \Delta r_{10,6} + \Delta r_{13,15} - \Delta r_{18,15})$$

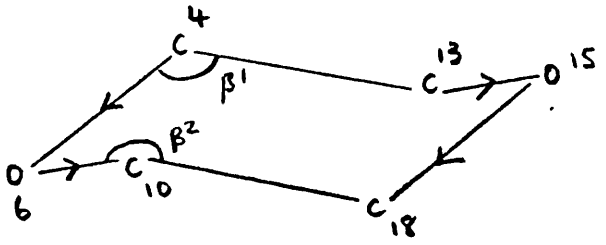

As S_{CO} changes, the two CC bonds move further apart (but still remain parallel), with a resulting change in the $\hat{OCC}$ angles: β_1 and β_2. These changes need to be quantified in order to set up the molecular geometry for input to Gaussian 76.

Thus the CO and CC bonds are defined as unit vectors:

$$\vec{R}_{4,6} = a\,\vec{e}_x + b\,\vec{e}_y + c\,\vec{e}_z$$

$$\vec{R}_{10,6} = d\,\vec{e}_x + \vec{e}\,e_y + f\,\vec{e}_z$$

$$\vec{R}_{4,13} = \vec{e}_y = \vec{R}_{10,18} \quad .$$

So,

$$b = \cos\beta_1 \; ; \quad e = \cos\beta_2 \qquad (3\text{-}10)$$

Two expressions which relate the coefficients for the adjacent CO bonds are:

$$r_{6,10}/r_{4,6} = c/f; \quad r_{6,10}/r_{4,6} = b/e \qquad (3\text{-}11)$$

Define a parameter ρ that is the ratio of bond lengths:

$$\rho = r_{6,10}/r_{4,6} = b/e = \frac{\cos\beta_1}{\cos\beta_2} = \frac{\cos(\beta+\Delta\beta)}{\cos(\beta-\Delta\beta)}$$

where β is the original $\hat{OCC}$ angle and $\Delta\beta$ the change due to the CO deformations.

$$\therefore \quad \rho = \frac{\cos\beta - \sin\beta\sin\Delta\beta}{\cos\beta + \sin\beta\sin\Delta\beta}$$

For β in radians and assuming $\Delta\beta$ is very small, this becomes:

$$\rho = \frac{\cos\beta - \Delta\beta\sin\beta}{\cos\beta + \Delta\beta\sin\beta} = \frac{r-\Delta r}{r+\Delta r}$$

'r' is the equilibrium CO bond length.

$$\therefore \quad (r+\Delta r)\cos\beta - r\Delta\beta\sin\beta$$

$$= (r-\Delta r)\cos\beta + r\Delta\beta\sin\beta$$

$$\therefore \quad \Delta r\cos\beta = r\Delta\beta\sin\beta$$

$$\therefore \quad \Delta\beta = \frac{\Delta r}{r}\cot\beta \qquad (3\text{-}12)$$

Thus, for $\Delta r = +.02\text{Å}$,

$$\Delta\beta_1 = \frac{.02}{1.4342}\cot(109.193^\circ) = -.004854 \text{ rad}$$

$$\equiv -.278^\circ = -\Delta\beta_2.$$

It is now necessary to develop further relationships between a, b, c and d, e, f in order to determine their individual values. From normalization,

$$a^2 = (1-b^2) - c^2$$

$$d^2 = (1-e^2) - c^2/\rho^2$$

$$\therefore \quad d^2 = (1-e^2) + \frac{a^2}{\rho^2} - \frac{(1-b^2)}{\rho^2} \qquad (3\text{-}13)$$

The COC angle is defined through the dot product of $\vec{R}_{4,6}$ and $\vec{R}_{10,6}$:

$$\cos COC = ad + be + c^2/\rho$$

$$\therefore \quad \cos COC = ad + be + \frac{(1-b^2)}{\rho} - \frac{a^2}{\rho} \qquad (3\text{-}14)$$

For $\Delta r = + .02\mathring{A}$,

$$\rho = \frac{1.4142}{1.4542} = 0.97249$$

From above, $\beta_1 = 108.915^\circ$ and $\beta_2 = 109.471^\circ$
$\therefore \quad b = -.32417; \quad e = -.33333.$

Substituting these values in equations (3-13) and (3-14),

$$d^2 = 1.05738\ a^2 - 0.05737$$

and $\cos\hat{COC} = \cos 113.5^\circ = - .39875$

$$= ad + 1.02829 - 1.02829\ a^2$$

$$\therefore \quad ad = -1.42704 + 1.02829\ a^2$$

These two expressions may now be solved for a and d:

$$\left(\frac{-1.42704+1.02829\ a^2}{a}\right)^2 = 1.05738\ a^2 - 0.05737$$

$$\therefore \quad a^2 = 0.70772, \quad a = -0.84126$$

and $d^2 = 0.69096, \quad d = 0.83124$

From the normalisation conditions,

$$c = (1-.70772 - .10509)^{\frac{1}{2}} = -.43266$$

$$f = (1-.69096 - .11111)^{\frac{1}{2}} = -.44489$$

So, $\vec{R}_{4,6} = -.84126\vec{e}_x - .32417\vec{e}_y - .43266\vec{e}_z$

$\vec{R}_{10,6} = + .83124\vec{e}_x - .33333\vec{e}_y - .44489\vec{e}_z$.

The quantities for data input may now be derived:

The x coordinates of positions '4' and '10' define the distances 1-3 and 1-9 respectively.

$$x_4 = -ar_{6,4} = 1.22336$$

$$x_{10} = dr_{6,4} = 1.17554$$

The distance 6-5 is given by:

$$r_{6,5} = [(y_6-y_5)^2 + (z_6-z_5)^2]^{\frac{1}{2}} \qquad (3\text{-}15)$$

($x_6 = x_5 = 0$ - these lie on the y axis)

Now, $b = \dfrac{y_6-y_4}{r_{6,4}}$, where $y_6-y_4 = y_6-y_5$

$\therefore \quad y_6-y_5 = br_{6,4} = -.47141$

and $z_6 = cr_{4,6} = -.62917$

Substituting these values into equation (3-15) gives

$$r_{6,5} = 0.78618$$

Finally, $\cos(6,\hat{5},14) = \dfrac{y_6-y_5}{r_{6,5}}$

$\therefore \quad 6,\hat{5},14 = 126.843^{\circ}$

Similarly, the CC bonds cannot be displaced without affecting the $\hat{OCC}$ angles. Consider the case where 4-13 expands, and 10-18 contracts by a magnitude Δr_{cc}. The CO bond vectors are defined as above. Here, c = f, and

$$r_{4,6}^{b} - \Delta r_{cc} = r_{6,10}^{e} \qquad (3\text{-}16)$$

Now,

$$b = \cos\beta_1 = \cos(\beta+\Delta\beta) = \cos\beta\cos\Delta\beta - \sin\beta\sin\Delta\beta$$

$$e = \cos\beta_2 = \cos(\beta-\Delta\beta) = \cos\beta\cos\Delta\beta + \sin\beta\sin\Delta\beta$$

Thus,

$$-\Delta r_{cc} + r_{4,6}(\cos\beta\cos\Delta\beta - \sin\beta\sin\Delta\beta)$$

$$= r_{6,10}(\cos\beta\cos\Delta\beta + \sin\beta\sin\Delta\beta)$$

$$\therefore \quad \frac{-\Delta r_{cc}}{r_{6,10}} + \cos\beta\cos\Delta\beta - \sin\beta\sin\Delta\beta$$

$$= \cos\beta\cos\Delta\beta + \sin\beta\sin\Delta\beta$$

$$\therefore \quad \sin\Delta\beta = \frac{-\Delta r_{cc}}{r_{co}} \cdot \frac{1}{2\sin\beta} \qquad (3\text{-}17)$$

where $r_{6,10} = r_{6,4} = r_{CO}$ (equilibrium CO bond length).

For $\Delta r_{cc} = +.02\text{Å}$, $\Delta\beta$ is calculated to be -0.423°. The calculations required for the input data are then exactly analogous to those above for CO, yielding

$$\vec{R}_{4,6} = -.83900\vec{e}_x - .32177\vec{e}_y - .43881\vec{e}_z$$

$$\vec{R}_{10,6} = +.83351\vec{e}_x - .33572\vec{e}_y - .43881\vec{e}_z$$

which in turn give the following desired quantities:

$$1\text{-}3 = 1.20329; \quad 1\text{-}9 = 1.19542$$

$$\hat{6,5,14} = 126.849^{\circ}; \quad r_{6,5} = 0.78636$$

B_g SYMMETRY COORDINATES.

Consider the bg CO symmetry coordinate.

$$S_{CO}(bg) = \tfrac{1}{2}(\Delta r_{4,6} - \Delta r_{10,6} - \Delta r_{13,15} + \Delta r_{18,15})$$

As previously,

$$\vec{R}_{4,6} = a\vec{e}_x + b\vec{e}_y + c\vec{e}_z$$

$$\vec{R}_{10,6} = d\vec{e}_x + e\vec{e}_y + f\vec{e}_z$$

$$\vec{R}_{4,13} = \vec{R}_{10,18} = \vec{e}_y$$

and $b = \cos(6,\hat{4},13)$; $e = \cos(6,\hat{1}0,18)$.

The four equations required to determine the four unknowns, a, c, d and f are given by:

The normalisation conditions:

$$a^2 + b^2 + c^2 = 1; \quad d^2 + e^2 + f^2 = 1$$

The expression for the $\hat{COC}$ angle:

$$\vec{R}_{4,6} \cdot \vec{R}_{10,6} = \cos COC = ad + be + cf$$

and finally, the ring closure condition

$$f = \frac{r_{4,6}}{r_{10,6}}\, c = \grave{\rho} c$$

The following expression is derived, defining as before $6,\hat{4},13 = \beta_1$, $6,\hat{1}0,18 = \beta_2$

$$\cos\beta_1 - \cos\beta_1\cos\beta_2 = \grave{\rho}(1-\cos^2\beta - a^2) - a\left[1-\cos^2\beta_2 - \grave{\rho}^2(1-\cos^2\beta_1 - a^2)\right]^{\frac{1}{2}} \qquad (3\text{-}18)$$

For $\Delta r_{CO} = .02\text{Å}$, $\grave{\rho} = \frac{1.4542}{1.4142}$, $b = -.32876 = e$; $\cos COC = -.39875$ (for no simultaneous bu OCC deformation) - note that this '$\grave{\rho}$' is the inverse of ρ employed in the a_u calculations.

This gives, from equation (3-18),

$$[-.39875 - .10808 - 1.0283(1-.10808-a^2)]^2$$

$$= a^2[1-.10808 - 1.0574(1-.10808-a^2)]$$

leading to $2.8775a^2 - 2.0278 = 0$ and $a = -.83947$.

$$\therefore \quad c = (1-.83947^2 - .32875^2)^{\frac{1}{2}} = -.43268$$

$$\therefore \quad \vec{R}_{4,6} = -.83947\vec{e}_x - .32875\vec{e}_y - .43268\vec{e}_z$$

$$\vec{R}_{10,6} = .83305\vec{e}_x - .32875\vec{e}_y - .44492\vec{e}_z$$

Examine the y coordinates of the carbon atoms 4 and 10:

$$y_4 - y_6 = -br_{6,4} = .47807$$

$$y_{10} - y_6 = -er_{6,4} = .46492$$

$$\therefore \quad y_5 - y_6 = .47150$$

- the CC bond 4-13 has moved along the y axis to be closer to oxygen atom 6, whilst 10-18 has moved in the opposite direction. This must be taken into account when defining the distance from carbon to the dummy atoms, which up to this point have remained unaltered. Thus,

$$4\text{-}3 = .75814 - (.47807 - .46492)/2$$

$$= .75157 = 18\text{-}9$$

and $$13\text{-}3 = .75814 + (.47807 - .46492)/2$$

$$= .76471 = 10\text{-}9$$

The rest of the input is calculated from the coefficients of the bond vectors, as previously, giving:

$6\text{-}5 = .7863$; $\hat{6,5,14} = 126.844^{o}$

$x_4\text{-}x_6 = 1.19038$; $x_6\text{-}x_{10} = 1.20353$

This satisfactorily fixes the geometry for the left hand side of the molecule. The right hand side now needs to be considered separately, since the symmetry of the deformation causes the two oxygen atoms to possess differing x coordinates, and the parameters from one side of the molecule may now not be simply transferred to the other. For the correct symmetry to be preserved, the input must correspond to the following Cartesian coordinates:

Atoms:	6	10	13	15	14
x	0	-1.1781	1.22076	.04266	0
y	-1.22964	-.76471	.76471	1.22964	.75814
z	-.62925	0	0	.62925	0

- note that atom 15 is moved along the x axis to yield the correct CO bond lengths.

Thus,

$14\text{-}15 = .78746$

$\hat{15,14,5} = 126.781^{o}$

This x axis motion of oxygen atom 15 results in an alteration of the dihedral angle 15,14,1,2 which is easily derived:

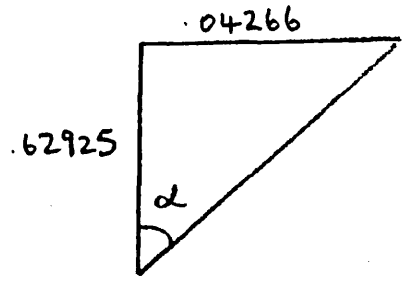

'.04266' is the x coordinate of the oxygen 15.

'.62925' is the z coordinate of this atom.

This gives $\alpha = 3.8784^{o}$.

This is actually the most complicated CO deformation to input, since both CC bonds are moved apart and also along the y axis, and a dihedral angle is varied for the first occasion.

The above has shown how a structure may be formed which corresponds to specifically chosen values of the molecular symmetry coordinates. On executing Gaussian 76 for this geometry a molecular potential energy is yielded, and this is the parameter to be utilised in the force constant determination.

Consider how one might proceed in order to obtain values for any two diagonal force constants and their interaction constant. The equation governing the potential energy, assuming simple harmonic motion, is:

$$E = E_o + \tfrac{1}{2}k_1\Delta S_1^{\,2} + \tfrac{1}{2}k_2\Delta S_2^{\,2} + k_{12}\Delta S_1\Delta S_2$$

'E' is the energy from the Gaussian 76 run, and there are six unknowns - E_o, the minimum of the potential energy well; the three force constants; and the two equilibrium values of the internal coordinates which combine to form the symmetry coordinates. Thus six suitably chosen runs will yield six equations which may then be solved for the parameters. A possible set of runs would be:

ΔS_1	ΔS_2	
+x	0	Determines E_o, k_1 and S_1
+y	0	
0	0	Determines E_o, k_2 and S_2
0	+a	
0	+b	
+x	+a	- Determines k_{12}

If $\Delta S_1 = \frac{1}{2}(R_1+R_2+R_3+R_4)$ where R is e.g. CO, then x and y might be .02 and .01Å. If $\Delta S_2 = \frac{1}{2}(\theta_1+\theta_2+\theta_3+\theta_4)$ where R is e.g. H^aCO then 'a' and 'b' might be 3^o and 2^o.

One problem when the geometry has not already been previously optimized is that there are additional terms in the energy equation arising from the interaction between those coordinates shifted from their equilibrium values and those being varied. The best approach is to gradually optimise the geometry through several cycles of varying one or two coordinates at a time, until force constants and geometry parameters are obtained that show only negligible changes upon any further optimization.

The approach adopted in this study was initially as above, but it was realised that much information on the interaction constants was being disregarded and as such was acting as a major source of error. Thus a program was developed to carry out the least squares fitting of a larger number of force constants at a time to the energy values obtained from all the runs.

The equations on which the employed perturbation technique is based are derived in the Appendix. The elements of the Jaccobian matrix were derived from the equation:

$$E = V_o + \sum_i \tfrac{1}{2}k_{ii}(R_i-R_{ei})^2 + \sum_{i\neq j}\sum k_{ij}(R_i-R_{ei})(R_j-R_{ej})$$

Thus,

$$\partial E/\partial V_o = 1$$

$$\partial E/\partial R_{ei} = -k_{ii}(R_i-R_{ei})$$

$$\partial E/\partial k_{ii} = \tfrac{1}{2}(R_i-R_{ei})^2$$

$$\partial E/\partial k_{ij} = 2(R_i-R_{ei})(R_j-R_{ej})$$

Various groups of force constants, such as CO, CC, COC, and OCC with their interactions, or the group of angle deformations $H^{a,e}CO$ and $H^{a,e}CC$, are then chosen in turn as parameters to be varied so as to give the best fit between the 'observed' ab initio energies and those calculated. The procedure is then continued until no further improvement occurs and the force constants have approached their optimum values - typically requiring 3 or 4 such cycles. The results from each symmetry block are obtained completely independently from each other.

The geometry employed for the Au, Bu and Bg runs, and for most of the Ag runs was that obtained from several cycles of optimising one or two coordinates (bond length, bond angles) in turn, as described previously. For the non-fully symmetric species this is adequate, since as long as the equilibrium on which the calculations are based is of the correct symmetry

(i.e. Ag) then all the other symmetry coordinates are by definition zero at this point and errors due to neglected interaction terms are not present. For the Ag force constant determination this can only be circumvented by providing enough data to ensure that all the interaction force constants are satisfactorily determined. The sets of calculated energies and derived force constants are listed in the Appendix.

The number of runs required to satisfy this condition, and to investigate the large number of force constants for a molecule of this size, means that such a project eventually becomes expensive in both computer time and the effort required to tackle the vector algebra required to determine the correct input. This is a factor which must be considered before embarking on similar procedures for new molecules.

TABLE 25.

Gaussian 76 dipole moment data for 1,4-dioxan.

Description of Run	(Debyes) x	y	z	TOT
$H^a(7)$, $\Delta x = +.01\text{Å}$	-.0005	-.0015	.0011	.0019
$H^a(7)$, $\Delta x = +.02\text{Å}$	-.0010	-.0029	.0022	.0038
$H^a(7)$, $\Delta x = +.03\text{Å}$	-.0016	-.0044	.0031	.0056
$H^a(7)$, $\Delta x = -.02\text{Å}$	.0008	.0030	-.0026	.0040
$H^a(7)$, $\Delta y = +.02\text{Å}$	-.0030	-.0019	.0052	.0063
$H^a(7)$, $\Delta z = +.02\text{Å}$	-.0068	.0091	-.0144	.0184
$H^e(8)$, $\Delta x = +.02\text{Å}$	-.0101	.0060	.0064	.0134
$H^e(8)$, $\Delta y = +.02\text{Å}$	.0048	.0037	-.0029	.0067
$H^e(8)$, $\Delta z = +.02\text{Å}$	.0073	-.0054	.0014	.0092
C(4), $\Delta x = +.02\text{Å}$	.0625	.0002	.0083	.0630
C(4), $\Delta y = +.02\text{Å}$	.0143	.0324	-.0019	.0354
C(4), $\Delta z = +.02\text{Å}$	.0186	-.0021	.0390	.0432
O(6), $\Delta x = +.02\text{Å}$	-.1054	+.0002	-.0005	.1054
O(6), $\Delta y = +.02\text{Å}$	0	-.0689	-.0011	.0689
O(6), $\Delta z = +.02\text{Å}$	0	-.0009	-.0550	.0550

Section 3.4 Ab Initio APT's.

The final piece of information in the Gaussian 76 output is the computed values of the x, y and z components of the dipole moment for that particular molecular configuration. By displacing an atom away from its equilibrium position and noting the resulting change in the components of the dipole moment, the corresponding atomic polar tensor may be determined.

E.g.

$$\frac{dp_x}{dy_1} \simeq \frac{\Delta p_x}{\Delta y_1}$$

change in x cpt of dipole moment / input change in y coordinate

By displacing the atom along each of the cartesian axes, by typically .02Å, the full polar tensor is obtained.

To this end, it is convenient to adopt the option of inputting the atomic positions simply in terms of their cartesian coordinates, as shown in the example below.

Section 3.5 1,4-Dioxan.

The results of the Gaussian 76 runs are shown below. The geometry employed was derived from the bond lengths and angles listed above (page 66). Several runs were performed to test the linearity of the dipole moment change with the distortion of the coordinate, using an axial hydrogen. It is seen that the results adhere to the expected direct proportionality.

Division of the results by .02 will give polar tensor elements in $D\text{Å}^{-1}$. Since it is customary to describe the charge flow in terms of electrons, this figure must be multiplied by 0.20822 to convert to 'e'. Thus the following set of atomic polar tensors is obtained:

$H^a(7)$	Δx	Δy	Δz	(in e)
ΔP_x	-.0104	-.0312	-.0708	
ΔP_y	-.0302	-.0198	+.0947	
ΔP_z	+.0229	+.0541	-.1499	

```
NETWORK(UHCA104,RUN=ULCC)
JOB(UHCA104,J12,T1000,M7600)
ATTACH(OVG,GAUSSIAN76,ID=PUBLIC)
OVG.
**EOR**
$  1
   23                                    1
   314                                  111        1
   4                                     1
   5                                     1
   6                                     1

 NEW  CYC  EQ
 0  1
    6    1.24107                    -.71653                  .2533
    6    0.00                       -1.43307                 -.2533
    6   -1.24107                   -0.71653                  .2533
    6   -1.24107                    0.71653                 -.2533
    6    0.0                        1.43307                  .2533
    6    1.24107                     .71653                 -.2533
    1    1.24107                    -.71653                  1.3663
    1    2.14984                   -1.24121                  -.1177
    1    0.00                       -2.48242                  .1177
    1    0.00                       -1.43307                  -1.3663
    1    -1.24107                  -.71653                   1.3663
    1    -2.14984                  -1.24121                  -.1177
    1    -2.14984                  1.24121                    .1177
    1    -1.24107                    .71653                   -1.3663
    1    0.0                        1.43307                    1,3663
    1    0.0                       2.48242                   -.1177
    1    2.14984                   1.24121                   .1177
    1   1.24107                     .71653                   -1.3663
   -1
**EOF**
```

$H^e(8)$

-.1052	+.0500	+.0760
+.0625	+.0385	-.0562
+.0666	-.0302	+.0146

C(4)

+.6507	+.1489	+.1936
+.0021	+.3373	-.0219
+.0864	-.0198	+.4060

O(6)

-1.0973	0	0
-.0021	-.7173	-.0094
-.0052	-.0115	-.5726

A small error is apparent on examining the oxygen polar tensor. Elements 2,1 and 3,1 should in fact be zero by symmetry; a fact which can be simply imposed without requiring any other changes.

At this stage, the tensor for one of each distinct type of atom has been obtained. It is now desired to transfer these to the equivalent atoms in the molecule. For instance, consider C(4) and C(10) - the elements of their respective tensors are obviously simply related by symmetry, and a small amount of thought should enable the tensor of C(10) to be written down immediately. Rigorously, the method is to rotate the coordinate system so that C(4) is then orientated with respect to the axes in the same way as C(10) was before the rotation. This is equivalent to performing a similarity transformation on the APT of C(4) with the matrix which brings about the transformation of the coordinates of C(4) to C(10):

$$P_x^{C(10)} = A\, P_x^{C(4)} A'$$

where A is

$$\begin{bmatrix} -1 & 0 & 0 \\ 0 & +1 & 0 \\ 0 & 0 & +1 \end{bmatrix}$$

the matrix which reflects C(4) into C(10).

$P_x^{C(10)}$ is the same as $P_x^{C(4)}$, apart from the signs of the elements 1,2, 1,3, 2,1, and 3,1, which are reversed. The same relationship naturally holds for all the atoms which are here related by the plane of reflection.

For atoms interconverted through the centre of inversion, the transforming matrix is now

$$A = \begin{bmatrix} -1 & 0 & 0 \\ 0 & -1 & 0 \\ 0 & 0 & -1 \end{bmatrix}$$

and the APT's in fact are equal - again this is apparent by simple inspection. In more complicated cases (e.g. see cyclohexane later on), however, this numerical method is the most straightforward route to the related APT's.

So a complete set of APT's has now been obtained. The constraint of the invariance of molecular dipole moment during translational motion imposes the relationship that the sum all the tensors should equal the null matrix. For the ab inito tensors:

$$\sum_{\alpha} P_x^{\alpha} = \begin{matrix} -.0542 & 0 & 0 \\ 0 & -.0106 & .0476 \\ 0 & -.0066 & -.0624 \end{matrix}$$

This condition is well obeyed here, showing a satisfying degree of consistency between the independently calculated APT's. This relationship is frequently used to find the tensor for a remaining type of atom once the rest have been determined. Here the constraint may be fully imposed by this approach through treating, say, the carbon APT as unknown. Then,

$$\begin{bmatrix} -4a & 0 & 0 \\ 0 & -4b & -4c \\ 0 & -4d & -4e \end{bmatrix} = \begin{bmatrix} -2.657 & 0 & 0 \\ 0 & -1.3598 & .1352 \\ 0 & .0726 & -1.6864 \end{bmatrix}$$

TABLE 26.

Gaussian 76 dipole moment data for cyclohexane.

Description of run	x	y	z	TOT
C1, x=+.02Å	.0110	-.0055	-.0024	.0126
C1, y=+.02Å	-.0065	.0050	.0015	.0083
C1, z=+.02Å	-.0022	.0013	.0149	.0151
C2, x=+.02Å	.0014	.0001	0	.0014
C2, y=+.02Å	0	.0167	-.0031	.0169
C2, z=-.02Å	0	.0026	-.0149	.0151
H^a7, x=+.02Å	.0036	-.0018	.0026	.0047
H^a7, y=+.02Å	-.0018	.0017	-.0019	.0031
H^a7, z=+.02Å	-.0029	.0017	-.0198	.0201
H^e8, x=+.02Å	-.0181	.0115	.0044	.0218
H^e8, y=+.02Å	.0109	-.0042	-.0025	.0119
H^e8, z=+.02Å	.0075	-.0043	.0034	.0093
H^a10, x=+.02Å	.0006	.0002	.0003	.0007
H^a10, y=+.02Å	0	.0045	.0034	.0057
H^a10, z=-.02Å	0	.0034	.0198	.0201
H^e9, x=+.02Å	.0020	.0004	0	.0020
H^e9, y=+.02Å	0	-.0232	.0049	.0237
H^e9, z=-.02Å	0	-.0087	-.0034	.0093

where the elements of one of the carbon APT's are given by

1,1 = a; 2,2 = b; 2,3 = c;
3,2 = d; 3,3 = e

Since the remaining elements do not contribute to the sum they are not determinable in this way, and shall simply be given their ab initio values. The APT for C(4) then becomes:

$$P_x^{C(4)} = \begin{matrix} +.6642 & + .1489 & + .1936 \\ + .0021 & + .3400 & -.0338 \\ + .0864 & - .0181 & + .4216 \end{matrix}$$

which as expected is very similar to that computed directly from Gaussian 76.

Section 3.6 Cyclohexane.

The cartesian coordinates used for the Gaussian 76 input were based on the following structural parameters:

C-C = 1.52Å
C-H = 1.113Å
$\hat{CCC}$ = 111.05°
$\hat{HCC}$ = tetrahedral;

obtained by electron diffraction measurements[29].

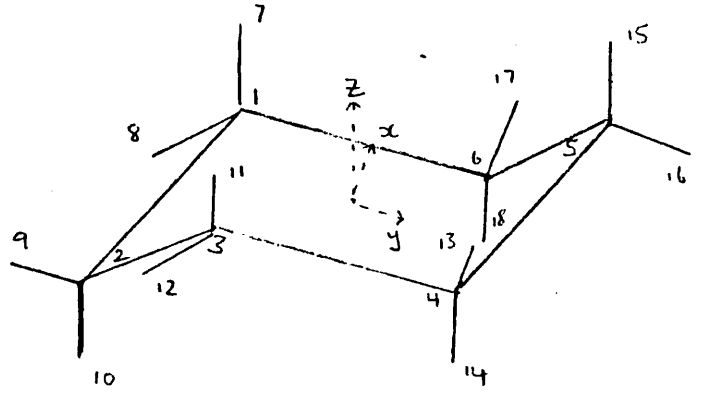

As previously, the data from each run is multiplied by .20822 to convert to electronic units, and divided by ± .02, the atomic displacement. This yields the following set of 'raw' APT's.

	.1145	-.0677	-.0229
C1	-.0573	.0521	.0135
	-.0250	.0156	.1551
	.0146	0	0
C2	.0010	.1739	-.0271
	0	-.0323	.1551
	.0375	-.0187	-.0302
H^a7	-.0187	.0177	.0177
	.0271	-.0198	-.2061
	.0062	0	0
H^a10	.0021	.0468	-.0354
	.0031	.0354	-.2061
	-.1884	.1135	.0781
H^e8	.1197	-.0437	-.0448
	.0458	-.0260	.0354
	.0208	0	0
H^e9	.0041	-.2415	.0906
	0	.0510	.0354

The relationship between the APT's for e.g. C1 and C3 is as in 1,4-dioxan, i.e. equal except for 1,2, 1,3, 2,1, and 3,1 which are opposite in sign, and APT's for C1 and C4 are equal. The sum of these raw tensors is then:

$$\sum_{\alpha} P_x^{\alpha} = \begin{matrix} -.0624 & 0 & 0 \\ .0144 & .0628 & .0018 \\ .0062 & -.0126 & -.0936 \end{matrix}$$

- not corresponding well to the expected null matrix. In fact, these tensors do not satisfy the D_{3d} molecular point group symmetry. This condition requires that the following should hold:

(1) The 'terminal' atoms (2,9,10,5,15,16) should posses APT's of the form:

$$\begin{matrix} a & 0 & 0 \\ 0 & b & c \\ 0 & d & e \end{matrix}$$

This is almost the case and is here simply imposed.

(2) The APT of C5 should transform into that of C3 on rotation of the axis system by 120^{o} clockwise about the C3(z) axis (the same applying for all thus related atoms) i.e.

$$\text{APT C3} = R^{120}\, P_x^{C5}\, (R^{120})^t$$

$$= \begin{bmatrix} -.5 & -.86603 & 0 \\ .86603 & -.5 & 0 \\ 0 & 0 & 1 \end{bmatrix} \begin{bmatrix} .0146 & 0 & 0 \\ 0 & .1739 & -.0271 \\ 0 & -.0323 & .1551 \end{bmatrix} \begin{bmatrix} -.5 & .86603 & 0 \\ -.86603 & -.5 & 0 \\ 0 & 0 & 1 \end{bmatrix}$$

$$= \begin{matrix} .1341 & .0690 & .0235 \\ .0690 & .0544 & .0135 \\ .0280 & .0161 & .1551 \end{matrix}$$

These constraints then yield the following set of APT's:

	.1341	-.0690	-.0235
C1	-.0690	.0544	.0135
	-.0280	.0161	.1551
	.0146	0	0
C2	0	.1739	-.0271
	0	-.0323	.1551
	.0366	-.0176	-.0307
H^a7	-.0176	.0163	.0177
	.0307	-.0177	-.2061
	-.1759	.1136	.0785
H^e8	.1136	-.0448	-.0453
	.0442	-.0255	.0354

$$H^e9 \quad \begin{matrix} .0208 & 0 & 0 \\ 0 & -.2415 & .0906 \\ 0 & .0510 & .0354 \end{matrix}$$

$$H^a10 \quad \begin{matrix} .0062 & 0 & 0 \\ 0 & .0468 & -.0354 \\ 0 & .0354 & -.2061 \end{matrix}$$

The sum of the tensors is now:

$$\sum_{\alpha} P_x^{\alpha} = \begin{matrix} .0624 & 0 & 0 \\ 0 & .0620 & 0 \\ 0 & 0 & -.0936 \end{matrix}$$

The null constraint may be imposed by determining the carbon APT's from those of the hydrogens.

$$\sum P_x^{H^a} = \begin{matrix} .1588 & 0 & 0 \\ 0 & .1588 & 0 \\ 0 & 0 & -1.2366 \end{matrix}$$

$$\sum P_x^{H^e} = \begin{matrix} -.662 & 0 & 0 \\ 0 & -.662 & 0 \\ 0 & 0 & .2124 \end{matrix}$$

$$\therefore \sum P_x^{c} = \begin{matrix} .5032 & 0 & 0 \\ 0 & .5032 & 0 \\ 0 & 0 & 1.0242 \end{matrix}$$

Applying a 120° similarity transformation to a generalised tensor having the same form as C2 yields:

$$\begin{bmatrix} -.5 & -.86603 & 0 \\ .86603 & -.5 & 0 \\ 0 & 0 & 1 \end{bmatrix} \begin{bmatrix} a & 0 & 0 \\ o & b & c \\ o & d & e \end{bmatrix} \begin{bmatrix} -.5 & .86603 & 0 \\ -.86603 & -.5 & 0 \\ 0 & 0 & 1 \end{bmatrix}$$

$$= \begin{bmatrix} (.25a+.75b) & (-.433a+.433b) & (-.866c) \\ (-.433a+.433b) & (.75a+.25b) & (-.5c) \\ (-.86603d) & (-.5d) & (e) \end{bmatrix}$$

$\therefore$ $.5032 = 4(.25a+.75b) + 2a$ (1)

$.5032 = 4(.75a+.25b) + 2b$ (2)

(1) $\rightarrow$ $a = .1677 - b$ (3)

In fact, it is not possible to solve for a and b since substitution of this value of 'a' into (2) only yields .5032 = .5032 !

Referring to the C2 APT, and using (3) as a constraint,

if $a = .0146$, $b = .1531$

or if $b = .1739$, $a = -.0062$

The latter has been accepted on the basis that the larger quantity, 'b', is perhaps more likely to be predicted accurately. This leads to the finally accepted set of polar tensors - as the last set listed above, except for the carbons which are now chosen to satisfy the summation to a null matrix of all the APT's:

$$\text{C2 APT} = \begin{matrix} -.0062 & 0 & 0 \\ 0 & .1739 & -.0271 \\ 0 & -.0323 & .1707 \end{matrix}$$

and from the 120° rotation of axes,

$$\text{C1 APT} = \begin{matrix} .1289 & -.0780 & -.0235 \\ -.0780 & .0388 & .0135 \\ -.0280 & .0161 & .1707 \end{matrix}$$

Section 3.7 Tetrahydropyran.

For the purposes of this set of calculations, the geometry of tetrahydropyran is constructed from those of 1,4-dioxan and cyclohexane - the former providing the Cartesian coordinates of the oxygen - containing half, and the latter corresponding to the remaining atoms.

The numbering is according to the following scheme:

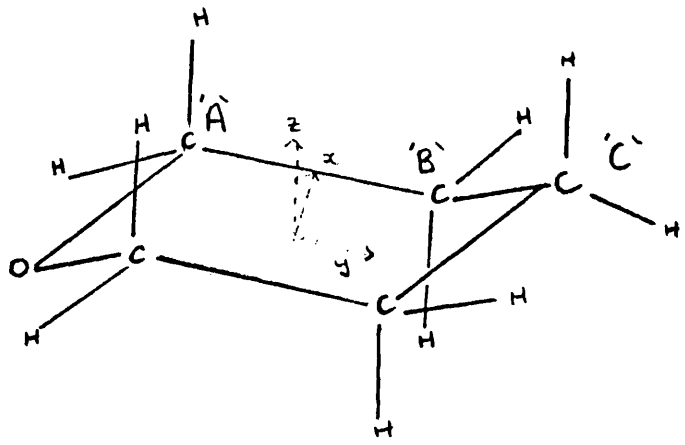

The following results were obtained:

TABLE 27.

Gaussian 76 dipole moment data for tetrahydropyran.

Description of run		x	y	z	TOT
C'A'	$\Delta x=+.02\mathring{A}$	.0674	1.4661	1.4792	2.0837
C'A'	$\Delta y=+.02\mathring{A}$	.0135	1.5054	1.4711	2.1048
C'A'	$\Delta z=+.02\mathring{A}$	.0182	1.4584	1.5114	2.1004
C'B'	$\Delta x=+.02\mathring{A}$	.0058	1.4705	1.4761	2.0836
C'B'	$\Delta y=+.02\mathring{A}$	.0018	1.4613	1.4687	2.0718
C'B'	$\Delta z=+.02\mathring{A}$	-.0004	1.4626	1.4867	2.0856
C'C'	$\Delta x=+.02\mathring{A}$	.0018	1.4640	1.4718	2.0759
C'C'	$\Delta y=+.02\mathring{A}$	0	1.4760	1.4679	2.0817
C'C'	$\Delta z=+.02\mathring{A}$	0	1.4640	1.4718	2.0759
O	$\Delta x=+.02\mathring{A}$	-.1070	1.4638	1.4713	2.0782
O	$\Delta y=+.02\mathring{A}$	0	1.3954	1.4695	2.0265
O	$\Delta z=+.02\mathring{A}$	0	1.4637	1.4184	2.0382
H^a'A'	$\Delta x=+.02\mathring{A}$	-.0020	1.4610	1.4741	2.0754
H^a'A'	$\Delta y=+.02\mathring{A}$	-.0034	1.4620	1.4765	2.0779
H^a'A'	$\Delta z=+.02\mathring{A}$	-.0071	1.4745	1.4549	2.0715
H^a'B'	$\Delta x=+.02\mathring{A}$	.0046	1.4662	1.4715	2.0772
H^a'B'	$\Delta y=+.02\mathring{A}$	.0003	1.4630	1.4780	2.0796

$H^a'B'$	$\Delta z=+.02\mathring{A}$	.0041	1.4711	1.4572	2.0707
$H^a'C'$	$\Delta x=+.02\mathring{A}$	0	1.4640	1.4715	2.0757
$H^a'C'$	$\Delta y=+.02\mathring{A}$	0	1.4676	1.4809	2.0849
$H^a'C'$	$\Delta z=+.02\mathring{A}$	0	1.4676	1.4524	2.0757
$H^e'A'$	$\Delta x=+.02\mathring{A}$	-.0111	1.4721	1.4785	2.0864
$H^e'A'$	$\Delta y=+.02\mathring{A}$	.0052	1.4647	1.4677	2.0735
$H^e'A'$	$\Delta z=+.02\mathring{A}$	.0073	1.4571	1.4728	2.0717
$H^e'B'$	$\Delta x=+.02\mathring{A}$	-.0161	1.4575	1.4641	2.0659
$H^e'B'$	$\Delta y=+.02\mathring{A}$	-.0072	1.4655	1.4689	2.0750
$H^e'B'$	$\Delta z=+.02\mathring{A}$	-.0113	1.4596	1.4721	2.0731
$H^e'C'$	$\Delta x=+.02\mathring{A}$	.0028	1.4638	1.4717	2.0757
$H^e'C'$	$\Delta y=+.02\mathring{A}$	0	1.4399	1.4688	2.0569
$H^e'C'$	$\Delta z=+.02\mathring{A}$	0	1.4644	1.4771	2.0799
Equilibrium		0	1.4641	1.4718	2.0760

This data is treated in the usual manner, and yields the following set of atomic polar tensors:

('e' units)

$\underline{O}$	-1.1140	0	0
(O)	-.0031	-.7152	-.0042
(O)	-.0052	-.0239	-.5559
$\underline{C}'A'$	.7017	.1405	.1895
	.0208	.4300	-.0593
	.0770	-.0073	.4123
$\underline{C}'B'$	.0604	.0187	-.0042
	.0666	-.0292	-.0156
	.0448	-.0323	.1551
$\underline{C}'C'$	.0187	0	0
	0	.1239	-.0094
	0	-.0406	.1645
$\underline{H}^a'A'$	-.0208	-.0354	-.0739
	-.0323	-.0219	.1083
	.0239	.0239	-.1759

$\underline{H}^{a}$'B'

.0479	.0031	.0467
.0219	-.0115	.0729
-.0031	.0645	-.1520

$\underline{H}^{a}$(C)

0	0	0
0	.0364	.0364
0	.0947	-.2020

$\underline{H}^{e}$'A'

-.1156	.0541	.0760
.0833	.0062	-.0729
.0698	-.0427	.0104

$\underline{H}^{e}$'B'

-.1676	-.0750	-.1176
-.0687	.0146	-.0468
-.0802	-.0302	.0031

$\underline{H}^{e}$'C'

.0292	0	0
0	-.2519	.0031
0	-.0312	.0552

Having corrected the 2,1 and 3,1 elements of the oxygen APT (symmetry dictates that these should be zero), the sum over all the APT's should be the null matrix. In fact,

$\sum_{\alpha} P_x^{\alpha} =$

-.0540	0	0
0	-.0304	-.0009
0	-.0492	-.0322

This small inconsistency may be removed by omitting C'C' from the sum, and then setting this equal to the negative of the resulting sum matrix. Then,

$\underline{C}$'C'

-.0728	0	0
0	-.1543	.0085
0	-.0086	-.1967

```
NETWORK(UHCA101,RUN=ULCC)
//UHCA101 JOB HOGAN
//         EXEC CRAY
//SYSUT1 DD *
JOB,US=UHCA101,M=3000,T=299.
ACCESS,DN=GAUSIAN,ID=TRIAL.
GAUSIAN.
/EOF
$0010000000000000000000000000000000000000000000000000000000000000000
0002300000000000000000000000000000001C000000000000000000000000000
0003140000000000000000000C000000000111000000010000000000000000
0004000000000000000000000C0000000C010C000000000000000000000000
0005000000000000000000000C000C000001000000000000000000000000
0006000000000000000000000C000C000001000000000000000000000000
```

```
  THP  EQN
 0  1
    6    1.1994                -.75814                0.0
    8    0.00                   -1.229663              -.629358
    1    1.239336              -1.124253              1.019712
    1    2.023258              -1.149081              -.574315
    6   -1.1994                -.75814                0.0
    1   -2.023258              -1.149081              -.574315
    1   -1.239336              -1.124253              1.019712
    6    1.253                  .76                    0.00
    6    0.00                  1.306004               .664953
    1    2.152342              1.131526               .540312
    1    1.309359              1.131526               -1.04764
    6   -1.253                 0.76                   0.0
    1   -1.309359              1.131526               -1.04764
    1   -2.152342              1.131526                .540312
    1    0.0                   1.027810               1.742630
    1    0.0                   2.417210               .601800
   -1
**EOF**
```

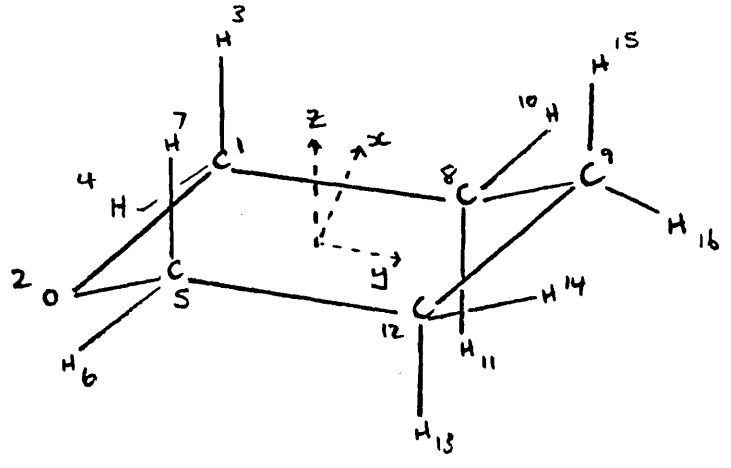

Section 3.8 Trioxan.

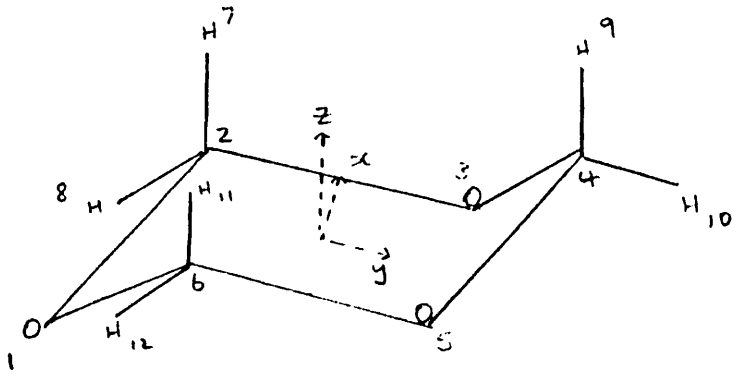

This molecule yields the following results:

TABLE 28.

Gaussian 76 dipole moment data for Trioxan.

Description of run		x	y	z(Debyes)
Equilibrium.		.0	0	3.3922
O	$\Delta x=+.02\mathring{A}$	-.1090	-.0005	3.3917
O	$\Delta y=-.02\mathring{A}$	0	.0757	3.3892
O	$\Delta z=-.02\mathring{A}$	0	-.0033	3.4553
C4	$\Delta x=+.02\mathring{A}$	.1074	0	3.3935
C4	$\Delta y=+.02\mathring{A}$	0	.0835	3.4079
C4	$\Delta z=+.02\mathring{A}$	0	.0259	3.4651
H^a9	$\Delta x=+.03\mathring{A}$	-.0068	0	3.3917
H^a9	$\Delta y=+.03\mathring{A}$	0	.0005	3.4013
H^a9	$\Delta z=+.03\mathring{A}$	0	-.0095	3.3640
H^e10	$\Delta x=+.03\mathring{A}$	.0079	0	3.3921
H^e10	$\Delta y=+.03\mathring{A}$	0	-.0112	3.3974
H^e10	$\Delta z=+.03\mathring{A}$	0	.0067	3.4021

The APT for C2 may be obtained from that for C4 by performing a similarity transformation based on the matrix corresponding to a 120° anticlockwise rotation about the z (C_3) axis. Symmetry thus enables the APT's for all atoms to be derived from the data presented above.

This set of APT's was found to satisfy very well the condition $\sum_{\alpha} P_x^{\alpha} = 0$, and so therefore can be employed without correction.

Trioxan ab initio APT's.

O(1)	-1.135	0	0
	0	-.788	.0344
	0	.0312	-.6569
C(4)	1.118	0	0
	0	.8693	.2696
	0	.1635	.7590
$H^a(9)$	- .0472	0	0
	0	.0035	-.0660
	0	.0063	-.1957
$H^e(10)$	.0548	0	0
	0	-.0777	.0464
	0	.0360	.0687
O(3)	-.8747	.1502	-.0298
	.1503	-1.0482	-.0172
	-.0270	-.0156	-.6569
C(6)	.9314	-.1077	-.2335
	-.1077	1.0558	-.1348
	-.1416	-.0817	.7590
$H^a(7)$	-.0092	-.0219	-.0572
	-.0219	-.0346	.0330
	.0055	-.0031	-.1957
$H^e(8)$	-.0446	.0574	.0402
	.0574	.0217	-.0232
	.0312	-.0180	.0687

```
NETWORK(UHCA101,RUN=ULCC)
//UHCA101  JOB STEELE
//         EXEC CRAY
//SYSUT1   DD *
JOB,US=UHCA101,M=3000,T=198.
ACCESS,DN=GAUSIAN,ID=TRIAL.
GAUSIAN.
/EOF
$0010000000000000000000000000000000000000
0002300000000000000000000000000001000000000000000000
0003140000000000000000000000000011100000001000000000
0004000000000000000000000000000010000000000000000000
0005000000000000000000000000000010000000000000000000
0006000000000000000000000000000010000000000000000000

  TRIOXAN DP/DQ
 0 1
   8    0.00000          -1.33997          -0.23177
   6    1.15573          -0.66726           0.20477
   8    1.16045           0.66998          -0.23177
   6    0.00000           1.33452           0.20477
   8   -1.16045           0.66998          -0.23177
   6   -1.15573          -0.66726           0.20477
   1    1.17653          -0.67927           1.29070
   1    2.02211          -1.16746          -0.20599
   1    0.00000           1.35854           1.29070
   1    0.00000           12.33493          -0.20599
   1   -1.17653          -0.67927           1.29070
   1   -2.02211          -1.16746          -0.20599
  -1
**EOF**
```

CHAPTER 4 - CYCLOHEXANE: ATOMIC POLAR TENSORS FROM EXPERIMENTAL BAND INTENSITIES.

Section 4.1 Method for the Analysis of Experimental Band Intensities.

A computer program SIGN has been constructed which evaluates the suitability of the possible sign combinations of the dp/dQ_i and computes the corresponding atomic polar tensors (for listing, see appendix). As well as the experimental band intensities, the following matrices are required as input:

B - Wilson B matrix; $B_{ij} = dR_i/dX_j$
F - Force constant matrix
M - diagonal matrix of atomic masses
Λ - diagonal matrix of vibrational frequencies
L - matrix which describes the form of each normal coordinate; $L_{ij} = dR_i/dQ_j$

These matrices (discussed previously in the Introduction) are produced by standard programs which carry out normal coordinate calculations. In this study the program F2.FOR, which had been previously written by D. Steele and co-workers, was employed. All these programs were written in FORTRAN, and the calculations performed on the VAX mainframe computer at Royal Holloway College.

The first step in SIGN is to derive the P_Q matrix from the experimental band intensities:

$$dp/dQ_i(eu^{-\frac{1}{2}}) = 0.03203[A_i(km\ mol^{-1})/d_i]^{\frac{1}{2}}$$

d_i being the degeneracy of the band.

A matrix is generated whose elements consist of +1 or -1, each row corresponding to a possible set of signs for the dp/dQ_i. At the end of each cycle of the full calculation this is used to change the signs of relevant entries in the P_Q matrix, to establish the suitability of a given sign combination.

The APT's are derived from P_Q using the relationship:

$$P_x = P_Q L^{-1} B$$

The L matrix is not inverted directly, but is calculated from

$$L^{-1} = \Lambda^{-1} L^t F$$

L^{-1} may be checked by ensuring that $L^{-1}L = E$, where E is a unit matrix.

The P_x thus obtained is then used to predict the band intensities of the fully deuterated compound:

$$P_Q = P_x AL$$

The product 'AL' is calculated using the expression

$$AL = M^{-1} B^t F L \Lambda^{-1}$$

and it is checked that BAL = L.

These calculated intensities are then compared with those obtained experimentally by defining a parameter 'f', the 'fit factor'

$$f = \sum_i |A_i(obs) - A_i(calc)|/A_i(obs)$$

The program yields a value of f for each possible combination of signs of selected $d\underline{p}/dQ_i$ (e.g. all the a_{2u} bands of cyclohexane). The magnitude of f is a measure of the suitability of each set of signs - the lower the value, the more likely that this is the correct sign combination.

Section 4.2 Cyclohexane Normal Coordinate Calculation.

The force constants required for input to 'P2', the program which carries out the normal coordinate computations, are taken from the hydrocarbon general valence force field developed by Snyder and Schachtschneider[30]. Its application to cyclohexane and its deuterated derivatives has been investigated by Wiberg

and Shrake.[31] The good agreement between calculated and observed vibrational frequencies led them to conclude that this was a satisfactory model for cyclohexane's force field. The results from this present calculation are tabulated below.

Due to the particular choice of axis system (see ab initio section) each infrared active mode produces a dipole moment change along only one of the x, y or z axes. For a_{2u} symmetry this along the z axis, and for the e_u bands half the intensity arises from changes in p_x alone and the other half from changes in p_y alone.

The first row of the APT will be determined only by the dp_x/dQ, the second row by dp_y/dQ, and the third by dp_z/dQ. Hence the signs of each Cartesian component of the dipole derivative may be varied independently since the a_{2u} and e_u intensities depend on different sets of independent parameters.

TABLE 29.

CALCULATED CYCLOHEXANE IR FREQUENCIES.

No.*	Cal.ν(cm^{-1})	Obs.ν(cm^{-1})	P.E. Distribution (%)
2	2930eu)	2933	52 CH^a, 48 CH^e
3	2930eu)		52 CH^a, 48 CH^e
4	$2927a_{2u}$	2914	50 CH^a, 50 CH^e
8	2856eu)	2863	48 CH^a, 52 CH^e
9	2856eu)		48 CH^a, 52 CH^e
12	$2855a_{2u}$	2863	60 CH^a, 40 CH^e
14	1457eu)	1449	76 HCH, 12 H^aCC, 12 H^eCC
15	1457eu)		76 HCH, 12 H^aCC, 12 H^eCC
18	$1449a_{2u}$	1449	76 HCH, 12 H^aCC, 12 H^eCC
21	1350eu)	1346	76 H^eCC, 12 H^aCC, 12 CC
22	1350eu)		76 H^eCC, 12 H^aCC, 12 CC
25	1258eu)	1257	64 H^aCC, 20 H^eCC
26	1258eu)		76 H^aCC, 14 H^eCC
35	$1005a_{2u}$	1038	42 CCC, 36 H^eCC, 12 H^aCC
36	897eu)	904	36 CC, 52 H^aCC
37	897eu)		36 CC, 52 H^aCC
38	860eu)	862	48 CC, 24 H^aCC, 24 H^eCC
39	860eu)		48 CC, 24 H^aCC, 24 H^eCC
43	$519a_{2u}$	524	40 CCC, 60 H^aCC
47	181eu)	241	76 CCC, 12 H^eCC
48	181eu)		76 CCC, 12 H^eCC

* Number in the full set of output frequencies - shall be used as a label below.

TABLE 30.

CALCULATED d_{12} CYCLOHEXANE FREQUENCIES.

No.	Cal.ν(cm^{-1})	Obs.ν(cm^{-1})	P.E. Distribution (%)
d2	2195eu)	2221	56 CD^a, 44 CD^e
d3	2195eu)		56 CD^a, 44 CD^e
d4	$2189a_{2u}$	2206	36 CD^a, 64 CD^e
d8	2092eu)	2111	40 CD^a, 56 CD^e
d9	2092eu)		50 CD^a, 50 CD
d12	$2086a_{2u}$	2104	66 CD^a, 30 CD^e
d16	1151eu)	1160	44 CC, 12 D^aCC, 44 D^eCC
d17	1151eu)		46 CC, 12 D^aCC, 42 D^eCC
d18	$1079a_{2u}$	1085	64 DCD, 12 CCC, 12 D^aCC
d23	1048eu)	1068	70 DCD, 12 D^aCC, 18 D^eCC
d24	1048eu)		70 DCD, 12 D^aCC, 18 D^eCC
d26	989eu)	988	8 CC, 60 D^aCC, 26 D^eCC
d27	989eu)		8 CC, 60 D^aCC, 8 D^eCC
d30	$885a_{2u}$	915	42 CCC, 36 D^eCC
d36	726eu)	719	48 CC, 10 D^aCC, 38 D^eCC
d37	726eu)		48 CC, 10 D^aCC, 40 D^eCC
d39	672eu)	685	64 D^aCC, 32 D^eCC
d40	672eu)		76 D^aCC, 24 D^eCC
d43	$388a_{2u}$	394	36 CCC, 50 D^aCC, 10 D^eCC
d47	145eu)	(190)	80 CCC
d48	145eu)		74 CCC

The L matrices for the molecular vibrations of cyclohexane. Contributions are given for representative internal coordinates. Others are deducible by symmetry.

A_{2u}

coordinate\ν/cm-1	2927	2855	1448	1005	519
Δr^a_7	-.277	-.320	.007	.002	.001
Δr^e_8	.327	-.268	.007	-.014	.002
$(rR)^{½}\Delta\beta^a_{716}$	.016	-.018	-.178	.101	.137
$(rR)^{½}\Delta\beta^e_{816}$	-.047	.012	-.141	-.222	-.077
$R\Delta\theta_{216}$	.079	-.069	-.079	.289	-.157
$r\Delta\alpha_{718}$	-.005	.059	.603	-.005	.012

E_u

coordinate\ν/cm-1	2930	2856	1457	1350	1257	897	860	181
Δr^a_7	.384	.348	.004	.001	.018	.010	.000	.000
Δr^e_8	-.358	.375	.010	.008	-.004	.000	-.008	.000
$r\Delta\alpha_{718}$	.000	-.070	.723	-.102	.087	.049	-.057	-.013
ΔR_{16}	-.002	-.044	.042	.104	.045	.115	-.128	.007
$R\Delta\theta_{216}$	.045	.045	-.033	-.059	-.097	-.149	.069	.086
$(rR)^{½}\Delta\beta^a_{712}$	-.052	.009	-.179	.107	-.133	.302	.207	-.007
$(rR)^{½}\Delta\beta^a_{716}$	-.100	-.004	-.251	-.131	.382	.079	.112	.002
$(rR)^{½}\Delta\beta^e_{812}$	.057	.002	-.141	.391	-.042	-.202	-.101	-.024
$(rR)^{½}\Delta\beta^e_{816}$	.057	.036	-.246	-.197	-.226	-.110	-.210	-.029

Evaluation of sign choices for d_o Cyclohexane $\frac{dp_z}{dQ}$.

Input d_o Sign Choice					Fit Factor	
4	12	18	33	43		
+	+	-	-	-	0.271	1
+	+	+	-	-	0.331	2
+	-	+	+	+	0.361	3
+	-	-	-	-	0.372	4
+	+	-	+	+	0.394	5
+	+	+	+	+	0.413	6
+	+	-	-	+	0.424	7
+	-	-	+	+	0.432	8
+	-	+	-	-	0.435	9
+	+	+	+	-	0.438	10
+	-	+	+	-	0.443	11
+	+	+	-	+	0.510	12
+	-	-	-	+	0.540	13
+	-	-	+	-	0.547	14
+	+	-	+	-	0.568	15
+	-	+	-	+	0.574	16

TABLE 31.

Section 4.4 Determination of Signs of dp_x/dQ and dp_y/dQ.

There are eight eu bands, but only seven values of dp_x/dQ to be varied, since the lowest frequency has zero experimental intensity. Since the magnitude of the dipole moment change must be equal for each component of the degenerate pair, the value of dp_x/dQ_i is obtained from half the observed intensity of the i^{th} d_o eu band. There are $2^7 = 128$ possible sign combinations of which 64 are actually completely independent, the rest just corresponding to a reversal of all these signs. The bands that contribute to the derived fit factor for the x components are d17, d24, d26, d36 and d40 - as before, the CD stretches are excluded due to the overlap problem.

Exactly the same reasoning applies to an investigation of the signs of the y components. In this case the bands which define the fit factor are d16, d23, d27, d37 and d39. The results for both components are listed below.

Once the sign has been chosen for a given dp_x/dQ_i, the sign of the corresponding dp_y/dQ_i is predetermined by symmetry. Similarly, once a given sign combination is chosen for the x-components, there is only one combination for the y-component which will pair with this to give polar tensors possessing the correct symmetry properties. As the table shows, the possible pairs of sign combinations are those sets which possess the same value of the fit factor. There still remains some ambiguity at this stage, however, since reversing the signs in each set will yield the same result. Thus there are four permutations of 'x-signs plus y-signs' that appear possible by simply considering the fit factor - only two of these yielding symmetrically correct tensors, only one of which is appropriate to physical reality. This ambiguity may be removed, as will be seen below, by use of the polar tensors derived from the ab initio calculations.

TABLE 32.

Evaluation of Sign Choices for d_o Cyclohexane dp_x/dQ and dp_y/dQ.

Order	Fit Factor	x Signs	y Signs
1	0.607	+ - + + - - -	+ - + + + - -
2	0.680	+ + + + - - -	+ + + + + - -
3	0.681	+ + - - + + +	+ + - - - + +
4	0.694	+ - - - + + +	+ - - - - + +
5	0.779	+ + - - + - +	+ + - - - - +
6	0.872	+ - + - - - -	+ - + - + - -
7	0.887	+ + - - + - -	+ + - - - - -
8	0.933	+ + - + + + +	+ + - + - + +
9	0.961	+ - - - + - -	+ - - - - - -
10	0.971	+ - + + - - +	+ - + + + - +
11	0.975	+ + + - - - -	+ + + - + - -
12	0.978	+ - - + + + +	+ - - + - + +
13	0.997	+ - - - + + -	+ - - - - + -
14	0.998	+ - - - + - +	+ - - - - - +
15	1.006	+ + + + - - +	+ + + + + - +
16	1.024	+ - + + - + -	+ - + + + + -
17	1.028	+ + - - + + -	+ + - - - + -
18	1.099	+ - + - - - +	+ - + - + - +
19	1.113	+ + - + + - -	+ + - + - - -
20	1.137	+ + - + + + -	+ + - + - + -
21	1.149	+ + - + + - +	+ + - + - + -
22	1.149	+ - - + + + -	+ - - + - + -
23	1.174	+ + + - - - +	+ + + - + - +
24	1.200	+ - + + - + +	+ - + + + + +
25	1.200	+ + + + - + -	+ + + + + + -
26	1.221	+ - - + + - -	+ - - + - - -
27	1.280	+ + + + - + +	+ + + + + + +
28	1.309	+ - - + + - +	+ - - + - - +
29	1.373	+ + - - - + +	+ + - - + + +
30	1.382	+ + - - - - +	+ + - - + - +
31	1.414	+ - + - - + -	+ - + - + + -
32	1.441	+ - + - - + +	+ - + - + + +
33	1.484	+ - + + + - -	+ - + + - - -
34	1.492	+ - - - - + +	+ - - - + + +
35	1.543	+ - + + + + -	+ - + + - + -
36	1.553	+ + + - - + +	+ + + - + + +
37	1.569	+ + - - - - -	+ + - - + - -
38	1.584	+ + + - - + -	+ + + - + + -

continued...

39	1.608	+ + + + + - -	+ + + + - - -
40	1.646	+ - - - - - +	+ - - - + - +
41	1.676	+ - - - - - -	+ - - - + - -
42	1.771	+ + - + - + +	+ + - + + + +
43	1.778	+ + - + - - +	+ + - + + - +
44	1.809	+ + + + + + -	+ + + + - + -
45	1.830	+ - + + + + +	+ - + + - + +
46	1.896	+ - + - + - -	+ - + - - - -
47	1.923	+ - - + - + +	+ - - + + + +
48	1.939	+ - - + - - +	+ - - + + - +
49	1.945	+ + - + - - -	+ + - + + - -
50	1.942	+ + + + + + +	+ + + + - + +
51	2.020	+ - + - + + -	+ - + - - + -
52	2.053	+ + + - + - -	+ + + - - - -
53.	2.077	+ + - - - + -	+ + - - + + -
54	2.085	+ - - + - - -	+ - - + + - -
55	2.111	+ - - - - + -	+ - - - + + -
56	2.181	+ + + - + + -	+ + + - - + -
57	2.220	+ - + - + + +	+ - + - - + +
58	2.223	+ - + + + - +	+ - + + - - +
59	2.268	+ + + + + - +	+ + + + - - +
60	2.286	+ + - + - + -	+ + - + + + -
61	2.363	+ - - + - + -	+ - - + + + -
62	2.365	+ + + - + + +	+ + + - - + +
63	2.452	+ - + - + - +	+ - + - - - +
64	2.539	+ + + - + - +	+ + + - - - +

In these tables, it is apparent that there is no great spread in the values obtained for the fit factor - .271 to .574 in the a_{2u} bands and .605 to 2.546 in the eu bands. This does not imply that two sign choices with very similar values of 'f' lead to similar values of derived d_{12} intensities. For instance, consider the following example from the dp_z/dQ sign variations.

No. 13: + - - - + , f = 0.540

d_{12} band	Obs. A_i/km mol^{-1}	Calc. A_i/km mol^{-1}
18	5.3	1.19
30	3.5	4.95
43	0.4	0.23

No. 14: + - - + - , f = 0.547

18	5.3	4.89
30	3.5	0.12
43	0.4	0.16

Note that although f is practically the same, the values calculated for d18 and d30 are very different.

Section 4.5 The use of Ab Initio Data to Help Resolve Sign Ambiguity.

At this stage, the only criterion offered for deciding the suitability of a given sign combination has been the value of the fit factor. How reliable a guide is this? The magnitude of this parameter will be influenced by experimental error and the quality of the force field employed.

An ab initio set of APT's was calculated for cyclohexane using the Gaussian 76 package, and these may be used to predict the signs of the dp/dQ_i and the magnitude of the band intensities, acting as a source of information completely independent from the experimental measurements. The results are shown in the following tables.

For both d_0 and d_{12} cyclohexane the calculated intensities are generally of the correct magnitude, as is the distribution across the total spectrum - the majority of intensity is found in the CH stretches (the predicted total being ~40% high), whilst the weakest bands are calculated to possess correspondingly low values.

Significantly, the signs of the calculated dipole derivatives for the a_{2u} bands are precisely those found to yield the optimum fit factor. This agreement must lead to optimism in the reliability of both procedures. However, the same is not immediately true for the eu bands - the ab initio sign combination being only 12th in the previous table. If the list is examined further, a group of signs very similar to the ab initio set is that possessing the 4th lowest fit factor. On reversing <u>all</u> the signs, the only discrepency is then the sign of the 1350cm^{-1} band, this being anyhow extremely weak. Thus this appears to be the correct sign choice for the x and y components.

Comparison of d_0 Cyclohexane experimental band intensities with those predicted using Ab Initio Atomic Polar Tensors.

Calc ν/cm^{-1}	Obs ν/cm^{-1}	Obs A_i/km mol^{-1}	Calc A_i/km mol^{-1}	Sign of dp/dQ	
2930(eu)	2933)	370	133.4	x	+
	)			y	-
2927(a_{2u})	2914?)		159.2	z	+
2856(eu)	2863)	103	269.2	x	-
	)			y	+
2855(a_{2u})	2863)		106.0	z	+
1457(eu)	1449)	23.65	10.0	x	-
	)			y	+
1449(a_{2u})	1449)		23.2	z	-
1350(eu)	1346	0.24	1.2	x	+
				y	-
1258(eu)	1257	3.6	0.6	x	+
				y	+
1005(a_{2u})	1038	2.0	2.5	z	-
897(eu)	904	2.8	1.0	x	+
				y	-
860(eu)	862	3.8	8.0	x	+
				y	-
519(a_{2u})	524	0.46	0.06	z	-
181(eu)	241	~0	0.4		

TABLE 33.

Comparison of d_{12} Cyclohexane Experimental Band Intensities with those predicted using Ab Initio Atomic Polar Tensors.

Calc ν/cm^{-1}	Obs ν/cm^{-1}	Obs A_i/km mol^{-1}	Calc A_i/km mol^{-1}
2195(eu)	2221	248.8	62.1
2189(a_{2u})	2206		73.3
2092(eu)	2111		143.0
2086(a_{2u})	2104		65.1
1151(eu)	1160	6.4	1.8
1079(a_{2u})	1085	5.3	9.1
1048(eu)	1068	1.2	4.5
999(eu)	988	5.9	2.4
885(a_{2u})	915	3.5	5.4
726(eu)	719	1.4	1.0
672(eu)	685	2.1	4.6
388(a_{2u})	394	0.43	.05
145(eu)	(190)	0	0.2

TABLE 34.

Section 4.6 Significance of the Intensity Distribution in Regions A, B and C.

Having examined the sign choices, it is now necessary to consider the repercussions of the band overlap in regions A(3030-2894 cm^{-1}), B(2894-2830 cm^{-1}) and C(1449 cm^{-1} band). Each of these contains an eu and an a_{2u} band. Three different parameters were used to investigate the effect of a redistribution of intensity (between eu and a_{2u} bands) within each region: the fit factor, the total calculated CD stretch intensity, and the effective atomic charges of the hydrogen atoms.

The only parameter found to be dependent on the splitting in region C is the fit factor. Increasing the proportion of intensity given to the a_{2u} band leads to an increase in the intensities predicted for the d_{12} a_{2u} bands.

d_{12} Band No.	Obs.A_i/km mol^{-1}	Calc.A_i (1)	Calc. A_i (2)
18	5.3	9.4	0.1
30	3.5	4.9	1.6
43	0.4	0.3	0.3

Splitting (1) is 0,0,23.7
Splitting (2) is 11.85, 11.85, 0

The splitting that yields the best fit for both a_{2u} and eu bands is 4.9, 4.9, 13.9:

d_{12} Band No.	Obs.A_i/km mol^{-1}	Calc. A_i/km mol^{-1}
d17	3.2	1.4
d18	5.3	5.1
d24	0.6	0.6
d26	3.0	3.7
d30	3.5	4.0
d36	0.7	0.0
d40	1.05	1.7
d43	0.4	0.3
d47	0	0

f = 0.356

So with the sign choice chosen, this represents the best partitioning of intensity within region C. But it is now necessary to check that, with this changed splitting, this sign choice still retains its position in the listing of choice against fit factor. The consequences for the five best combinations for x and z components are shown below.

x Sign	Old Fit Factor	New Fit Factor
+ - + + - - -	.607	.414
+ + + + - - -	.680	.482
+ + - - + + +	.681	.603
+ - - - + + +	.694	.487
+ + - - + - +	.779	.640

z Sign	Old Fit Factor	New Fit Factor
+ + - - -	.271	.138
+ + + - -	.331	.562
+ - + + +	.361	.320
+ - - - -	.372	.328
+ + - + +	.394	.611

These show that the splitting in block C can alter the relative ordering of the sign combinations, though in the above the chosen sets retain their positions.

Considering the a_{2u} bands alone, if all the intensity of the 1449cm^{-1} band is attributed to the eu band, a subsequent variation of sign choices then gives:

+ + - - - , f = .562
+ - + - + , f = .502

and the latter becomes top of the z sign list. But, in conclusion, the best pairing of 'sign choice + splitting' is that which yields a low value of the fit factor, and the chosen sign combination cannot lose its position in such a list without the fit factor rising overall. Thus the lowest z sign choice with the 4th lowest x and y sign choice are the best combinations, the latter being in accord with the ab initio calculation, and the best splitting is 4.9, 4.9, 13.9 in block C.

The splittings in regions A and B are found to affect the fit factor to a completely negligible degree - the intensity contained in these regions only determines the magnitude of the dipole change along the direction of the CH bonds. Again, the total CD stretch intensity is insensitive to the splitting, and remains steady at a value of ~0.97 of that observed experimentally. The parameter which is found to be sensitive to the redistribution of intensity from eu to a_{2u} bands is the hydrogen effective atomic charge, and more specifically, the relative values for the axial and equatorial hydrogen.

The ab initio calculations give $X_{H^a} = .125$, $X_{H^e} = .154$, whilst experiment yields the average value of $X_H = .115$. The average ab initio value of ~.139 is 21% too high. Since part of this error could be an overestimation of the equatorial value, it would probably be unwise to impose the suggested differentiation between the hydrogens at this stage. Thus, in parallel with the equality of axial and equatorial stretching force constants employed in the normal coordinate calculations, the values of X_{H^a} and X_{H^e}, which are dependent on the splitting in regions A and B, will be constrained to be equal.

The procedure adopted is to decide on a sensible intensity distribution in region A, and then vary that in section B so as to achieve this equalization. If the assignment of the 2914cm^{-1} band, a weak shoulder, as the a_{2u} fundamental is correct, then most of the intensity should be given to the overlapping eu band. However, it is possible that this represents a scissoring combination band. This interpretation is supported by the ab initio calculations, which suggest that 54% of the total intensity in A should be given to the a_{2u} band.

The reliability of the Gaussian 76 results is shown by the satisfactory accord between observed and calculated band intensities, and especially in the prediction of correct sign choices for the $d\underline{p}/dQ$. An encouraging sign as far as the splitting is concerned appears on referring back to the 1449cm^{-1} d_0 bands. Even though the total intensity of this band is calculated 42% too high, the a_{2u} band is calculated to possess 70% of the intensity, which is close to the value of 59% which is derived from the fit factor calculations above. Thus, in

the absence of any better information, the quantum mechanical prediction of splitting in region A is adopted - a_{2u} = 212 km mol^{-1}, eu = 158 km mol^{-1}.

This does represent the most arbitrary assumption in this cyclohexane analysis. It should be recalled, however, that any subsequent error will only transfer to the magnitude of the dipole changes along the direction of the CH bonds, and will not invalidate the other features of the APT's calculated.

The splitting in region B that equalises the effective charges is a_{2u} = 51 km mol^{-1}, eu = 52 km mol^{-1}, and $\chi_{H^a} = \chi_{H^e} = 0.118$, which is in good agreement with the experimental value of 0.115.

Thus, the sign choices and intensity distributions have been derived, and now the APT's which result may themselves be considered.

Section 4.7 Atomic Polar Tensors for Cyclohexane.

The following sign combinations were employed in deriving the set of experimental APT's for cyclohexane:

	~2930cm^{-1}	2863cm^{-1}	1449cm^{-1}	1038cm^{-1}	524cm^{-1}
dp_z/dQ	+	+	-	-	-

	2930	2963	1449	1346	1257	904	862cm^{-1}
dp_x/dQ	+	-	-	-	+	+	+
dp_y/dQ	-	+	+	+	+	-	-

The splitting of total intensity within regions A, B, and C is:

A(~2930cm^{-1}): a_{2u} = 212km mol^{-1}, eu = 158 km mol^{-1}
B(~2863cm^{-1}): a_{2u} = 51 km mol^{-1}, eu = 52 km mol^{-1}
C (1449cm^{-1}): a_{2u} = 13.9km mol^{-1}, eu = 9.8 km mol^{-1}

The APT's calculated under these conditions are now presented alongside those derived from the Gaussian 76 package. The following numbering system is employed:

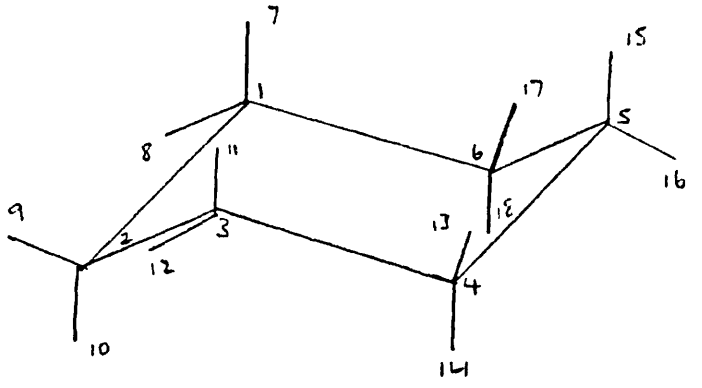

	EXPERIMENTAL			AB INITIO		
C1	.085	-.034	-.038	.129	-.078	-.023
	-.034	.046	.022	-.078	.039	.013
	-.072	.042	.176	-.028	.016	.171
C2	.026	0	0	-.006	0	0
	0	.105	-.044	0	.174	-.027
	0	-.083	.177	0	-.032	.171
H^a7	.032	-.022	.051	.037	-.018	-.031
	-.022	.006	-.029	-.018	.016	.018
	.020	-.011	-.190	.031	-.018	-.206
H^a10	-.007	0	0	.006	0	0
	0	.045	.058	0	.047	-.035
	0	.023	-.190	0	.035	-.206
H^e8	-.127	.074	.057	-.176	.114	.078
	.074	-.042	-.033	.114	-.045	-.045
	.078	-.045	.014	.044	-.025	.035
H^e9	0	0	0	.021	0	0
	0	-.169	.066	0	-.241	.091
	0	.090	.014	0	.051	.035

A detailed analysis of these APT's is delayed until later chapters, but one obvious feature that is very encouraging is the close correspondence between the 'experimental' and ab initio sets. Perhaps it is unclear to what extent this is made inevitable by the constraints imposed on the experimental APT's, but the fact remains that these were derived from observed d_0 intensities, and are capable of accurately predicting those found for the d_{12} compound.

CHAPTER 5. THE 1,4-DIOXAN FORCE FIELD.

Section 5.1 Evaluation of the Snyder and Zerbi Ether Force Field.

A prerequisite for the analysis of the experimental band intensities of a compound is the possession of a molecular force field that is able to correctly predict the form of each vibrational mode. Snyder and Zerbi[32] have derived a model general valence force field for aliphatic ethers from a procedure in which an initial field was refined so as to match the observed and calculated frequencies for ten compounds, one of which was 1,4-dioxan This force field forms the starting point for this investigation, and the numerical values of the force constants appear in Table35.

An indication of the suitability of this S+Z field for this study is the extent to which calculated vibrational frequencies match up with those that occur experimentally for undeuterated (d_0) and completely deuterated (d_8) 1,4-dioxan. These are presented in Tables 36 and 37.

TABLE 35. Snyder and Zerbi Force Constants.

Force Constant	Value*	Force Constant	Value
CH	4.626	CC/HCC	0.367
CO	5.090	COC/OCC	0.005
CC	4.261	COC/HCO_g	0.002
COC	0.640	COC/HCO_t	-0.062
OCC	0.545	OCC/OCC_g	-0.005
HCO	0.579	OCC/HCO	-0.017
HCH	0.403	OCC/HCC	-0.016
HCC	0.457	OCC/HCC_t	0.014
CH/CH	-.046	OCC/HCC_g	-0.059
CO/CO	0.288	HCO/HCO	-0.003
CO/CC	0.101	HCO/HCC	0.070
CO/COC	0.339	HCC/HCC	0.062
CO/OCC	0.420	HCC/HCC_g	0.002
CO/HCO	0.310	HCC/HCC_t	0.071
CC/OCC	0.274		

* Unless stated otherwise, the following units are used for constants:

Stretch, Stretch/stretch in mdyn $\AA^{-1}$

Bend, bend/bend in mdyn $\AA^{-1}(rad)^{-2}$

Stretch/bend in mdyn $\AA^{-1}(rad)^{-1}$

i.e. bend force constants are scaled by the lengths of the bonds that form the angle.

TABLE 36.

Snyder and Zerbi F.Field - Calculated Frequencies.

Obs.ν(cm^{-1})	Calc.ν(cm^{-1})	Potential Energy Distribution(%)
Ag		
2968	2971	48 CH^e, 50 CH^a
2856	2864	51 CH^e, 49 CH^a
1444	1470	65 HCH, 8 H^eCO, 10 H^aCO
1397	1354	17 H^eCO, 50 H^aCC, 41 H^aCO
1305	1245	21 H^eCC, 67 H^eCO, 26 H^aCO
1128	1141	8 OCC, 21 CO, 36 H^eCC, 25 H^aCC,8 H^aCO
1015	1057	72 CC, 26 CO, 17 H^eCC, 8 H^aCO, 9 OCC
837	825	38 CC, 59 CO
435	501	8 CC, 30 OCC, 55 COC
424	343	11 H^eCC, 47 OCC, 44 COC
Bg		
2968	2963	51 CH^e, 47 CH^e
2856	2862	48 CH^e, 52 CH^a
1459	1458	66 HCH, 12 H^eCC, 9 H^aCC
1335	1404	36 H^eCC, 45 H^eCO, 25 H^aCO
1217	1227	13 CO, 31 H^eCO, 58 H^aCO
1110	1150	70 CO, 10 H^eCC, 12 H^aCO, 11 OCC
853	841	23 CO, 31 H^eCC, 10 H^eCO, 36 H^aCO
490	483	23 H^aCO, 78 OCC
Au		
2970	2969	47 CH^e, 51 CH^a
2863	2863	52 CH^e, 48 CH^a
1449	1464	66 HCH, 10 H^eCO, 7 H^aCC, 7 H^aCO
1369	1356	10 H^eCC, 31 H^eCO, 50 H^aCC, 26 H^aCO
1256	1283	27 CO, 15 H^eCC, 26 H^eCO, 17 H^aCC, 28 H^aCO
1136	1122	24 CC, 53 CO, 25 H^eCO, 11 H^aCO
1086	1078	55 H^eCC, 14 H^aCC, 21 H^aCO
881	900	76 CC, 26 CO, 8 H^aCC, 10 OCC
288	175	75 OCC

continued...

continuation...

Bu

2970	2965	53 CH^e, 46 CH^a
2863	2863	47 CH^e, 54 CH^a
1457	1457	68 HCH, 10 H^eCC, 8 H^aCC
1378	1413	9 CO, 37 H^eCC, 37 H^eCO, 30 H^aCC
1291	1254	37 H^eCO, 12 H^aCC, 55 H^aCO
1052	1020	11 CO, 17 H^eCC, 16 H^eCO, 16 H^aCC, 25 OCC
889	880	95 CO, 18 COC
610	654	43 H^aCC, 42 OCC, 13 COC
274	224	24 OCC, 70 COC

TABLE 37.

Obs.ν(cm^{-1})	Calc.ν(cm^{-1})	Potential Energy Distribution(%)
Ag		
2242	2230	46 CH^e, 49 CH^a
2098	2098	51 CH^e, 47 CH^a
1225	1145	29 CC, 52 CO, 10 HCH, 30 H^eCO 14 H^aCC, 18 H^aCO
1108	1053	14 CC, 52 HCH, 31 H^aCC
1008	969	30 CC, 9 HCH, 15 H^eCC, 13 H^eCO, 36 H^aCO, 10 OCC
832	956	14 CC, 35 H^aCC, 30 H^aCO
808	868	58 H^eCC, 46 H^eCO, 8 H^aCC
752	768	28 CC, 49 CO
490	492	34 OCC, 49 COC
348	282	14 H^eCC, 41 OCC, 45 COC
Bg		
2226	2210	53 CH^e, 44 CH^a
2088	2093	44 CH^e, 55 CH^a
1070	1186	73 CO, 27 H^eCC, 17 H^aCO
1023	1056	70 HCH, 10 H^aCC
956	1039	13 H^eCC, 50 H^eCO, 16 CO
888	877	26 H^eCO, 11 H^aCC, 64 H^aCO
711	691	12 CO, 37 H^eCC, 27 H^aCC, 12 OCC
422	420	39 H^aCC, 66 OCC
Au		
2235	2226	44 CH^e, 52 CH^a
2086	2094	54 CH^e, 44 CH^a
1191	1188	25 CC, 81 CO. 12 H^aCC, 16 H^aCO
1117	1051	60 HCH, 22 H^eCO
1030	1017	9 CC, 8 HCH, 10 H^eCC, 36 H^eCO, 51 H^aCC
922	940	62 CC, 29 H^eCC, 12 H^aCC, 13 OCC
809	870	17 H^eCO, 68 H^aCO
762	789	22 CC, 17 CO, 46 H^eCC, 11 H^eCO, 15 H^aCC
254	142	74 OCC

continued...

continuation...

Bu

2232	2216	56 CH^e, 41 CH^a
2098	2095	40 CH^e, 58 CH^a
1153	1161	40 CO, 39 H^eCC, 28 H^eCO, 21 H^aCO
1087	1066	68 HCH, 10 H^aCC
1042	976	16 CO, 28 H^eCO, 51 H^aCO, 12 COC
896	885	18 H^eCO, 9 H^aCC, 9 H^aCO, 32 OCC, 11 COC
732	767	56 CO, 17 H^eCC, 16 H^eCO, 11 COC
490	522	21 H^eCC, 62 H^aCC, 31 OCC
238	198	21 OCC, 71 COC

Note: Inclusion of the S+Z torsion f.c. has a completely negligible effect on all frequencies except for the lowest in each symmetry species, which are raised by 10-20 cm^{-1}.

First consider d_0-dioxan. Overall there is a reasonably good agreement between observed and calculated frequencies, although in a number of cases some large discrepancies appear. In their paper, Snyder and Zerbi gave 1335 cm^{-1} as an Ag band, and 1397 cm^{-1} as a Bg band - here the reverse assignment has been made, since the latter appears definately polarised in the Raman spectrum. This explains why 1335 cm^{-1} seems poorly predicted as 1404 cm^{-1}.

It is in Table37, with d_8-dioxan, that the largest discrepancies are apparent. The replacement of hydrogen by deuterium completely changes the character of corresponding normal modes, the severe degree of mixing providing a stringent test of the accuracy of the suggested interaction force constants. Errors of the order of ~100 cm^{-1}, e.g. 832 (956) cm^{-1} Ag, 1070 (1186) cm^{-1} Bg, indicate that this force field cannot be used with confidence to generate the L matrix required for the intensity analyses, so an attempt has been made to obtain a field that will describe the normal modes more accurately.

Section 5.2 Force Field Refinement.

In this section it is described how the standard force constant perturbation procedure has been applied, in an attempt to fit the experimental frequencies of d_0 and d_8 - dioxan to a common general valence type force field.

In this procedure, an initial trial force field is modified so as to minimize an error vector, which is defined by

$$X^1 = \sum_i \omega_i (\lambda_i{}^{obs} - \lambda^1{}_i)^2$$

$\lambda_i{}^{obs}$ is the observed vibrational frequency; ω_i is the weighting factor for the ith observed frequency.

$\lambda_i{}^1$ is the frequency predicted by the trial force field.

The way the force field is modified is determined by the equation

$$J^t{}_\omega \Delta\Lambda = J^t{}_\omega J \Delta\Phi$$

or

$$\Delta\Phi = (J^t\omega J)^{-1}J^t\omega\Delta\Lambda$$

$\Delta\Phi$ is a column matrix, whose elements are the force constants, ϕj.
$\Delta\Lambda$ is a column matrix, where elements are $\Delta\lambda_i^n$:
$\Delta\lambda_i^n = \lambda_i^{obs} - \lambda_i^n$, 'n' being the number of the iteration cycle.
ω is a square diagonal matrix - the i, ith element is ω_i.
J is the Jacobian matrix:

$$J_{ij} = \left| \frac{\partial\lambda_i}{\partial\phi_j} \right|$$

In fact,

$$\frac{\partial\lambda_k}{\partial F_{ij}} = 2L_{ik}\,L_{jk} \quad (i\neq j)$$

and

$$\frac{\partial\lambda_k}{\partial F_{ii}} = (L_{ik})^2$$

Thus starting from the initial force field Φ^1, J^1 and $\Delta\Lambda^1$ may be calculated and then $\Delta\Phi^1$. A new field is then formed, $\Phi^2 = \Phi^1 + \Delta\Phi^1$.

If the assumptions on which the equation is based (that the relationship between the force constant correction and frequency correction, $\Delta\lambda_i$, is <u>linear</u>) are completely obeyed, then the best force field would be obtained in one cycle only. However, in reality this procedure is carried out until the error vector reaches its minimum value.

In order to successfully apply a perturbation procedure to the problem of deriving force constants from observed vibrational frequencies, the latter must be assigned to their correct symmetry species. In this study, the assignments employed are those suggested by Ellestad and Klaboe. In the Raman spectra, the differentiation between Ag and Bg modes is made primarily on the basis of polarisation data, whilst in the infrared spectra the bands may theoretically be classified as Au or Bu according to their contours in the gas phase.

In d_0-dioxan, the intermediate inertial axis I_B coincides with the two-fold symmetry axis, but in d_8-dioxan the latter

coincides with the lowest axis of inertia, I_A. Thus for d_0-dioxan, a_u bands should have B-type contours and b_u bands should have A/C hybrid contours. In d_8-dioxan, a_u bands will have A-type contours and b_u bands B/C hybrid contours. Typically, the three forms of band envelope assume the following shape:

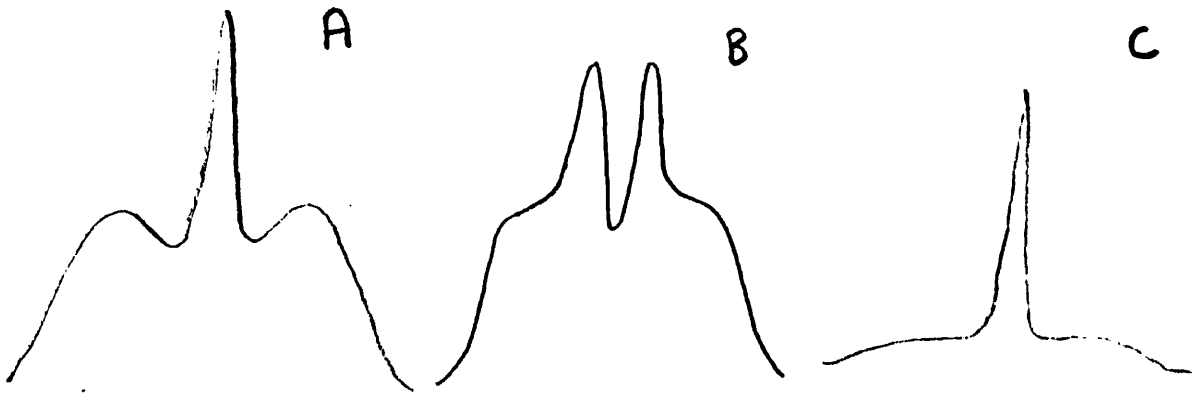

In reality, the bands are often overlapping and often possess an indistinctive contour. The difference between A and B/C is anyhow a rather subjective quantity.

Ellestad and Klaboe have listed their arguments for their assignments, and call upon evidence from additional sources of information, such as normal coordinate calculations on similar molecules, and low temperature spectra. In this project it is considered that these assignments are satisfactory, and are not investigated further.

Any residual doubt concerning the assignment or exact frequency of a band may be expressed by imposing a weighting factor on that frequency which is less than unity. The following bands were treated in this way:

Band	Weighting.	Reason.
d_0, 1110(Bg)	0.5	Polarization in question.
d_0, 2863(Au)	0.5	B type contour not discernable.
d_0, 1449(Au)	0.5	Ill defined contour.
d_0, 288(Au)	0.0	Not observed.
d_0, 881(Au)/ 889(Bu)	0.5 0.5	Overlapping, ill defined contours.
d_8, 808(Ag)	0.1	Weak band between two strong polarized bands.
d_8, 2088(Bg)	0.5	Polarization in question.
d_8, 1023(Bg)	0.2	" " "
d_8. 2086(Au)	0.8	Uncertain band contour.
d_8, 1030(Au)	0.2	" " "
d_8. 922(Au)	0.1	Extremely weak band.
d_8. 254(Au)	0.0	Not observed.

This is a rather arbitrary procedure since it attempts to compensate for an unknown degree of error. This simply reflects the uncertainties that must remain inherent to the perturbation method.

Section 5.3 Force Field A.

In the derivation of this force field, the initial Snyder and Zerbi dioxan force constants were varied through five cycles of iteration. The resulting field contained many ill-defined elements with large standard deviations, so this in turn formed the basis for further investigation, various interactions being set equal to zero and then the rest of the field perturbed in order to discover those force constants which were both important and determinable.

During this procedure, the HCH diagonal force constant was held at its Snyder and Zerbi value since it is a redundant coordinate - angle changes around the carbon atom are completely defined by the OCC, H^aCC, H^eCC, H^aCO and H^eCO internal coordinates. All the force constants then assume values consistent with that chosen for f_{HCH}.

It is found necessary to similarly fix the CC/OCC interaction in order to adequately determine f_{CC} and CO/CO, since it is very highly correlated with these.

Thus 'Force Field A' has been produced - a 22 parameter field that reasonably reproduces the experimental frequencies for both undeuterated and completely deuterated compounds. The details from this calculation are tabulated below, but before this is a description of the methods used to obtain a rather different, but at this point equally reliable field - 'Force Field B'.

Section 5.4 Derivation of Constraints Based on Ab Initio Force Constants.

It has been described how the quantum mechanical package Gaussian 76 was used to obtain a set of 'ab initio' symmetrized force constants. (Note that the units employed for force constants in this section only are Nm^{-1} for stretches and stretch/stretch interactions, $Nm^{-1}(rad)^{-2}$ for bends and bend/bend interactions, and $Nm^{-1}(rad)^{-1}$ for stretch/bend interactions. To convert from Nm^{-1} to mdyn $\AA^{-1}$, simply divide the former by 10^2.) In this section it will be demonstrated that an analysis of these leads to a series of constraints which may then be imposed on the force constant perturbation procedure.

At this stage it should be emphasized that one of the aims of this study is to obtain force constants that are not necessarily unique to 1,4-dioxan, but which may prove transferable to chemically related compounds such as tetrahydropyran and trioxan. For this to be possible, they should be related to an internal coordinate basis set rather than based on symmetry coordinates. It is then necessary to examine the relationship between these in order to proceed.

The transformation between internal and symmetry coordinates is given by

$$S = UR$$

and that between symmetrized and non-symmetrized force constants is

$$F(sym) = UFU^t$$

This transformation may result in a modification of the numerical values of both diagonal and off diagonal force constants - a simple case will illustrate how this occurs.

Consider the CO,CC portion of the force constant matrix,

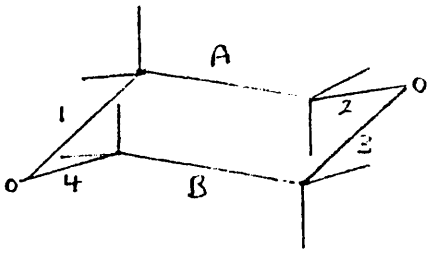

$$\begin{array}{c} \\ S_1{}^{Ag} \\ S_2{}^{Ag} \end{array} \begin{bmatrix} CO_1 & CO_2 & CO_3 & CO_4 & CC^A & CC^B \\ \frac{1}{2} & \frac{1}{2} & \frac{1}{2} & \frac{1}{2} & 0 & 0 \\ 0 & 0 & 0 & 0 & \frac{1}{\sqrt{2}} & \frac{1}{\sqrt{2}} \end{bmatrix}$$

$$F = \begin{array}{c} \\ CO^1 \\ CO^2 \\ CO^3 \\ CO^4 \\ CC^A \\ CC^B \end{array} \begin{bmatrix} CO^1 & CO^2 & CO^3 & CO^4 & CC^A & CC^B \\ f_{CO} & & & CO/CO & CO/CC & \\ & f_{CO} & CO/CO & & CO/CC & \\ & CO/CO & f_{CO} & & & CO/CC \\ CO/CO & & & f_{CO} & & CO/CC \\ CO/CC & CO/CC & & & f_{CC} & \\ & & CO/CC & CO/CC & & f_{CC} \end{bmatrix}$$

The above gives the form of the F matrix which includes the CO/CO and CO/CC interactions. (Below this will be expanded to include CO/CO opp, between e.g. CO^1 and CO^2.)

$$UF = \begin{bmatrix} \frac{1}{2}(f_{CO}+CO/CO), \frac{1}{2}(f_{CO}+CO/CO), \frac{1}{2}(f_{CO}+CO/CO), \frac{1}{2}(f_{CO}+CO/CO), CO/CC, CO/CC \\ \frac{1}{\sqrt{2}}(CO/CC), \frac{1}{\sqrt{2}}(CO/CC), \frac{1}{\sqrt{2}}CO/CC, \frac{1}{\sqrt{2}}CO/CC, \frac{1}{\sqrt{2}}f_{CC}, \frac{1}{\sqrt{2}}f_{CC} \end{bmatrix}$$

and finally,

$$UFU^t = \begin{bmatrix} f_{CO} + CO/CO, & CO/CC \\ CO/CC & f_{CC} \end{bmatrix}$$

Thus F_{CO}^{Ag} actually differs from the non-symmetrized force constant by the CO/CO interaction term. The mixing of these terms may change when considering different symmetry species. Using the above example but now considering the Bg block, the row of the U matrix is derived from

$$S_{CO}^{Bg} = \tfrac{1}{2}(CO_1 - CO_2 + CO_3 - CO_4)$$

and on computing UFU^t,

$$F_{CO}^{Bg} = f_{CO} - CO/CO$$

Hence in principle, f_{CO} and CO/CO may be calculated from a knowledge of the numerical values of these two symmetrized force constants.

Having made this preliminary discussion, the above approach will be utilized in analysing the ab initio results in detail. The symmetrized force constants are tabulated for the Ag, Bu and Au blocks, together with the CO/OCC portion of the Bg block in the ab initio chapter.

An important feature which is apparent in these results is that all the symmetrized force constants associated with H^aCO, H^eCO, H^aCC, H^eCC and OCC are disproportionately large and the corresponding interaction constants have all adopted a similar value. This may be shown to be a consequence of omitting the redundant HCH coordinate. The redundancy condition involving the angles around the carbon atom (assuming they are tetrahedral) may be written:

$$\Delta OCC + \Delta H^aCO + \Delta H^eCO + \Delta H^aCC + \Delta H^eCC + \Delta HCH = 0$$

The following symmetry coordinates may then be constructed:

$$S_1 = \frac{1}{\sqrt{2}}(\Delta OCC - \Delta HCH); \qquad S_2 = \frac{1}{\sqrt{2}}(\Delta H^eCO - \Delta HCH)$$

$$S_3 = \frac{1}{\sqrt{2}}(\Delta H^aCO - \Delta HCH); \qquad S_4 = \frac{1}{\sqrt{2}}(\Delta H^eCC - \Delta HCH)$$

$$S_5 = \frac{1}{\sqrt{2}}(\Delta H^aCC - HCH).$$

The relevant portion of the F matrix is:

	OCC	H^eCO	H^aCO	H^eCC	H^aCC	HCH
OCC	f_{OCC}	OCC/H^eCO	OCC/H^aCO	OCC/H^eCC	OCC/H^aCC	-
H^eCO		f_{H^eCO}	H^eCO/H^aCO	H^eCO/H^eCC	-	HCH/H^eCO
H^aCO			f_{H^aCO}	-	H^aCO/H^aCC	HCH/H^aCO
H^eCC				f_{H^eCC}	H^eCC/H^aCC	HCH/H^eCC
H^aCC					f_{H^aCC}	HCH/H^aCC
HCH						f_{HCH}

The impact of the redundancy on the corresponding ab initio force constants may be examined by forming UFU^t.

It is convenient to revert to the following notation in these matrices:

$\alpha \equiv HCH$, $\theta \equiv OCC$, $\beta_a^o = H^aCO$, $\beta_e^o = H^eCO$, $\beta_e^c = H^eCC$, $\beta_a^c = H^aCC$ See following page.

It is seen that the f_{HCH} constant is added to all the elements of this portion of the $\mathcal{F}$ matrix. This means that f_{OCC}, f_{H^eCO}, f_{H^aCC}, f_{H^eCC}, f_{H^aCO} and all their interaction constants cannot individually be determined. However, since the calculated results show that the off diagonals have approximately the same value, the average of these may be associated with f_{HCH} and the symmetrized force constants accordingly 'corrected' - this f_{HCH} being subtracted from the diagonals and the interactions then set equal to zero.

This is actually not the only redundancy condition to influence the calculated ab initio force constants. In the section describing the calculations required for the input to Gaussian 76, a redundancy was revealed in the A_u block, it not being possible to deform either CO or CC without simultaneously changing the OCC angle:

$$
UF = \begin{array}{c} \begin{matrix} \delta\theta & \delta\beta_e^o & \delta\beta_a^o & \partial\beta_e^c & \partial\beta_a^c & \partial\alpha \end{matrix} \\ \begin{bmatrix} \frac{1}{\sqrt{2}} & & & & & -\frac{1}{\sqrt{2}} \\ & \frac{1}{\sqrt{2}} & & & & -\frac{1}{\sqrt{2}} \\ & & \frac{1}{\sqrt{2}} & & & -\frac{1}{\sqrt{2}} \\ & & & \frac{1}{\sqrt{2}} & & -\frac{1}{\sqrt{2}} \\ & & & & \frac{1}{\sqrt{2}} & -\frac{1}{\sqrt{2}} \end{bmatrix} \end{array} \begin{bmatrix} f_\theta & \theta/\beta^o & \theta/\beta^o & \theta/\beta^c & \theta/\beta^c & \\ & f_{\beta e}^o & \beta^o/\beta^o & \beta^o/\beta^c & & \alpha/\beta^o \\ & & f_{\beta a}^o & & \beta^o/\beta^c & \alpha/\beta^o \\ & & & f_{\beta e}^c & \beta^c/\beta^c & \alpha/\beta^c \\ & & & & f_{\beta a}^c & \alpha/\beta^c \\ & & & & & f_\alpha \end{bmatrix}
$$

$$
= 2^{-\frac{1}{2}} \begin{bmatrix} f_\theta, & \theta/\beta^o-\alpha/\beta^o, & \theta/\beta^o-\alpha/\beta^o, & \theta/\beta^c-\alpha/\beta^c, & \theta/\beta^c-\alpha/\beta^c, & -f_\alpha \\ \theta/\beta^o, & f_{\beta 2}^o-\alpha/\beta^o, & \beta^o/\beta^o-\alpha/\beta^o, & \beta^o/\beta^c-\alpha/\beta^c, & -\alpha/\beta^c, & \alpha/\beta^o-f_\alpha \\ \theta/\beta^o, & \beta^o/\beta^o-\alpha/\beta^o, & f_{\beta a}^o-\alpha/\beta^o, & -\alpha/\beta^c & \beta^o/\beta^c-\alpha/\beta^c, & \alpha/\beta^o-f_\alpha \\ \theta/\beta^c, & \beta^o/\beta^c-\alpha/\beta^o, & -\alpha/\beta^o, & f_{\beta e}^c-\alpha/\beta^c & \beta^c/\beta^c-\alpha/\beta^c, & \alpha/\beta^c-f_\alpha \\ \theta/\beta^c, & -\alpha/\beta^o, & \beta^o/\beta^c-\alpha/\beta, & \beta^c/\beta^c-\alpha/\beta^c, & f_{\beta a}^c-\alpha/\beta^c, & \alpha/\beta^c-f_\alpha \end{bmatrix}
$$

$$UFU^{t}=2^{-1}\begin{bmatrix} f_{\theta}+f_{\alpha}, & \theta/\beta^{o}-\alpha/\beta^{o}+f_{\alpha}, & \theta/\beta^{o}-\alpha/\beta^{o}+f_{\alpha}, & \theta/\beta^{c}-\alpha/\beta^{c}+f_{\alpha}, & \theta/\beta^{c}-\alpha/\beta^{c}+f_{\alpha} \\ \theta/\beta^{o}-\alpha/\beta^{o}+f_{\alpha}, & f^{o}_{\beta e}-2\alpha/\beta^{o}+f_{\alpha}, & \beta^{o}/\beta^{o}-\alpha/\beta^{o}-\alpha/\beta^{o}+f_{\alpha}, & \beta^{o}/\beta^{c}-\alpha/\beta^{o}-\alpha/\beta^{c}+f_{\alpha}, & -\alpha/\beta^{c}-\alpha/\beta^{o}+f_{\alpha} \\ \theta/\beta^{o}-\alpha/\beta^{o}+f_{\alpha}, & \beta^{o}/\beta^{o}-2\alpha/\beta^{o}+f_{\alpha}, & f^{o}_{\beta a}-2\alpha/\beta^{o}+f_{\alpha}, & -\alpha/\beta^{c}-\alpha/\beta^{o}+f_{\alpha}, & \beta^{o}/\beta^{c}-\alpha/\beta^{c}-\alpha/\beta^{o}+f_{\alpha} \\ \theta/\beta^{c}-\alpha/\beta^{c}+f_{\alpha}, & \beta^{o}/\beta^{c}-\alpha/\beta^{o}-\alpha/\beta^{c}+f_{\alpha}, & -\alpha/\beta^{o}-\alpha/\beta^{c}+f_{\alpha}, & f^{c}_{\beta e}-2\alpha/\beta^{c}+f_{\alpha}, & \beta^{c}/\beta^{c}-2\alpha/\beta^{c}+f_{\alpha} \\ \theta/\beta^{c}-\alpha/\beta^{c}+f_{\alpha}, & -\alpha/\beta^{o}-\alpha/\beta^{o}+f_{\alpha}, & \beta^{o}/\beta^{c}-\alpha/\beta^{o}-\alpha/\beta^{c}+f_{\alpha}, & \beta^{c}/\beta^{c}-2\alpha/\beta^{c}+f_{\alpha}, & f^{c}_{\beta a}-2\alpha/\beta^{c}+f_{\alpha} \end{bmatrix}$$

$$\Delta R_{CC} = -2R_{CO}(\sin OCC)\sin\Delta OCC$$

$$= -2.7089\Delta OCC \quad (OCC \text{ in radians})$$

$$\Delta R_{CO} = \Delta OCC \times R_{CO}/\text{cot } OCC$$

$$= -4.120\,\Delta OCC$$

The A_u CO, CC and OCC symmetry coordinates are given by:

$$\begin{array}{c} \\ S_a \\ S_b \\ S_c \end{array} \begin{array}{c} \begin{array}{cccccccccc} CO^1 & CO^2 & CO^3 & CO^4 & CC^A & CC^B & OCC^1 & OCC^2 & OCC^3 & OCC^4 \end{array} \\ \begin{bmatrix} \frac{1}{2} & \frac{1}{2} & -\frac{1}{2} & -\frac{1}{2} & 0 & 0 & 0 & 0 & 0 & 0 \\ 0 & 0 & 0 & 0 & \frac{1}{\sqrt{2}} & -\frac{1}{\sqrt{2}} & 0 & 0 & 0 & 0 \\ 0 & 0 & 0 & 0 & 0 & 0 & \frac{1}{2} & \frac{1}{2} & -\frac{1}{2} & -\frac{1}{2} \end{bmatrix} \end{array}$$

From the equations which express the redundancy conditions, the normalised 'redundant' symmetry coordinates may be constructed:-

$$S_1^R = (\sqrt{2} \times 2.7089S_b - S_c)/(1 + 2 \times 2.7089^2)^{\frac{1}{2}}$$

$$= .2444S_b - .0638S_c$$

$$S_2^R = (4.12S_a - S_c)/(1 + 4.12^2)^{\frac{1}{2}}$$

$$= .2292S_a - .0556S_c$$

Substituting for S_a, S_b and S_c gives the following U matrix

$$\begin{array}{c} \\ S_1^R \\ S_2^R \end{array} \begin{array}{c} \begin{array}{cccccc} CO^1 & CO^2 & CO^3 & CO^4 & CC^A & CC^B \end{array} \\ \begin{bmatrix} .4859 & .4859 & -.4859 & -.4859 & 0 & 0 \\ 0 & 0 & 0 & 0 & .6842 & -.6842 \end{bmatrix} \end{array}$$

$$\begin{array}{cccc} OCC^1 & OCC^2 & OCC^3 & OCC^4 \\ \begin{bmatrix} -.1180 & -.1180 & .1180 & .1180 \\ -.1263 & -.1263 & .1263 & .1263 \end{bmatrix} \end{array}$$

As with the HCH redundancy, performing the UFU^t operation will reveal the effect of the mixing with OCC on the individual CO and CC symmetrized force constants, F =

	CO^1	CO^2	CO^3	CO^4	CC^A	CC^B	OCC^1	OCC^2	OCC^3	OCC^4
CO^1	fco	(5)		(1)	(2)		(3)	(6)		(7)
CO^2	(5)	fco	(1)		(2)		(6)	(3)	(7)	
CO^3		(1)	fco	(5)		(2)		(7)	(3)	(6)
CO^4	(1)		(5)	fco		(2)	(7)		(6)	(3)
CC^A	(2)	(2)			fcc		(4)	(4)		
CC^B			(2)	(2)		fcc			(4)	(4)
OCC^1	(3)	(6)		(7)	(4)		focc			
OCC^2	(6)	(3)	(7)		(4)			focc		
OCC^3		(7)	(3)	(6)		(4)			focc	
OCC^4	(7)		(6)	(3)		(4)				focc

The force constants are numbered in the following manner:

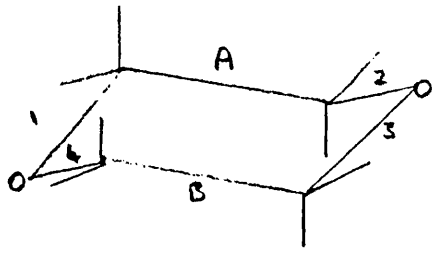

(1) = CO/CO
(2) = CO/CC
(3) = CO/OCC
(4) = CC/OCC
(5) = CO/CO(Opp) [Eg 1/2]
(6) = CO/OCO [Eg CO^1/OCC^2]
(7) = CO/OCC [Eg CO^1/OCC^4]

Here a number of force constants have been introduced which would normally be assumed to take negligible values - (5), (6) and (7). These have been included since the analysis below indicates that in this ab initio treatment they are too significant to be ignored.

UF

$$1,1 = .4859[f_{CO} + (5) - (1)] + .1180[(7) - (3) - (6)]$$
$$= 1,2 = -1,3 = -1,4$$

$$1,5 = 2[.4859(2) - .1180\ (4)] = -1,6$$

$$1,7 = .4859[(3) + (6)] - .1180\ f_{OCC}$$
$$= 1,8 = -1,9 = -1,10$$

$$2,1 = .6842\ (2) - .1263[(3) + (6)]$$
$$= 2,2 = -2,3 = -2,4$$

$$2,5 = .6842\ f_{CC} - 2[.1263\ (4)]$$
$$= -2,6$$

$$2,7 = .6842\ (4) - .1263\ f_{OCC}$$
$$= 2,8 = -2,9 = -2,10$$

Finally, the elements of UFU^t are given by

$$1,1 = .9444[f_{CO} + (5) - (1)] + .4587[(7) - (3) - (6)] + .0557 f_{OCC}$$

$$1,2 = 1.3298\ (2) + .2455\ [(7) - (3) - (6)] - .3229\ (4) + .0596\ f_{OCC}$$

$$2,2 = .9363 f_{CC} - .6913\ (4) + .0638 f_{OCC}.$$

Hence the redundancy causes the F^{Au}_{CO} and F^{Au}_{CC} to be functions of f_{OCC} and the corresponding interaction constants.

The next step is to illustrate how numerical values may be attached to these force constants by examining the results from Ag, Bg and Bu ab initio data. Calculating UFU^t for these species yields the following relationships

$$F^{Ag}_{CO} = f_{CO} + CO/CO + CO/CO(Opp)$$
$$F^{Bu}_{CO} = f_{CO} + CO/CO - CO/CO(Opp)$$
$$F^{Bg}_{CO} = f_{CO} - CO/CO - CO/CO(Opp)$$
$$F^{Ag}_{OCC} = f_{OCC} + OCC/OCC$$
$$F^{Bu}_{OCC} = f_{OCC} - OCC/OCC = F f^{Bg}_{OCC}$$
$$F^{Ag}_{CO/OCC} = CO/OCC + CO/O\overset{o}{C}C + CO/\overset{o}{O}CC$$
$$F^{Bu}_{CO/OCC} = CO/OCC - CO/O\overset{o}{C}C + CO/\overset{o}{O}CC$$
$$F^{Bg}_{CO/OCC} = CO/OCC - CO/O\overset{o}{C}C - CO/\overset{o}{O}CC$$
$$F^{Ag}_{CO/CC} = \sqrt{2}\,CO/CC\ ;\ F\, f^{Ag}_{CC} = f_{CO}$$

Thus a series of simultaneous equations is generated which may be solved for the constituent force constants on substitution of the appropriate values from the ab initio force constant tables. For instance:

$$577 = f_{CO} + CO/CO + CO/CO'(Opp)$$
$$592 = f_{CO} + CO/CO - CO/CO\ (Opp)$$
$$550 = f_{CO} - CO/CO - CO/CO\ (Opp)$$

These yield:

$f_{CO} = 563.5$; $CO/CO = 21$; $CO/CO\ (Opp) = -7.5$

Similarly,

$CO/OCC = 39.4$; $CO/O\overset{o}{C}C = -30.2$; $CO/\overset{o}{O}CC = 15.7$
$CO/CC = 25.7$; $f_{CC} = 472$; $f_{OCC} = 109.3$ (includes f_{HCH})

The f_{OCC} value is simply the average of the results from the three symmetry species since they are in good agreement, indicating that $OCC/OCC \sim 0$. To test the consistancy of the calculated values, these may be substituted into the equations obtained for the Au force constants, and the result compared with the values listed.

Care should be taken in comparing 'like with like', the tabulated values needing to be scaled by the same coefficient that appears in the relevant equation - i.e. in the 1,1 Au force constant listed above, f_{CO} is multiplied by .9444, and for compatibility, the tabulated '554' should be scaled similarly.

Thus,

$$523 = .9444[f_{CO} + CO/CO(Opp) - CO/CO] + .4587[CO/\overset{o}{O}CC - CO/OCC - CO/O\overset{o}{C}C] + .0557\ f_{OCC}$$
$$= 514, \text{ on substitution of the values derived for these force constants.}$$

This represents very good agreement, when considering the large number of parameters involved.

The same procedure for $F_{CO/CC}$ suggests that $F^{Au}_{CO/CC}$ should be 29.7 as opposed to the 'observed' 10.8 - the poor agreement perhaps indicating that a CO/CC(Opp) term should be included. Finally, the f_{OCC} term:

$$F^{Au}_{CC} = .9363\ f_{CC} - .6913(CC/OCC) + .0638\ f_{OCC}$$

$$= .9363 \times 472$$

and this gives $f_{CC} = 471$, compared with $f_{CC} = 479$ from the Ag block - again, good agreement.

The above has shown how the symmetrized force constants can be analysed into their unsymmetrized components by an examination of the UFU^t transformation. The rest of the results from these calculations are now listed:

$CO/H^aCC \sim 0$ (Note that the stretches with all the angles except COC actually contain the stretch/HCH interaction).

<u>CO/H^eCC</u>.

$$F^{Ag}_{CO/H^eCC} = 10.2 = CO/H^eCC + CO/H^eC^oC$$

$$F^{Bu}_{CO/H^eCC} = 40.1 = CO/H^eCC - CO/H^eC^oC$$

$\therefore$ $CO/H^eCC = 25.2$, $CO/H^eC^oC = -15.0$.

<u>CO/H^aCO</u>

$$F^{Ag}_{CO/H^aCO} = F^{Bu}_{CO/H^aCO}$$

i.e. no CO/H^aC^oO term can explain the large discrepancy between 36.7 (Ag) and 8.5 (Bu).
Average = 22.6.

<u>CO/H^eCO</u> = $\frac{1}{2}(41.9 + 45.1) = 43.5$ - a good agreement between Ag and Bu.

<u>CO/COC</u> = $\frac{1}{2}(56.0 + 82.3) = 69.1$

To explain the difference in Ag and Bu results, a CO/COC(Opp) interaction would be required.

$CC/H^aCC = 28.2/\sqrt{2} = 19.9$
$CC/H^eCC = -14.1$
$CC/H^aCO = 5.4$
$CC/H^eCO = -25.7$
$CC/COC = -14.0/2 = -7.0$
$CC/OCC = 9.1$

These CC interactions are derived from the Ag results - the Au values are more complicated and less reliable functions due to the redundancy complication.

$\underline{CH^a} = \frac{1}{3}(565 + 562 + 577) = 568$

$\underline{CH^e} = \frac{1}{3}(591 + 585 + 578) = 585$

All the CH interactions are considered to be zero since these coordinates produce vibrations widely separated in frequency.

$\underline{COC} = \frac{1}{2}(69.7 + 85.2) = 77.5$
and COC/COC Opp $= -7.8$ to explain the Ag/Bu difference.

The force constants which follow all contain f_{HCH} due to the redundancy around the carbon atom. As described previously, this is here taken as the average of the corresponding Ag interaction constants ~39.5, and this is to be subtracted from the diagonal term.

$\underline{H^aCC}$

$$F^{Ag}_{H^aCC} = F^{Au}_{H^aCC} = fH^aCC + H^aCC/H^aCC + fHCH$$

$$F^{Bu}_{H^aCC} = fH^aCC - H^aCC/H^aCC(CC) + fHCH$$

$\therefore \quad H^aCC/H^aCC(CC) = 7.6$

$fH^aCC = [\frac{1}{2}(103.3 + 94.9) - 39.5] - 7.6 = 52$

$\underline{H^eCC}$ Same form of relationship as H^aCC:

$fH^eCC = 51.1, \quad H^eCC/H^eCC(CC) = -2.5$

$\underline{H^aCO} = \frac{1}{3}(101.7 + 104.1 + 103.6) - 39.5 = 63.6$

$\underline{H^eCO} = \frac{1}{3}(101.6 + 104.1 + 100.5) - 39.5 = 62.6$

The excellent agreement between the symmetry species for HCO means that no additional interactions are required.

The CO, CC and OCC force constants were discussed prior to this list.

Thus a set of 'ab initio' force constants is derived that is based on the internal coordinate basis set. These are the parameters that furnish a set of constraints on the force constant perturbation procedure. The diagonals are to be allowed to vary whilst the off-diagonal elements are maintained at the same relative value to these principle diagonal terms as is predicted in the ab initio calculations. For example, CO/CO = 21; $f_{CO} = 563.5$, $\therefore$ CO/CO = .037 f_{CO}.
Thus the following table of constraints is finally constructed.

TABLE 38.

Force Constant	Constrained Value
CO/CO	.037 f_{CO}
CO/CO(Opp)	.013 f_{CO}
CO/H^aCC	0
CO/$H^e\overset{o}{C}C$	-.027 f_{CO}
CO/H^eCC	.045 f_{CO}
CO/H^aCO	.040 f_{CO}
CO/H^eCO	.077 f_{CO}
CO/OCC	.070 f_{CO}
CO/$O\overset{o}{C}C$	-.054 f_{CO}
CO/$\overset{o}{O}$CC	.028 f_{CO}
CO/COC	.123 f_{CO}
CC/H^aCC	.042 f_{CC}
CC/H^eCC	-.030 f_{CC}
CC/H^aCO	.011 f_{CC}
CC/H^eCO	-.054 f_{CC}
CC/OCC	.019 f_{CC}
H^aCC/H^aCC(CC)	.145 f_{H^aCC}
H^eCC/H^eCC(CC)	-.050 f_{H^eCC}
OCC/OCC	0
COC/COC(Opp)	0

5.5 Perturbation Procedure for 'Constrained Force Field'.

The force field matrix, part of the input for the force constant refinement computer program, is listed in the form of row, column, number of force constant and the coefficient by which this is multiplied. In order to impose a given constraint, all that is required is to substitute the last two pieces of data by the number of the diagonal force constant that is to be varied, and the coefficient which defines the appropriate relationship to be maintained during the perturbation procedure - these being the figures listed in Table . Thus the only force constants that are actually varied are the diagonals, the rest being set to zero - in principle.

In fact, several modifications were required to produce a satisfactory fit. The $CO/H^eC\overset{o}{C}$, CO/H^eCC and CO/H^aCO interaction constants had their constraints removed, and were initially varied - in the end only CO/H^aCO approached a significant value, so the other two were set equal to zero.

Again, to improve the fit, two more interaction constants were introduced - COC/CCO and H^eCO/H^eCC. This does not amount to a contradiction of the ab initio results, since the latter was seen to be 'swamped' by the inbuilt f_{HCH} contribution, whilst COC/CCO had been fixed at zero simply due to the inconsistency of its value between different symmetry blocks.

A further amendment was to alter f_{HCH} from a fixed value of .403 to .365, the latter appearing to be the optimum value on letting f_{HCH} vary along with the other diagonals.

Although the final resulting field, 'Force Field B', contains a number of surprising elements - e.g. $CO/OC\overset{o}{C}$ = -.2575, CC/H^eCO = -.2301 - the degree of agreement between observed and calculated frequencies is essentially the same as that achieved with Force Field A.

The results of these calculations are now presented. Table39 contains the force constants that constitute Force Field A; Table40 contains those for Force Field B. Table41 lists these together with the Snyder and Zerbi force constants, for purposes of comparison. Table42 shows the frequencies

calculated for 1,4-dioxan (d_0) from the two force fields, and Table 41 shows the results for dioxan - d_8. Table 42 gives the potential energy distributions derived from Force Field A, and Table 45 that from Force Field B.

Both field A (unconstrained) and field B (constrained) produce a differentiation between the axial and equatorial CH stretch diagonal force constants:

$$F^{A}_{CH^a} = F^{B}_{CH^a} = 4.49$$
$$F^{A}_{CH^e} = F^{B}_{CH^e} = 4.77$$

The ab initio values were ~ 25% higher than these, but again show CH^e to be larger in magnitude than CH^a, and also predict a similar ratio for these:

$$\left(\frac{F_{CH^e}}{F_{CH^a}}\right)_{A,B} = 1.062$$

$$\left(\frac{F_{CH^e}}{F_{CH^a}}\right)_{\text{ab initio}} = 1.030$$

Caillod et al. in their study of the CH stretching region of dioxan obtained values which are consistent with the above: $F_{CH^a} = 4.530$, $F_{CH^e} = 4.805$, $(F_{CH^e}/F_{CH^a})_c = 1.061$.

The ab initio values of F_{CO} and f_{cc} are ~ 10% higher than those of fields A and B, but again similar ratios are found:

$$\left(\frac{F_{CO}}{F_{CC}}\right)_{\text{ab initio}} = 1.194; \quad \left(\frac{F_{CO}}{F_{CC}}\right)_{A} = 0.972; \quad \left(\frac{F_{CO}}{F_{CC}}\right)_{B} = 1.119$$

The ab initio values of F_{H^aCC} and F_{H^eCC} are equal as are F_{H^aCO} and F_{H^eCO}. Whilst the values in A and B are now of the same magnitude as the ab initio they do not reflect this pattern. Both A and B give the equatorial greater than the axial force constants. However, the ab initio gives $F_{HCO} > F_{HCC}$ and this does reflect fields A and B.

The ab initio F_{COC} is larger than the other angle diagonals, and again this is found in A and B.

Most of the major off-diagonal force constants in A and B are similar in value. Field B possesses a number of unexpectedly large values, due to the ab initio constraints: CO/ÔCC = -.257, COC/COC(Opp) = -.116. Initially there is a temptation to say these terms should really be neglected, since they describe long range electronic effects, but the fact is that, as will be seen later, field B is actually more successful than field A in the analysis of the band intensities.

TABLE 39.

Unconstrained Force Field.

Force Constant	Value	Variance
CH^e	4.772	0.048
CH^a	4.490	0.050
CO	4.543	0.340
CC	4.673	0.350
COC	0.809	0.117
OCC	0.623	0.063
HCH	0.403	-
H^eCO	0.605	0.048
H^aCO	0.553	0.034
H^eCC	0.496	0.063
H^aCC	0.345	0.037
CO/CO	0.810	0.205
CO/CC	0.037	0.152
CO/COC	0.505	0.150
CO/CCO	0.266	0.140
CO/H^eCO	0.243	0.071
CO/H^aCO	0.409	0.089
CC/CCO	0.274	-
CC/H^eCC	0.153	0.081
CC/H^aCC	0.143	0.054
COC/OCC	0.162	0.038
H^eCO/H^eCC	0.143	0.021

TABLE 40.

Constrained Force Field.

Force Constant	Value	Variance
CH^e	4.767	0.056
CH^a	4.489	0.059
CO	4.769	0.214
CC	4.261	0.340
COC	1.146	0.136
OCC	0.560	0.056
H^eCO	0.721	0.040
H^aCO	0.513	0.020
H^eCC	0.497	0.030
H^aCC	0.290	0.019
HCH	0.365	
CO/CC	0.192	0.173
COC/OCC	0.105	0.048
H^eCO/H^eCC	0.119	0.029
CO/H^aCO	0.427	0.086
CO/CO	0.176	
CO/COC	0.587	
CO/OCC	0.334	
CO/H^eCO	0.367	
CC/OCC	0.081	
CC/H^eCO	-.230	
CC/H^aCO	0.047	
CC/H^eCC	-.128	
CC/H^aCC	0.179	
HCC/HCC_g	-.025	
HCC/HCCt	0.042	
CO/CO(Opp)	0.062	
$CO/OC\overset{o}{C}$	-.257	
$CO/\overset{o}{O}CC$	0.133	
COC/COC(Opp)	-.116	

TABLE 41.

Comparison of Force Fields.

Force Constant	S+Z		Uncon.	Constrained	
CH^e	4.626		4.772	4.767	
CH^a	4.626		4.490	4.489	
CO	5.090		4.543	4.769	
CC	4.261		4.673	4.261	
COC	0.640		0.809	1.146	
OCC	0.545		0.623	0.560	
HCH	0.403	↔	0.403	0.365	
H^eCO	0.579		0.605	0.721	
H^aCO	0.579		0.553	0.513	
H^eCC	0.457		0.496	0.497	
H^aCC	0.457		0.345	0.290	
CH/CH	-.046		0	0	
CO/CO	0.288		0.810	0.176	
CO/CC	0.101		0.037	0.192	
CO/COC	0.339		0.505	0.587	
CO/OCC	0.420		0.266	0.334	
CO/H^eCO	0.310		0.243	0.367	
CO/H^aCO	0.310		0.409	0.427	
CO/H^eCC	0		0	0	*
CO/H^aCC	0		0	0	*
CC/OCC	0.274	↔	0.274	0.081	
CC/H^eCC	0.367		0.153	-.128	
CC/H^aCC	0.367		0.143	0.179	
COC/OCC	0.005		0.162	0.105	
COC/HCO_g	0.002		0	0	
COC/HCOt	-.062		0	0	
OCC/OCC	-.005		0	0	
$OCC/H^{a,e}CO$	-.017		0	0	
$OCC/H^{a,e}CC$	-.016		0	0	
OCC/HCCt	0.014		0	0	
HCO/HCO	-.003		0	0	
H^eCO/H^eCC	0.070		0.143	0.119	
H^aCO/H^aCC	0.070		0	0	
HCC/HCC	0.062		0	0	
HCC/HCC_g	0.002		0	-.025	
HCC/HCCt	0.071		0	0.042	
CO/CO(Opp)	0		0	0.062	
$CO/^{\delta}CC$	0		0	-.257	
CO/OC^{δ}	0		0	0.133	
COC/COC(Opp)	0		0	-.116	

TABLE 42.

d_0 Calculated Frequencies.

	Obs.(cm^{-1})	A	B
Ag	2968	2978	2976
	2856	2861	2864
	1444	1483	1481
	1397	1359	1381
	1305	1280	1306
	1128	1126	1103
	1015	1024	975
	837	835	814
	435	459	501
	424	419	397
Bg	2968	2972	2971
	2856	2855	2854
	1459	1461	1470
	1335	1352	1379
	1217	1245	1228
	1110	1090	1100
	853	857	836
	490	502	482
Au	2970	2973	2970
	2863	2861	2864
	1449	1480	1487
	1369	1348	1399
	1256	1227	1264
	1136	1112	1120
	1086	1035	1079
	881	868	833
	288	185	169
Bu	2970	2975	2976
	2863	2856	2854
	1457	1460	1454
	1378	1376	1381
	1291	1304	1302
	1052	1042	1036
	889	891	804
	610	612	642
	274	273	294

TABLE 43.

d_8 Calculated Frequencies.

	Obs.(cm^{-1})	A	B
Ag			
	2242	2231	2229
	2098	2107	2116
	1225	1237	1244
	1108	1122	1101
	1008	1025	1006
	832	858	861
	808	811	831
	752	765	728
	490	449	474
	348	342	332
Bg			
	2226	2214	2212
	2088	2091	2088
	1070	1098	1120
	1023	1059	1097
	956	991	983
	888	902	894
	711	705	692
	422	446	418
Au			
	2235	2217	2214
	2086	2104	2116
	1191	1217	1238
	1117	1095	1144
	1030	981	1074
	922	882	885
	809	835	832
	762	746	687
	254	151	138
Bu			
	2232	2221	2227
	2098	2094	2087
	1153	1145	1142
	1087	1067	1065
	1042	1017	1011
	896	894	871
	732	728	727
	490	525	509
	238	239	260

TABLE 44(a).

Unconstrained Force Field d_0.

Obs ν_i	Potential Energy Distribution (%)
Ag	
2968	86 CH^e, 12 CH^a
2856	12 CH^e, 86 CH^a
1444	60 HCH, 7 H^eCC, 17 H^eCO, 11 H^aCO
1397	23 CC, 14 H^eCC, 28 H^aCC, 47 H^aCO
1305	10 CC, 11 CO, 14 H^eCC, 59 H^eCO, 21 H^aCO
1128	10 CO, 51 H^eCC, 7 H^eCO, 26 H^aCC, 7 COC
1015	49 CC, 10 CO, 9 H^eCO, 19 H^aCC
837	19 CC, 74 CO
435	8 CO, 34 OCC, 99 COC
424	7 H^eCC, 57 OCC, 11 COC
Bg	
2968	89 CH^e, 11 CH^a
2856	11 CH^e, 89 CH^a
1459	65 HCH, 15 H^eCO
1335	30 H^eCC, 15 H^eCO, 22 H^aCC, 48 H^aCO
1217	38 H^eCC, 55 H^eCO, 24 H^aCO
1110	59 CO, 20 OCC
853	39 CO, 15 H^eCC, 9 H^eCO, 30 H^aCC
490	9 CO, 9 H^aCC, 70 OCC
Au	
2970	87 CH^e, 13 CH^a
2863	13 CH^e, 86 CH^a
1449	62 HCH, 16 H^eCO, 8 H^eCC, 9 H^aCO
1369	28 CC, 17 H^eCC, 13 H^eCO, 29 H^aCC, 38 H^aCO
1256	33 H^eCC, 61 H^eCO, 21 H^aCO
1136	32 CC, 40 CO, 7 H^eCC, 7 H^aCO
1086	12 CC, 15 H^eCC, 41 H^aCC, 10 H^aCO
881	30 CC, 62 CO, 15 H^eCC, 10 OCC
288	77 OCC

continued...

Bu

2970	89 CH^e, 11 CH^a
2863	11 CH^e, 89 CH^a
1457	67 HCH, 16 H^eCO
1378	23 H^eCC, 21 H^aCC, 59 H^aCO
1291	14 CO, 42 H^eCC, 56 H^eCO, 13 H^aCO
1052	11 CO, 10 H^eCC, 20 H^eCO, 16 H^aCC, 25 OCC
889	70 CO, 16 H^eCC, 19 H^aCC, 10 COC
610	19 CO, 15 H^aCC, 10 H^aCO, 57 OCC, 45 COC
274	13 OCC, 57 COC

TABLE 44(b).

Unconstrained Force Field d_8

Obs ν_i	Potential Energy Distribution (%)
Ag	
2242	71 CH^e, 25 CH^a
2098	26 CH^e, 70 CH^a
1225	57 CC, 32 CO, 23 H^eCO, 12 H^aCO
1108	12 CC, 10 CO, 46 HCH, 17 H^eCC, 12 H^eCO
1008	14 HCH, 62 H^aCO, 11 COC
832	30 H^eCC, 10 H^eCO, 50 H^aCC
808	26 CO, 19 H^eCC, 44 H^eCO
752	27 CC, 41 CO, 17 H^eCC
490	64 OCC, 69 COC
348	9 H^eCC, 26 OCC, 35 COC
Bg	
2226	79 CH^e, 19 CH^a
2088	19 CH^e, 79 CH^a
1070	51 CO, 42 H^eCC, 24 H^aCO
1023	66 HCH, 23 H^eCO
956	29 CO, 18 H^eCO, 15 H^aCC, 11 H^aCO, 10 OCC
888	22 H^eCC, 48 H^eCO, 39 H^aCO
711	23 CO, 27 H^eCC, 27 H^aCC
422	20 H^aCC, 62 OCC
Au	
2235	71 CH^e, 27 CH^a
2086	27 CH^e, 69 CH^a
1191	69 CC, 19 CO, 8 H^eCC, 9 H^eCO, 13 H^aCC, 14 H^aCO
1117	55 HCH, 11 H^eCC, 17 H^eCO
1030	58 CO, 13 H^eCC, 23 H^eCO
922	30 H^eCO, 63 H^aCO
809	12 HCH, 12 H^eCC, 61 H^aCC
762	23 CC, 24 CO, 50 H^eCC, 17 H^eCO
254	76 OCC

continued...

Bu

2232	79 CH^e, 18 CH^a
2098	18 CH^a, 80 CH^e
1153	51 CO, 32 H^eCC, 32 H^eCO, 17 H^aCO
1087	38 HCH, 14 H^eCC, 9 H^eCO, 15 H^aCC, 14 H^aCO
1042	9 CO, 27 HCH, 43 H^aCO, 9 COC
896	35 H^eCO, 13 H^aCC, 33 OCC, 16 COC
732	43 CO, 37 H^eCC, 13 H^eCO, 16 H^aCC, 15 COC
490	12 CO, 30 H^aCC, 9 H^aCO, 48 OCC, 21 COC
238	9 OCC, 61 COC

TABLE 45(a).

Constrained Force Field d_0

Obs ν_i	Potential Energy Distribution (%)
Ag	
2968	86 CH^e, 13 CH^a
2856	13 CH^e, 85 CH^a
1444	51 HCH, 10 H^eCC, 20 H^eCO
1397	18 CC, 33 H^eCC, 59 H^eCO, 16 H^aCO
1305	20 H^eCO, 61 H^aCO
1128	10 HCH, 59 H^aCC, 8 H^eCC
1015	52 CC, 50 CO, 16 H^eCC, 17 COC
837	14 CC, 61 CO, 11 H^eCC
435	16 CC, 11 CO, 9 H^aCO, 13 OCC, 81 COC
424	70 OCC
Bg	
2968	88 CH^e, 11 CH^a
2856	11 CH^e, 89 CH^a
1459	26 HCH, 70 H^eCO
1335	31 HCH, 64 H^eCC, 11 H^eCO
1217	15 H^aCC, 80 H^aCO
1110	84 CO, 14 HCH, 15 OCC
853	27 CO, 19 H^eCC, 12 H^eCO, 34 H^aCC
490	15 H^aCC, 78 OCC
Au	
2970	86 CH^e, 13 CH^a
2863	13 CH^e, 85 CH^a
1449	49 HCH, 27 H^eCO
1369	16 CC, 39 H^eCC, 49 H^eCO
1256	12 CO, 19 H^aCC, 66 H^aCO
1136	10 CC, 86 CO, 15 H^eCO
1086	11 CC, 14 HCH, 47 H^aCC
881	60 CC, 39 H^eCC, 11 H^aCO
288	8 CO, 79 OCC

continued...

Bu

2970	88 CH^e, 11 CH^a
2863	11 CH^e, 88 CH^a
1457	21 HCH, 11 H^eCC, 81 H^eCO
1378	41 HCH, 53 H^eCC
1291	10 H^aCC, 72 H^aCO
1052	7 CO, 19 H^eCC, 24 H^aCC, 22 OCC, 28 COC
889	100 CO, 21 COC
610	13 CO, 36 H^aCC, 45 OCC, 12 COC
274	35 OCC, 43 COC

TABLE 45(b).

Constrained Force Field d_8

Obs ν_i	Potential Energy Distribution (%)
Ag	
2242	69 CH^e, 27 CH^a
2098	28 CH^e, 67 CH^a
1225	51 CC, 12 HCH, 19 H^eCC, 10 H^aCO
1108	8 CC, 33 CO, 15 HCH, 76 H^eCO, 10 COC
1008	23 HCH, 56 H^aCO, 14 COC
832	16 CO, 23 H^eCC, 9 H^eCO, 48 H^aCC
808	47 CO, 17 H^aCC, 7 CC, 7 H^eCO
752	26 CC, 19 CO, 32 H^eCC, 12 COC
490	16 CC, 8 CO, 11 H^aCO, 37 OCC, 56 COC
348	13 H^eCC, 45 OCC, 21 COC
Bg	
2226	78 CH^e, 20 CH^a
2088	20 CH^e, 79 CH^a
1070	73 CO, 43 H^eCC, 11 H^aCO
1023	12 HCH, 10 H^eCC, 72 H^eCO
956	24 CO, 57 HCH, 14 H^eCC, 8 OCC
888	13 H^eCO, 10 H^aCC, 70 H^aCO
711	13 CO, 26 H^eCC, 8 H^eCO, 27 H^aCC, 14 OCC
422	27 H^aCC, 65 OCC
Au	
2235	67 CH^e, 31 CH^a
2086	31 CH^e, 63 CH^a
1191	53 CC, 13 HCH, 18 H^eCC, 7 CO
1117	81 CO
1030	8 CO, 25 HCH, 67 H^eCO, 12 H^aCO
922	11 HCH, 9 H^eCC, 28 H^eCO, 49 OCC
809	19 HCH, 65 H^aCC
762	44 CC, 56 H^eCC, 15 H^aCO
254	8 CO, 79 OCC

continued...

Bu

2232	77 CH^e, 19 CH^a
2098	19 CH^e, 79 CH^a
1153	28 CO, 23 H^eCC, 77 H^eCO, 17 COC
1087	35 H^eCC, 42 H^aCO, 16 COC
1042	67 HCH, 9 H^eCC
896	13 H^eCC, 17 H^aCC, 30 H^aCO, 27 OCC, 11 COC
732	100 CO, 11 H^eCO, 8 H^aCO, 14 COC
490	6 CO, 9 H^eCC, 48 H^aCC, 36 OCC
238	28 OCC, 47 COC

CHAPTER 6. DIOXAN: ANALYSIS OF EXPERIMENTAL INTENSITIES.

Section 6.1 Use of the Ab Initio APT'S.

In this section it is described how an attempt has been made to obtain the set of atomic polar tensors for 1,4-dioxan, through an analysis of the experimental infra red band intensities. Both of the derived force fields; A (unconstrained) and B (constrained), have been utilized in the calculations, and much use is made of the ab initio polar tensors in determining how to proceed with the investigation.

In cyclohexane, the experimental intensities may be conveniently and rigorously apportioned to the changes along the x, y and z axes, according to the symmetry of the particular normal coordinate. In 1,4-dioxan, in the au bands the intensity is due to changes in the dipole moment along the x axis. The bu bands involve changes along the y and z axes simultaneously. Therefore, the problem immediately arises - how is it possible to split the bu intensities so as to yield the experimental dp_y/dQ_i and dp_z/dQ_i?

The method adopted here is to calculate these intensities from the ab initio polar tensors, and then impose the resulting suggested manner of splitting on the actual experimental intensities. The following tables show the results of these calculations: Table46 Calculated d_0 intensities (force field A); Table47 - Calculated d_0 intensities (force field B); Table48 - Splitting corresponding to Table 46; Table 49 - Splitting corresponding to Table 47; Table 50- Calculated d_8 intensities (force field A); Table51 - Calculated d_8 intensities (force field B).

It is apparent that the two force fields produce estimates of the intensities that are significantly different - it is difficult to say which one is most appropriate for use since force field A seems best for d_0-dioxan, and force field B best for d_8-dioxan.

For instance, in Table46 the most intense bands 1136cm^{-1} (au) and 881cm^{-1} (au) are predicted as intense, and the weak bands such as 1378 (bu), 1052 (bu), and 288 (au) are predicted as low. The intermediate bands in several cases are estimated very well - e.g. 1291 (bu), [1449 (au) + 1457 (bu)], but there is a degree

TABLE 46.

d_o - Unconstrained Force Field.

OBS. $\nu_i(cm^{-1})$	CALC. $\nu_i(cm^{-1})$	OBS. $A_i(km\ mol^{-1})$	CALC. $A_i(km\ mol^{-1})$
2970 bu	2975)	176.6	59.1
2970 au	2973)		62.7
2863 au	2861)	153.4	60.9
2863 bu	2856)		148.5
1449 au	1480)	16.19	0.1
1457 bu	1457)		17.4
1378 bu	1376	2.11	3.0
1369 au	1348	11.28	33.9
1291 bu	1304	12.19	12.9
1256 au	1227	33.00	18.5
1136 au	1112	158.1	102.3
1052 bu	1042	8.05	4.5
1086 au	1035	10.35	1.7
889 bu	891	17.51	51.0
881 au	868	75.2	123.0
610 bu	612	14.64	58.3
274 bu	273	20.22	41.2
288 au	185	0	4.4

TABLE 47.

d_0 Constrained Force Field.

OBS. $\nu_i(cm^{-1})$	CALC. $\nu_i(cm^{-1})$	OBS. $A_i(km\ mol^{-1})$	CALC. $A_i(km\ mol^{-1})$
2970 bu	2976)	176.6	61.6
2970 au	2970)		62.8
2863 au	2864)	153.4	63.4
2863 bu	2854)		146.6
1449 au	1487)	16.19	5.7
1457 bu	1454)		5.4
1369 au	1399	11.28	0.35
1378 bu	1381	2.11	14.6
1291 bu	1302	12.19	10.0
1256 au	1264	33.00	69.6
1136 au	1120	158.1	186.6
1086 au	1079	10.35	4.9
1052 bu	1036	8.05	17.8
881 au	833	75.2	8.4
889 bu	804	17.51	76.6
610 bu	642	14.64	14.2
274 bu	294	20.22	49.2
288 au	169	0	5.8

TABLE 48.

d_0 Unconstrained Ab Initio Sign Choices and Intensity Distributions.

OBS.ν_i (cm^{-1})		x	y, %	z, %	
2970	bu	0	-, 7.3	-, 92.7	*
2970	au	-	0	0	
2863	au	+	0	0	
2863	bu	0	+, 37.5	-, 62.5	
1449	au	+	0	0	*
1457	bu	0	-, 64.0	+, 36.0	
1378	bu	0	+, 64.1	-, 35.9	
1369	au	+	0	0	*
1291	bu	0	+, 5.9	-, 94.1	
1256	au	-	0	0	*
1136	au	-	0	0	*
1052	bu	0	-, 22.0	+, 78.0	*
1086	au	+	0	0	
889	bu	0	-, 36.6	-, 63.4	
881	au	-	0	0	*
610	bu	0	+, 97.8	+, 2.2	*
274	bu	0	-, 55.5	+, 44.5	*
288	au	-	0	0	*

* Normal coordinate reversed, so do same to signs of dipole changes to compare with 'constrained' results.

TABLE 49.

d_0 Constrained.

Ab Initio Sign Choices and Intensity Distributions.

OBS.ν_i (cm^{-1})		x	y, %	z, %
2970	bu	0	+, 6.9	+, 93.1
2970	au	-	0	0
2863	au	+	0	0
2863	bu	0	+, 38.4	-, 61.6
1449	au	+	0	0
1457	bu	0	-, 82.1	+, 17.9
1369	au	+	0	0
1378	bu	0	-, 38.8	+, 61.2
1291	bu	0	+, 6.6	-, 93.4
1256	au	+	0	0
1136	au	+	0	0
1086	au	-	0	0
1052	bu	0	+, 99.4	+, 0.6
881	au	+	0	0
889	bu	0	-, 58.2	-, 41.8
610	bu	0	-, 73.8	+, 26.2
274	bu	0	+, 59.6	-, 40.4
288	au	+	0	0

TABLE 50.

d_8 Unconstrained Force Field.

OBS. $\nu_i(cm^{-1})$		CALC. $\nu_i(cm^{-1})$	OBS. $A_i(km\ mol^{-1})$	CALC. $A_i(km\ mol^{-1})$
2232	bu	2221)	87.3	46.1
2235	au	2218)		24.9
2086	au	2104)	101.4	58.3
2098	bu	2094)		86.8
1191	au	1217	91.5	90.5
1153	bu	1145	29.4	20.1
1117	au	1095	97.8	9.2
1087	bu	1067	13.0	1.1
1042	bu	1017	28.0	23.2
1030	au	981	13.0	133.7
896	bu	894	17.4	12.8
922	au	882	0	0.2
809	au	835	0	0.0
762	au	746	39.14	38.9
732	bu	728	5.2	35.8
490	bu	525	9.6	43.6
238	bu	239	13.9	29.0
254	au	151	0	2.9

TABLE 51.

d_8 Constrained Force Field.

OBS. $\nu_i(cm^{-1})$		CALC. $\nu_i(cm^{-1})$	OBS. $A_i(km\ mol^{-1})$	CALC. $A_i(km\ mol^{-1})$
2232	bu	2228)	87.3	50.1
2235	au	2214)		22.5
2086	au	2117)	101.4	67.8
2098	bu	2087)		84.1
1191	au	1238	91.5	36.5
1117	au	1144	97.8	204.1
1153	bu	1142	29.4	23.3
1030	au	1075	13.0	15.6
1087	bu	1065	13.0	2.4
1042	bu	1011	28.0	7.4
922	au	885	0	1.8
896	bu	871	17.4	24.0
809	au	832	0	0.3
732	bu	726	5.2	55.6
762	au	687	39.14	6.2
490	bu	509	9.6	16.2
238	bu	260	13.9	35.5
254	au	138	0	3.9

of inconsistancy. Table47 shows less satisfactory agreement - 881(au) is now far too low, and 1378(bu) too high, though the predicted intensities are still generally of the correct order of magnitude.

In Table50 there are a number of major faults - 1117 cm^{-1} (au) is far too low, and 1030cm^{-1} (au) far too large. Table 51 shows overall a better pattern of predicted intensities and these faults are no longer present.

The two force fields should be expected to give different results, since many of the corresponding vibrational modes are predicted to be rather different in character. For instance, for the d_0 881 cm^{-1} band force field A calculates 62% CO in the potential energy distribution, whilst B calculates 0% CO - the former then predicts $A_{881\ cm^{-1}}$ = 123 km mol^{-1}, and the latter 8.4 km mol^{-1}. Obviously the extent of motion of the oxygen atoms is a prime factor in determining the intensity of a band.

Section 6.2 Determination of Signs of dp_x/dQ_i.

There are 9 au bands, one of which has effectively zero experimental intensity, so there are 2^8 = 248 possible sign choices for the set of dp_x/dQ_i, or in fact 124 taking into account the equivalence of results on reversing a given collection of signs.

As in the analysis of the cyclohexane band intensities, the suitability of a given sign combination is examined by using the resulting APT's to calculate the intensities for the completely deuterated compound, which are then compared with those observed experimentally.

Tables48 and 49 show the signs predicted for the d_0 dp/dQ on the basis of the force fields combined with the ab initio APT's.

Force Field A.

The following represents the ab initio sign choice for the dp_x/dQ

2970 cm^{-1}	2863	1449	1369	1256	1136	1086	881
-	+	+	+	-	-	+	-

Four d_8 intensities are chosen to contribute to the fit factor - these are 1191, 1117, 1030 and 762 cm^{-1}. The two au CD str band intensities are not experimentally available, and the three au bands with effectively zero intensity - 922, 809 and 254 cm^{-1} may be used as a further guide by inspection.

This sign choice yields the following d_8 intensities:

ν	A_i(obs)	A_i(calc)
1191	91.5	92.9
1117	97.8	12.2
1030	13.0	162.8
922	0.0	0.0
809	0.0	1.7
762	39.1	10.4
254	0.0	0.0

f = 3.288

The au bands contribute only to the first row of the APT's - here they are for this sign choice:

C^4	.646	.222	.204
H^{a7}	-.017	.014	-.026
H^{e8}	-.092	.106	.100
O^6	-1.073	0	0

Although the low intensity bands are well predicted, 1117 cm^{-1} comes out far too low, and 1030 cm^{-1} far too high.

The predicted signs that are most likely to be in error are those corresponding to intensities predicted high when they should be low, and those which are predicted low when they should be high - the latter case having the greatest effect on the derived APT. This leads to the signs for d_0 1449 cm^{-1} and 1086 cm^{-1} perhaps being the most likely to fall under suspicion. In fact, changing these signs has no great effect on either the fit factor or APT's.

Actually, the value of f can be drastically improved by changing just the sign of the last d_0 band, 881 cm^{-1}, leading to the following:

ν	A_i(obs)	A_i(calc)
1191	91.5	121.4
1117	97.8	0.5
1030	13.0	13.5
922	0.0	0.3
809	0.0	2.1
762	39.1	95.4
254	0.0	0.0

f = 0.699

C^4	.167	.619	.047
H^{a7}	.002	.042	.048
H^{e8}	-.087	.230	.098
O^6	-.163	0	0

The improvement in 'f' is simply due to the better prediction for the 1030 cm^{-1} band. 1117 cm^{-1} is still very poor. The band whose sign has been changed, 881 cm^{-1} (d_0) is large in magnitude (75.2 km mol^{-1}) and has been predicted even larger using the ab initio APT's (123.0 km mol^{-1}), and hence would only be a likely candidate for a sign change if either the ab initio APT's, or force field, or both were totally unreasonable. The polar tensorsthen derived are very different - notably $dp_x/dx(0)$ has changed from -1.073 to -.163.

There are a large number of sign combinations that yield f ~0.6, some of which can be ignored on the basis of prediction of large intensities for 922 and 809 cm^{-1}, but all of which have three or four signs different from the ab initio choice. Furthermore, the resulting polar tensors are very different from the ab initio set. The success achieved with the cyclohexane ab initio APT's suggests that it is the force field employed, rather than the Gaussian 76 package, that is most at fault.

Force Field B.

This is the ab initio sign combination:

2970	2863	1449	1369	1256	1136	1086	881
-	+	+	+	+	+	-	+

This gives the following predicted results:

ν	A_i(obs)	A_i(calc)
1191	91.5	3.4
1117	97.8	216.2
1030	13.0	1.9
922	0.0	5.6
809	0.0	0.4
762	39.14	41.6
254	0.0	

C^4	.679	-.175	.179
H^{a7}	-.011	-.017	-.027
H^{e8}	-.096	.009	.126
O^6	-1.144	0	0

The signs most likely to be in error are 1369 cm^{-1} (Obs 11.3, Calc 0.35), 1086 cm^{-1} (Obs 10.35, Calc 4.9), and 881 cm^{-1} (Obs 75.2, Calc 8.4). The fit factor may be improved through the variation simply of these questionable signs.

If 881 cm^{-1} is -1, then it is found that 1369 cm^{-1} must be -1 to yield a low f. The sign of 1086 cm^{-1} in this case has no great influence, although the negative is preferred. The - - - combination for these three bands gives: [SIGN CHOICE 1]

ν	A_i(Obs)	A_i(Calc)
1191	91.5	64.8
1117	97.8	123.8
1030	13.0	8.7
922	0.0	1.1
809	0.0	6.6
762	39.1	56.6
254	0.0	0.0

f = 0.333

C^4	.427	.507	.211
H^{a7}	.034	.059	-.024
H^{e8}	-.096	.179	.086
O^6	-.730	0	0

If 881 cm^{-1} is +1, then 1369 cm^{-1} must be +1, and 1086 cm^{-1} must be -1 to give a low fit factor. The + - + combination for the bands gives: [SIGN CHOICE 2]

ν	A_i(Obs)	A_i(Calc)
1191	91.5	53.4
1117	97.8	127.6
1030	13.0	12.3
922	0.0	1.3
809	0.0	11.1
762	39.1	50.7
254	0.0	0.0

f = 0.269 [lowest value out of <u>all</u> the sign combinations]

C^4	.688	.131	-.017
H^{a7}	-.065	.033	-.037
H^{e8}	-.132	-.050	.115
O^6	-.981	0	0

The fact that the calculated d_8 intensities agree so much better with the observed data than with those obtained with force field A, and that these sign choices are straightforwardly obtained from the ab initio results, strongly suggests that this constrained force field is the more reliable of the two from which an 'experimental' set of atomic polar tensors may be derived.

Section 6.3 2nd and 3rd Rows of Dioxan APT's.

The second and third rows of the APT's are determined by the experimental values of dp_y/dQ and dp_z/dQ, which in turn must be derived from the observed b_u d_0 band intensities. Tables 48 and 49 show the ab initio sign choices for the two force fields together with the calculated splitting of the b_u bands from which these dipole derivatives may be obtained.

The analysis of these b_u bands presents a formidable problem, since the 9 values of dp_y/dQ and the 9 values of dp_z/dQ may have their signs varied completely independently - thus there are $2^{18}/2 = 131072$ possible sign combinations that each produce a new set of APT's. Even if a particular sign choice is singled out, the problem still remains of how to then split the bands into the y and z components, for if the ab initio sign choice is not deemed satisfactory, then the subsequently predicted splittings are meaningless.

The success of force field B in favouring a set of signs consistent with the ab initio results can lead to some optimism in believing that the majority (if not all) of the b_u signs in Table 49 are reliable. The fact that most of the observed b_u intensities are only low to intermediate in value means that one or two errors of sign are unlikely to significantly change the form of the derived APT's. The y/z splitting is of still less consequence to the numerical value of the APT elements.

The procedure adopted here, then, is to impose all the constraints that appear in Table 49 on the d_0 b_u bands, and calculate the APT's that result. This yields the following:

ν	A_i(Obs)	A_i(Calc)
1153	29.4	10.3
1087	13.0	6.3
1042	28.0	3.9
896	17.4	11.5
732	5.2	10.4
490	9.6	10.8
238	13.9	14.9

Overall there is reasonable agreement between the observed and calculated b_u d_8 intensities, which are all intermediate in magnitude. The final APT's are now presented - the first row being derived from sign choice 1 (that from sign choice 2 is in brackets), and the second and third rows derived as was described immediately above. The ab initio APT's are listed for comparison.

Section 6.4 1,4-Dioxan Experimental APT's.

	EXPT.			AB INITIO		
C^4	.427(.688)	.507(.131)	.211(-.017)	.664	.149	.194
	-.069	.258	-.042	.002	.340	-.034
	-.124	-.017	.313	.086	-.018	.422
H^{a7}	.034(-.065)	.059(.033)	-.024(-.037)	-.010	-.031	-.071
	-.030	-.015	.077	-.030	-.020	.095
	.006	.090	-.133	.023	.054	-.150
H^{e8}	-.096(-.132)	.179(-.050)	.086(.115)	-.105	.050	.076
	.042	-.006	-.053	.062	.038	- 056
	.079	-.036	-.004	.067	-.030	.015
O^6	-.730(-.981)	0	0	-1.097	0	0
	0	-.473	.036	0	-.717	-.009
	0	-.074	-.352	0	-.011	-.573

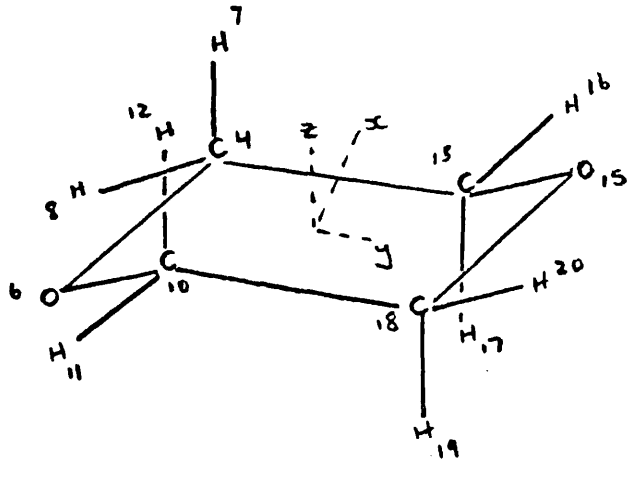

APT's:

$O^6 \equiv O^{15}$

$C^4 \equiv C^{18}$

$\equiv C^{10} \equiv C^{13}$ (*)

$H^{a7} \equiv H^a19$

$\equiv H^a12 \equiv H^a17$ (*)

$H^{e8} \equiv H^e20$

$\equiv H^e11 \equiv H^e16$ (*)

* - apart from reversal of sign of elements 1,2; 1,3; 2,1; 3,1.

Generally, there is very good agreement between the 'experimental' and ab initio APT's - the most significant terms are predicted correctly in both direction and magnitude. Of course, these results have been obtained by using the ab initio APT's to render the problem manageable, by placing constraints on the sign choices and b_u splitting. This in itself would not force the derived set of APT's to assume the same form as the ab initio set, since this experimental set is also determined by both the experimentally observed intensities, and the force field.

It is true that the force field B itself has been constrained by the results from the ab initio calculations, and might be expected to mirror those properties of electron flow exhibited by the ab initio APT's, even though the relationship between the parameters is ultimately rather obscure. If these may be used successfully in conjunction with the experimental intensities, then this would imply that the ab initio picture is actually close to that of physical reality. Surely though the perturbation procedure has destroyed any dependence of force field on APT's, even if they have both originated from the same source, Gaussian 76.

Thus the two sets of APT's may be considered to be independent, and it is certainly correct to take their similarity as being an encouraging sign that a realistic model is being constructed to describe the flow of charge as the molecule vibrates.

Section 7.1.
Atomic Polar Tensors - Analysis and Discussion.

To compare the APT's that have been derived for atoms in different molecules, it is necessary for these to be based on the same cartesian axis system. That employed for cyclohexane and trioxan (z-axis being the C_3 axis and the x-axis passing through the mid point of the in plane C-C or C-O bond respectively) has been different from that for dioxan and tetrahydropyran (y-axis parallel to the C-C bond; again the x-axis passes through its mid point) in order to take advantage of the simplifications that result from molecular symmetry.

The transition from one axis system to the other may be brought about simply by a rotation about the x-axis. For instance consider trioxan.

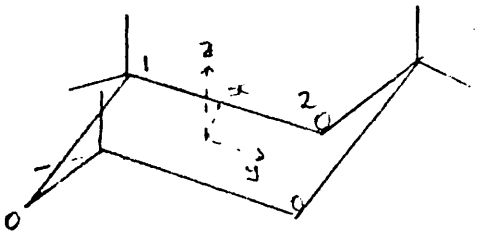

Coordinates:

C^1:	x	1.16614
	y	-.67327
	z	.23177
O^2:	x	1.16045
	y	.66998
	z	-.23177

From the Cartesian coordinates, the unit vector for the CO bond may be derived:

$$\underline{e}_{12} = -.0040\ \underline{e}_x + .94529\ \underline{e}_y - .32621\ \underline{e}_z$$

Since .94529 = cos 19.040°, this is the angle through which the molecule should be rotated around the x-axis (anti-clockwise) to bring the C-O parallel to the y-axis (neglecting the tiny x-component).

As previously, the effect of this molecular rotation on the APT's is realized through the application of a similarity transformation.

$$P_x(\text{new axes}) = RP_x(\text{old})R^t$$

$$R \text{ is } \begin{matrix} 1 & 0 & 0 \\ 0 & \cos\theta & -\sin\theta \\ 0 & \sin\theta & \cos\theta \end{matrix}$$

This procedure has been applied to the cyclohexane and trioxan APTs, and the results are listed below with the corresponding parameters for dioxan and tetrahydropyran. The atoms are labelled according to the following numbering scheme,

Cyclohexane

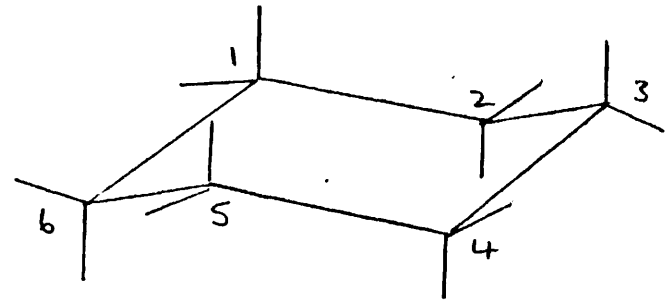

Tetrahydropyran: region 6 replaced by an oxygen atom.

Dioxan: regions 3 and 6 replaced by oxygen atoms.

Trioxan: regions 2,4 and 6 replaced by oxygen atoms.

TABLE 52.

APT's IN DIOXAN - TYPE AXIS SYSTEM.

Carbon Atoms.

Cyclohexane(1) (Ab initio)	.1289	-.0657	-.0482
	-.0642	.0442	-.0313
	-.0524	-.0287	.1653
Cyclohexane(1) (Experimental)	.085	-.019	-.047
	-.008	.040	-.026
	-.079	-.006	.182
Cyclohexane(3) (Ab initio)	-.0062	0	0
	0	.1922	-.0195
	0	-.0247	.1524
Cyclohexane(3) (Experimental)	.026	0	0
	0	.153	-.052
	0	-.091	.129
Tetrahydropyran(1) (Ab initio)	.7017	.1405	.1895
	.0208	.4300	-.0593
	.0770	-.0073	.4123
Tetrahydropyran(3) (Ab initio)	.0187	0	0
	0	.1239	-.0094
	0	-.0406	.1645
Tetrahydropyran(2) (Ab initio)	.0604	.0187	-.0042
	.0666	-.0292	-.0156
	.0448	-.0323	.1551
1,4-Dioxan(1) (Ab initio)	.6642	.1489	.1936
	.0021	.3400	-.0338
	.0864	-.0181	.4216
1,4-Dioxan(1) (Experimental)	.668	.131	-.017
	-.069	.258	-.042
	-.124	-.017	.313
Trioxan(1) (Ab initio)	.9314	.0256	.2559
	.0556	1.0910	-.0020
	.1690	.0329	.7238
Trioxan(3) (Ab initio)	1.118	0	0
	0	.7240	.2575
	0	.1515	.9043

Note: Original cyclohexane APT's have been rotated 19.473° anticlockwise about the x-axis. Trioxan APT's have been rotated 19.04° about the x-axis.

TABLE 53.

Axial Hydrogens.

Cyclohexane(1) (Ab initio)	.0366	-.0064	-.0348
	-.0268	-.0084	.0876
	.0231	.0522	-.1814
Cyclohexane(1) (Experimental)	.032	-.038	.041
	-.027	-.003	.037
	.011	.055	-.181
Cyclohexane(3) (Ab initio)	.0062	0	0
	0	.0187	.0440
	0	.1149	-.1780
Cyclohexane(3) (Experimental)	-.007	0	0
	0	-.006	.123
	0	.088	-.138
Tetrahydropyran(1) (Ab initio)	-.0208	-.0354	-.0739
	-.0323	-.0219	.1083
	.0239	.0239	-.1759
Tetrahydropyran(3) (Ab initio)	0.000	0	0
	0	.0364	.0364
	0	.0947	-.2020
Tetrahydropyran(2) (Ab initio)	.0479	.0031	.0467
	.0219	-.0115	.0729
	-.0031	.0645	-.1520
1,4-Dioxan(1) (Ab initio)	-.0104	-.0312	-.0708
	-.0302	-.0198	.0947
	.0229	.0541	-.1499
1,4-Dioxan(1) (Experimental)	-.065	.033	-.037
	-.030	-.015	.077
	.006	.090	-.133
Trioxan(1) (Ab initio)	-.0092	.0020	.0612
	.0225	-.0610	.0795
	.0019	.0434	-.1693
Trioxan(3) (Ab initio)	-.0472	0	0
	0	-.0176	.0548
	0	.0678	-.1746

TABLE 54.

Equatorial Hydrogen.

Cyclohexane(1) (Ab initio)	-.1759	.0809	.1119
	.0924	-.0134	-.0626
	.0795	-.0429	.0043
Cyclohexane(1) (Experimental)	-.127	.051	.078
	.044	-.011	-.042
	.098	-.054	-.017
Cyclohexane(3) (Ab initio)	.0208	0	0
	0	-.2552	-.0122
	0	-.0518	.0492
Cyclohexane(3) (Experimental)	.000	0	0
	0	-.198	-.009
	0	.015	.043
Tetrahydropyran(1) (Ab initio)	-.1156	.0541	.0760
	.0833	.0062	-.0729
	.0698	-.0427	.0104
Tetrahydropyran(3) (Ab initio)	.0292	0	0
	0	-.2519	.0031
	0	-.0312	.0552
Tetrahydropyran(2) (Ab initio)	-.1676	-.0750	-.1176
	-.0687	.0146	-.0468
	-.0802	-.0302	.0031
1,4-Dioxan(1) (Ab initio)	-.1052	.0500	.0760
	.0625	.0385	-.0562
	.0666	-.0302	.0146
1,4-Dioxan(1) (Experimental)	-.132	-.050	.115
	.042	-.006	-.053
	.079	-.036	-.004
Trioxan(1) (Ab initio)	-.0446	.0411	.0567
	.0441	.0394	-.0334
	.0482	-.0281	.0510
Trioxan(3) (Ab initio)	.0548	0	0
	0	-.0875	-.0074
	0	-.0179	.0786

TABLE 55.

Oxygen.

Tetrahydropyran(6) (Ab initio)	-1.1140	0	0
	0	-.7152	-.0042
	0	-.0239	-.5559
1,4-Dioxan(6) (Ab initio)	-1.0973	0	0
	0	-.7173	-.0094
	0	-.0115	-.5726
1,4-Dioxan(6)	-.981	0	0
	0	-.473	.036
	0	-.074	-.352
Trioxan(6) (Ab initio)	-1.1350	0	0
	0	-.7943	-.0130
	0	-.0162	-.6506

Bond Coordinate System.

In the literature, many APTs are reported that are based on the 'bond coordinate' system in which the molecular z-axis is chosen so that it points along (or is parallel to) a specified band, Depending on the symmetry of the site of the bonded atom, the corresponding APT may assume a particularly simple form that will facilitate subsequent analysis.

In the molecules under consideration in this study this axis system is primarily of interest for the hydrogen atoms, the z-axis then pointing along the C-H bond. Motion of the hydrogen in the z-direction is then a pure stretch. The dioxan-type system employed in the previous section actually has the y-axis parallel to C-C bonds, but motion of a carbon atom in this direction results in other internal coordinate distortions apart from a C-C stretch, due to the cyclic nature of the structure.

To swing the z-axis along a C-H bond actually requires two rotations: one about the z-axis to give the same y coordinate as the carbon, and then a subsequent rotation about the y-axis to give the same y coordinate as the carbon. Consider the procedure for the cyclohexane equatorial hydrogen (ab initio data).

For simplification the coordinates are adjusted so that the carbon atom becomes the origin 0,0,0. In this calculation the initial APT is based on the cyclohexane-type axis system, and these atoms have the following coordinates:

C: (0,0,0)
H^e: (.90877, -.52468, -.37100)

The two rotation matrices multiply to give

$$\begin{bmatrix} \cos\theta & 0 & -\sin\theta \\ 0 & 1 & 0 \\ \sin\theta & 0 & \cos\theta \end{bmatrix} \begin{bmatrix} \cos\phi & -\sin\phi & 0 \\ \sin\phi & \cos\phi & 0 \\ 0 & 0 & 1 \end{bmatrix}$$

$$= \begin{bmatrix} \cos\phi\cos\theta & -\cos\phi\sin\theta & -\sin\phi \\ \sin\theta & \cos\theta & 0 \\ \sin\phi\cos\theta & -\sin\phi\sin\theta & \cos\phi \end{bmatrix} \equiv R$$

It is required that

$$R \begin{bmatrix} .90877 \\ -.52468 \\ -.37100 \end{bmatrix} = \begin{bmatrix} 0 \\ 0 \\ 1.113 \end{bmatrix}$$

Three equations may be generated and then solved for the angles θ and ϕ.

① $.90877 \cos\phi\cos\theta + .52468 \cos\phi\sin\theta + .371 \sin\phi = 0.$

② $.90877 \sin\theta - .52468 \cos\theta = 0.$

③ $.90877 \sin\phi\cos\theta + .52468 \sin\phi\sin\theta - .371 \cos\phi = 1.113.$

② yields $\tan\theta = .52468/.90877 \therefore \theta = 30^{\circ}$

Substituting this into ① gives

$$\tan\phi = -2.8283 \quad \therefore \phi = 109.472^{\circ}$$

and ③ may be used to confirm these figures.

Thus the transformation matrix R may be constructed. Then

$$P_x(\text{bond coordinate system}) = R\, P_x(\text{old})\, R^t$$

and

$P_x(\text{old}) \rightarrow P_x(\text{new})$ as:

$$\begin{bmatrix} -.1759 & .1136 & .0785 \\ .1136 & -.0448 & -.0453 \\ .0442 & -.0255 & .0354 \end{bmatrix} \rightarrow \begin{bmatrix} .0492 & 0 & .0517 \\ 0 & .0208 & 0 \\ .0089 & 0 & -.2553 \end{bmatrix}$$

The APTs for hydrogen, in different molecules, in the bond coordinate system are listed below. Also given are the changes in the atomic coordinates produced by the shift of axes. The atoms are labelled as in the preceding section. In each case, the hydrogen coordinates listed are those bonded to the carbon at the origin.

TABLE 56.

APT's IN BOND COORDINATE AXIS SYSTEM.

* Cyclohexane H^e (Ab initio); $\theta = 30^o$, $\phi = 109.472^o$

	Old Coordinates	New Coordinates
C^1	0,0,0	0,0,0
C^2	0,1.43306,-.5066	.7164,1.2410,-.5067
C^6	-1.24107,-.71654,-.5066	.7164,-1.2410,-.5067
H^a	0,0,1.113	-1.0493,0,-.3710
H^e	-.90877,-.52468,-.37100	0,0,1.113

Old APT			New APT		
-.1759	.1136	.0785	.0492	0	.0517
.1136	-.0448	-.0453	0	0.208	0
.0442	-.0255	.0354	.0089	0	-.2553

Cyclohexane H^e (Expt).

Coordinates are listed above.

Old APT			New APT		
-.127	.074	.057	.042	0	-.015
.074	-.042	-.033	0	.001	0
.078	-.045	.014	.009	0	-.198

Note: In the cyclohexane-type axis system, the C-H^a actually points along the z direction, i.e. no computation is required.

TABLE 57.

Dioxan H^a (Ab initio) $\theta = 81.475^\circ$, $\phi = 20.079^\circ$

	Old Coordinates	New Coordinates
C^1	0,0,0	0,0,0
C^2	0,-1.5163,0	-1.4084,.2248,-.5148
O^6	-1.1935,-.4809,-.6283	.4962,-1.2516,-.4875
H^a	.0552,-.3680,1.0182	0,0,1.0841
H^e	.8368,-.3915,-.5554	.4962,-1.2516,-.4875

Old APT			New APT		
-.0104	-.0312	-.0708	.0227	.0178	-.0411
-.0302	-.0198	0.0947	.0486	-.0196	-.0419
.0229	.0541	-.1499	.0130	.0391	-.1832

Dioxan H^a (Expt)

Coordinates as listed above.

Old APT			New APT		
-.065	.033	-.037	.024	.015	-.024
-.030	-.015	.077	-.029	-.063	-.037
.006	.090	-.133	-.031	.026	-.174

continued...

continued....

Dioxan H^e (Ab initio) $\theta = 25.075^o$, $\phi = 121.014^o$

	Old Coordinates	New Coordinates
C^1	0,0,0	0,0,0
C^2	0,1.5163,0	.3311,1.3734,-.5507
O^6	-1.1935,-.4809,-.6283	.9904,-.9414,.1056
H^a	.0552,-.3680,1.0181	-.9787,-.3100,-.3481
H^e	.8368,-.3915,-.5554	0,0,1.0780

Old APT			New APT		
-.1052	.0500	.0760	.0514	.0123	.0315
.0625	.0385	-.0562	.0226	.0559	-.0014
.0666	-.0302	.0146	.0119	-.0222	-.1594

Dioxan H^e (Expt)

Coordinates as listed above.

Old APT			New APT		
-.132	-.050	.115	.063	.049	.015
.042	-.006	-.053	.002	-.032	-.005
.079	-.036	-.004	-.025	-.083	-.173

TABLE 58.

Tetrahydropyran H^a1 (Ab initio) $\theta = 83.774^o$, $\phi = 19.858^o$

Old Coordinates	New Coordinates
C^1 0,0,0	0,0,0
C^2 .0536, 1.5181,0	-1.4140,.2179,-.5107
O^6 -1.1994,-.4715,-.6294	.5323,-1.2434,-.4769
H^a .0399,-.3661,1.0197	0,0,1.084
H^e .8239,-.3910,-.5743	.6447,.7766,-.3778

Old APT			New APT		
-.0208	-.0354	-.0739	.0105	.0208	-.0484
-.0323	-.0219	.1083	.0536	-.0281	-.0463
.0239	.0239	-.1759	.0462	.0355	-.2010

Tetrahydropyran H^e1 (Ab initio) $\theta = 25.385^o$, $\phi = 122.201^o$

Old Coordinates	New Coordinates
C^1 0,0,0	0,0,0
C^2 .0536,1.5181,0	.3210,1.3945,-.5098
O^6 -1.1994,-.4715,-.6294	1.0023,-.9402,-.4104
H^a .0399,-.3661,1.0197	-.9657,-.3136,-.3801
H^e .8239,-.3910,-.5743	0,0,1.0780

Old APT			New APT		
-.1156	.0541	.0760	.0476	.0171	.0408
.0833	.0062	-.0729	.0224	.0362	.0269
.0698	-.0427	.0104	.0223	-.0109	-.1836

continued...

Tetrahydropyran H^a2 (Ab initio) $\theta = 98.626^\circ$, $\phi = 199.733^\circ$

	Old Coordinates	New Coordinates
C^1	-.0536,-1.5181,0	-1.4203,.1747,-.5095
C^2	0,0,0	0,0,0
C^3	-1.2530,-5460,.6649	.5557,-1.3207,-.5071
H^a	.0564,.3715,-1.0476	0,0,1.113
H^e	.8993,.3715,.5403	.6551,.8334,-.3391

Old APT			New APT		
.0479	.0031	.0467	.0222	.0241	-.0166
.0219	-.0115	.0729	.0226	.0429	-.0293
-.0031	.0645	-.1520	-.0008	.0222	-.1807

Tetrahydropyran H^e2 (Ab initio) $\theta = 157.554^\circ$, $\phi = -60.957^\circ$

C^1	-.0536,-1.5181,0	.3055,1.3823,-.5501
C^2	0,0,0	0,0,0
C^3	-1.2530,.5460,.6649	1.0424,-.9830,-.5073
H^a	.0564,.3715,-1.0476	-1.0101,-.3218,-.3391
H^e	.8993,.3715,.5403	0,0,1.113

Old APT			New APT		
-.1676	-.0750	-.1176	.0473	.0026	.0471
-.0687	.0146	-.0468	.0066	.0387	-.0152
-.0802	-.0302	.0031	.0062	-.0103	-.2359

continued...

continued...

Tetrahydropyran H^a3 (Ab initio) $\theta = -14.470^\circ$, $\phi = 0$

Old Coordinates	New Coordinates
C^2 1.2530,-.5460,-.6649	1.2530,-.6949,-.5074
C^3 0,0,0	0,0,0
C^4 -1.2530,-.5460,-.6649	-1.235,-.6949,-.5074
H^a 0,-.2782,1.0777	0,0,1.113
H^e 0,1.1112,-.0431	0,1.0652,-.3195

Old APT			New APT		
0	0	0	0	0	0
0	.0364	.0364	0	.0532	-.0294
0	.0947	-.2020	0	.0288	-.2189

Tetrahydropyran H^e3 (Ab initio) $\theta = -87.776^\circ$, $\phi = 0$

Old Coordinates	New Coordinates
C^2 1.2530,-.5460,-.6649	1.2530,.6856,-.5198
C^3 0,0,0	0,0,0
C^4 -1.2530,-.5460,-.6649	-1.2530,.6856,-.5198
H^a 0,-.2782,1.0777	0,-1.0660,-.3198
H^e 0,1.1112,-.0431	0,0,1.113

Old APT			New APT		
.0292	0	0	.0292	0	0
0	-.2519	.0031	0	.0537	.0430
0	-.0312	.0552	0	.0087	-.2503

TABLE 59.

Trioxan H^a (Ab initio) $\theta = -30^\circ$, $\phi = -.514^\circ$

Old Coordinates	New Coordinates
C^1 0,0,0	0,0,0
O^2 -.0057,1.3432,-.4635	1.3479,.0048,-.4514
O^6 -1.1661,-.6677,-4635	-1.3479,.0048,-.4514
H^a -.0149,.0086,1.0899	0,0,1.09
H^e .8664,-.5002,-.4108	.4965,-.8664,-.4151

Old APT			New APT		
-.0092	-.0219	-.0572	-.0348	-.0220	-.0345
-.0219	-.0346	.0330	-.0215	.0093	.0574
.0055	-.0031	-.1957	.0018	-.0053	-.1954

Trioxan H^e (Ab initio) $\theta = 30^\circ$, $\phi = 112.323^\circ$

Old Coordinates	New Coordinates
C^1 0,0,0	0,0,0
O^2 -.0057,1.3432,-.4635	.6837,1.1604,-.4467
O^6 -1.1661,-.6677,-.4635	.6837,-1.1604,-.4467
H^a -.0149,.0086,1.0899	-.9967,.0149,-.4298
H^e .8664,-.5002,-.4108	0,0,1.0814

Old APT			New APT		
-.0446	.0574	.0402	.0758	0	.0274
.0574	.0217	-.0232	0	.0548	0
.0312	-.0180	.0687	.0171	0	-.0847

Invariants of Atomic Polar Tensors.

The identification of the effective atomic charge χ_α through a reformulation of the Crawford G sum rule has enabled an experimental sum of integrated band intensities to be analyzed into separate 'atomic' contributions. The most significant trend to have been identified is that in many cases the values of χ_α seem to be independent of the host molecule. For instance χ_H = .101e (± .005) in all hydrocarbons except acetylene and χ_H = .072e(± .012) in the methyl halides. This implies that χ_α represents some particularly localized combination of chemical bond properties which is sensitive to the nature of the atom α rather than those atoms in its immediate vicinity or their geometrical arrangement.

There are two possible methods for determining χ_α:

a) From the APT for that atom, by calculating $[\underline{P}_x{}^\alpha(P_x{}^\alpha)^t]$. The effective charges may then be derived for all the atoms in the molecule and these will automatically satisfy those constraints imposed by the translational symmetry of the dipole moment.

b) Through measurements of the band intensities of isotopically substituted molecules and use of the sum rule (as used in the chapter presenting the experimental data).

The first method will yield χ_α that suffer from the same errors that are inherent to the determination of the APTs, namely uncertainties due to overlapping of bands, the sign choices of the experimental dipole derivatives and in the normal coordinates.

The second method is not usually viable for elements other than hydrogen. Isotopic data is scarce, and anyway the method would not be ideal for the heavier atoms (carbon, oxygen, fluorine etc.) since these provide only the minor terms in the intensity sums (the latter being weighted by the inverse of the atomic masses), and are thus particularly susceptible to errors from experimental measurements.

It is thus not realistic to expect the values of χ_α derived from the two different approaches to be exactly equal. In this work, the χ_H values obtained from the sum rule are:

$\chi_H = 0.115$ for cyclohexane
$\chi_H = 0.118$ for 1,4-dioxan

The values derived from the experimental APTs are:

$\chi_H = 0.118$ for cyclohexane
$\chi_{Ha} = 0.115$; $\chi_{He} = 0.124$ for 1,4-dioxan

It appears that the two sets of values exhibit good agreement. It should be recalled, however, that a number of assumptions were made concerning the band-splitting in the CH stretch regions and that these strongly influence the experimental effective charges on axial and equatorial hydrogens separately.

All derived effective atomic charges are tabulated below. Two additional quantities are also listed, the Mulliken total atomic charge[33] and the 'charge deformability' parameter.

The Mulliken charge is derived from molecular wavefunctions produced by quantum mechanical calculations.

Consider any normalized molecular orbital ϕ of a diatomic molecule, written as a linear combination of normalized atomic orbitals χ_r and χ_s of two respective atoms k and ℓ.

$$\phi = c_r \chi_r + c_s \chi_s$$

The occupancy of the molecular orbital, N (usually 2), may be envisaged as consisting of three 'sub-populations' whose distributions in space are given by the terms in the following expression

$$N\phi^2 = Nc_r^2(\chi_r)^2 + 2Nc_rc_s(\chi_r\chi_s) + Nc_s^2(\chi_s)^2$$

On integration over all space,

$$N = Nc_r^2 + 2Nc_rc_sS_{rs} + Nc_s^2$$

S_{rs} is the overlap integral: $\int_{\infty} \chi_r \chi_s d\tau$

The first and last terms are the 'net atomic populations' and the central term is the 'overlap population'. In attempting to allocate the total population to the atomic centres alone, each atom is assigned exactly half of the overlap.

$$N(k) = N(c_r^2 + c_r c_s S_{rs})$$
$$N(\ell) = N(c_s^2 + c_r c_s S_{rs})$$

The above logic may be expanded to fit the general case of a polyatomic molecule:

$$N(i;r_k) = N(i) c_{ir_k} (c_{ir_k} + \sum_{\ell \neq k} c_{is_\ell} S_{r_k s_\ell})$$

c_{ir_k} is the coefficient of the r^{th} atomic orbital (on atom k) in the i^{th} molecular orbital. $N(i;r_k)$ is the partial gross population in molecular orbital ϕ and atomic orbital χ_{r_k}.

$$N(i;k) = \sum_r N(i;r_k)$$

$N(i;k)$ is the subtotal in MO ϕ on atom k.

$$N(k) = \sum_i N(i;k)$$

$N(k)$ is the total gross population on atom k.

So in this scheme the total electronic charge is divided amongst the individual atomic centres. This analysis is performed by the Gaussian 76 program and is presented in the full computer print-out. Some caution should be exercised before attaching a direct physical meaning to the Mulliken atomic charge and all the sub-populations since the procedure suffers from a number of deficiencies.

(1) The equal division of the overlap charge between two atoms of a bond may be unrealistic.

(2) It is possible for an atomic orbital electron population calculated from this scheme to be negative or greater than 2.

(3) The charge Nc_A^2 is assigned entirely to atom A even though the function ϕ_A may have its maximum at a significant distance from A, perhaps even in the vicinity of a neighbouring nucleus.

(4) The values obtained are dependent on the basis set.

At one stage in this project it was hoped that changes in the Mulliken populations due to atomic displacements might give a valuable insight into the origins of the molecular dipole moment change. In fact the dipole moment calculated on considering each atom as a point mass possessing the Mulliken charge bore no relationship to the value generated by that same Gaussian 76 run from the wavefunctions directly. Quite possible this is due to the inability of the Mulliken approach to cater for the directional and unsymmetrical nature of the bonding.

It has been found[34] that charges correspond better with those found experimentally on increasing the size of the basis set. STO 4-31 G values are generally too positive.

Here it is considered that the Mulliken charges obtained may be most profitably used to identify trends that appear amongst atoms in different molecules, rather than attaching too much significance to their absolute magnitudes.

The 'charge deformability' parameter is a function of two terms which are invariants of the APT for the atom α.

$$\bar{p}_\alpha = \frac{1}{3} \mathrm{Tr}\, P_x^{\alpha}$$

$$\beta_\alpha^2 = \tfrac{1}{2}[(p_{xx}-\bar{p}_{yy})^2 + (p_{yy} - p_{zz})^2 + (p_{zz} - p_{xx})^2 + 3(p_{xy}^2 + p_{yz}^2 + p_{xz}^2 + p_{zx}^2 + p_{yx}^2 + p_{zy}^2)]$$

$\bar{p}_\alpha$ is the 'mean dipole derivative' and β_α is the anisotropy of the APT for atom α. These are related to the effective atomic charge by the relationship

$$\chi_\alpha^2 = (\bar{p}_\alpha)^2 + (2/9)\beta_\alpha^2$$

The charge deformability of atom α is defined as the ratio of $\bar{p}_\alpha$ to β_α, $|\bar{p}/\beta|_\alpha$.[35]

To understand the significance of this parameter, consider the form of the APT for an atom A in a diatomic molecule.

$$P_x^A = \begin{matrix} q_A^o & 0 & 0 \\ 0 & q_A^o & 0 \\ 0 & 0 & [q_A^o + (\delta q_A/\delta r_{AB})^o r_{AB}^o] \end{matrix}$$

q_A^o is the charge on atom A when the structure is at equilibrium.
r_{AB}^o is the equilibrium bond length.
$(\delta q_A/\delta r_{AB})^o$ gives the change in the value of the charge on A as the bond is stretched: the charge flux.

The expressions for the invariants take the form

$$\bar{p}_A = q_A^o + \tfrac{1}{3}(\delta q_A/\delta r_{AB})^o r_{AB}^o$$

$$\chi_A^2 = (q_A^o)^2 + \tfrac{2}{3} q_A^o (\delta q_A/\delta r_{AB})^o r_{AB} + \tfrac{1}{3}[(\delta q_A/\delta r_{AB})^o r_{AB}^o]^2$$

$$\beta_A^2 = [(\delta q_A/\delta r_{AB})^o r_{AB}^o]^2$$

$$\int_o |\bar{p}_A|\beta_A| = \left| \frac{q_A^o}{(\delta q_A/\delta r_{AB})^o r_{AB}^o} + \tfrac{1}{3} \right|$$

Thus if $(\delta q_A/\delta r_{AB})^o$ is very small $|\bar{p}_A/\beta_A|$ will become correspondingly large, whereas if $(\delta q_A/\delta r_{AB})^o$ is the leading term in the expression it will be small. This is equivalent to saying that atoms in bonds that have a prevalently ionic character (i.e. practically fixed charges) will have a high value of the parameter, >1.0. In this case the expressions for χ_A and q_A^o become very similar.

This argument may be extended to polyatomic molecules, where an APT may be written in the form (z axis being parallel to r_{AB}^o):

$$P_x^A = \begin{matrix} f[q_A^o, (\delta q_A/\delta R_t)^o] & f[(\delta q_A/\delta R_t)^o] & f[(\delta q_A/\delta R_t)^o] \\ f[(\delta q_A/\delta R_t)^o] & f[q_A^o, (\delta q_A/\delta R_t)^o] & f[(\delta q_A/\delta R_t)^o] \\ f[(\delta q_A/\delta R_t)^o] & f[(\delta q_A/\delta R_t)^o] & f[q_A^o, (\delta q_A/\delta R_t)^o, \\ & & (\frac{\delta q_A}{\delta r_{AB}})^o] \end{matrix}$$

where $R_t \neq r_{AB}$.

In hydrocarbons the off-diagonal charge flows are always smaller than q_A^o and $(\delta q_A/\delta r_{AB})^o$. If these are then neglected, the above expression reduces to a form very similar to that given for a diatomic molecule, as do the corresponding expressions for the invariants. Within this approximation $|\bar{p}/\beta|$ may be interpreted in the same way. Thus in a non-polar molecule such as ethane $|\bar{p}_H/\beta_H| = 0.144$, which can be compared with values of 1.2 for H in H_2O and 21.6 for H in HCN.

Before considering the tabulated results it should be recalled that in order to impose the constraint $\Sigma P_x^\alpha = 0$ for a molecule it was found necessary to recalculate the APT for a specific chosen atom, in the ab initio calculations. This procedure has the disadvantage of concentrating the error from the full set on the APT for that certain atom, and it may prove misleading to compare subsequently derived parameters such as the invariants with those from the unmanipulated APTs. For this reason the original carbon APT results have been included in the list, and these actually give a greater degree of consistency to the full set.

Firstly consider the data for the carbon atoms. It is here that the greatest fluctuation is observed on passing through the series cyclohexane, tetrahydropyran, dioxan, trioxan. This should be expected since carbon experiences the greatest bonding changes, being connected to zero, one, one and two oxygen atoms respectively. Thus it is observed that the Mulliken charge becomes correspondingly more positive and that the effective charge also increases (q_m increases by ~ + 0.3e on the addition of each oxygen and χ_c increases by ~ 0.4e). $|\bar{p}/\beta|_c$ is found to increase with the greater charge on the carbon as would be expected from the above discussion.

The variations in the properties of the hydrogen atoms are less significant since the replacement of carbon by oxygen occurs at a site two bonds away. Nevertheless, as the Mulliken charge becomes more positive, within the separate axial and equatorial sets the effective charge is seen to drop in magnitude. This trend is not consistent with

the values derived from the sum rule and experimental band intensities: cyclohexane, $\chi_H = 0.115$; dioxan, $\chi_H = 0.118$. No particular regularity is seen in the $|\bar{p}/\beta_H|$ data.

A further feature that is apparent is that in each site in each molecule the Mulliken charge on the equatorial hydrogen is more positive than on the axial hydrogen. If a new parameter is defined

$$\Delta = MC_{He} - MC_{Ha}$$

for hydrogens as the same carbon in the same molecule, then the following trend becomes clear:

Molecule	Δ(e)
Cyclohexane	.004
1,4-dioxan	.019
Tetrahydropyran(1)	.037
Trioxan	.066

Δ increases by ~ .03e on the inclusion of each oxygen, but the 1,4-dioxan figure suggests that addition of an oxygen separated by a C-C bond can reduce the discrepancy (the equatorial value is similar to that in THP but the axial hydrogen becomes more positive). Δ = .012 for tetrahydropyran hydrogens attached to both carbons 2 and 3.

The data for oxygen remains quite constant through the series. Thus whilst this atom is the source of the electronic rearrangements, it seems that the end result is actually an exchange of charge between the carbon and hydrogen atoms.

TABLE 60 INVARIANTS OF ATOMIC POLAR TENSORS.

Atom	Mulliken Charge(e)	χ_α(e)	$\lvert\bar{p}/\beta\rvert$
C(CYC,AB)	-.297	.143	.607
C(CYC,AB)*	-.297	.137	.718
C(CYC,EXPT)		.131	.590
C1(THP,AB)	+.029	.552	1.223
C2(THP,AB)	-.324	.111	.320
C3(THP,AB)	-.312	.150	1.320
C3(THP,AB)*	-.312	.122	.727
C(Dioxan,AB)	+.002	.517	1.096
C(Dioxan,AB)*	+.002	.507	1.080
C(Dioxan,EXPT)		.475	.889
C(Trioxan,AB)	+.295	.945	1.824
O(THP,AB)	-.704	.829	1.596
O(Dioxan,AB)	-.705	.826	1.693
O(Dioxan,EXPT)		.663	1.022
O(Trioxan,AB)	-.683	.884	1.980
H^a(CYC,AB)	+.147	.125	.211
H^a(CYC,EXPT)		.118	.231
H^a1(THP,AB)	+.146	.132	.312
H^a2(THP,AB)	+.155	.112	.173
H^a3(THP,AB)	+.147	.132	.217
H^a(Dioxan,AB)	+.166	.119	.275
H^a(Dioxan,EXPT)		.115	.370
H^a(Trioxan,AB)	+.161	.116	.447
H^e(CYC,AB)	+.151	.154	.206
H^e(CYC,EXPT)		.117	.237
H^e1(THP,AB)	+.183	.122	.215
H^e2(THP,AB)	+.167	.144	.174
H^e3(THP,AB)	+.159	.151	.187
H^e(Dioxan,AB)	+.185	.106	.078
H^e(Dioxan,EXPT)		.123	.197
H^e(Trioxan,AB)	+.227	.076	.097

* Corresponds to result obtained before imposition of constraint $\sum_\alpha P^\alpha_x = 0$.

Section 7.4.

Atomic Polar Tensors.

Any trends to have appeared in the invariants of the APTs must ultimately arise from relationships amongst the actual elements of these tensors. These in turn are functions of electro-optical parameters μ_i and $\partial\mu_i/\partial R_j$ (μ_i is the i^{th} bond moment, R_j is the j^{th} internal coordinate) which form the most direct interpretation of the electron flow. In this present study the analysis is not taken to this depth, the emphasis being rather on a comparison of the tensors of different compounds. Once trends have been identified they will promote the possibility of extending the work to prediction of the intensities of related molecules.

For convenience, the APT elements for atoms in different molecules are tabulated together below.

Consider first the carbon APTs (dioxan-type axis system). It should be recalled that the 2nd and 3rd rows of the dioxan experimental APTs contain a high measure of uncertainty due to the ab initio constraints that had to be introduced during their acquisition. The diagonal elements increase in magnitude on passing through the cyclohexane-trioxan series, paralleling correctly the trend in the experimental APT elements. Out of the six off-diagonal elements four show a definite trend through the series: dp_x/dz, dp_y/dx, dp_z/dx and dp_z/dy. Of these, only dp_x/dz mirrors the difference between the cyclohexane and dioxan experimental APT elements. However, both the ab initio dp_x/dy and dp_y/dz do reflect this difference.

For the hydrogen atoms the APT's are based on the bond coordinate system. Consider the axial and equatorial atoms separately. The diagonals of ab initio axial hydrogen only exhibit a trend in dp_x/dx but all mirror the experimental APTs. No off-diagonals show an obvious trend but all reflect the experimental figures except for dp_y/dx and dp_y/dz. For equatorial hydrogen, dp_y/dy and dp_z/dz do and dp_x/dx does not show a progression, whilst dp_x/dx and dp_z/dz mirror the experimental results. Many off-diagonal elements for cyclohexane and trioxan are forced to zero by molecular symmetry. Of those which are not, dp_x/dz and dp_z/dx, only

the former shows any trend. The experimental dp_x/dy and dp_z/dy changes are correctly predicted by the ab initio values. Most of the hydrogen APT elements are small in magnitude and so are of questionable significance.

For oxygen the values of the APT elements are independent of the host molecule, as was noted for the invariants. It seems that the inclusion of this atom strongly influences the carbon to which it is bonded and also the equatorial hydrogen attached to that carbon, but not the axial hydrogen. The diagonal elements of the carbon and equatorial hydrogen APTs typically have values directly proportional to the number of adjoining oxygen atoms.

One of the most interesting points to have emerged is the differentiation between axial and equatorial hydrogen. Such a phenomenon has been found to occur in many compounds containing atoms with lone pair electrons, as is indicated by the positions of the CH stretching modes. It is found that the lone pair weakens the CH bond that is trans to it. In dioxan the the other cyclic molecules studied here this is the carbon-axial hydrogen bond.

Thus the equatorial hydrogen is calculated to be more positively charged than its axial counterpart throughout this series of molecules. The CH^e stretching force constant is higher than that for CH^a in both the ab initio calculations and the unconstrained and constrained perturbation treatments.

The negative value of dp_z/dz for the hydrogens implies that as the CH bond stretches the hydrogen acquires a greater positive charge. The drop from -.2553 for H^e in cyclohexane to -.0847 in trioxan can be seen as being consistent with the greater equilibrium positive charge on the latter. It is more difficult to produce an electron flow away from a centre with an already high positive charge. For the addition of each oxygen the equatorial hydrogen Mulliken atomic charge increases by ~ 0.3 → 0.4e and the dp_z/dz also increases (i.e. becomes less negative) by a constant value, ~ .075e.

TABLE 61.

Diagonal Elements of Hydrogen Atomic Polar Tensors(/e) (Bond Coordinate System).

Atom, Molecule	$\frac{dp_x}{dx}$	$\frac{dp_y}{dy}$	$\frac{dp_z}{dz}$
H^a1,CYC(AB)	.0366	.0163	-.2061
H^a1,CYC(EXPT)	.032	.006	-.190
H^a1,THP(AB)	.0105	-.0281	-.2010
H^a1,Dioxan(AB)	.0227	-.0196	-.1832
H^a1,Dioxan(EXPT)	.024	-.063	-.174
H^a1,Trioxan(AB)	-.0348	.0093	-.1954
H^e1,CYC(AB)	.0492	.0208	-.2553
H^e1,CYC(EXPT)	.042	.001	-.198
H^e1,THP(AB)	.0476	.0362	-.1836
H^e1,Dioxan(AB)	.0514	.0559	-.1594
H^e1,Dioxan(EXPT)	.063	-.032	-.173
H^e1,Trioxan(AB)	.0758	.0548	-.0847

TABLE 62.

Off-Diagonal Elements of Hydrogen Atomic Polar Tensors(/e) (Bond Coordinate System).

Atom, Molecule	$\frac{dp_x}{dy}$	$\frac{dp_x}{dz}$	$\frac{dp_y}{dx}$	$\frac{dp_y}{dz}$	$\frac{dp_z}{dx}$	$\frac{dp_z}{dy}$
H^a1,CYC(AB)	-.0176	-.0307	-.0176	.0177	.0307	-.0177
H^a1,CYC(EXPT)	-.022	.051	-.022	-.029	.020	-.011
H^a1,THP(AB)	.0208	-.0484	.0536	-.0463	.0462	.0355
H^a1,Dioxan(AB)	.0178	-.0411	.0486	-.0419	.0130	.0391
H^a1,Dioxan(EXPT)	.015	-.024	-.029	-.037	-.031	.026
H^a1,Trioxan(AB)	-.0220	-.0345	-.0215	.0574	.0018	-.0053
H^e1,CYC(AB)	0	.0517	0	0	.0089	0
H^e1,CYC(EXPT)	0	-.015	0	0	.009	0
H^e1,THP(AB)	.0171	.0408	.0224	.0269	.0223	-.0109
H^e,Dioxan(AB)	.0123	.0315	.0226	-.0014	.0119	-.0222
H^e1,Dioxan(EXPT)	.049	.015	.002	-.005	-.025	-.083
H^e1,Trioxan(AB)	0	.0274	0	0	.0171	0

TABLE 63.

Diagonal Elements of Carbon Atomic Polar Tensors (Dioxan Type Axis System).

Atom, Molecule	$\frac{dp_x}{dx}$	$\frac{dp_y}{dy}$	$\frac{dp_z}{dz}$
Cl,CYC(AB)	.1289	.0442	.1653
Cl,CYC(EXPT)	.085	.040	.182
Cl,THP(AB)	.7017	.4300	.4123
Cl,Dioxan(AB)	.6642	.3400	.4216
Cl,Dioxan(EXPT)	.688	.258	.313
Cl,Trioxan(AB)	.9314	1.0910	.7238

TABLE 64.

Off-Diagonal Elements of Carbon Atomic Polar Tensors (Dioxan Type Axis System).

Atom, Molecule	$\frac{dp_x}{dy}$	$\frac{dp_x}{dz}$	$\frac{dp_y}{dx}$	$\frac{dp_y}{dz}$	$\frac{dp_z}{dx}$	$\frac{dp_z}{dy}$
Cl,CYC(AB)	-.0657	-.0482	-.0642	-.0313	-.0524	-.0287
Cl,CYC(EXPT)	-.019	-.047	-.008	-.026	-.079	-.006
Cl,THP(AB)	.1405	.1895	.0208	-.0593	.0770	-.0073
Cl,Dioxan(AB)	.1489	.1936	.0021	-.0338	.0864	-.0181
Cl,Dioxan(EXPT)	.131	-.017	-.069	-.042	-.124	-.017
Cl,Trioxan(AB)	.0256	.2559	.0556	-.0020	.1690	.0329

TABLE 65.

Oxygen APT Elements (Dioxan Type Axis System).

Atom, Molecule	$\frac{dp_x}{dx}$	$\frac{dp_y}{dy}$	$\frac{dp_z}{dz}$	$\frac{dp_y}{dz}$	$\frac{dp_z}{dy}$
O6,THP(AB)	-1.1140	-.7152	-.5559	-.0042	-.0239
O6,Dioxan(AB)	-1.0973	-.7173	-.5726	-.0094	-.0115
O6,Dioxan(EXPT)	-.981	-.473	-.352	.036	-.074
O6,Trioxan(AB)	-1.1350	-.7943	-.6506	-.0130	-.0162

Section 7.5.

Prediction of Tetrahydropyran Band Intensities.

The ultimate test for the proposed force fields and APTs is their usefulness in predicting the infrared spectra of other molecules. A series of measurements have been made for tetrahydropyran, leading to a full set of experimental band intensities. In this section these are compared with figures predicted employing the force fields and APTs of cyclohexane and 1,4-dioxan.

The tetrahydropyran force field has here been formed by selecting appropriate force constants from those already used for cyclohexane and 1,4-dioxan. The latter supplies the constants for the oxygen-containing section of the molecule, and cyclohexane the other half.

Dioxan Force constants →

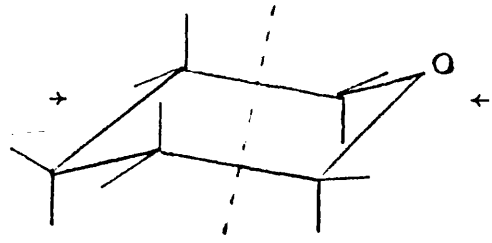

← Cyclohexane Force constants

The f_{cc} value is the average of that from the two fields.

Two fields were investigated for dioxan so this procedure accordingly yields a 'constrained' and 'unconstrained' tetrahydropyran field.

One set of APT's for tetrahydropyran was constructed in a similar fashion using the experimental tensors obtained for cyclohexane and dioxan. A different set was obtained from the Gaussian 76 ab initio calculations, which actually allows differentiation between the three types of carbon present.

Thus there are four different possible combinations of force field plus APTs, which each produce a different set of predicted band intensities. These are tabulated below.

Due to the large number of closely spaced modes, all of these being infrared active, and the approximate nature of the force fields, matching the observed and calculated

frequencies is a somewhat arbitrary process. All that can be done is to assume that it is correct to compare those bands of the same symmetry species (a' or a") that are closest in frequency. The quality of the frequency match will not determine the accuracy of the predicted intensity since these are different aspects of the molecular charge distribution.

A lot of data is listed. Overall there seems to be little to choose between constrained and unconstrained force fields in predicting the intensities. The ab initio APTs, however, appear to give better results than those constructed from experimental APTs. This is apparent in the predictions for the most intense experimentally observed bands:

	Constrained		Unconstrained	
ν_i, A_i(obs.)	Ab initio	Expt.	Ab initio	Expt.
1195, 41.2	49.9	26.4	5.9	2.9
1090, 70.2	64.7	52.2	74.4	56.6
1046, 25.7	1.5	3.8	7.6	1.6
875, 23.6	32.2	4.5	23.6	1.3

The ab initio APTs are successful except for the 1046 cm^{-1} band, whilst the experimental ones are satisfactory for only the 1090 cm^{-1} (most intense) band.

Many bands are intermediate in magnitude (between 4 and 20 km mol^{-1}) and on the whole are satisfactorily predicted. Two low intensity bands that seem particularly poor are the 880 cm^{-1} and 856 cm^{-1} bands.

	Constrained		Unconstrained	
ν_i, A_i(obs.)	Ab initio	Expt.	Ab initio	Expt.
880, 0	0.8	25.4	18.8	48.9
856, 4.3	22.8	4.2	29.1	5.4

These will be very sensitive to the amount of CO stretch predicted in the normal mode.

Overall, the reasonable measure of agreement must lead to some optimism in hoping that these fields and APTs form a viabl foundation on which to base further refinements.

TABLE 66.

Tetrahydropyran - 'Constrained' Force Field.

Obs ν (cm^{-1})	Calc ν (cm^{-1})	Obs A_i (km mol^{-1})	Calc A_i (km mol^{-1})	Ab initio
			EXPT	
2958a'	2980			
2958a"	2974			
2942a'	2928	114.4	281.3	190.5
2933a'	2921			
2924a"	2923			
2860a'	2860			
2860a"	2860			
2849a'	2856	218.1	150.0	280.2
2849a"	2855			
2842a'	2855			
1468a'	1463	4.0	0.0	0.8
1454a'	1449	4.3	1.8	5.9
1441a"	1474			
1434a'	1443	11.6	15.9	21.24
1420a"	1449			
1384a'	1399	5.85	0.5	5.3
1360a"	1401	1.1	4.4	3.2
1347a"	1393	4.75	12.8	1.0
1338a"	1339	0.0	5.2	0.9
1297a'	1356	5.6	1.3	1.8
1271a"	1216	5.8	9.2	9.2
1254a'	1300	3.45	3.8	3.5
1242a"	1179	0.0	0.8	3.5
1195a"	1264	41.2	26.4	49.9
1170a'	1227	0.0	0.8	6.2
1155a'	1123	2.3	0.3	1.5
1090a"	1114	70.2	52.2	64.7
1046a"	1095	25.7	3.8	1.5
1030a'	1042	11.6	4.1	4.8
1009a'	962	9.5	3.7	9.3
969a"	963	2.4	2.5	15.4

continued...

continued...

880a"	849	0	25.4	0.8
875a'	851	23.6	4.5	32.2
856a'	819	4.3	4.2	22.8
818a'	776	4.0	0.1	6.2
811a"	762	0.0	1.8	2.0
565a'	580	3.7	6.3	3.9
458a"	463			
432a'	500	7.2	19.3	10.4
400a'	369			
252a'	200			
252a"	171	4.3	1.3	13.72

TABLE 67.

Tetrahydropyran - 'Unconstrained' Force Field.

Obs ν (cm^{-1})	Calc ν (cm^{-1})	Obs A_i (km mol^{-1})	Calc A_i (km mol^{-1}) EXPT	Ab initio
2958a'	2979			
2958a"	2975			
2942a'	2923	114.4	281.1	190.0
2933a'	2922			
2924a"	2923			
2860a'	2859			
2860a"	2859			
2849a'	2856	218.1	149.7	279.2
2849a"	2855			
2842a'	2855			
1468a'	1471	4.0	2.2	5.6
1454a'	1453	4.3	4.4	8.1
1441a"	1471			
1434a'	1444	11.6	12.2	19.3
1420a"	1449			
1384a'	1398	5.85	0.7	5.3
1360a"	1407	1.1	0.0	4.0
1347a"	1371	4.75	10.7	8.2
1338a"	1345			
1297a'	1294	5.6	2.3	6.3
1271a"	1332	5.8	22.2	13.1
1254a'	1218	3.45	1.1	4.2
1242a"	1250	0	1.5	1.6
1195a"	1200	41.2	2.9	5.9
1170a'	1174	0	0.4	4.6
1155a'	1125	2.3	1.2	1.8
1090a"	1061	70.2	56.6	74.4
1046a"	1109	25.7	1.6	7.6
1030a'	1070	11.6	1.1	2.9
1009a'	960	9.5	2.4	5.8

continued...

continued...

969a"	956	2.4	1.4	9.1
880a"	881	0.0	48.9	18.8
875a'	878	23.6	1.3	23.6
856a'	811	4.3	5.4	29.1
818a'	797	4.0	0.0	2.2
811a"	766	0.0	1.0	6.5
565a'	568	3.7	5.8	10.3
458a"	480			
432a'	463	7.2	24.2	11.0
400a'	379			
252a'	197			
252a"	176	4.3	1.4	13.5

Section 7.6.

An 'Average' Dioxan Force Field.

Out of curiosity it was decided to test a third force field for dioxan formed by combining the constrained and unconstrained fields. The new field is taken as their average:

$$F_{Av} = (F_{constr} + F_{unconstr})/2$$

where F is an element in the force field matrix. Where there is no corresponding element (as with some interaction terms) F_{Av} is simply half of the non-zero value.

This field, in conjunction with the dioxan ab initio APTs, was used to calculate the dioxan frequencies and intensities. The results are tabulated below.

TABLE 68.

d_o Dioxan - Average Force Field.

Obs ν_i (cm^{-1})	Calc ν_i (cm^{-1})	Obs A_i (km mol^{-1})	Calc A_i (km mol^{-1})
2970bu	2975	176.6	123.1
2970au	2971		
2863au	2863	153.4	209.6
2863bu	2855		
1457bu	1440	16.19	16.6
1449au	1476		
1378bu	1368	2.11	1.9
1369au	1359	11.28	8.2
1291bu	1322	12.19	13.3
1256au	1261	33.00	54.6
1136au	1101	158.1	150.5

continued...

continued...

1086au	1057	10.35	13.0
1052bu	1035	8.05	7.0
889bu	850	17.51	69.0
881au	883	75.2	50.0
610bu	652	14.6	35.8
288au	178	0	5.2
274bu	287	20.2	45.6

TABLE 69.

d_8 Dioxan - Average Force Field.

Obs ν_i (cm^{-1})	Calc ν_i (cm^{-1})	Obs A_i (km mol^{-1})	Calc A_i (km mol^{-1})
2235au	2216	87.3	72.1
2232bu	2224		
2098bu	2090	101.4	148.0
2086au	2110		
1191au	1217	91.5	68.4
1153bu	1122	29.4	20.3
1117au	1093	97.8	89.2
1087bu	1057	13.0	4.4
1042bu	1023	28.0	11.5
1030au	1059	13.0	91.3
922au	881	0	1.7
896bu	894	17.4	19.6
809au	836	0	0.1
762au	732	39.1	17.6
732bu	737	5.2	49.9
490bu	531	9.6	26.9
238bu	253	13.9	32.4
254au	145	0	3.4

It was found that in nearly every case the intensity calculated is close to the average of those calculated with the initial two fields. In a number of cases this leads to a great improvement in the agreement with the experimental

results. For instance, the unconstrained field calculated the d_8 1117cm^{-1} band as 9.2, the constrained field gave 204.1 and this new field gives 89.2, compared with the experimental value of 97.8. Similarly the unconstrained field gave d_o 881cm^{-1} as 123.0, the constrained gave 8.4 and the new field gives 50.0, compared with the experimental value of 75.2. Of course there are a number of instances where the good agreement from one field is spoiled by the poor result from the other - e.g. the d_8 1191cm^{-1} band: unconstrained gives 90.5, the constrained 36.5 and the average field gives 68.4, compared with 91.5 experimentally.

This has illustrated that it seems possible to roughly estimate the consequences for the intensities on modifying the force field. Since ideally in future studies there will be a combined iterative refinement of fields and APTs to frequencies plus intensities, such a conclusion may lead to valuable constraints for the procedure.

Section 7.7.

ASSESSMENT OF RESULTS.

The initial aim of this project was to perform a thorough analysis of the vibrational spectra of 1,4-dioxan. The acquisition of experimental band intensities from gas and solution phase spectra, although time-consuming, is a straightforward procedure once the necessary instrumentation has been assembled and the computer programs have been written.

It was decided that MO calculations, carried out with Gaussian 76, would provide a set of constraints for later force field perturbation treatments, to ensure that realistic force constants could be produced for the analysis of the experimental data. Any subsequent success from these results would then show that Gaussian 76 and the STO 4-31G basis set could properly be used for molecules of this size.

The ease with which atomic polar tensors could be obtained from Gaussian 76 made it feasible to calculate these for a range of related molecules, and this effectively decided the course of the rest of the research: experimental data was acquired for d_0- and d_8-dioxan, d_0- and d_{12}-cyclohexane and tetrahydropyran, ab initio APTs were generated for dioxan, cyclohexane, tetrahydropyran and trioxan, and software was constructed to analyse the experimental band intensities and derive APTs from them.

Initially it was expected that the ab initio data would basically be employed to give some insight into the experimental figures. However, due to the greater quantity of the former at present, a rather different approach has been adopted. When agreement has appeared between the ab initio and experimental results, this has been used to justify some degree of confidence in the ab initio results, and conclusions have been drawn from these which are then taken as being realistic.

Perhaps it is correct to be somewhat sceptical about such an approach. How much faith should really be attached to the figures that the computer generates in its quantum

mechanical calculations? Any indication of internal consistency is given great significance - maybe there is too much of a temptation to ignore those numbers which are not so satisfactory. When possible, conclusions ought to be drawn from real experiments in a real laboratory! The manner in which the dioxan constrained force field was derived is particularly open to this form of criticism; this is a least-squares fit (to experimental frequencies) of a least-squares fit (to energies calculated from Gaussian 76) to an MO calculation, which itself is based on a hierachy of assumptions (validity of LCAO approach, viability of basis set, etc.). A cynic would argue that the force constants finally produced might well be valid solutions to certain sets of equations, but actually lack any physical significance.

It is hoped that the success of the cyclohexane calculations will go some way to subduing such criticism. The fact that the ab initio sign combinations are those generated by the completely independent force field plus experimental intensities must at least confirm the validity of this MO procedure for the calculation of APTs for this molecule.

Incorporation of oxygen atoms into the ring will certainly change the character of the molecule, so this success is not necessarily relevant. However, again the signs for dp_x/dQ gained via the experimental intensities correspond with those from the ab initio calculations apart from those for several weak bands. Certainly ab initio force constants were used in generating the force field but these are several steps removed from the actual field employed, and the band intensities are completely independent. The fact is that it is the constrained force field that was most successful in analysing the intensities - this would have to be pure coincidence if the MO approach led to wholly abstract and meaningless force constants.

The force fields certainly need more thorough investigation since these are the prerequisites for any analysis of the experimental work. The next stage must be to carry out

a force field refinement simultaneously on all frequencies for the molecules studied. Certainly more isotopic data should be incorporated, especially ^{13}C or ^{18}O derivatives which would yield valuable information on the ring deformations (it was found that dioxan could be successfully prepared by the self-condensation of 1g of ethylene glycol (70% yield) in concentrated sulphuric acid, and this can be bought commercially in the isotopically substituted forms).

In summary, it is hoped that this research has shown that Gaussian 76 can prove valuable in the analysis of the infrared spectra of these cyclic molecules. The degree of consistency between the ab initio results and those from experiment leads to optimism in believing that the derived atomic polar tensors are reasonable and that a procedure has evolved that will form the basis for future extensions of these studies.

ACKNOWLEDGMENTS

I would like to express my warmest gratitude to my supervisor, Dr. Derek Steele, whose encouragement and patience have enabled me to carry out the work described in this thesis. I would also like to thank the technical staff of the Chemistry Department, Royal Holloway College, for their assistance, and to acknowledge the support provided by the provision of a three year grant by the Science and Engineering Research Council.

APPENDIX

CONTENTS

References

1. B. Crawford, Jr., J. Chem. Phys., 20 (1952) 977.

2. B. Crawford, Jr., J. Chem. Phys., 29 (1958) 1042.

3. D. G. Bourgin, Phys. Rev., 29 (1927) 794.

4. E. Bartholome, Z. Phys. Chem., (Leipzig), B23 (1933) 131.

5. E. B. Wilson, Jr., and A. J. Wells, J. Chem. Phys., 14(1946) 578.

6. R. Coulon, B. Oksengorn, J. Robin and B. Vodar, J. Phys. Radium., 14 (1953) 63.

7. H. L. Welsh, M. F. Crawford, J. C. F. McDonald and D. Chisholm, Phys. Rev., 83 (1951) 1264.

   D. A. Chisholm, Phys. Rev., 83 (1951) 1264.

   J. Fahrenfort and J. A. A. Ketelaar, J. Chem. Phys., 22 (1954) 1631.

8. D. M. Dennison, Phys. Rev., 31 (1928) 503.

9. R.Ladenburg and F. Reiche, Ann. Physik., 42 (1911) 181.

10. D. A. Ramsey, J. Am. Chem. Soc., 74 (1952) 72.

11. H. J. Kostowsky and A. M. Bass, J. Opt. Soc. Am., 46 (1956) 1060.

12. A. Savitsky and M. J. E. Golay, Analyt. Chem., 36 (1964) 1627.

13. H. C. Burger and P. H. van Cittert, Z. Physik., 79 (1952) 722.

14. H. F. Herget, W. E. Deeds, N. M. Goular, R. J. Lovell and A. H. Nielsen, J. Opt. Soc. Am., 52 (1962) 1113.

15. R. N. Jones, R. Venkataragharan and J. W. Hopkins, Spectrochim. Acta, 23A (1967) 925.

16. D. F. Hornig and D. C. McKean, J. Phys. Chem., 59 (1955)

17. L. A. Gribov, Intensity Theory for Infrared Spectra of Polyatomic Molecules, Consultants Bureau, New York, 1964.

18. W. T. King, G. B. Mast and P. P. Blanchette, J. Chem. Phys., 56 (1972) 4440; 58 (1973) 1272; 64 (1976) 3036.

19. C. C. J. Roothan, Rev. Mod. Phys., 23 (1951) 69.

20. For example;

H. F. Schaefer, The Electronic Structure of Atoms and Molecules, Addison-Wesley, Reading, Massachusetts, 1972.

E. Clements, Proc. Nat. Acad. Sci. U.S.A., 69 (1972) 2942.

P. Pulay and W. Meyer, J. Mol. Spectrosc., 40 (1971) 59.

21. J. A. Pople and D. L. Beveridge, Approximate MO Theory, McGraw-Hill, New York, 1970.

22. G. A. Segal and M. L. Klein,J. Chem. Phys., 47 (1967) 4236.

23. R. Ditchfield, W. S. Hehre and J. A. Pople, J. Chem. Phys., 54 (1970) 724.

24. C. E. Blom, P. J. Slingerland and C. Altona, Mol. Phys., 31 (5) (1976) 1359.

25. A. Garrett and I. Mills, J. Chem. Phys., 49 (1968) 1719.

26. P. Pulay, Mol. Phys., 17 (2) (1969) 197.

27. D. Steele, W. B. Person and K. G. Brown, J. Phys. Chem., 85 (1981) 2007.

28. J. A. Pople et al., Quantum Chemistry Package Exchange, 11 (1978) 368.

29. H. R. Buys and H. J. Goise, Tetrahedron Lett., 34 (1970) 2997.

30. R. G. Snyder and J. H. Schachtsneider, Spectrochim. Acta, 21 (1965)169.

31. K. B. Wiberg and A. Shrake, Specrochim. Acta, 27A (1971) 1139; 29A (1973) 567; 29A (1973) 583.

32. R. G. Snyder and G. Zerbi, Spectrochim. Acta, 23A (1967) 391.

33. R. S. Mulliken, J. Chem. Phys., 23 (1955) 1833.

34. M. Gussoni, C. Castiglioni and G. Zerbi, Chem. Phys. Lett., 95 (1983) 483.

35. M. Gussoni, P. Jona and G. Zerbi, J. Chem. Phys., 80 (1984) 1377.

TEKTRONIX PROGRAM FOR THE INPUT AND ANALYSIS OF SPECTRAL DATA

The following is a listing of the program that was developed to store and manipulate spectra from the Perkin-Elmer 325 spectrometer. The operations performed by the program are described in Section 2.1.

```
80 GO TO 8300
81 GO TO 181
82 GO TO 3000
83 GO TO 3200
84 GO TO 1800
85 GO TO 5000
86 GO TO 8500
87 GO TO 9600
88 GO TO 5800
89 GO TO 5801
90 GO TO 8200
91 GO TO 9800
92 GO TO 18100
93 GO TO 12000
100 GO TO 9300
101 PAGE
102 PRINT "PROGRAM TO ACCEPT DATA FROM PE325 "
103 PRINT
105 PRINT "IS THIS A BACKGROUND RUN?    YES = 1,  NO = 2"
106 INPUT Z9
110 PRINT "INPUT ABSOLUTE STARTING FREQUENCY"
120 INPUT Y2
130 PRINT "INPUT FINAL FREQUENCY"
140 INPUT Y3
141 Z1=1
145 X=0.14285714286
146 PRINT "ENTER TITLE"
147 INPUT T$
148 PRINT "ENTER FILE NUMBER"
149 INPUT Z5
150 IF Y2<2500 THEN 190
170 Y4=5000
180 PRINT "SCAN ON 5000-2000 RANGE"
185 GO TO 300
190 IF Y2<1000 THEN 230
200 X=X/2
210 Y4=2500
220 PRINT "SCAN ON 2500-1000 RANGE "
225 GO TO 300
230 IF Y2<500 THEN 270
240 X=X/5
250 Y4=1000
260 PRINT "SCAN ON 1000-400 RANGE "
265 GO TO 300
269 IF Y2<200 THEN 295
270 X=X/10
280 Y4=450
285 PRINT "SCAN ON 450-200 RANGE"
290 GO TO 300
295 PRINT "FREQUENCY OUT OF RANGE"
296 END
300 N1=INT((Y2-Y3)/X)
310 PRINT "TOTAL NUMBER OF POINTS = ";N1
320 PRINT "INPUT SAMPLING INTERVAL"
330 INPUT N2
340 N1=INT(N1/N2)
350 Y5=X*N2
355 Y6=INT(Y5*1000)
356 Y6=Y6*1.0E-3
360 PRINT "POINTS TO BE COLLECTED AT ";Y6;" CM-1 INTERVALS"
370 V1=INT((Y4-Y2)/X)+1
380 V2=Y4-V1*X
390 IF V1<=99 THEN 430
400 Y6=INT(V1/100)
410 Y6=100*Y6
420 V1=V1-Y6
430 Y1=199-Y1
431 IF V1<100 THEN 440
432 V1=V1-100
```

```
440 CALL "RATE";1200,8,2
450 DELETE F2
460 DIM F2(N1),F3(N1)
465 F2=0
466 F3=0
470 PRINT "COMMENCE SCANNING AT ";V1;" ON THE INTERFACE"
480 PRINT @40,30:
1300 GOSUB 2500
1320 IF A<>V1 THEN 1300
1325 PRINT A;B
1330 A2=V1
1360 F2(1)=B
1400 IF N2=1 THEN 1640
1480 FOR J1=2 TO N2
1500 GOSUB 2500
1502 M9=M9+1
1505 PRINT A;B
1520 F2(1)=F2(1)+B
1540 NEXT J1
1560 F2(1)=F2(1)/N2
1640 FOR I1=2 TO N1
1660 F2(I1)=0
1680 FOR I2=1 TO N2
1700 GOSUB 2500
1702 M9=M9+1
1704 IF M9<>20 THEN 1710
1706 PAGE
1707 CALL "WAIT";1.0E-3
1708 M9=1
1709 PRINT "POINTS COLLECTED=";I1
1710 PRINT A;B
1720 F2(I1)=F2(I1)+B
1740 NEXT I2
1750 F2(I1)=F2(I1)/N2
1752 A3=A2-A
1752 A3=A2-A
1770 A2=A
1780 NEXT I1
1781 IF Z9=3 THEN 1800
1782 F2=883-F2
1783 Z9=3
1800 PAGE
1810 V3=V2-(N1-1)*X*N2
1815 MOVE 60,1800
1820 PRINT "      FREQUENCY AT TERMINATION EQUALS ";V3
1825 PRINT "                ";T$;" FILE NUMBER ";Z5
1840 WINDOW 0,N1,0,1000
1845 VIEWPORT 10,120,10,100
1846 Z=V2-N1*X*N2
1850 AXIS N1/20,100
1855 MOVE 0,10
1860 CALL "DISP",F2
1861 CALL "DISP",F3
1862 GOSUB 2910
1870 INPUT X9
1880 GO TO 9300
1900 END
2500 INPUT @40:A$,B$,C$,D$,E$
2520 A1=VAL(A$)
2540 B1=VAL(B$)
2560 C1=VAL(C$)
2580 D1=VAL(D$)
2600 E1=VAL(E$)
2620 A=10*D1+E1
2640 B=100*A1+10*B1+C1
2660 RETURN
2680 PRINT "FREQ COUNTER IS OUT OF STEP"
2690 END
2910 MOVE INT(N1/2),0
2915 PRINT "JJJJJJJJJFREQUENCY IN CH-1"
2920 FOR I=0 TO N1 STEP INT(N1/10)
```

```
2820 FOR I=0 TO N1 STEP INT(N1/10)
2830 MOVE INT(CD),0
2835 W=INT(Y2-I*X*M2)
2840 PRINT "HJ";W
2845 NEXT I
2846 IF Z1<>1 THEN 2960
2848 MOVE 0,1000
2850 PRINT "HHHH100"
2853 MOVE 0,800
2856 PRINT "HHHKJJJJJTHJRHJWHJNHJSHJMHJIHJSHJSHJIHJOHJN"
2960 RETURN
3000 PAGE
3010 PRINT "ENTER DATA FILE NUMBER"
3020 INPUT Z5
3060 FIND Z5
3070 PRINT "INPUT TITLE"
3080 INPUT T$
3090 WRITE T$,N1,N2,X,Y2,Y3,F2
3092 CLOSE
3095 GO TO 9300
3096 END
3200 PRINT "ENTER DATA FILE NUMBER"
3201 INPUT Z5
3202 PRINT "IS THIS BACKGROUND DATA?        YES = 1   NO =2"
3203 INPUT Z9
3204 FIND Z5
3210 READ @33:T$,N1,N2,X
3212 WINDOW 0,N1,0,1000
3220 IF Z9=2 THEN 3280
3240 DIM F2(N1)
3250 READ @33:Y7,Y8,F2
3260 Y2=Y7
3262 Y3=Y8
3270 GO TO 3320
3280 DELETE F3
3290 DIM F3(N1)
3300 READ @33:Y9,Y8,F3
3302 Y2=Y9
3304 Y3=Y8
3310 Z1=1
3320 PAGE
3330 IF Z9=2 THEN 3360
3340 CALL "DISP",F2
3350 GO TO 3370
3360 CALL "DISP",F3
3365 MOVE 0,1000
3370 GO TO 9300
3380 END
5000 PAGE
5006 WINDOW 0,N1,0,1000
5007 IF Z9=4 THEN 5071
5070 CALL "DISP",F2
5071 CALL "DISP",F3
5075 GOSUB 8000
5080 FOR I=1 TO N1
5082 F3(I)=LOG(F2(I)/F3(I))/2.302585
5084 NEXT I
5085 PRINT "JJJJJJJJJJ"
5086 PRINT "F3 NOW CONTAINS ABSORBANCE"
5087 INPUT Z0
5088 GOSUB 7000
5089 INPUT Z0
5090 GO TO 9300
5091 DELETE F2
5092 DIM F2(N1)
5093 CALL "INT",F3,F2
5095 MOVE 0,-0.1
5100 PAGE
5101 PRINT "INTENSITY OF BAND IS ";F2(N1)*X*M2
5105 PRINT "JJJJJ"
5110 GOSUB 9000
```

```
5120 INPUT X9
5130 GO TO 9300
6000 END
7000 CALL "MAX",F3,M4,M5
7010 CALL "MIN",F3,M6,M7
7020 M8=INT(10*M4)+1
7030 M8=M8/10
7055 PAGE
7060 M9=-M8/10
7070 WINDOW 0,N1,0,M8
7071 VIEWPORT 10,120,10,95
7075 AXIS N1/20,0.1
7076 Z1=2
7077 GOSUB 2910
7080 CALL "DISP",F3
7090 MOVE 0,M8
7095 PRINT "HHHHHK "
7100 PRINT M8
7110 MOVE 0,0.8*M8
7120 PRINT "HHHHAHJPHJSHJOHJRHJPHJAHJNHJCHJE"
7130 MOVE 0.7*N1,M8
7135 END
7140 PRINT "FILE NUMBER ";Z5;"HHHHHHHHHHHHHJJ";T$
7200 RETURN
8000 PRINT "JJJJJ"
8001 PRINT "AT WHAT FREQUENCY IS THE FIXED POINT?";
8010 INPUT F8
8020 N5=INT((Y2-F8)/(X*N2))
8030 PRINT "WHAT IS THE BGRD/SAMPLE INTENSITY RATIO HERE?";
8032 INPUT I8
8034 PRINT "HOW MANY POINTS DO YOU WISH TO AVERAGE OVER?";
8036 INPUT N7
8038 DIM S1(N7)
8039 DIM K1(N7)
8040 FOR I=1 TO N7
8042 S1(I)=F3(N5-(N7-1)/2+I)
8043 K1(I)=F2(N5-(N7-1)/2+I)
8044 NEXT I
8046 S2=0
8047 K2=0
8048 FOR J=1 TO N7
8050 S2=S2+S1(J)
8051 K2=K2+K1(J)
8052 NEXT J
8054 S3=S2/N7
8055 F2(N5)=K2/N7
8056 S=S3*I8/F2(N5)
8060 FOR I=1 TO N1
8070 F2(I)=F2(I)*S
8080 NEXT I
8090 PRINT "BACKGROUND INTENSITIES HAVE BEEN SCALED BY";S
8100 CALL "DISP",F2
8105 CALL "DISP",F3
8110 RETURN
9000 H=INT(N1/100)
9005 M3=0
9006 C1=0
9010 FOR J=1 TO H
9012 C=100*X*N2*J
9014 C2=C
9016 DELETE F2
9020 DIM H1(100),H2(100)
9030 FOR I=1 TO 100
9040 H1(I)=F3(I+(J-1)*100)
9050 NEXT I
9060 CALL "INT",H1,H2
9065 H2(100)=H2(100)*X*N2
9066 C3=Y2-C1
9067 C4=Y2-C2
9070 PRINT "INT OF SECTION ";C3;" TO ";C4;" IS ";H2(100)
```

```
9075 H3=H3+H2(100)
9080 DELETE H1,H2
9085 C1=C2
9090 NEXT J
9091 PRINT
9095 PRINT "TOTAL INTENSITY OF SECTIONS IS ";H3
9100 RETURN
9200 PAGE
9210 PRINT T$;"                                        FILE NUMBER ";Z5
9215 PRINT
9216 PRINT
9217 PRINT
9220 PRINT "V2 = ";V2;"     V3 = ";V3
9225 PRINT
9226 PRINT
9227 PRINT
9230 PRINT "INTENSITY OF BAND IS ";F2(H1)*X*N2
9235 PRINT
9240 PRINT "FREQUENCY OF FIXED POINT IS ";F8
9245 PRINT
9250 PRINT "BACKGROUND/SAMPLE RATIO AT THIS POINT IS ";I8
9255 PRINT
9260 PRINT "AVERAGED OVER ";N7;" POINTS"
9265 PRINT
9270 PRINT "BACKGROUND INTENSITIES HAVE BEEN SCALED BY ";S
9275 PRINT
9280 GOSUB 9300
9285 END
9290 ON SRQ THEN 9300
9300 PAGE
9305 PRINT "          PROGRAM TO ACCEPT DATA FROM PE325"
9306 PRINT
9310 PRINT "          INPUT THE OPTION NUMBER REQUIRED"
9320 PRINT
9321 PRINT
9325 PRINT "1    COLLECT DATA FROM PE325"
9326 PRINT
9330 PRINT "2    STORE TRANSMITTANCE ON MAGNETIC TAPE"
9331 PRINT
9332 PRINT "3    COLLECT TRANSMITTANCE FROM TAPE"
9333 PRINT
9340 PRINT "4    DISPLAY DATA IN STORE"
9341 PRINT
9350 PRINT "5    RATIO AND ABSORBANCE"
9351 PRINT
9360 PRINT "6    STORE ABSORBANCE ON MAGNETIC TAPE"
9361 PRINT
9362 PRINT "7    COLLECT ABSORBANCE FROM TAPE"
9370 PRINT
9371 PRINT "8    DISPLAY ABSORBANCE"
9372 PRINT
9373 PRINT "9    INTEGRATE"
9374 PRINT
9375 PRINT "10   LIST INTEGRATION DATA"
9376 PRINT
9377 PRINT "11   PLOT ABSORBANCE"
9378 PRINT
9379 PRINT "12   LIST INTEGRATION DATA ON PLOTTER"
9380 PRINT
9381 PRINT "13   END"
9382 PRINT
9400 INPUT Z0
9410 GO TO Z0 OF 81,82,83,84,85,86,87,88,89,90,91,92,93
9420 END
9500 REM STORE ABSORBANCE
9501 PRINT "ENTER DATA FILE NUMBER"
9505 INPUT Z5
9510 FIND Z5
9515 PRINT "ENTER TITLE"
9520 INPUT T$
```

```
9525 WRITE T$,N1,N2,X,V2,V3,F8,I8,N7,S,F3
9530 GO TO 9300
9600 REM COLLECT ABSORBANCE
9601 PRINT "ENTER DATA FILE NUMBER"
9605 INPUT Z5
9610 FIND Z5
9615 READ @33:T$,N1,N2,X
9619 DELETE F3
9620 DIM F3(N1)
9625 READ @33:V2,V3,F8,I8,N7,S,F3
9630 GO TO 9300
9700 PRINT "INPUT 2 IF F2 TO BE CHECKED OR 3 FOR F3"
9705 INPUT Z9
9710 PRINT
9720 PRINT "INPUT NUMBER OF POINTS TO BE CHECKED"
9730 INPUT Z8
9740 FOR J=1 TO Z8
9750 IF Z9=2 THEN 9780
9760 PRINT "F3(";N1-Z8+J;") =";F3(N1-Z8+J)
9770 IF Z9=3 THEN 9790
9780 PRINT "F2(";N1-Z8+J;") =";F2(N1-Z8+J)
9790 NEXT J
9800 CALL "MAX",F3,M4,M5
9810 CALL "MIN",F3,M6,M7
9820 M8=INT(10*M4)+1
9830 M8=M8/10
9840 WINDOW 0,N1,0,M8
9850 VIEWPORT 10,120,10,95
9860 AXIS @25:N1/20,0.1
9870 Z1=2
9880 MOVE @25:INT(N1/2),0
9890 PRINT @25:"JJJJJJJJJFREQUENCY IN CM-1"
9900 FOR I=1 TO N1 STEP INT(N1/10)
9910 MOVE @25:INT(I),0
9920 W=INT(V2-I*X*M2)
9930 PRINT @25:"HJ";W
9940 NEXT I
9945 MOVE @25:0,F3(1)
9950 FOR I=2 TO N1
9960 DRAW @25:I,F3(I)
9970 NEXT I
9980 MOVE @25:0,M8
9990 PRINT @25:"HHHHHHK "
10000 PRINT @25:M8
10010 MOVE @25:0,0.8*M8
10020 PRINT @25:"HHHHHAHJHHJSHJOHJHHJHHJAHJHHJCHJE"
10030 MOVE @25:0.7*N1,M8
10035 END
10040 PRINT @25:"FILE NUMBER ";Z5;"HHHHHHHHHHHHHJ";T$
10050 GO TO 9300
10060 END
10100 PRINT @25:T$;"                                    FILE NUMBER ";Z5
10101 PRINT @25:
10110 PRINT @25:
10120 PRINT @25:
10130 PRINT @25:"V2 = ";V2;"    V3 = ";V3
10140 PRINT @25:
10150 PRINT @25:
10160 PRINT @25:
10170 PRINT @25:"INTENSITY OF BAND IS ";F2(N1)*X*M2
10180 PRINT @25:
10190 PRINT @25:"FREQUENCY OF FIXED POINT IS ";F8
10200 PRINT @25:
10210 PRINT @25:"BACKGROUND/SAMPLE RATIO AT THIS POINT IS ";I8
10220 PRINT @25:
10230 PRINT @25:"AVERAGED OVER ";N7;" POINTS"
10240 PRINT @25:
10250 PRINT @25:"BACKGROUND INTENSITIES HAVE BEEN SCALED BY ";S
10260 PRINT @25:
10270 M=INT(N1/100)
```

```
18288 H3=0
18298 FOR J=1 TO H
18300 DIM H1(100),H2(100)
18310 FOR I=1 TO 100
18320 H1(I)=F3(I+(J-1)*100)
18330 NEXT I
18340 CALL "INT",H1,H2
18350 H2(100)=H2(100)*X*N2
18360 PRINT @25:"INTENSITY OF SECTION ";J;" IS ";H2(100)
18370 H3=H3+H2(100)
18380 DELETE H1,H2
18390 NEXT J
18400 PRINT @25:
18410 PRINT @25:"TOTAL INTENSITY OF SECTIONS IS ";H3
18420 GO TO 9300
12000 END
14035 DIM F2(N1)
14036 DIM F3(N1)
15000 PRINT "INPUT NUMBER OF SEPARATE BANDS"
15010 INPUT N8
15015 S3=N2*X
15016 FOR I=1 TO N1
15017 F3(I)=0
15018 NEXT I
15020 FOR J=1 TO N8
15022 GOSUB 16000
15024 FOR I=1 TO N1
15026 F3(I)=F3(I)+F2(I)
15028 NEXT I
15030 NEXT J
15080 REM COMBINED SPECTRUM IS NOW IN F3
15092 STOP
15095 N2=1
15096 GO TO 9900
16000 PRINT "INPUT BAND CENTRE,MAX ABSORBANCE,HALF-HALF-WIDTH"
16010 INPUT F1,I1,H5
16015 PRINT "INPUT EXP FACTORS"
16018 INPUT A5,B5
16020 FOR K=1 TO N1
16025 K=-K
16030 A=H5^2+(V2+K*S3-F1)^2
16040 B=I1*H5^2
16070 D=-A5*ABS(V2+K*S3-F1)^B5
16080 E=EXP(D)
16085 K=-K
16090 F2(K)=B/A*E
16100 NEXT K
16110 GO TO 15024
20000 PRINT "INPUT RANGE OF INTEGRATION"
20010 INPUT F6,F7
20020 N6=(V2-F6)/(N2*X)
20022 N6=INT(N6)
20030 N7=(V2-F7)/(N2*X)
20032 N7=INT(N7)
20040 N8=N7-N6
20050 DIM F5(N8)
20060 DIM Q(N8)
20070 FOR J=1 TO N8
20080 F5(J)=F3(N6+J)
20090 NEXT J
20100 CALL "INT",F5,Q
20105 Q(N8)=Q(N8)*X*N2
20110 PRINT "INT OF SECTION IS";Q(N8)
58000 FOR I=1 TO 10
58010 PRINT "PLEASE DO NOT START USING TEKTRONIX!-TIM"
58020 NEXT I
58030 END
```

GAS PHASE SPECTRA

d_0-Dioxan

Spectrum	Region (cm^{-1})	Pathlength (m)	Pressure (mm Hg)
1	3100-2600	1.25	1.34
2	1520-1410	1.25	1.18
3	1410-1200	1.25	0.96
4	1200-1000	1.25	0.48
5	960-820	1.25	0.80
6	660-550	1.25	1.34
7	320-220	1.25	1.56
d_8-Dioxan			
8	2315-2150	1.25	0.6
9	2150-1900	1.25	0.6
10	1300-1000	1.25	0.71
11	1000-840	1.25	0.97
12	840-700	1.25	0.71
13	560-440	1.25	3.88
14	270-200	1.25	2.50
d_0-Cyclohexane			
15	3030-2830	1.25	0.15
16	1500-1400	1.25	1.52
17	1400-1310	5	30.00
18	1310-1190	5	3.82
19	1100-1000	5	7.65
20	1000-800	5	2.58
21	560-480	5	14.53

Spectrum	Region (cm^{-1})	Pathlength (m)	Pressure (mm Hg)
d_{12}-Cyclohexane			
22	2300-2150	1.25	0.48
23	2150-2000	1.25	0.48
24	1300-1000	5	1.58
25	1000-850	5	1.58
26	770-600	5	2.98
27	450-350	5	13.92
Tetrahydropyran			
28	3100-2780	1.25	0.42
29	1550-1335	1.25	2.50
30	1325-1235	1.25	5.05
31	1235-1000	1.25	0.84
32	1000-925	5	3.48
33	620-520	5	3.48
34	450-340	5	3.24
35	290-200	5	2.54

Note: In all the spectra presented the absorbance is $\log_{10}(I_0/I)$, i.e. ordinate values should be multiplied by 2.303 to give the natural logarithmic absorbance value.

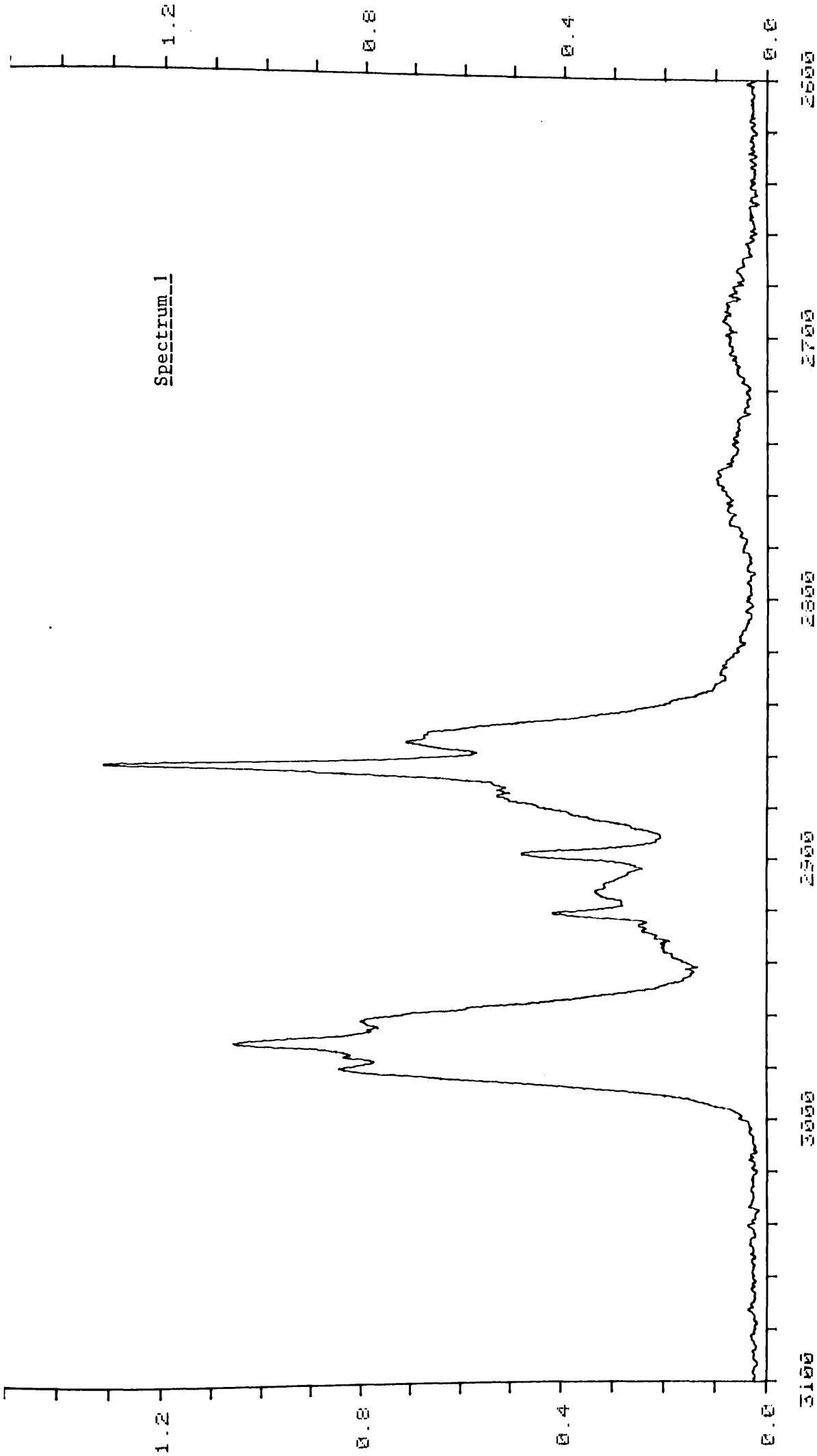
Spectrum 1
1.2
0.8
0.4
0.0
29000
28000
27000
26000
25000
24000
23000

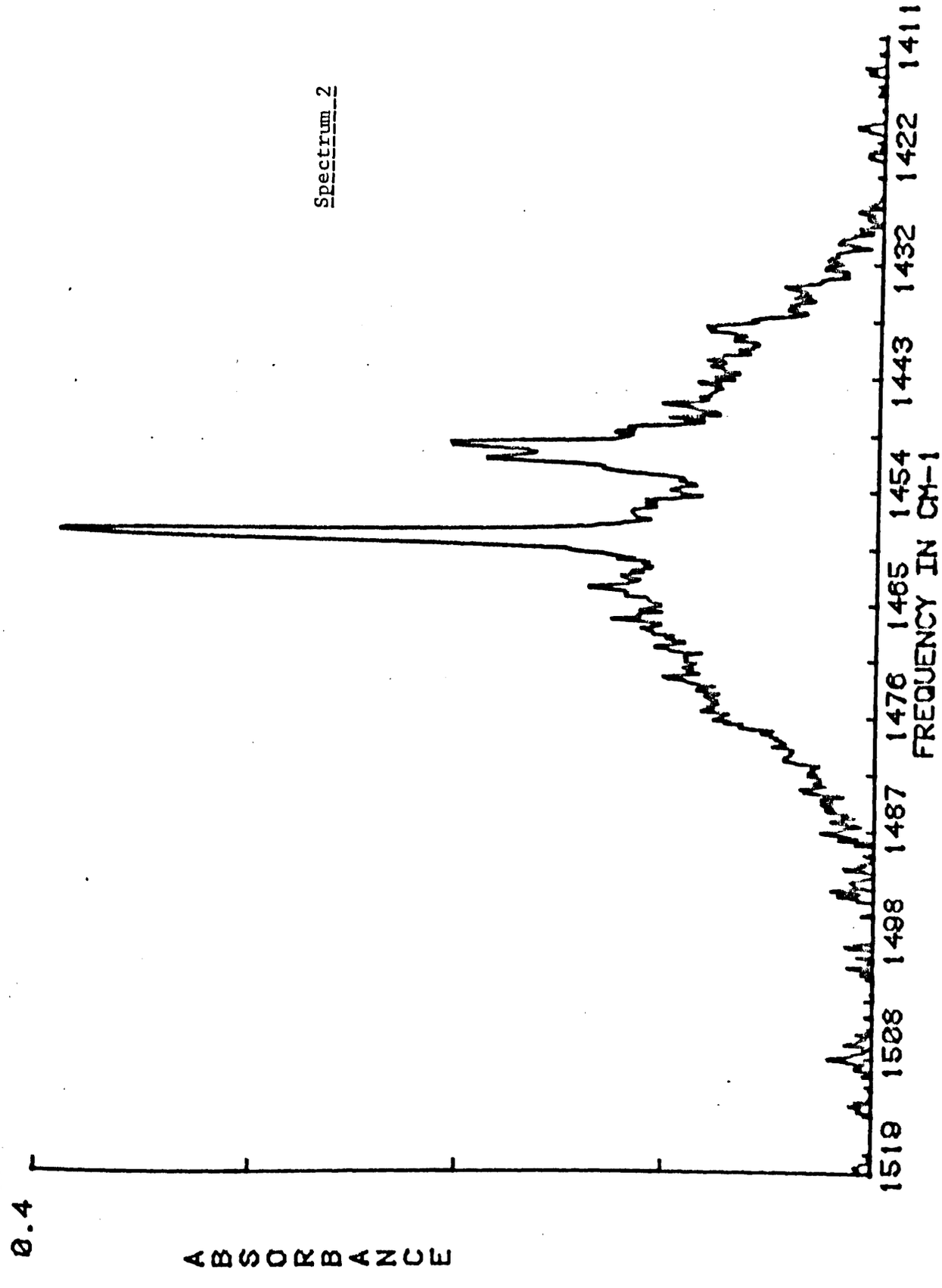
Spectrum_2
0.4
ABSORBANCE
1519 1508 1498 1487 1476 1465 1454 1443 1432 1422 1411
FREQUENCY IN CM-1

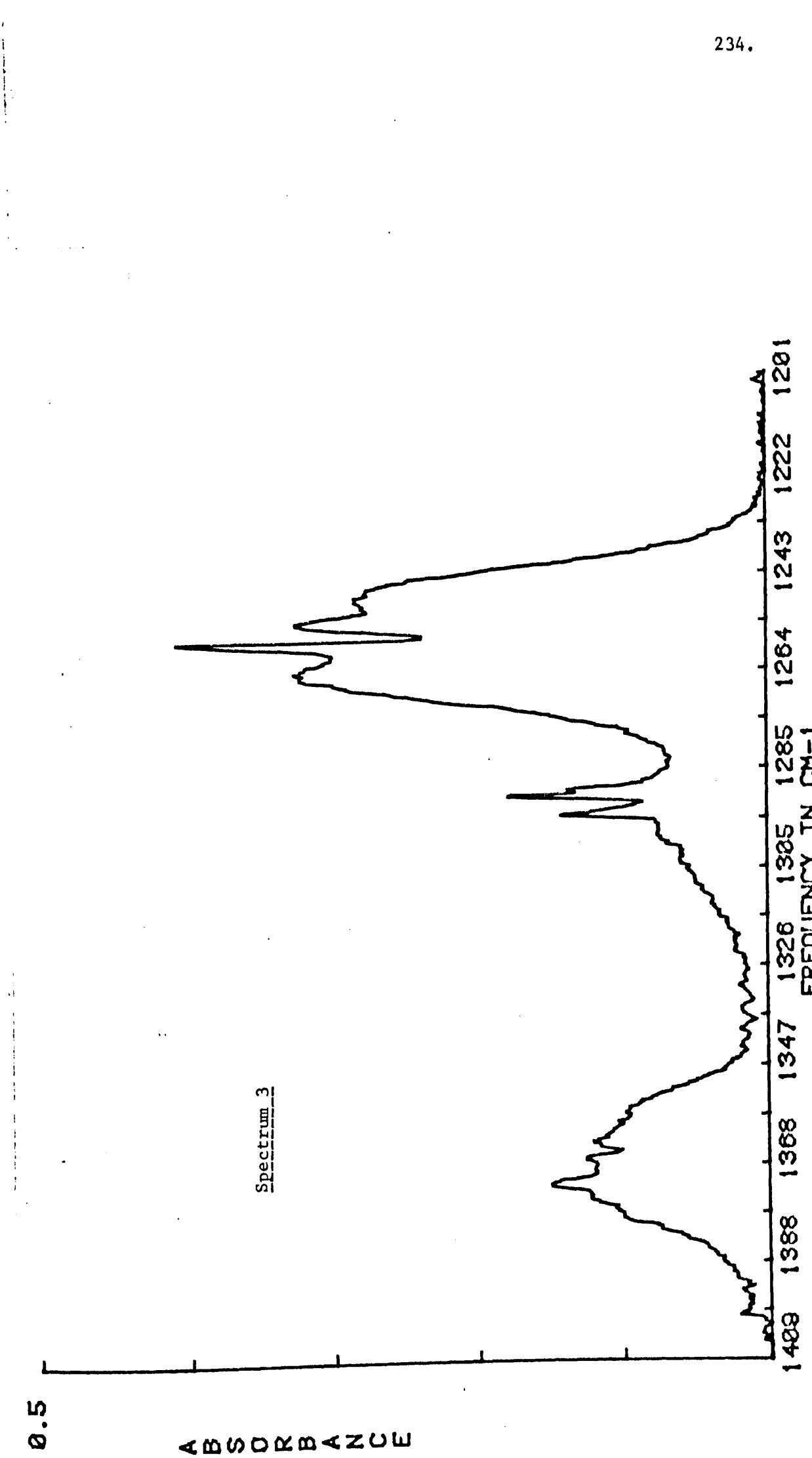
0.5
ABSORBANCE
Spectrum 3
1409
1388
1368
1347
1326
1305
1285
1264
1243
1222
1201
FREQUENCY IN CM-1

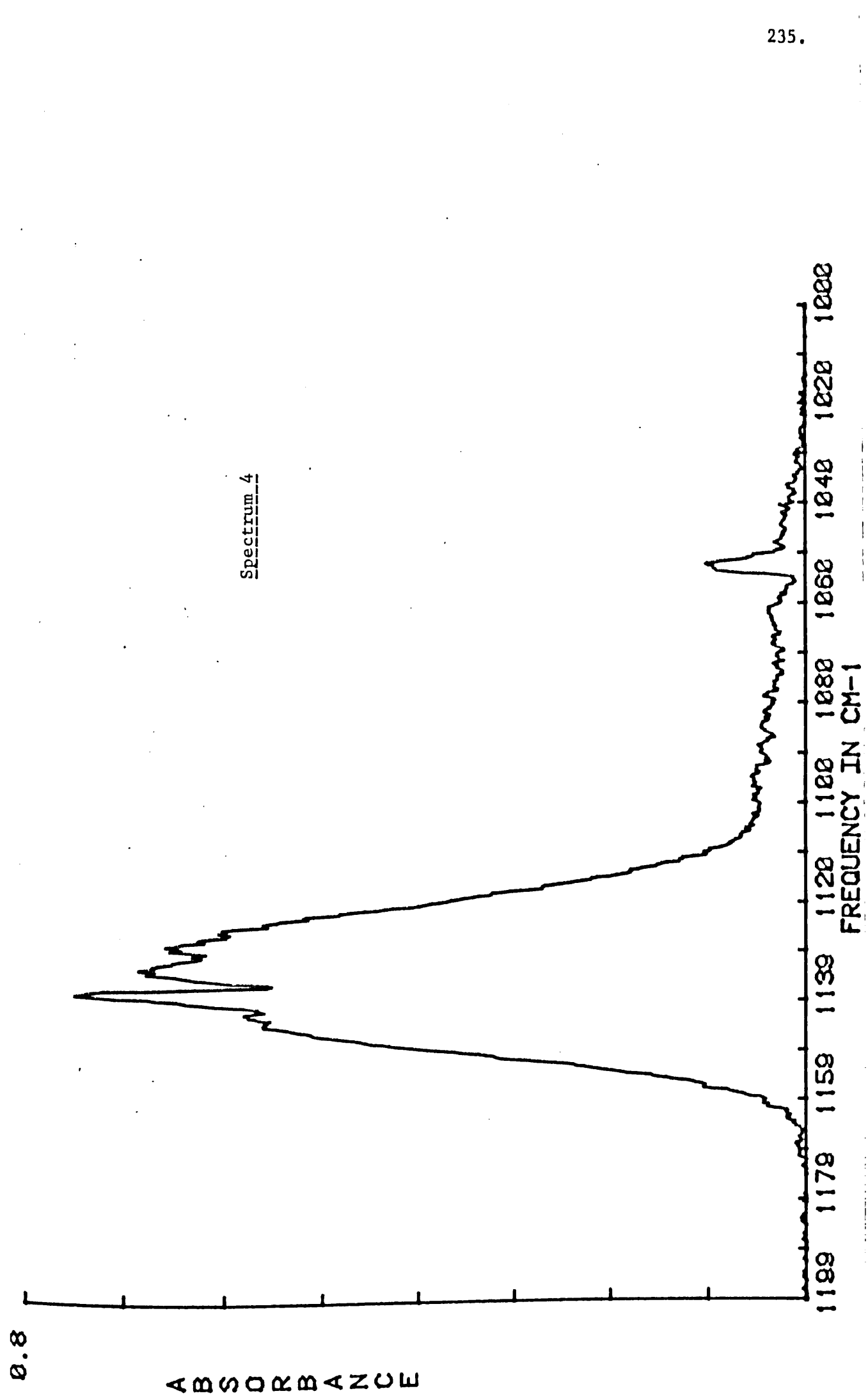
Spectrum 4
0.8
ABSORBANCE
1189
1179
1159
1139
1120
1100
1080
1060
1040
1020
1000
FREQUENCY IN CM-1

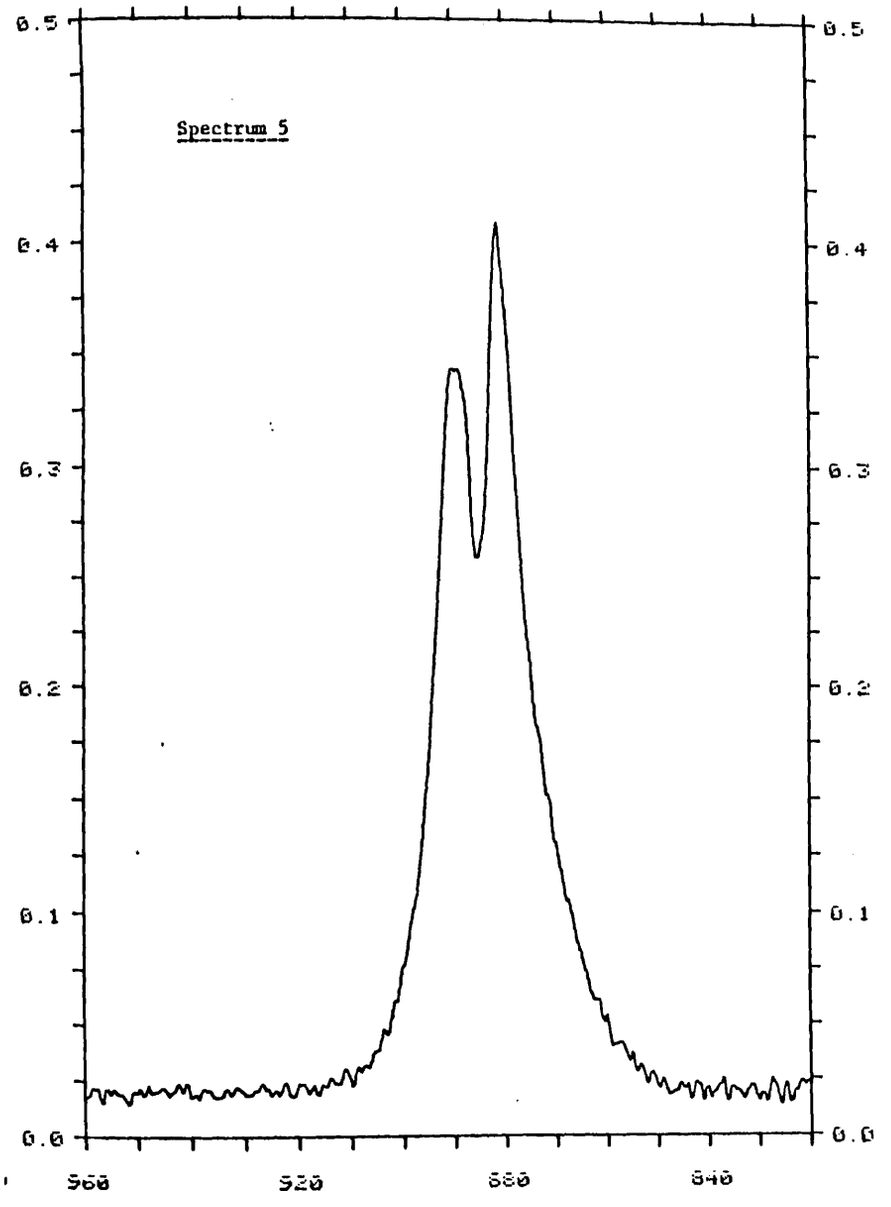
Spectrum 5
0.5
0.4
0.3
0.2
0.1
0.0
960
920
880
840

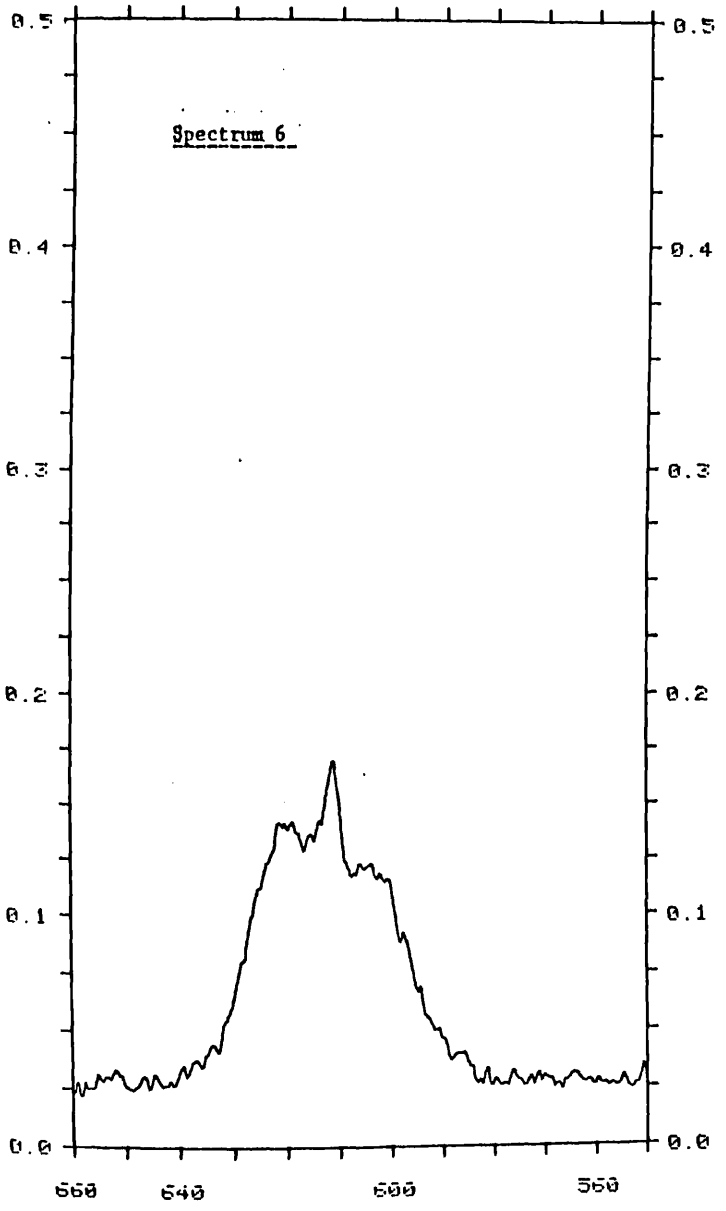
Spectrum 6
0.5
0.4
0.3
0.2
0.1
0.0
660
640
600
560

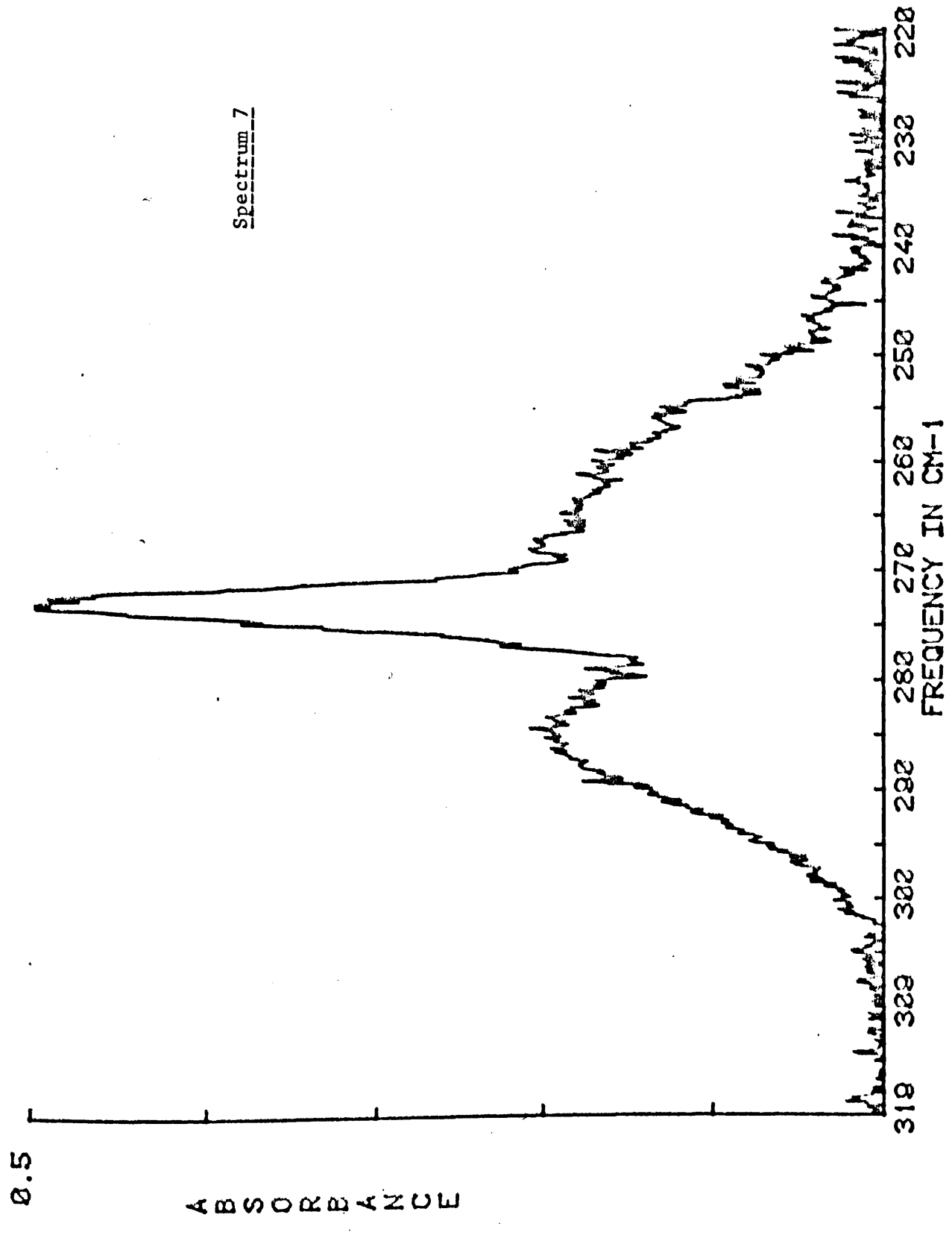
Spectrum_7
0.5
ABSORBANCE
318
328
338
282
272
262
252
242
232
228
FREQUENCY IN CM-1

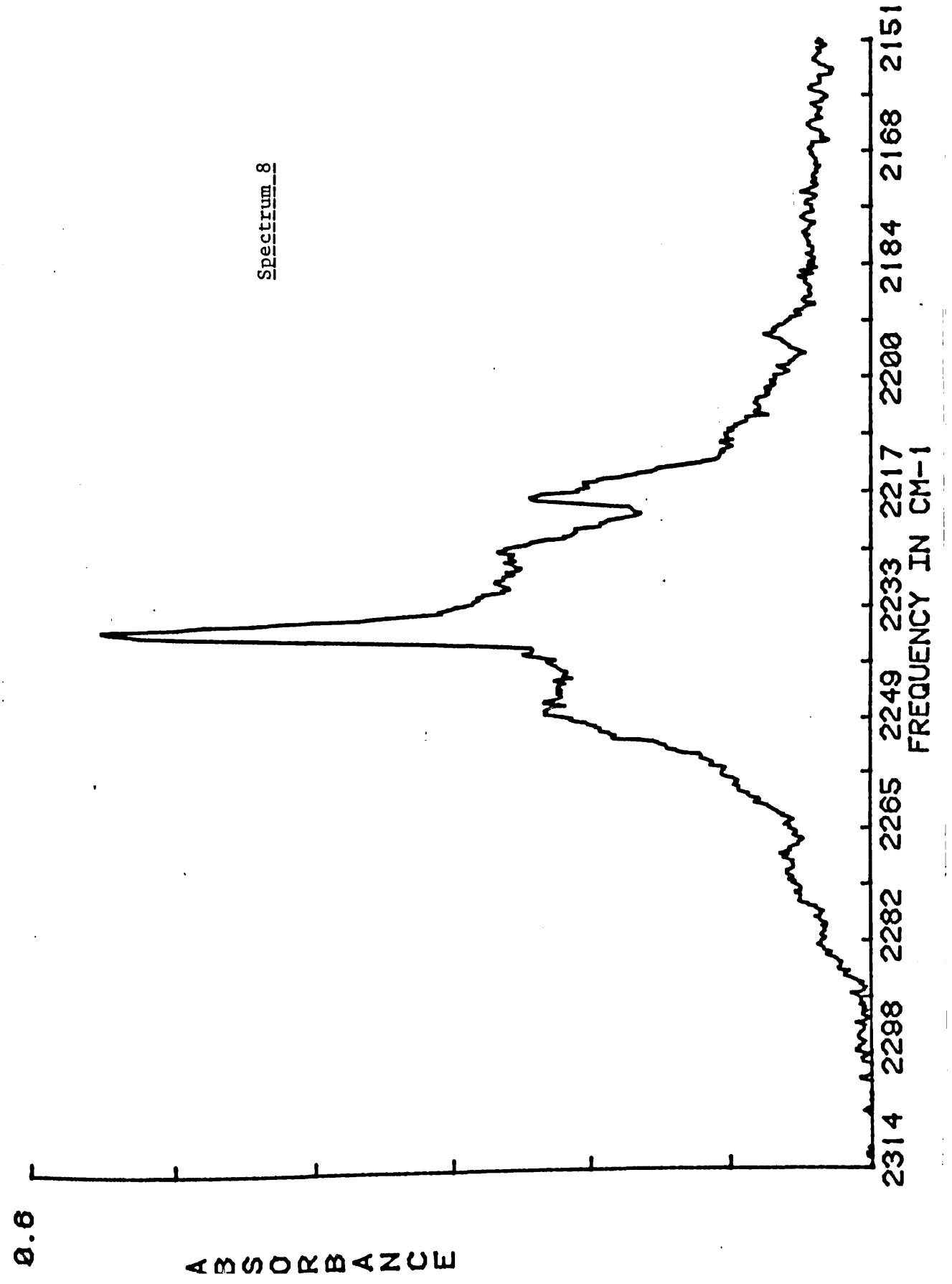
Spectrum 8
0.6
ABSORBANCE
2314 2288 2282 2265 2249 2233 2217 2200 2184 2168 2151
FREQUENCY IN CM-1

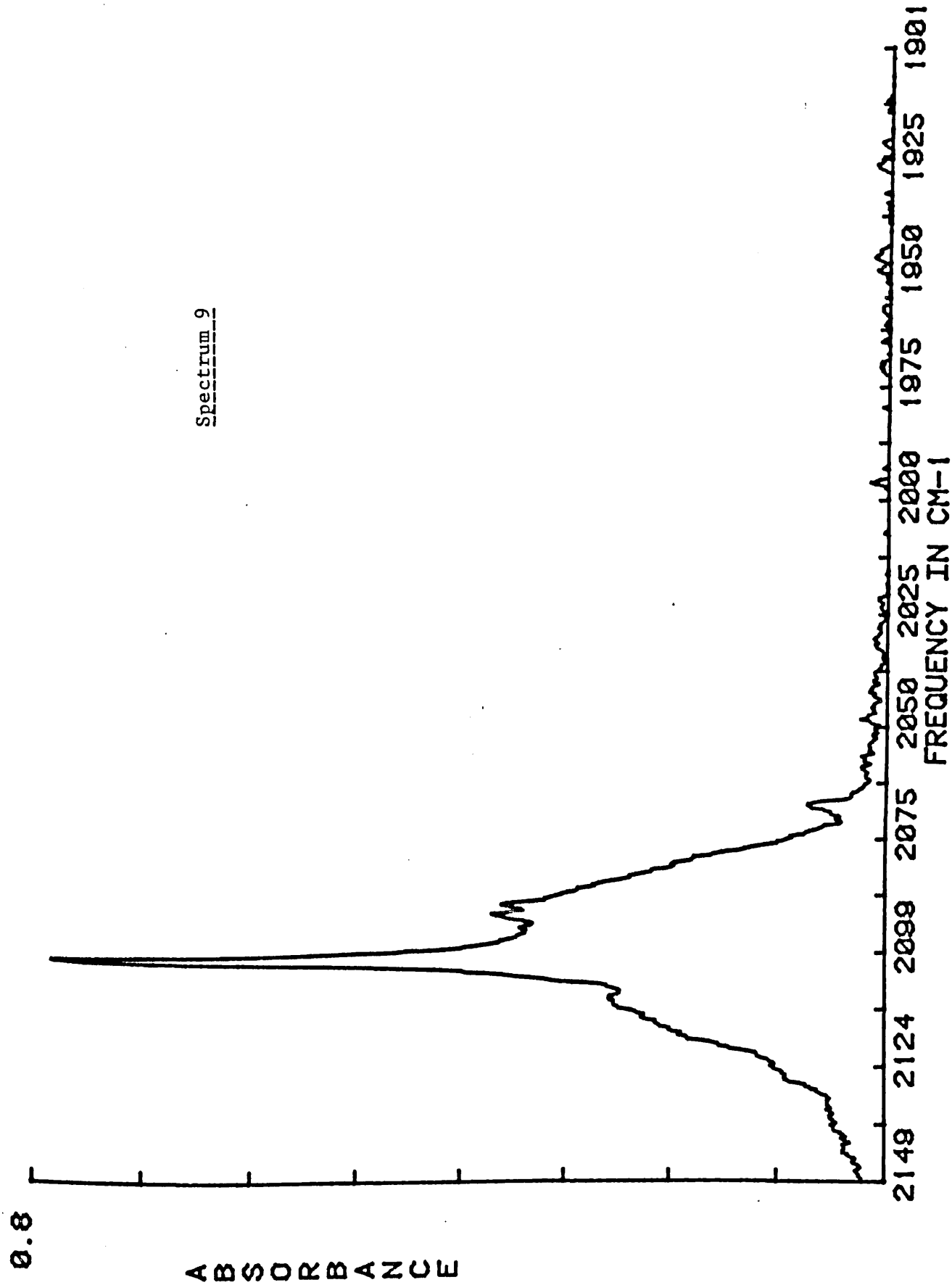
Spectrum 9
0.8
ABSORBANCE
2149 2124 2099 2075 2050 2025 2000 1975 1950 1925 1901
FREQUENCY IN CM-1

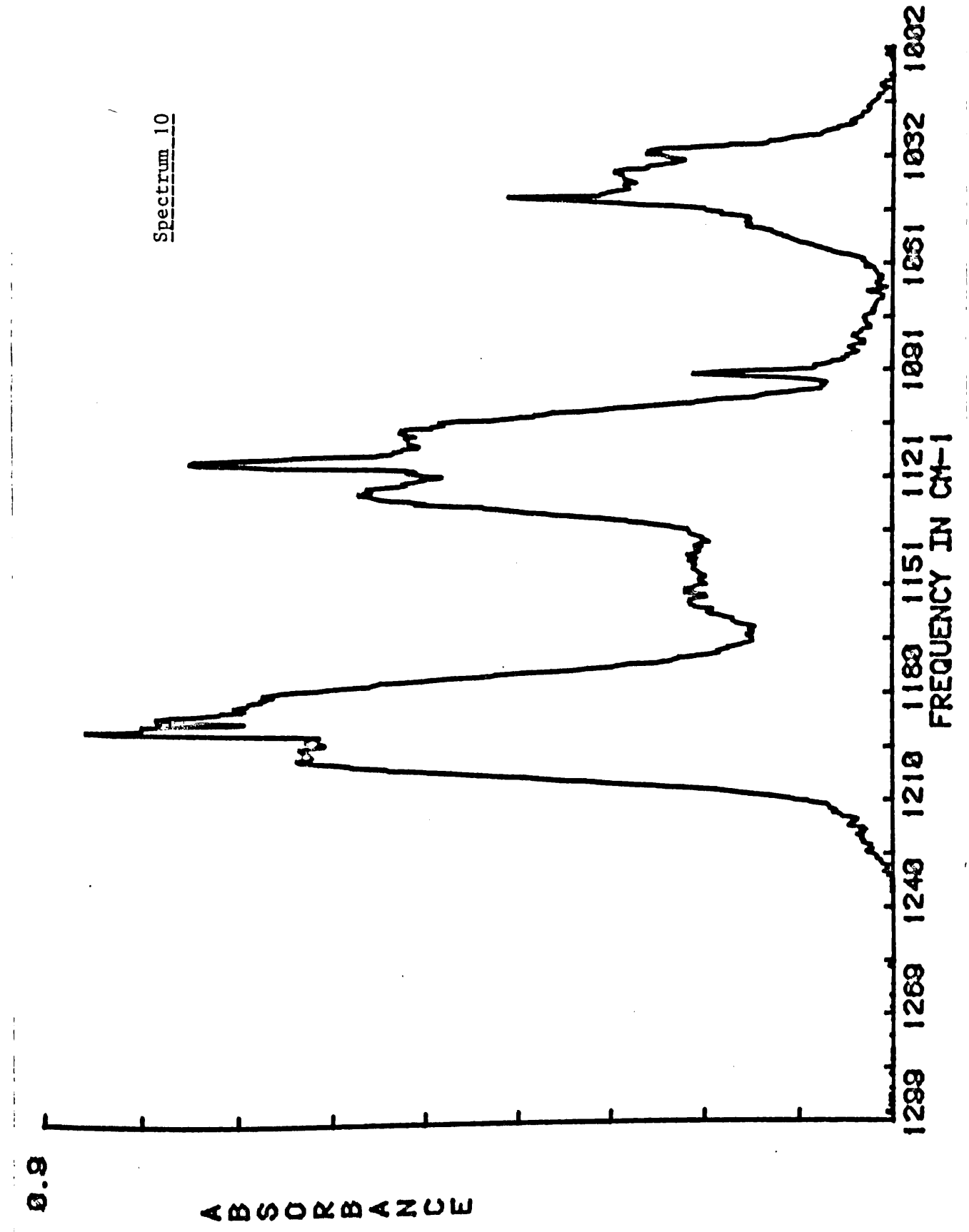
Spectrum 10
0.9
ABSORBANCE
1289
1269
1249
1210
1180
1151
1121
1091
1061
1032
1002
FREQUENCY IN CM-1

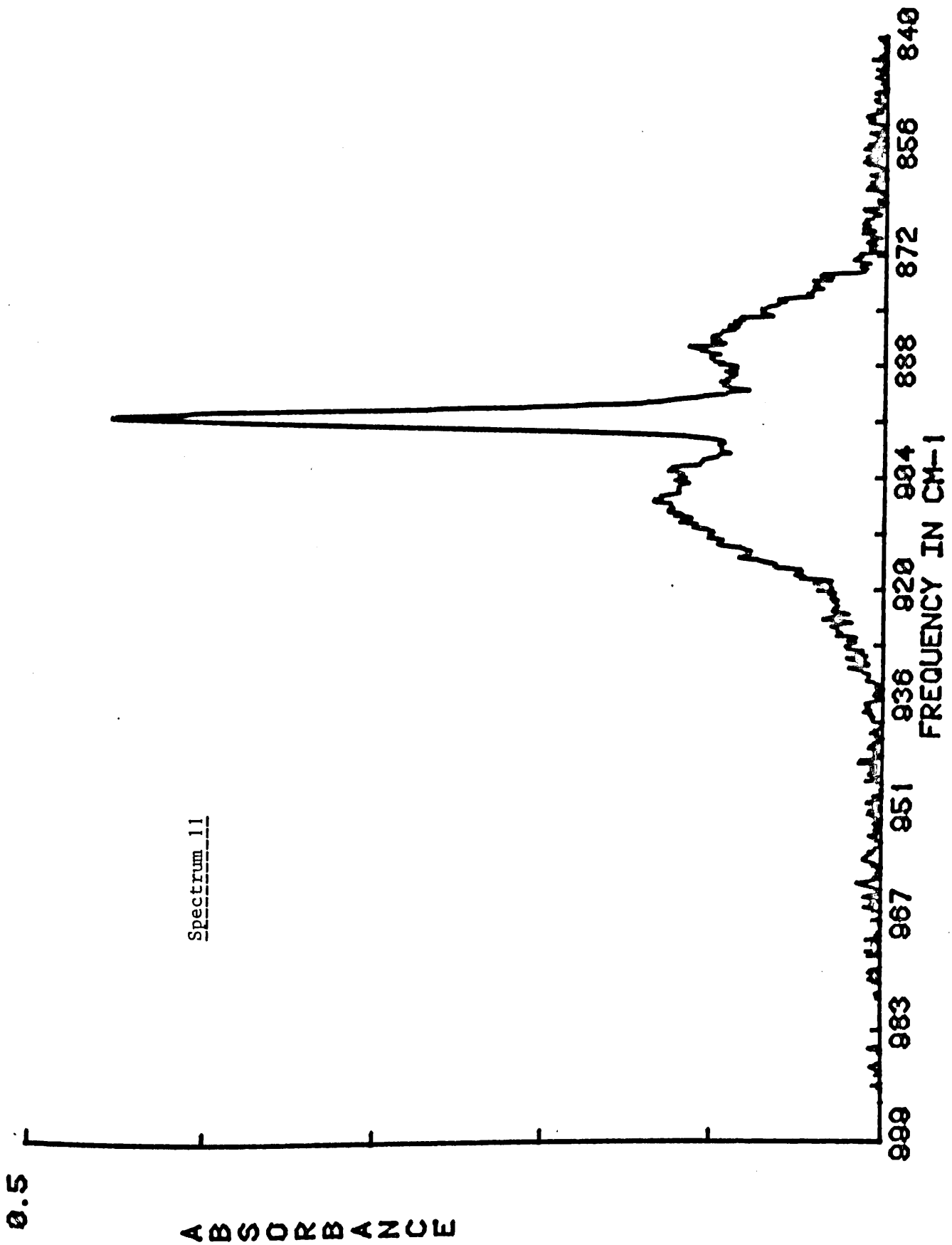
0.5
ABSORBANCE
999
983
967
951
936
920
904
888
872
856
840
FREQUENCY IN CM-1
Spectrum 11

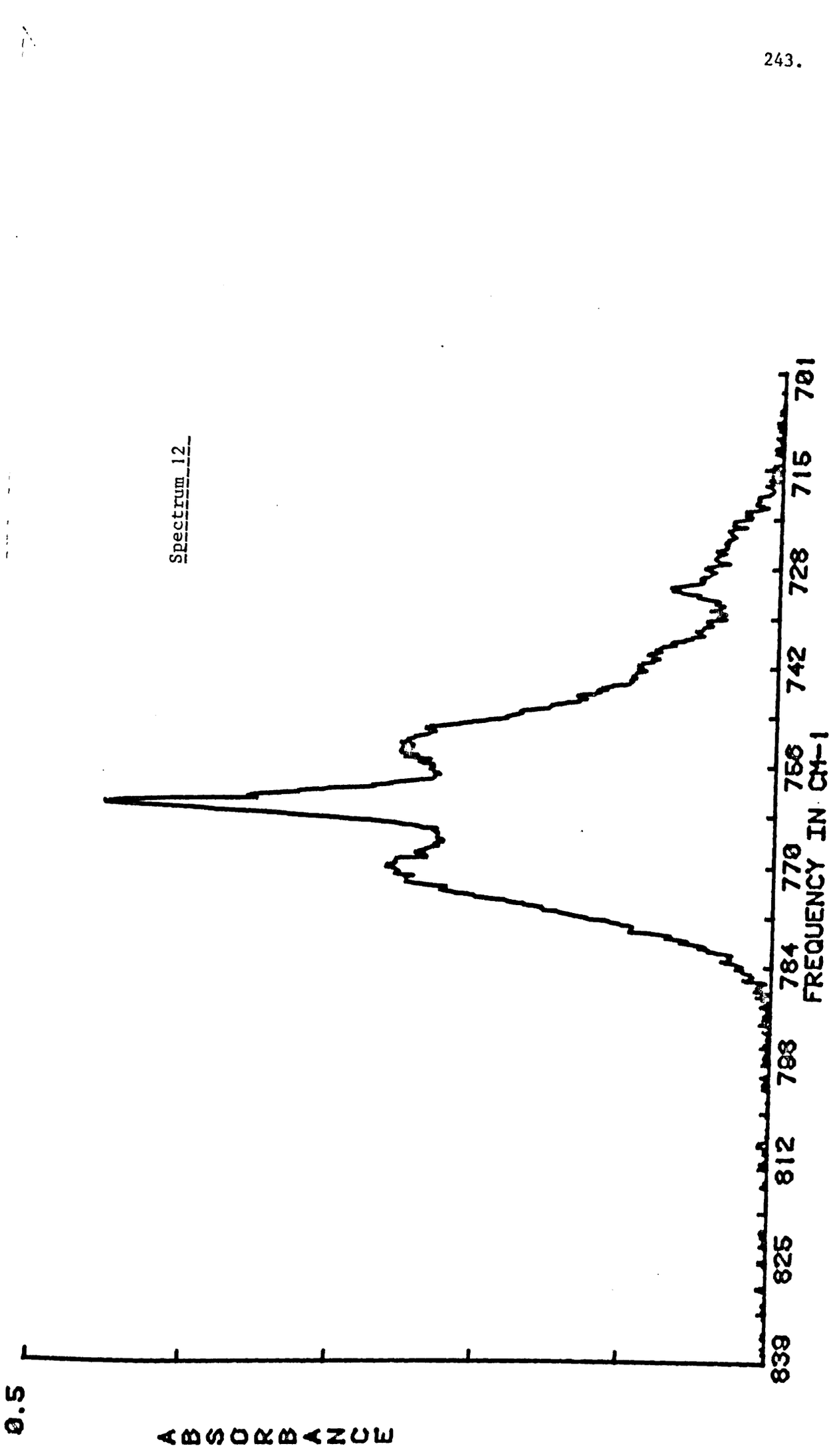
Spectrum 12
0.5
ABSORBANCE
839
825
812
798
784
770
756
742
728
715
701
FREQUENCY IN CM-1

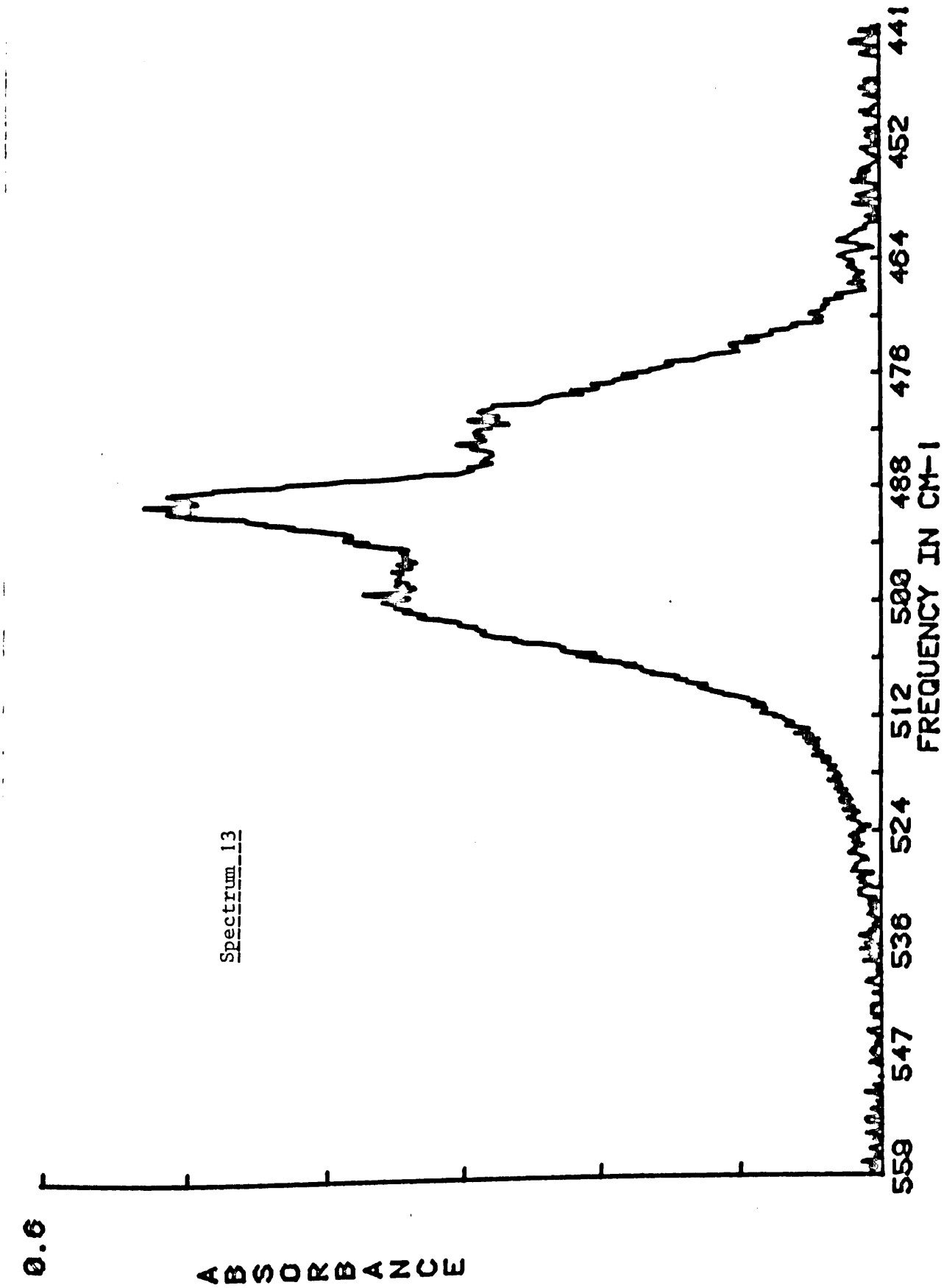
0.6
ABSORBANCE
559
547
538
524
512
500
488
476
464
452
441
FREQUENCY IN CM-1

Spectrum 13

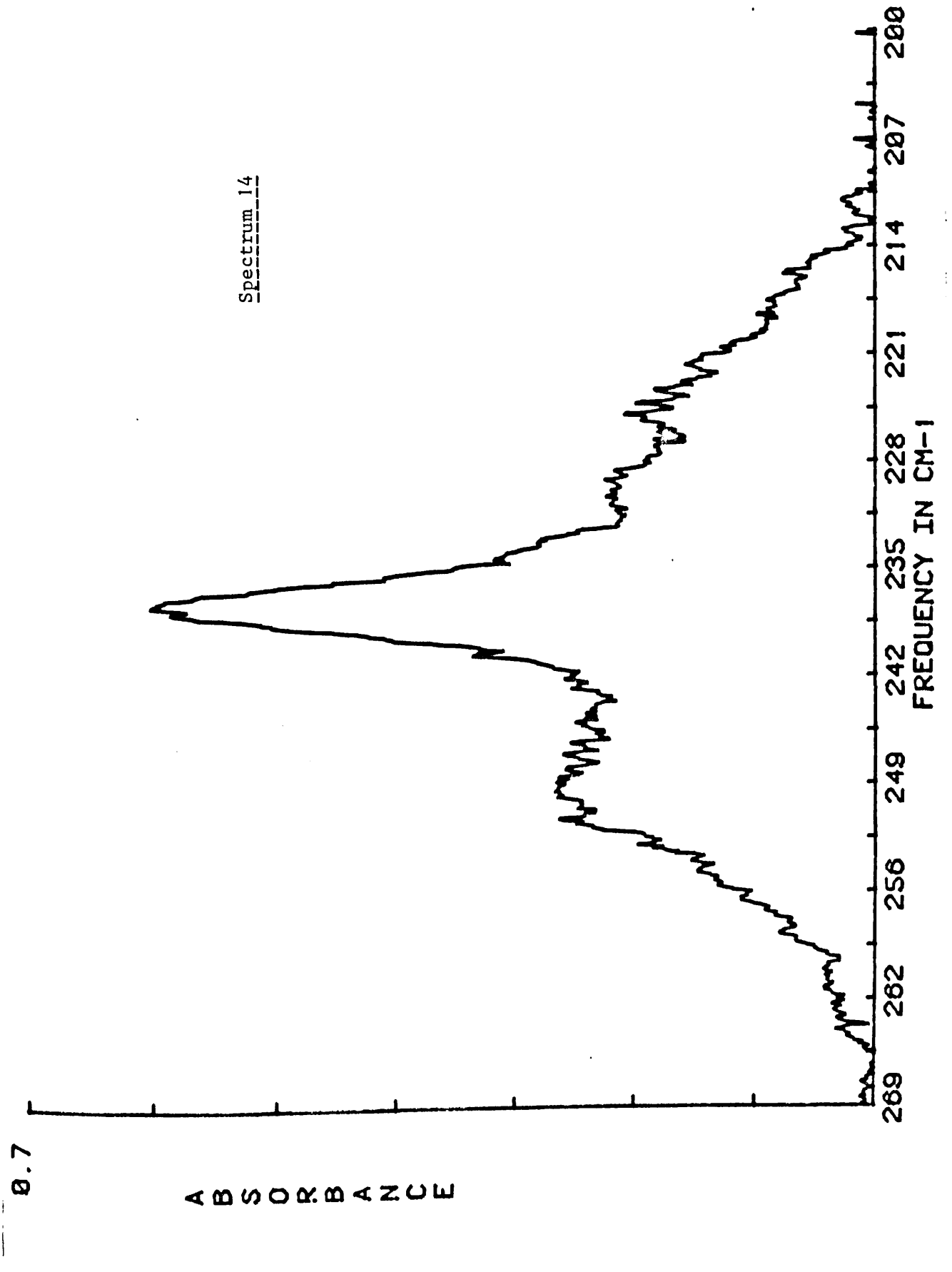
Spectrum 14
0.7
ABSORBANCE
269
262
256
249
242
235
228
221
214
207
200
FREQUENCY IN CM-1

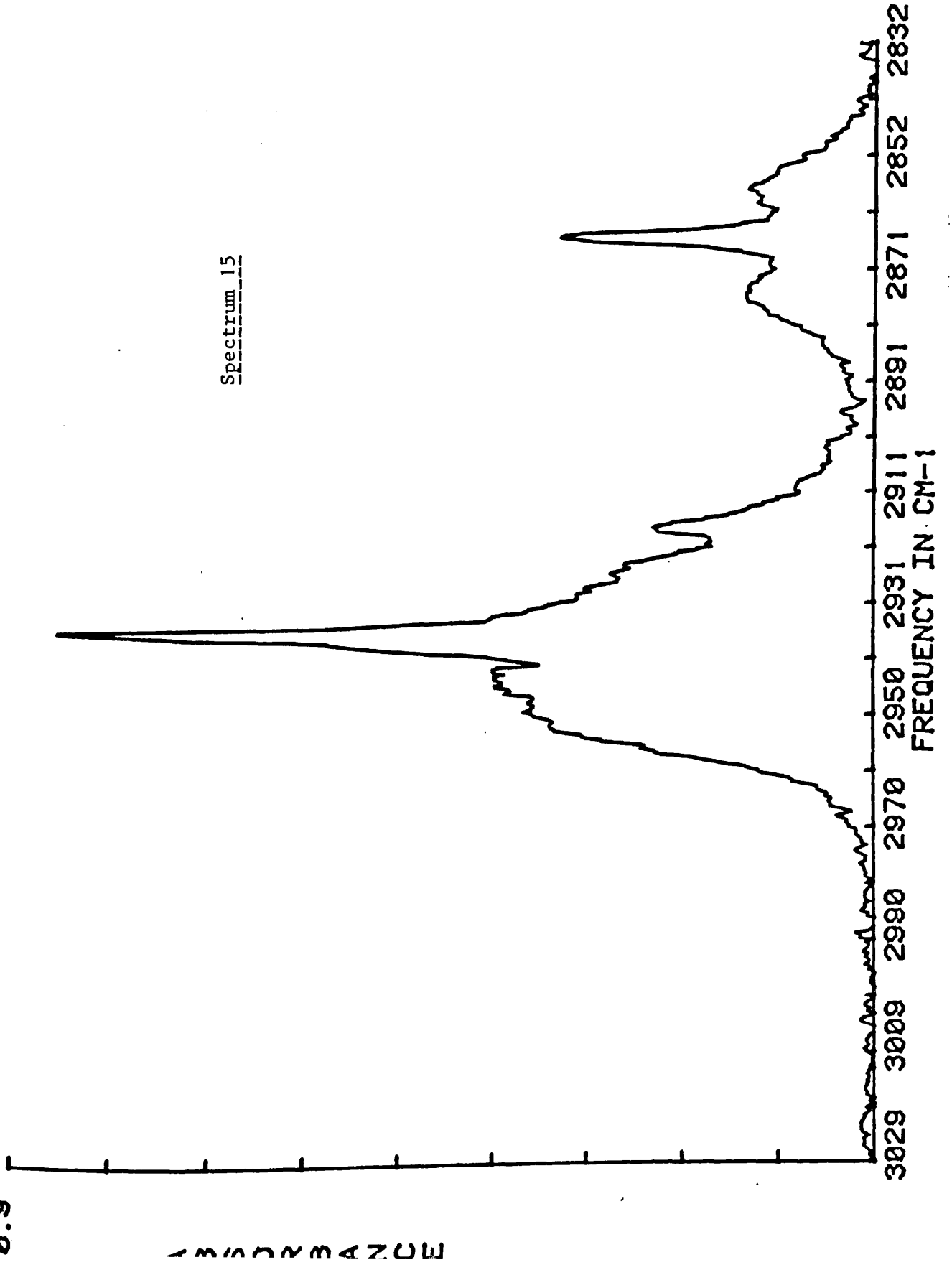
Spectrum 15
3029
3009
2990
2970
2950
2931
2911
2891
2871
2852
2832
FREQUENCY IN CM-1
0.9

Spectrum 16

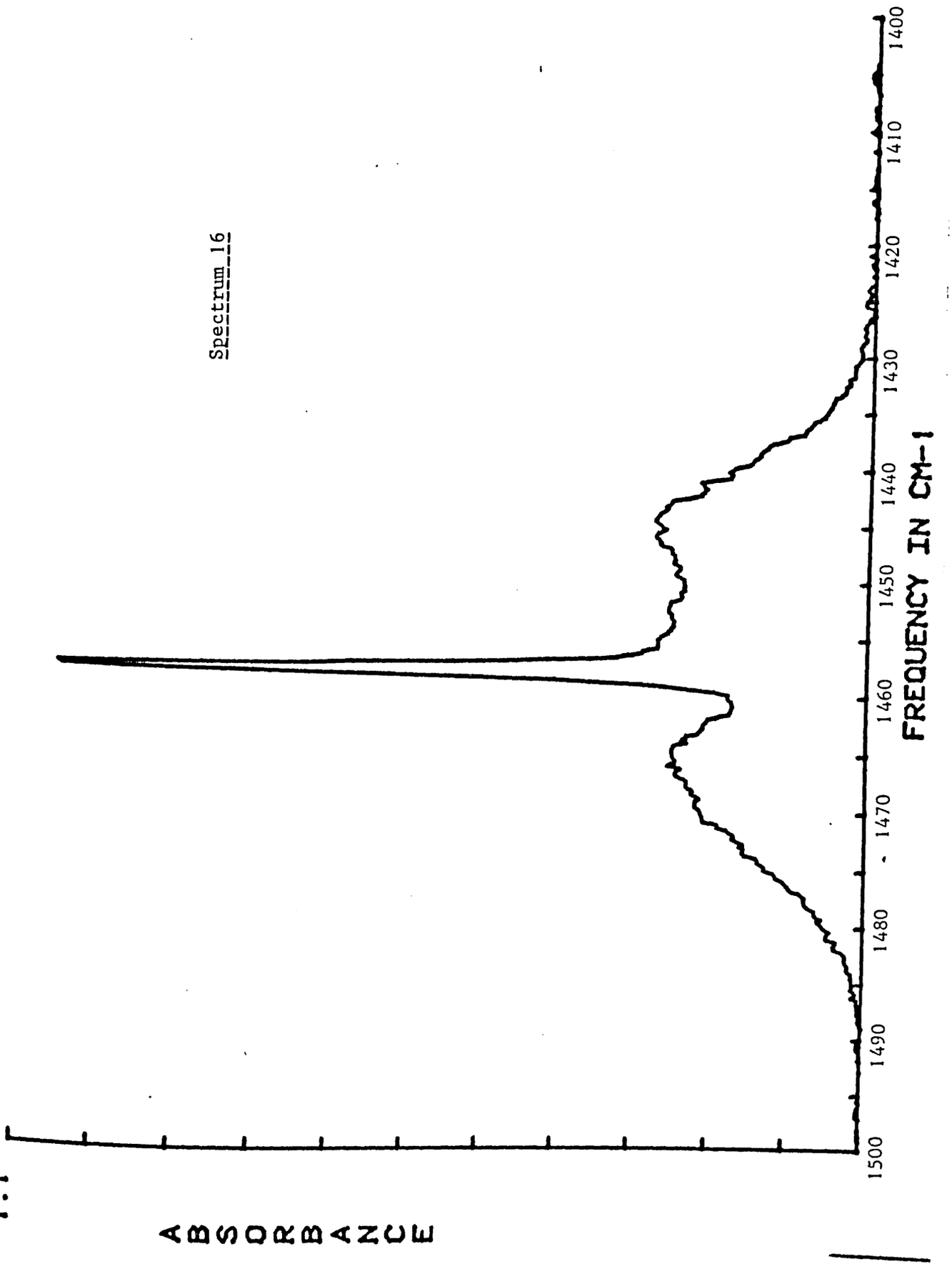
1.1
ABSORBANCE
1500
1490
1480
1470
1460
1450
1440
1430
1420
1410
1400
FREQUENCY IN CM-1

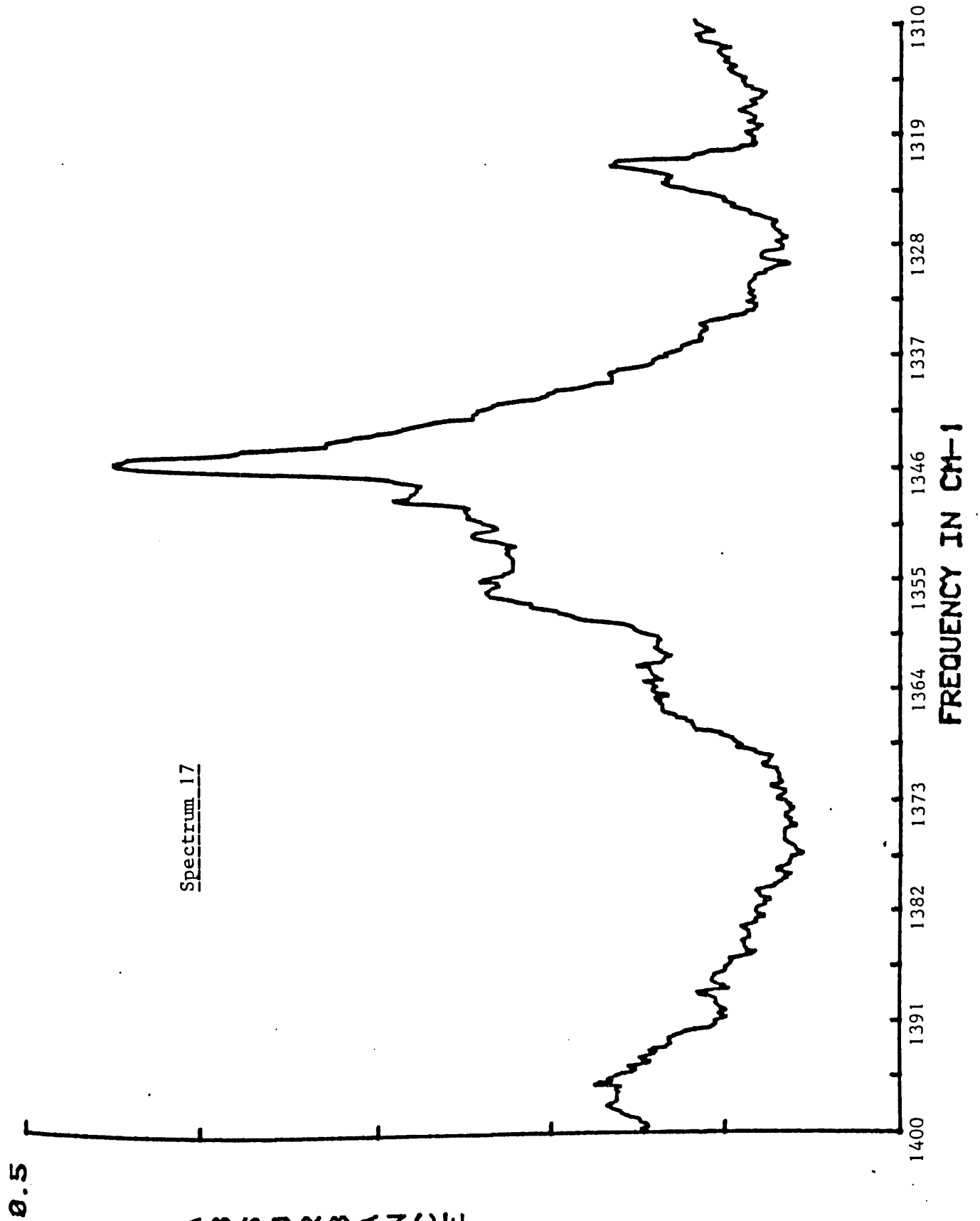
0.5
ABSORBANCE
Spectrum 17
1400
1391
1382
1373
1364
1355
1346
1337
1328
1319
1310
FREQUENCY IN CM-1

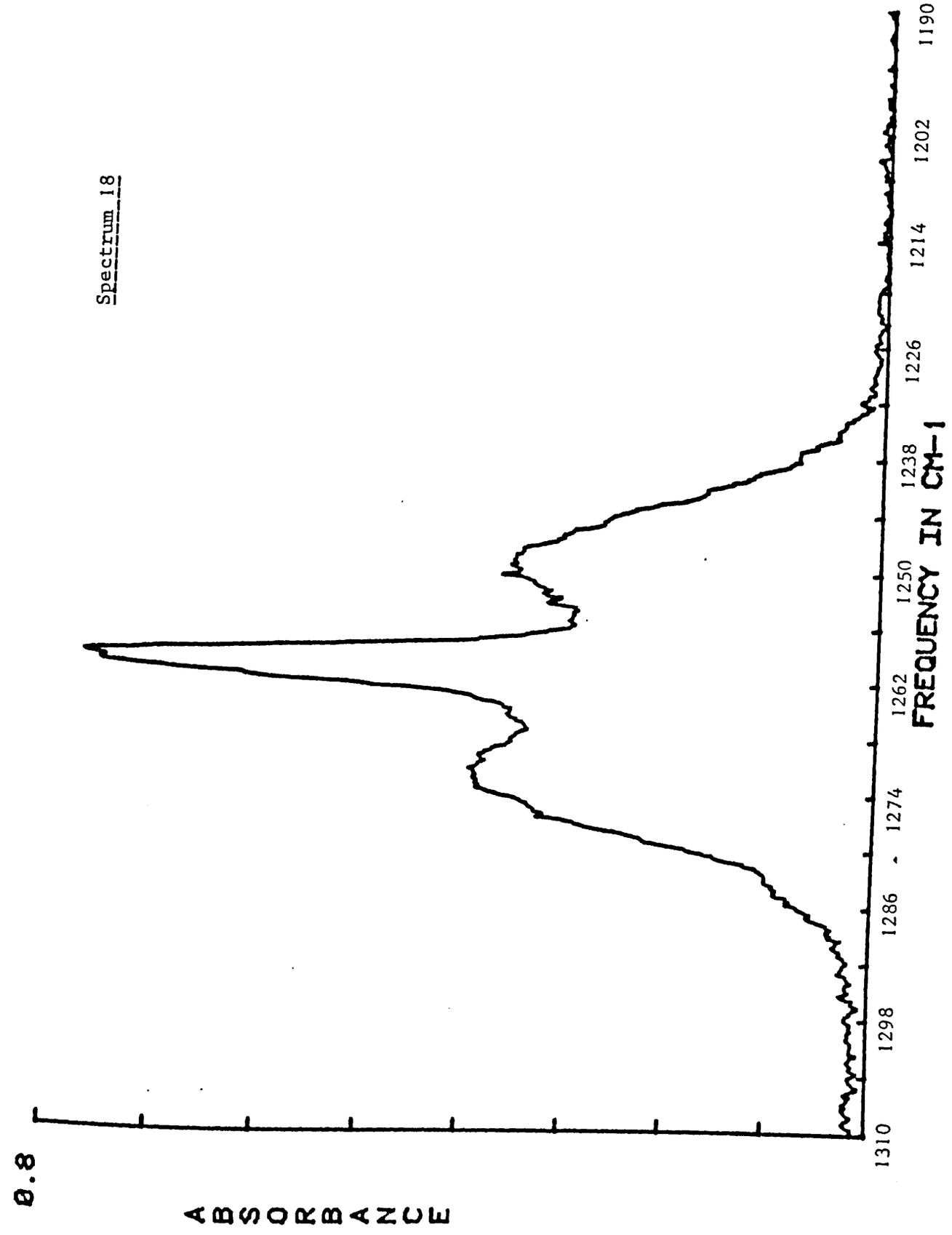
Spectrum 18
0.8
ABSORBANCE
1310
1298
1286
1274
1262
1250
1238
1226
1214
1202
1190
FREQUENCY IN CM-1

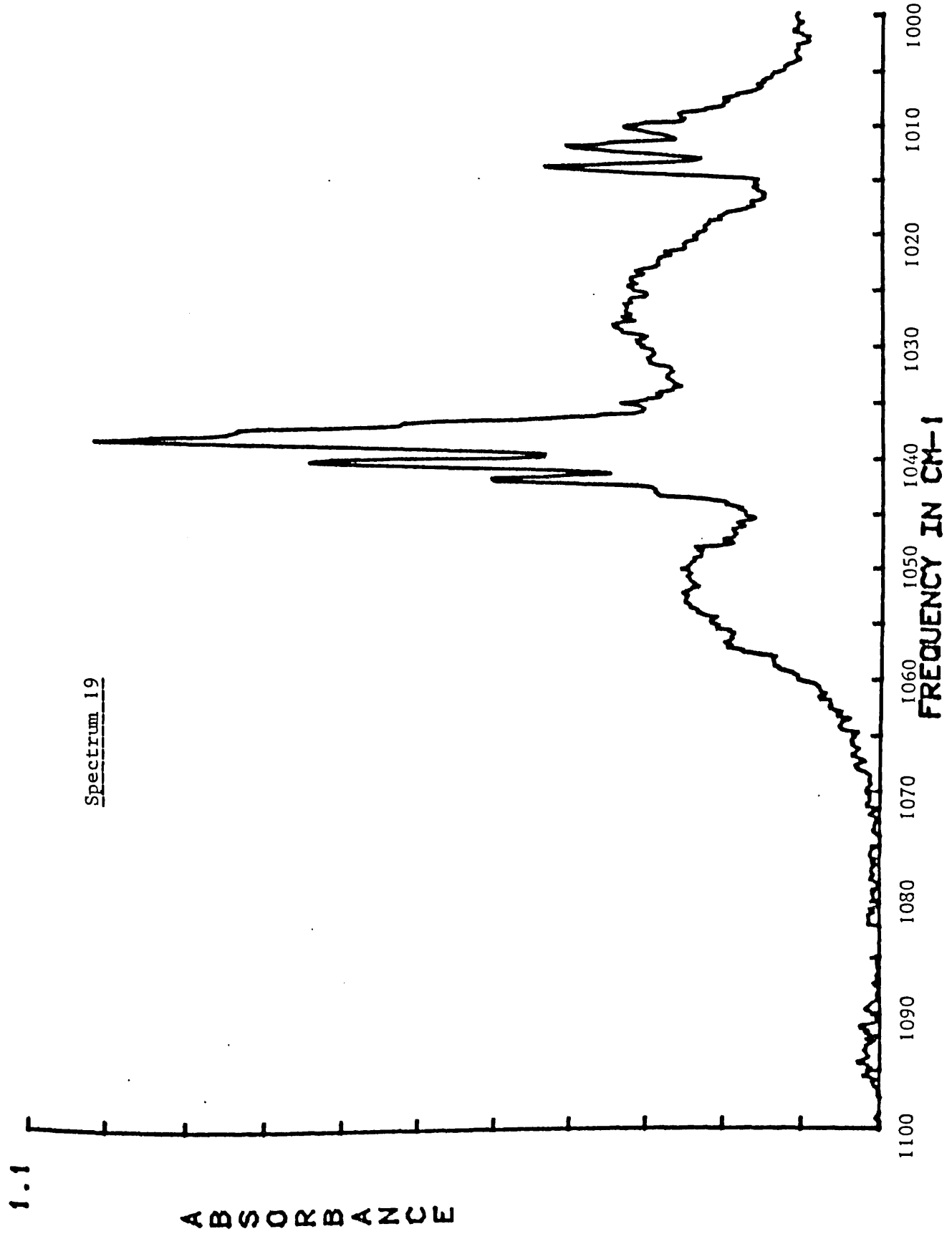
Spectrum 19
1.1
ABSORBANCE
1100
1090
1080
1070
1060
1050
1040
1030
1020
1010
1000
FREQUENCY IN CM-1

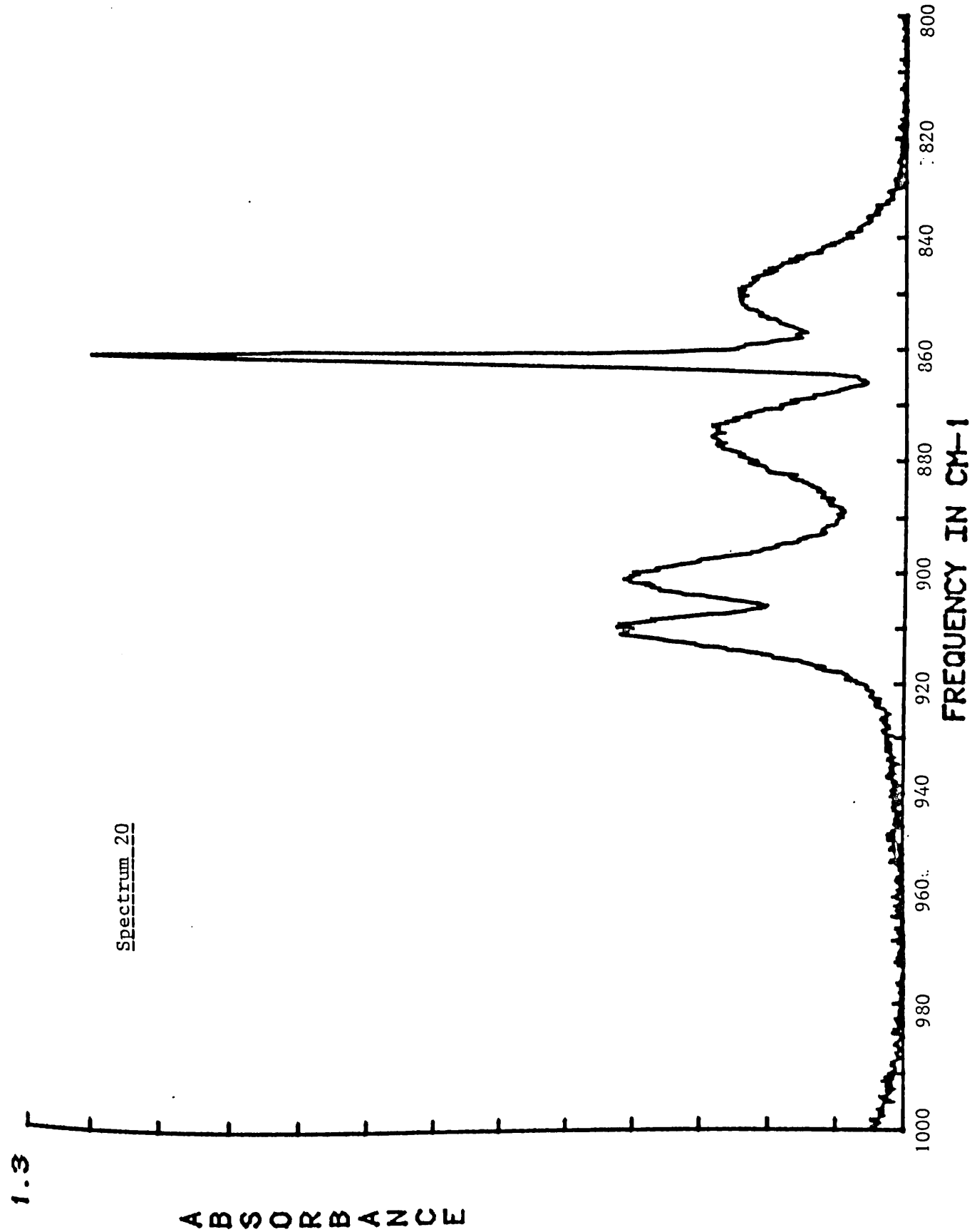
Spectrum 20
1.3
ABSORBANCE
1000
980
960
940
920
900
880
860
840
820
800
FREQUENCY IN CM-1

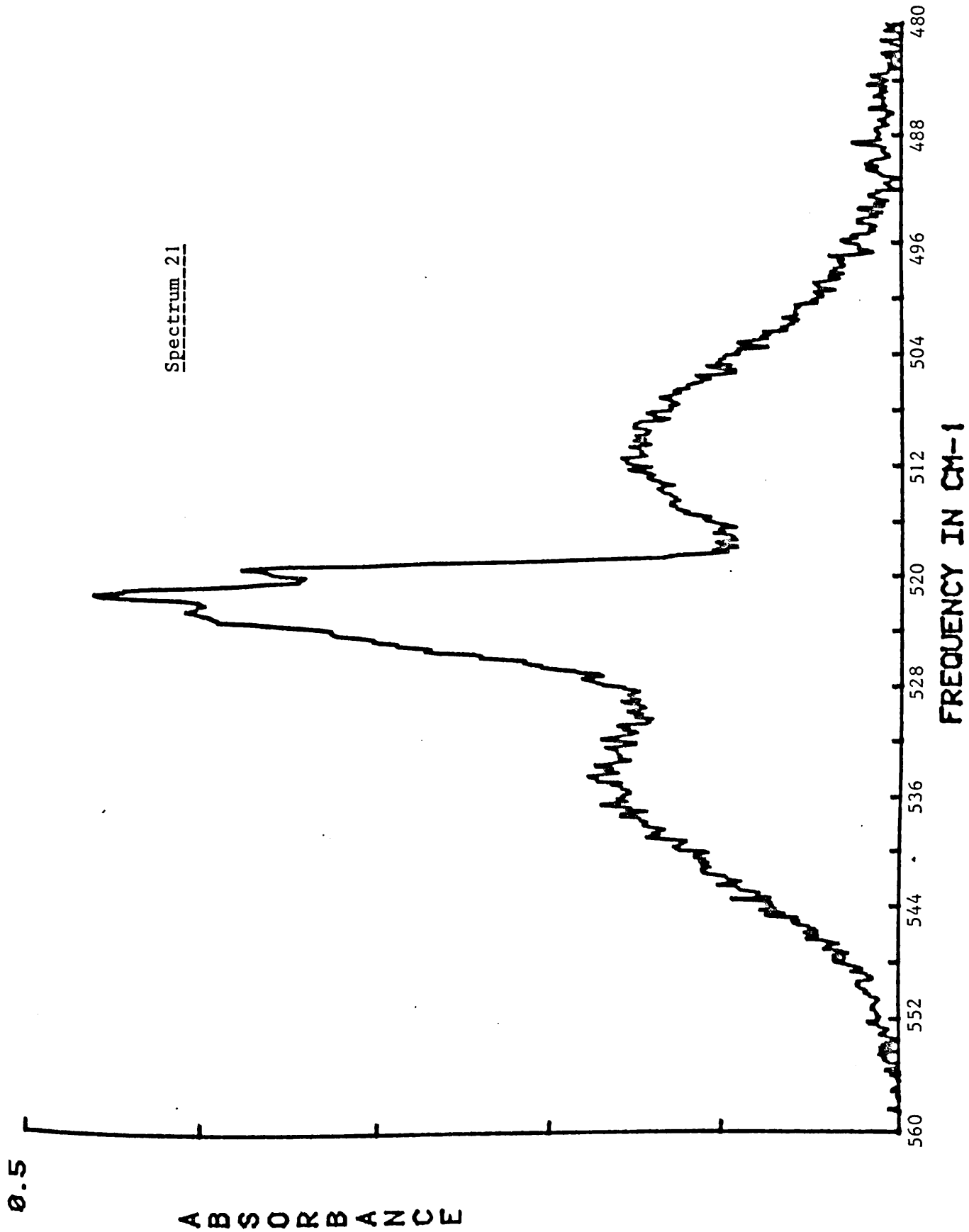
Spectrum 21
0.5
ABSORBANCE
560
552
544
536
528
520
512
504
496
488
480
FREQUENCY IN CM-1

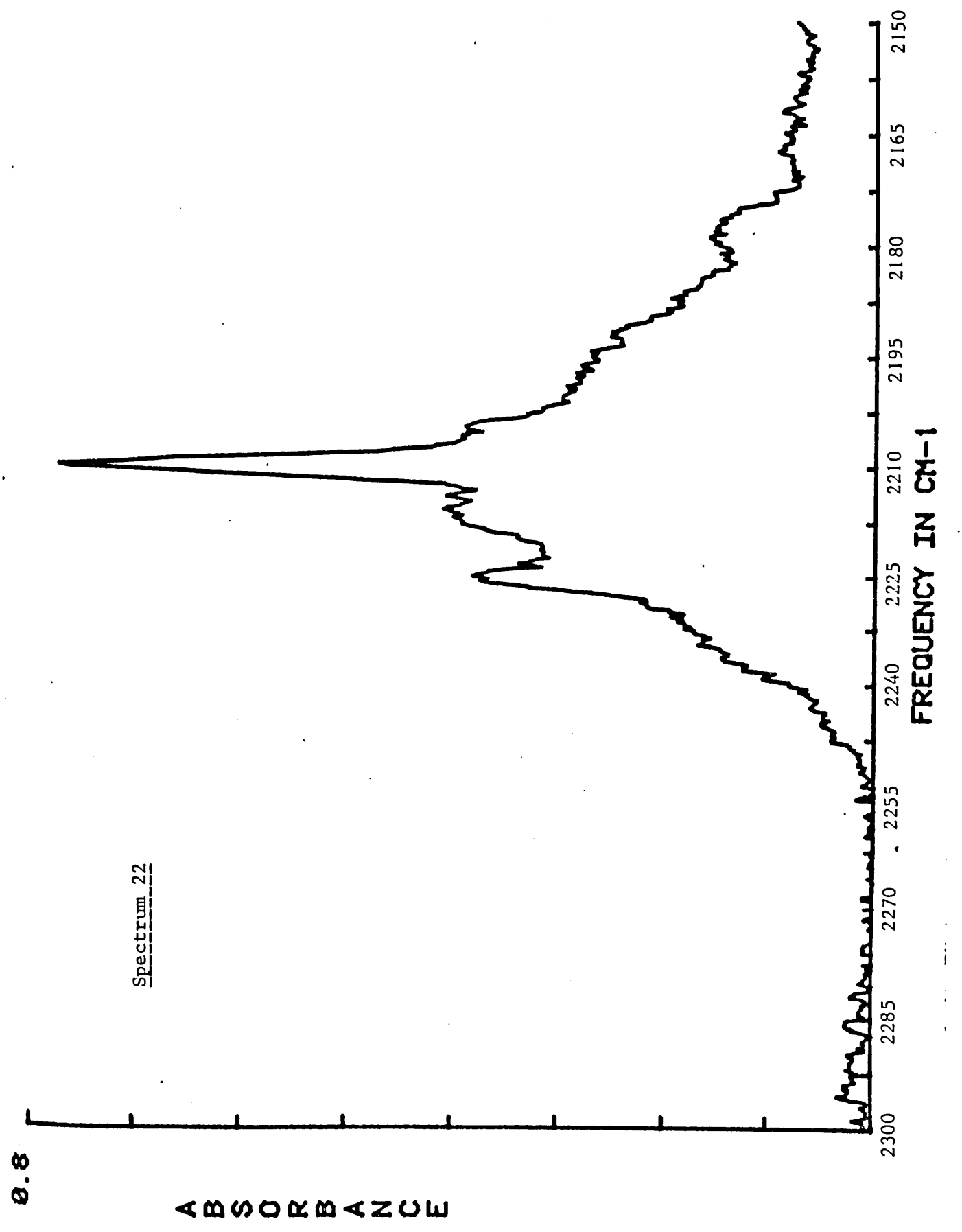
0.8
ABSORBANCE
Spectrum 22
2300
2285
2270
2255
2240
2225
2210
2195
2180
2165
2150
FREQUENCY IN CM-1

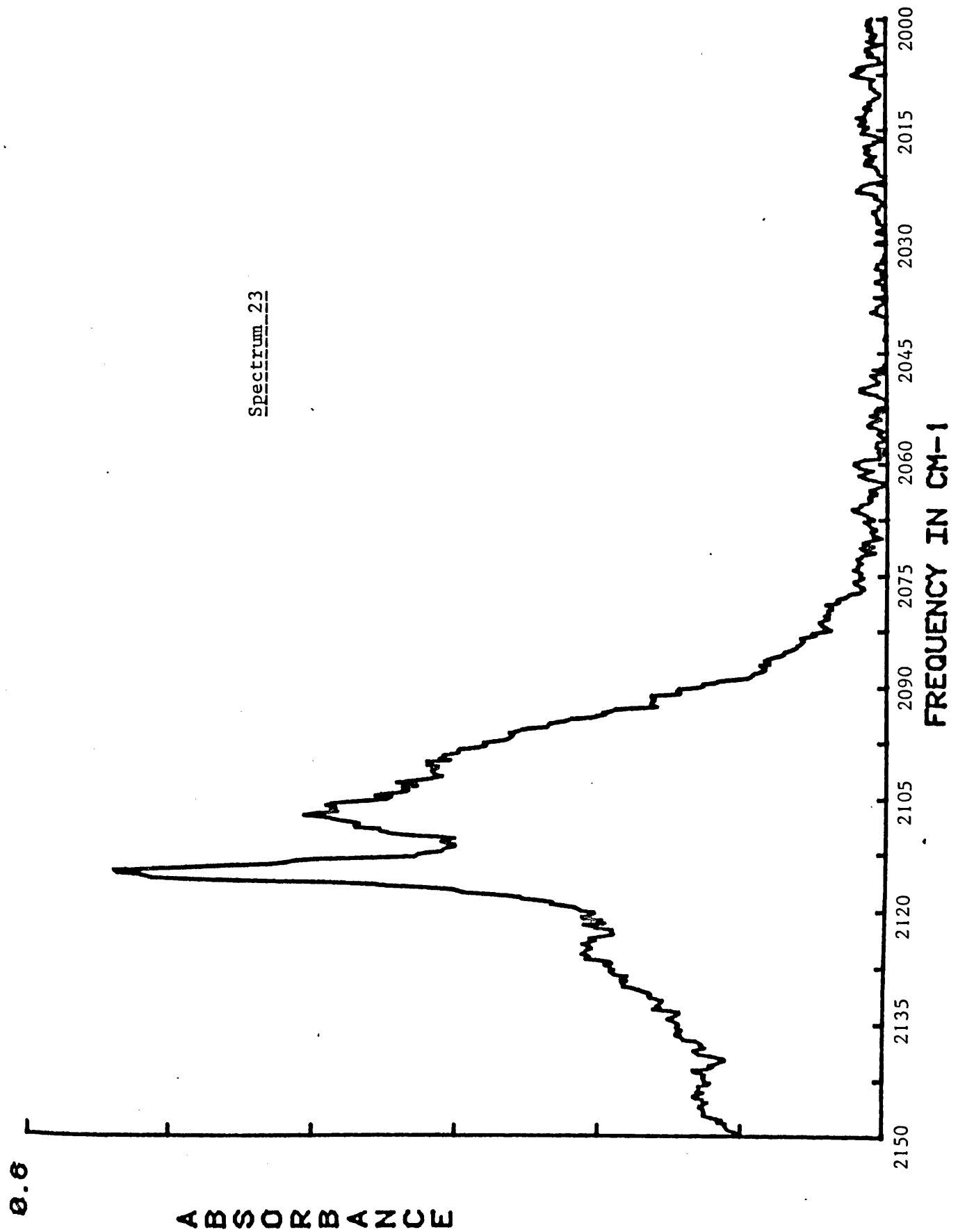
Spectrum 23
0.6
ABSORBANCE
2150
2135
2120
2105
2090
2075
2060
2045
2030
2015
2000
FREQUENCY IN CM-1

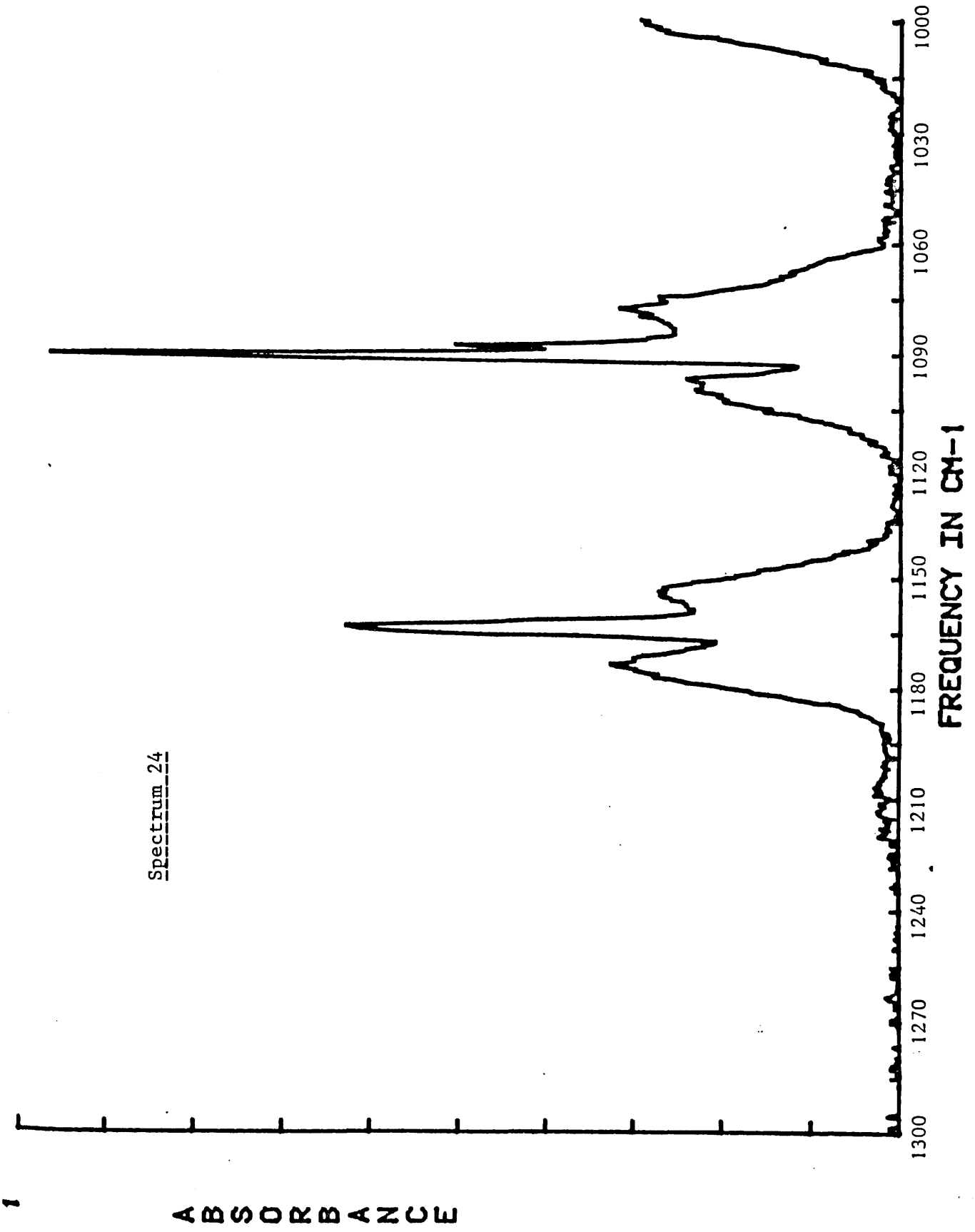
Spectrum 24
1
ABSORBANCE
1300
1270
1240
1210
1180
1150
1120
1090
1060
1030
1000
FREQUENCY IN CM-1

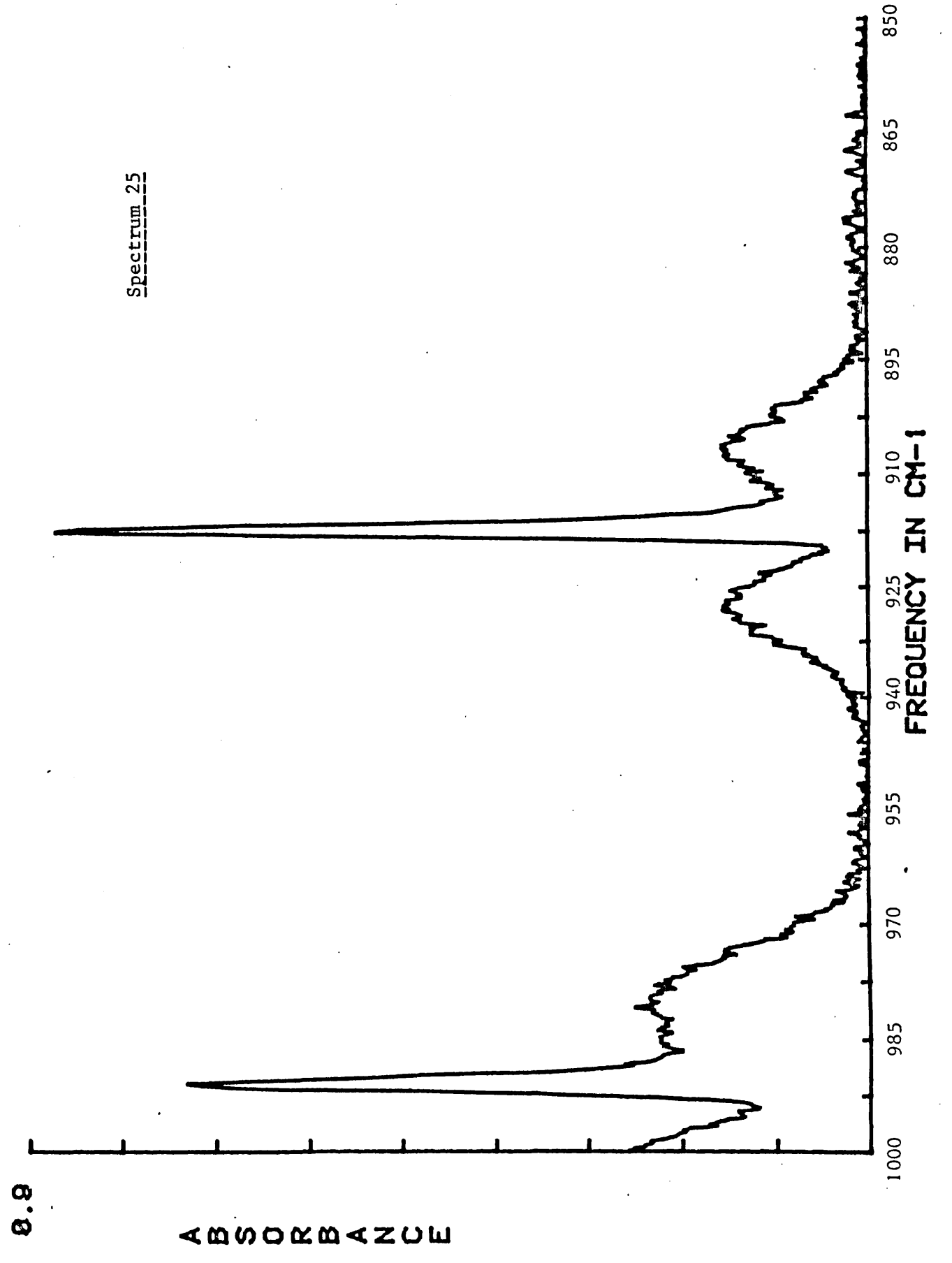
Spectrum 25
0.8
ABSORBANCE
1000
985
970
955
940
925
910
895
880
865
850
FREQUENCY IN CM-1

Spectrum 26

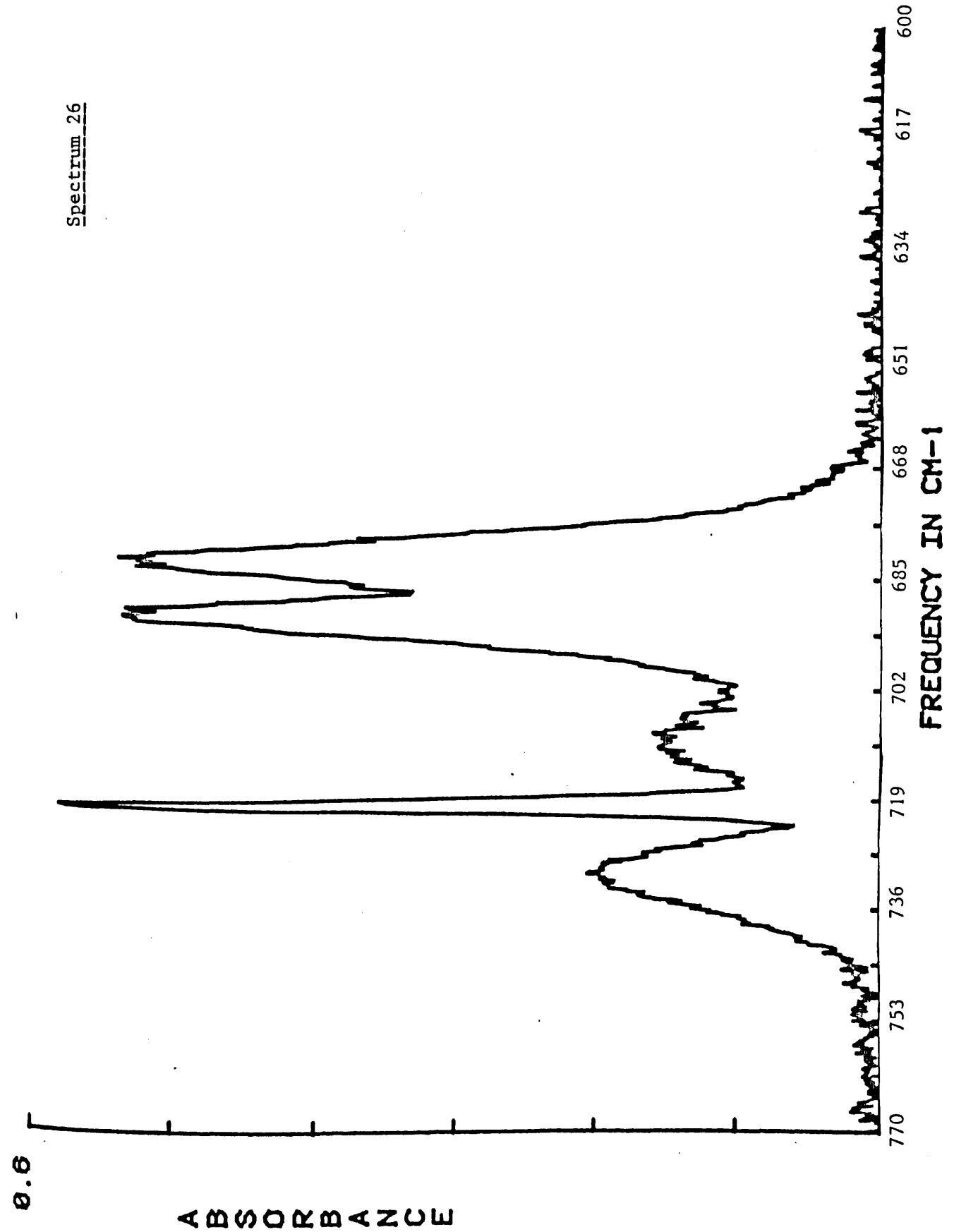
0.6
ABSORBANCE
770
753
736
719
702
685
668
651
634
617
600
FREQUENCY IN CM-1

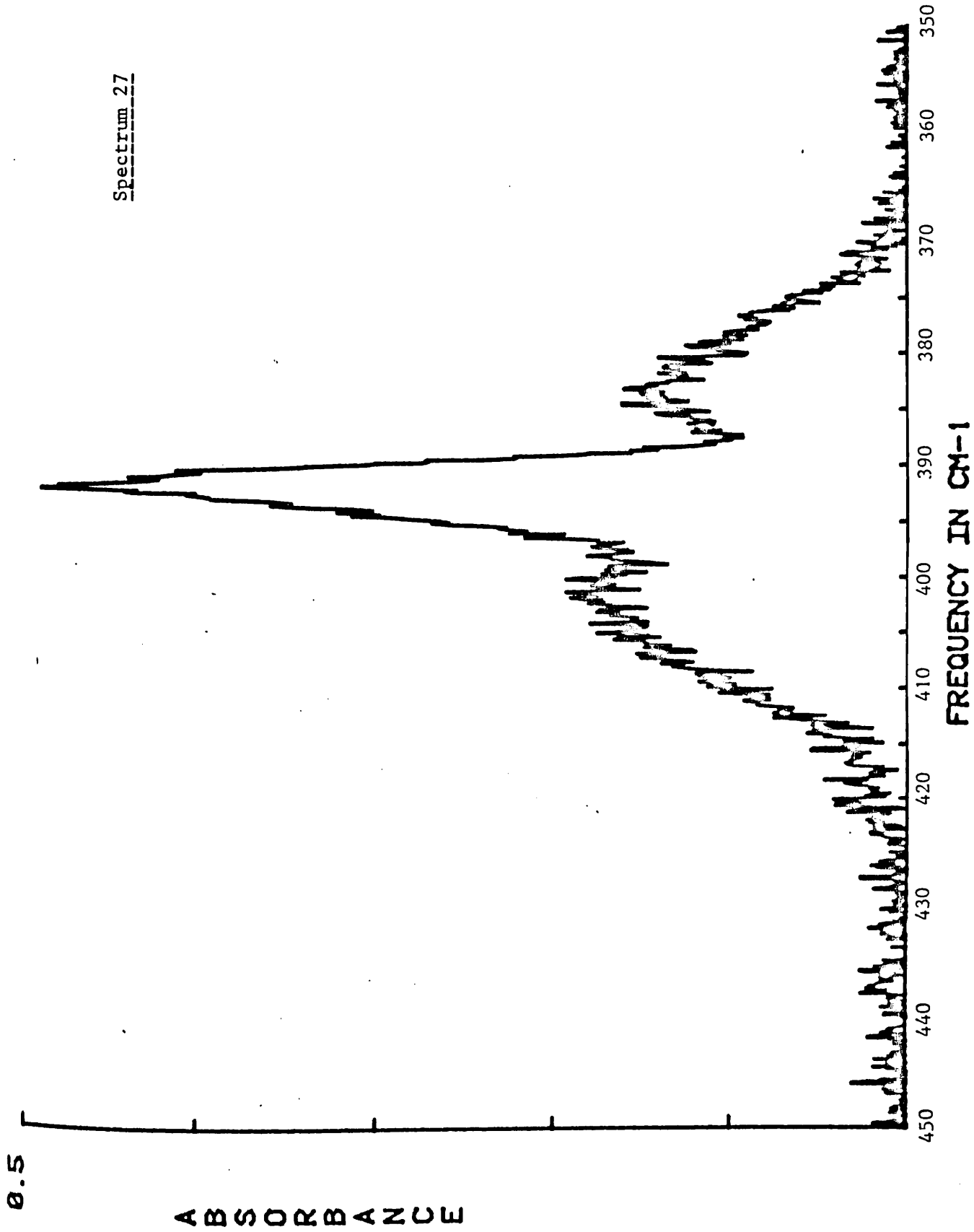
Spectrum 27
0.5
ABSORBANCE
450
440
430
420
410
400
390
380
370
360
350
FREQUENCY IN CM-1

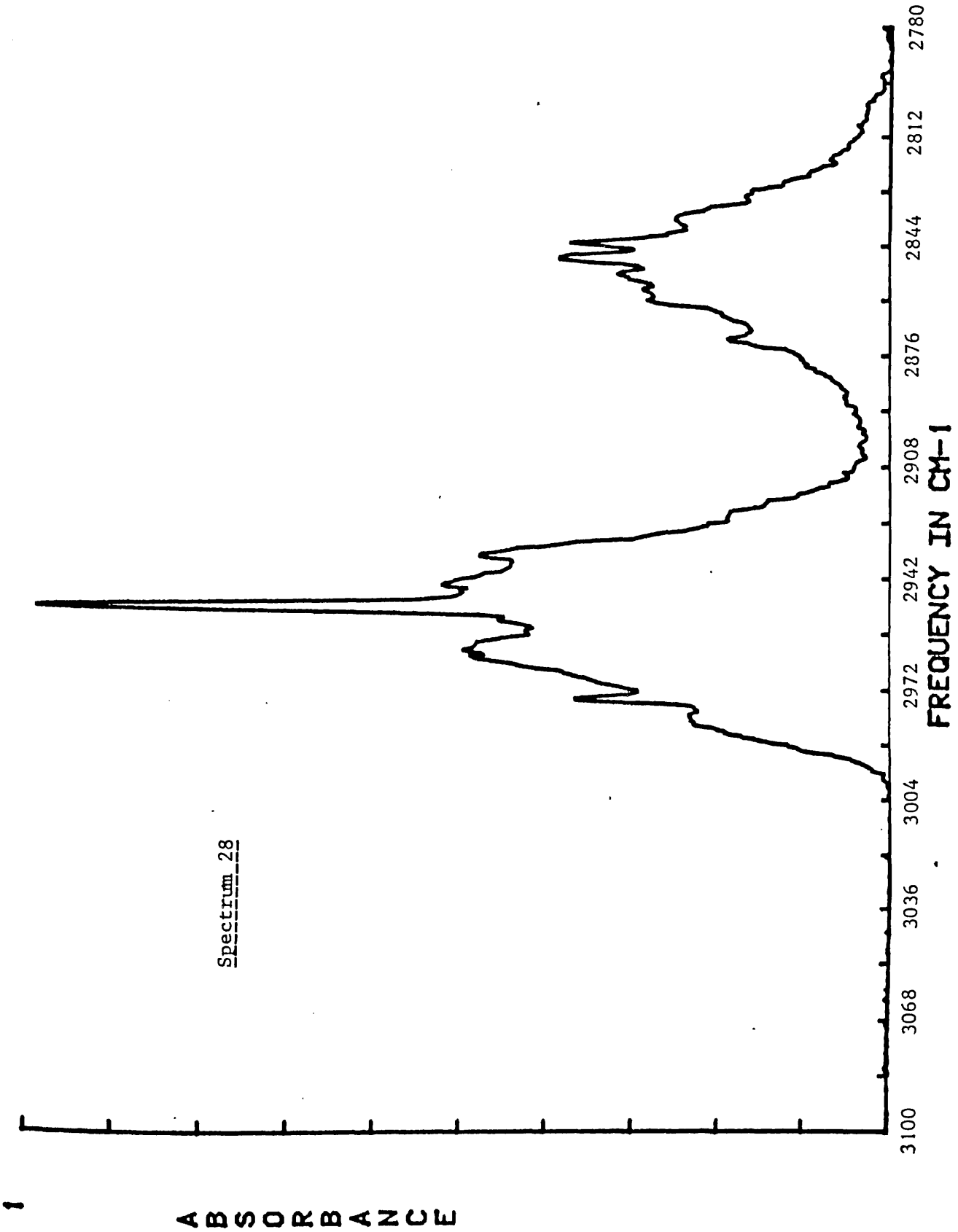
Spectrum 28
ABSORBANCE
1
3100
3068
3036
3004
2972
2942
2908
2876
2844
2812
2780
FREQUENCY IN CM-1

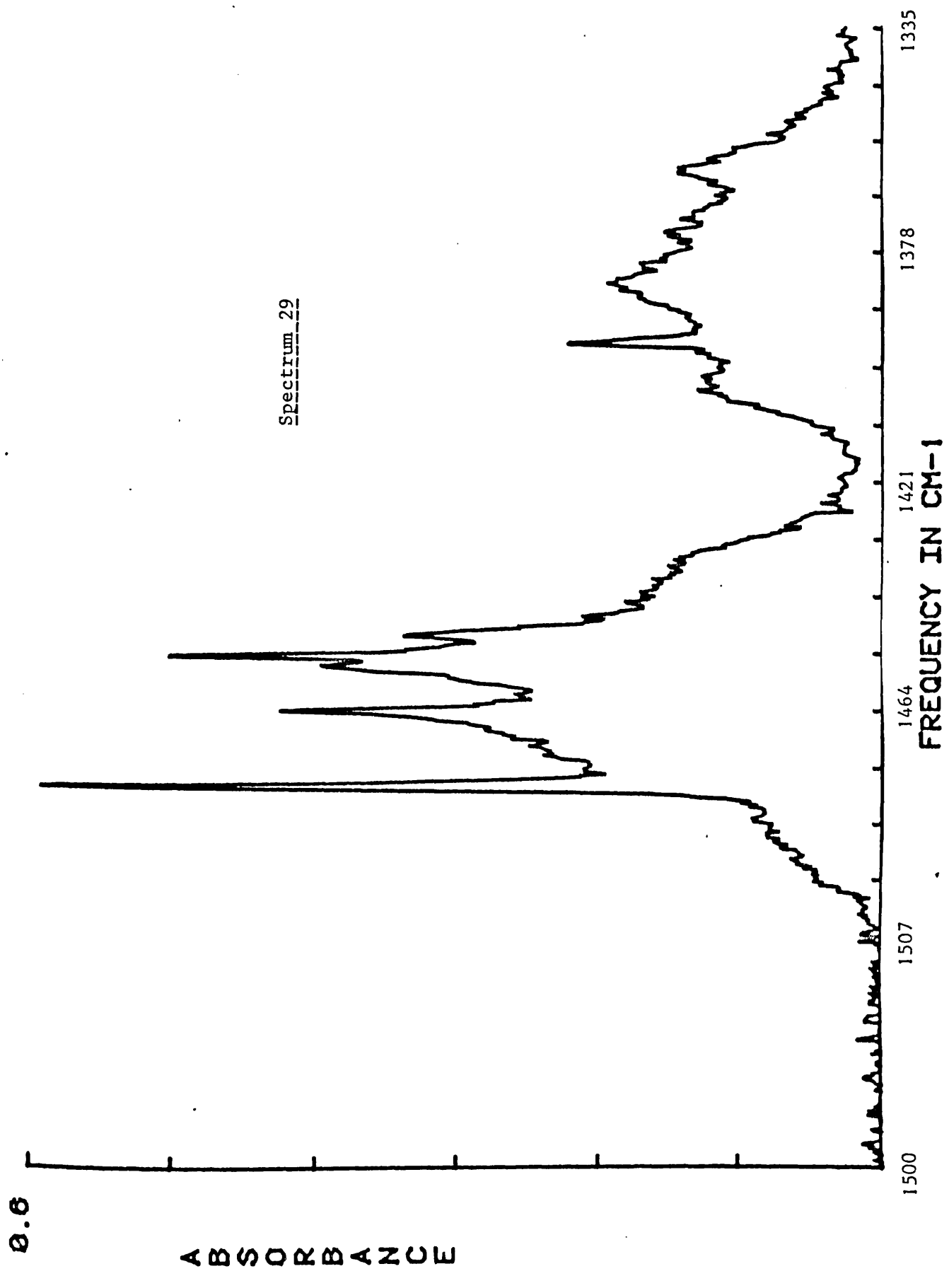
Spectrum 29
0.6
ABSORBANCE
1500
1507
1464
1421
1378
1335
FREQUENCY IN CM-1

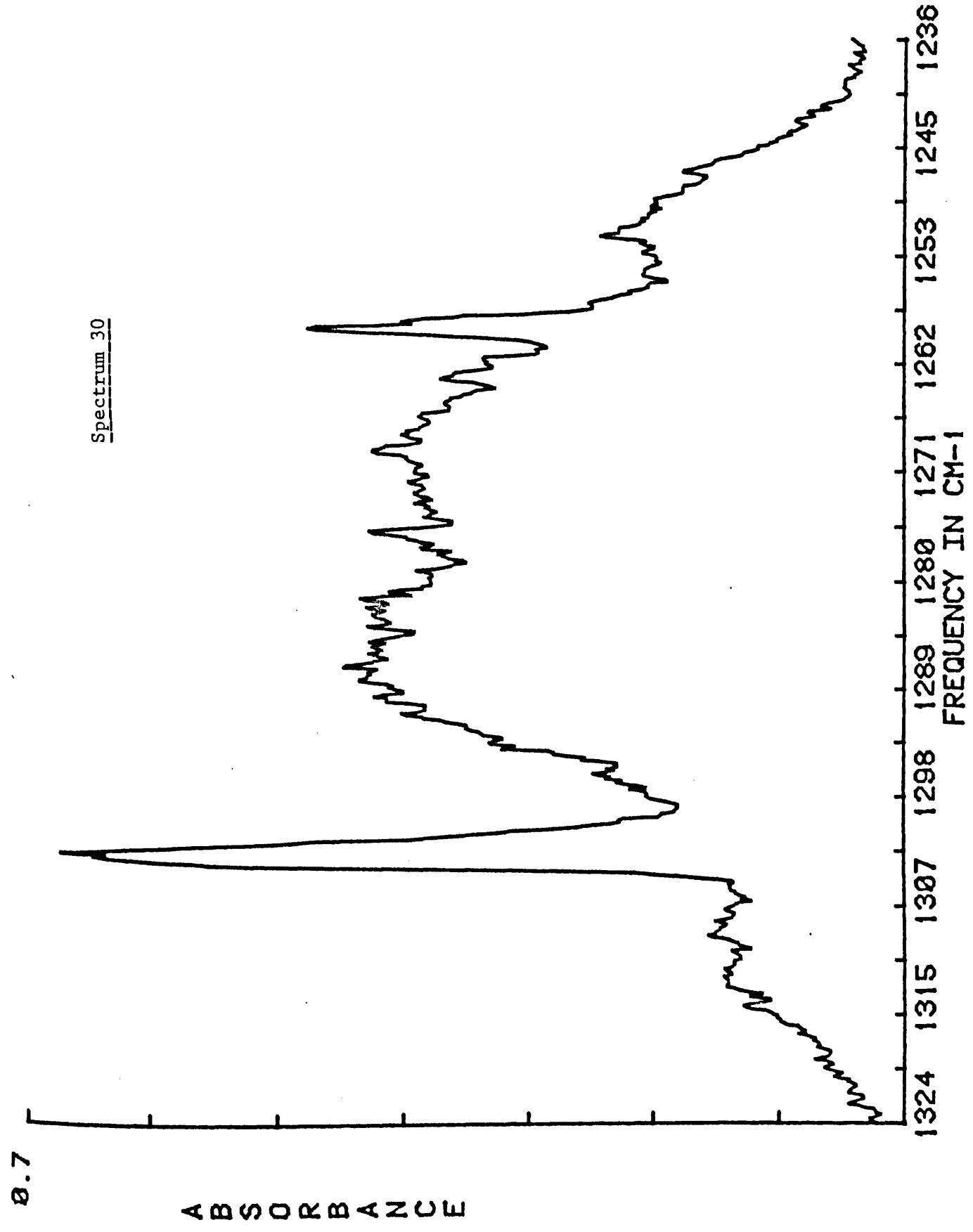
Spectrum 30
0.7
ABSORBANCE
1324 1315 1307 1298 1289 1280 1271 1262 1253 1245 1236
FREQUENCY IN CM-1

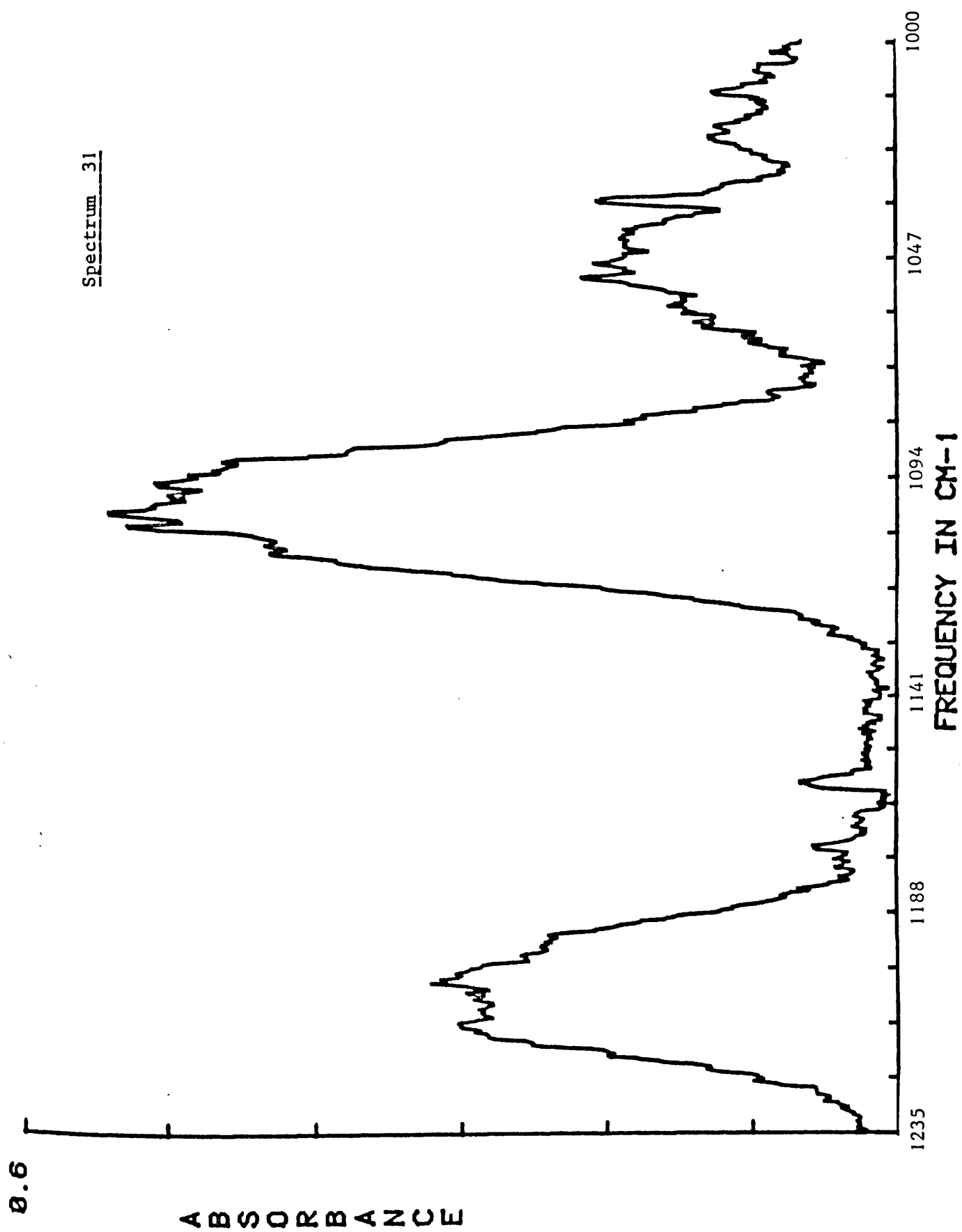
Spectrum 31
0.6
ABSORBANCE
1235
1188
1141
1094
1047
1000
FREQUENCY IN CM-1

Spectrum 32

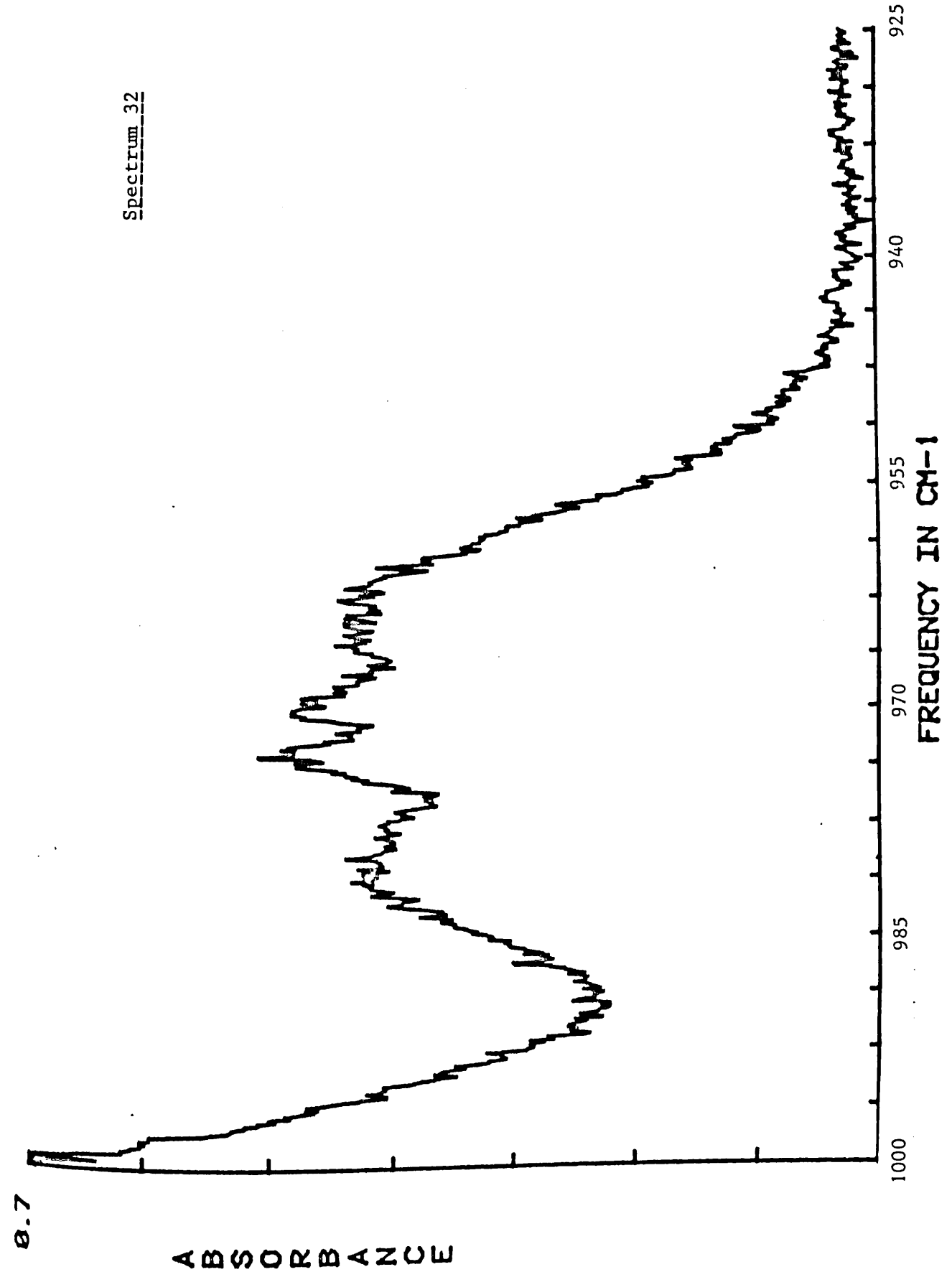

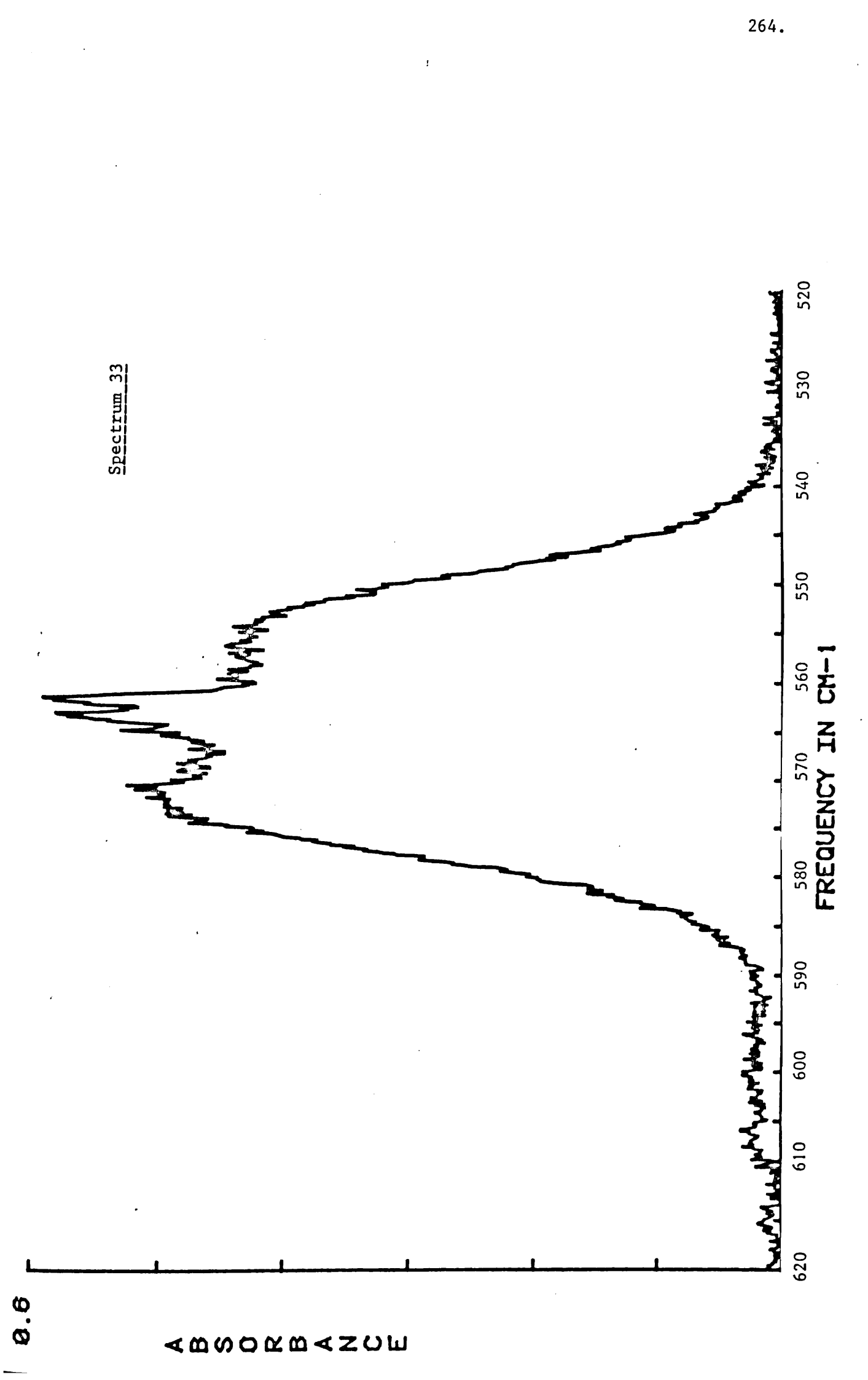
Spectrum 33
0.6
ABSORBANCE
620
610
600
590
580
570
560
550
540
530
520
FREQUENCY IN CM-1

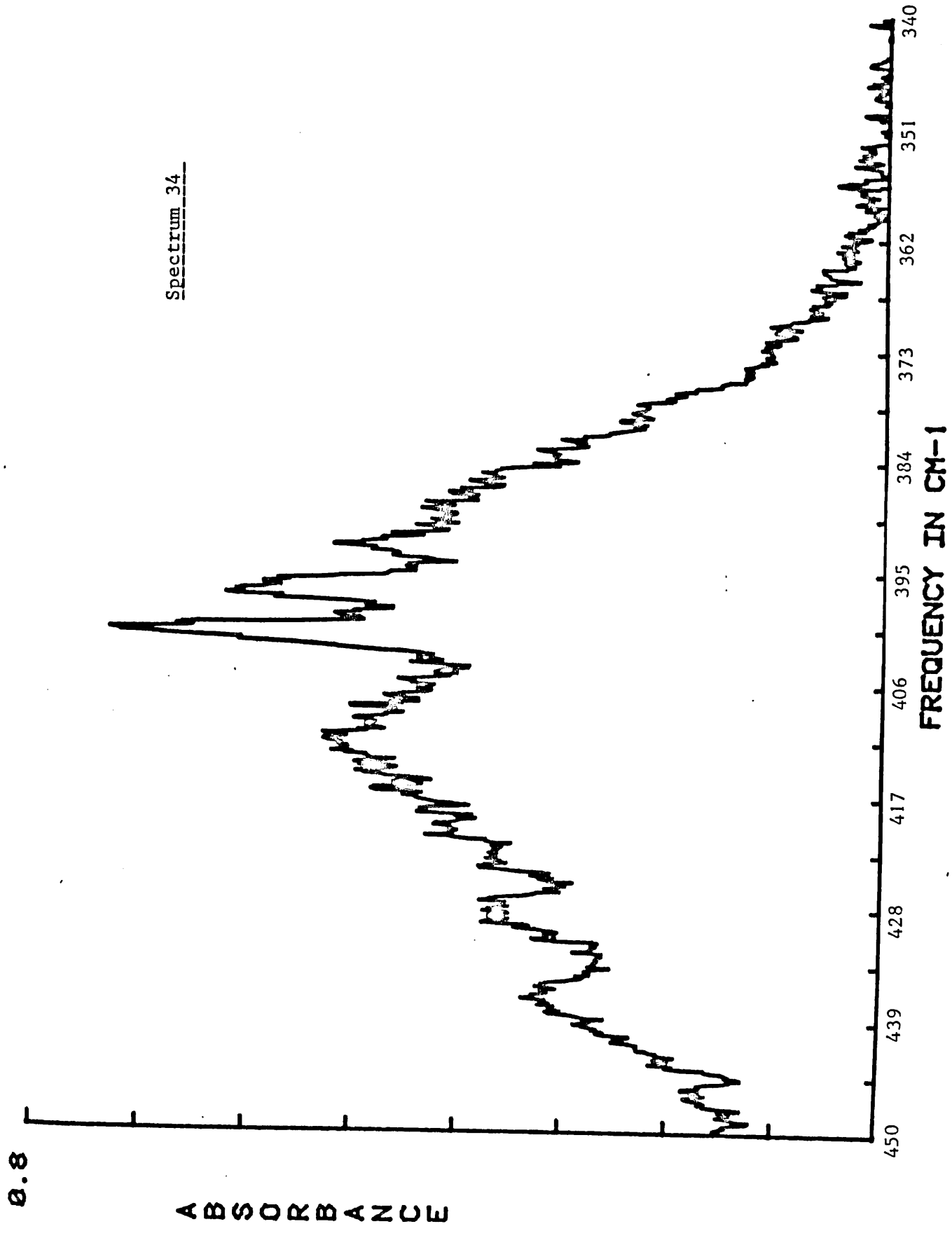
Spectrum 34
0.8
ABSORBANCE
450
439
428
417
406
395
384
373
362
351
340
FREQUENCY IN CM-1

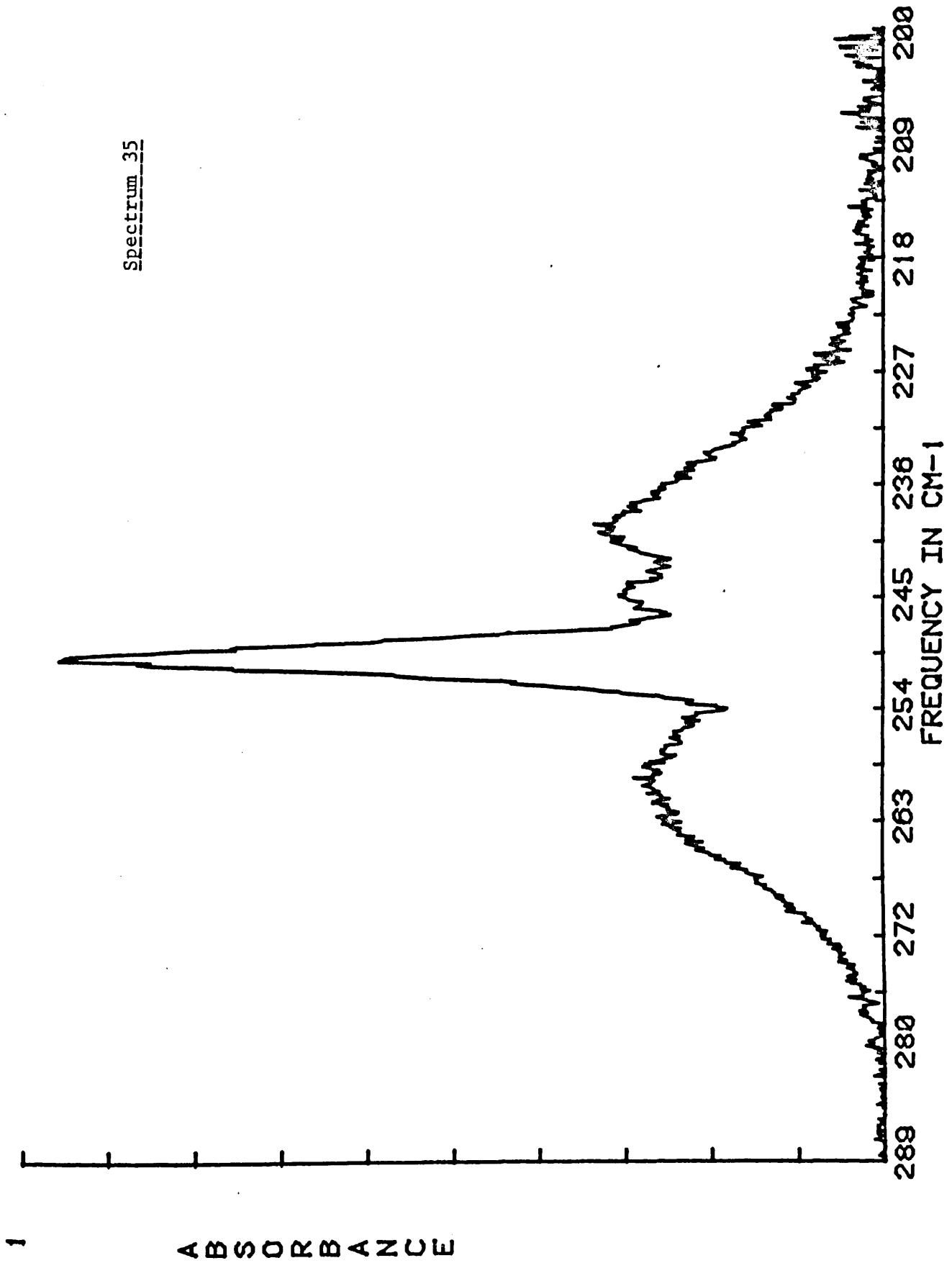
Spectrum 35
1
ABSORBANCE
289
280
272
263
254
245
236
227
218
209
200
FREQUENCY IN CM-1

SOLUTION SPECTRA

Spectrum	Range (cm^{-1})	Concentration (M)	Solvent
d_0-Dioxan			
36	3100-2600	0.111	CS_2
37	1520-1220	0.177	CCl_4
38	1300-1000	0.135	CCl_4
39	970-840	0.060	CCl_4
40	660-540	0.277	CCl_4
41	340-200	0.084	C_6H_{12}
d_8-Dioxan			
42	2350-1950	0.214	CS_2
43	1300-850	0.092	CS_2
44	840-700	0.125	CS_2
45	600-400	0.214	CS_2
46	300-200	0.214	CS_2
d_0-Cyclohexane			
47	3100-2750	0.126	CCl_4
48	1500-1200	0.188	CCl_4
49	1300-1200	0.961	CCl_4
50	1100-970	1.410	CS_2
51	950-850	0.961	CCl_4
52	600-500	0.961	CCl_4
d_{12}-Cyclohexane			
53	2500-1900	0.266	CCl_4
54	1200-850	0.726	CCl_4
55	850-600	0.489	CS_2

Spectrum	Range (cm^{-1})	Concentration (M)	Solvent
Tetrahydropyran			
56	3300-2500	0.208	CCl_4
57	1490-925	0.208	CCl_4
58	910-770	0.512	CS_2
59	650-500	0.512	CS_2
60	350-200	0.512	CS_2

Spectrum 36

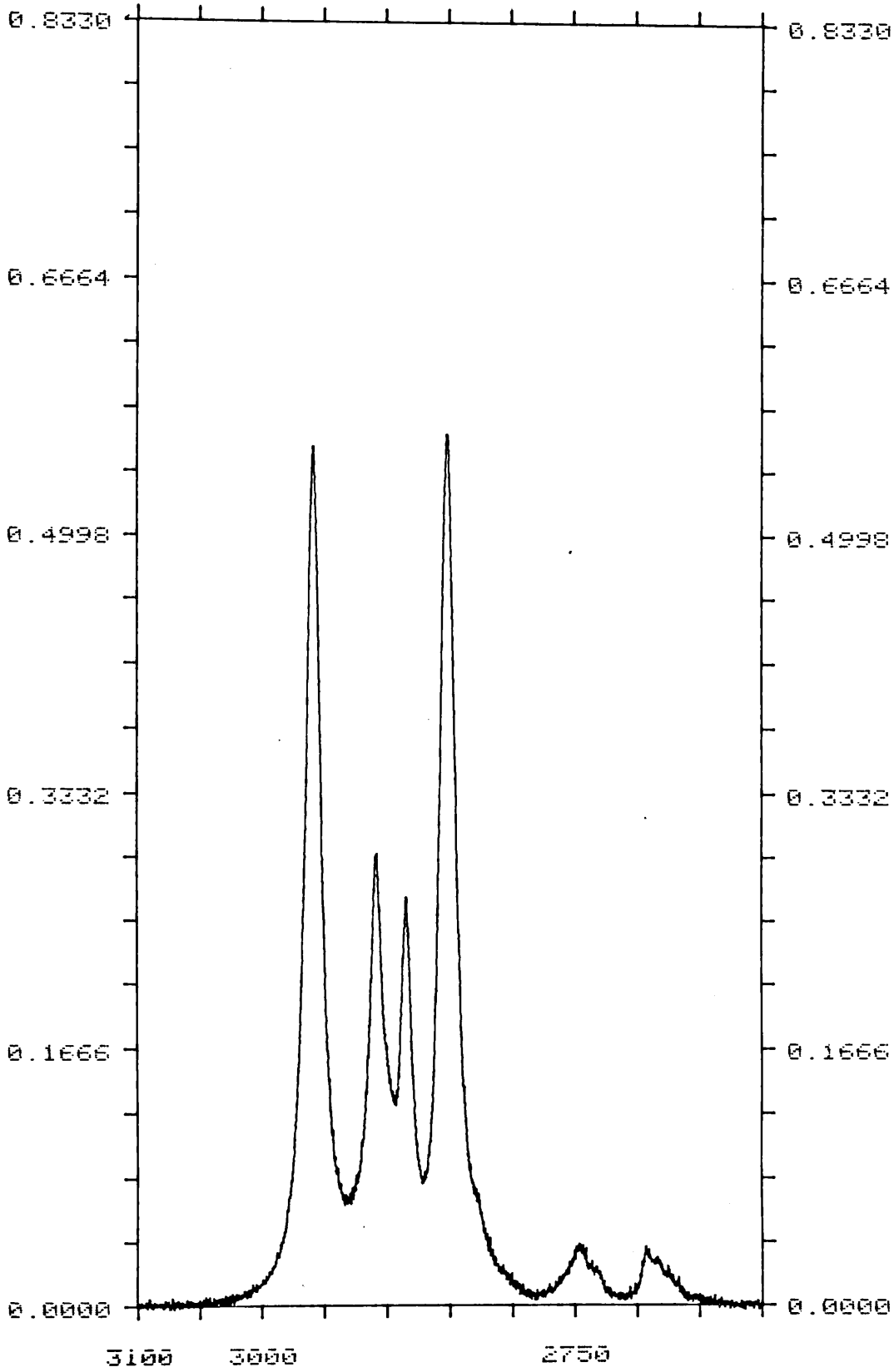

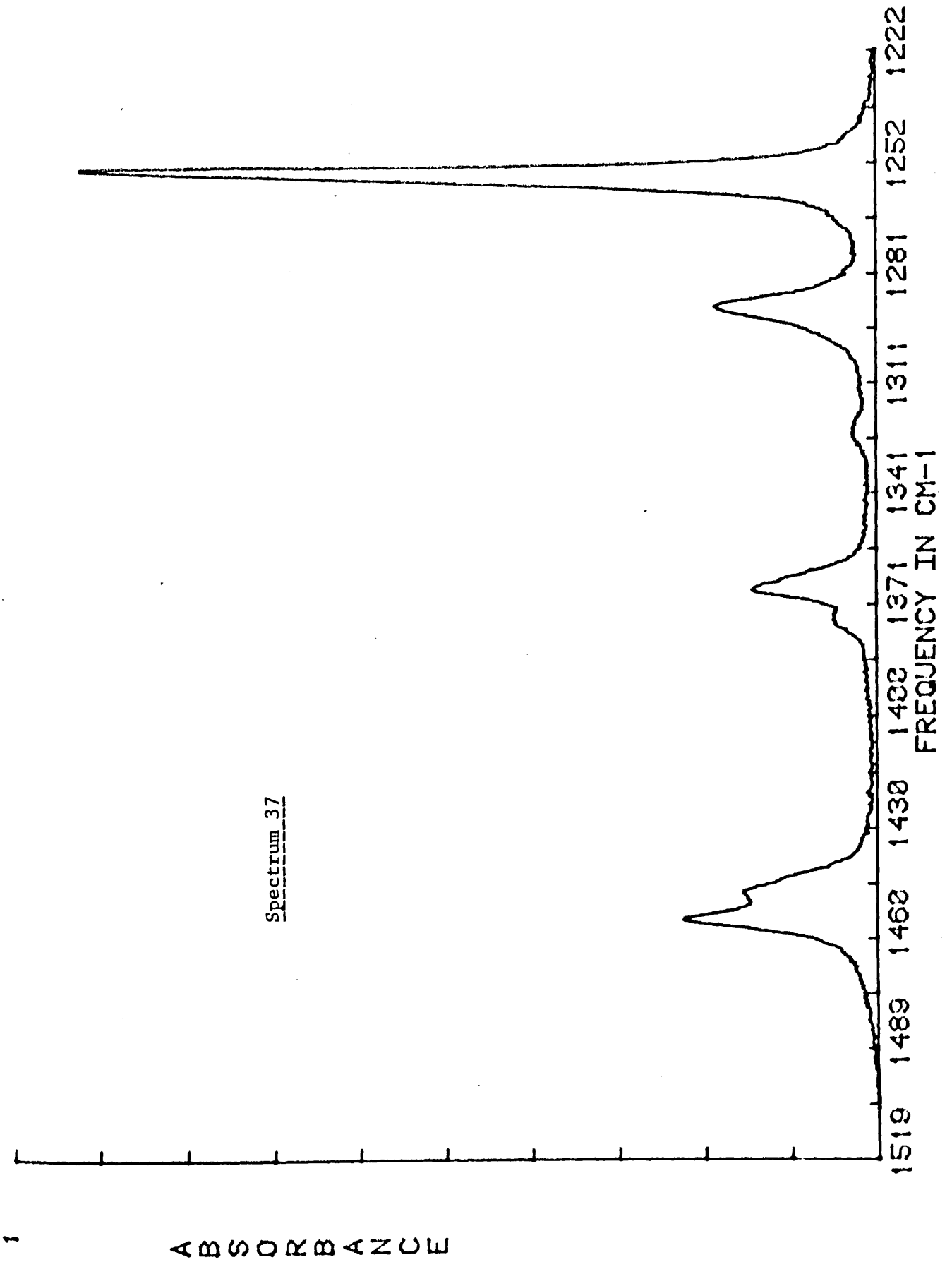
Spectrum 37
1519
1489
1462
1438
1432
1371
1341
1311
1281
1252
1222
FREQUENCY IN CM-1
ABSORBANCE
1

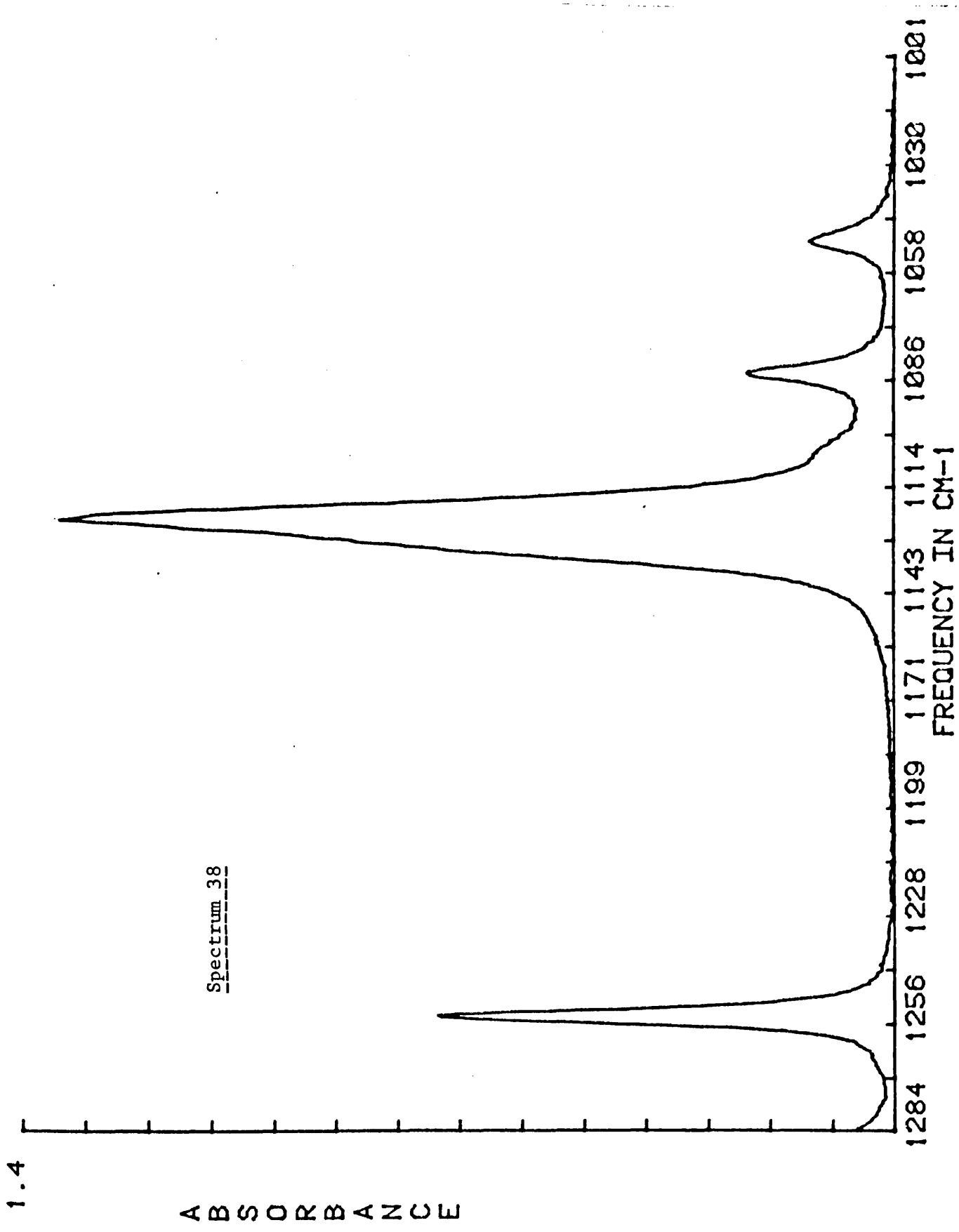
Spectrum 38
1.4
ABSORBANCE
1284
1256
1228
1199
1171
1143
1114
1086
1058
1030
1001
FREQUENCY IN CM-1

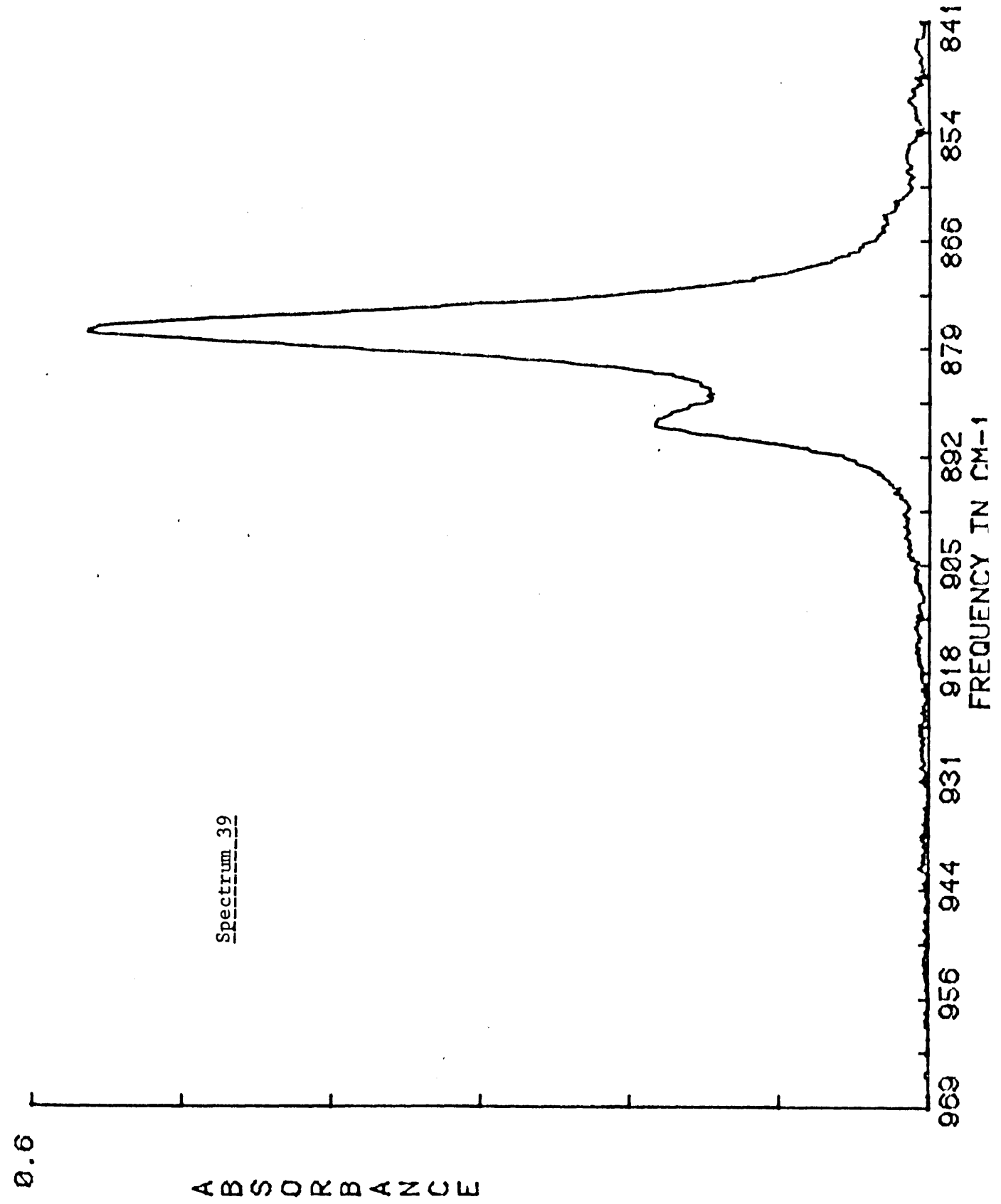
0.6
ABSORBANCE
969
956
944
931
918
905
892
879
866
854
841
FREQUENCY IN CM-1
Spectrum_39

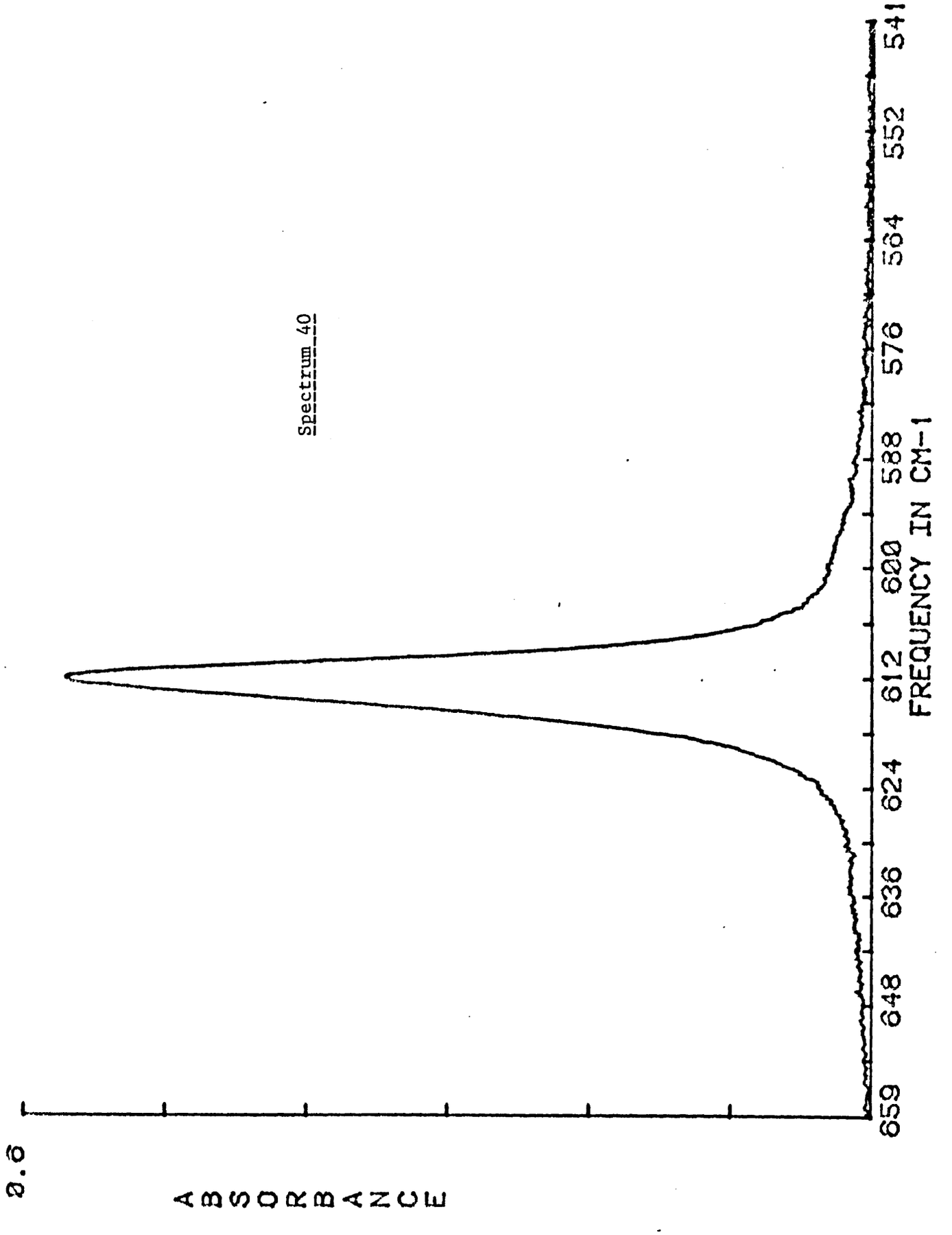
Spectrum 40
2.6
ABSORBANCE
659
648
636
624
612
600
588
576
564
552
541
FREQUENCY IN CM-1

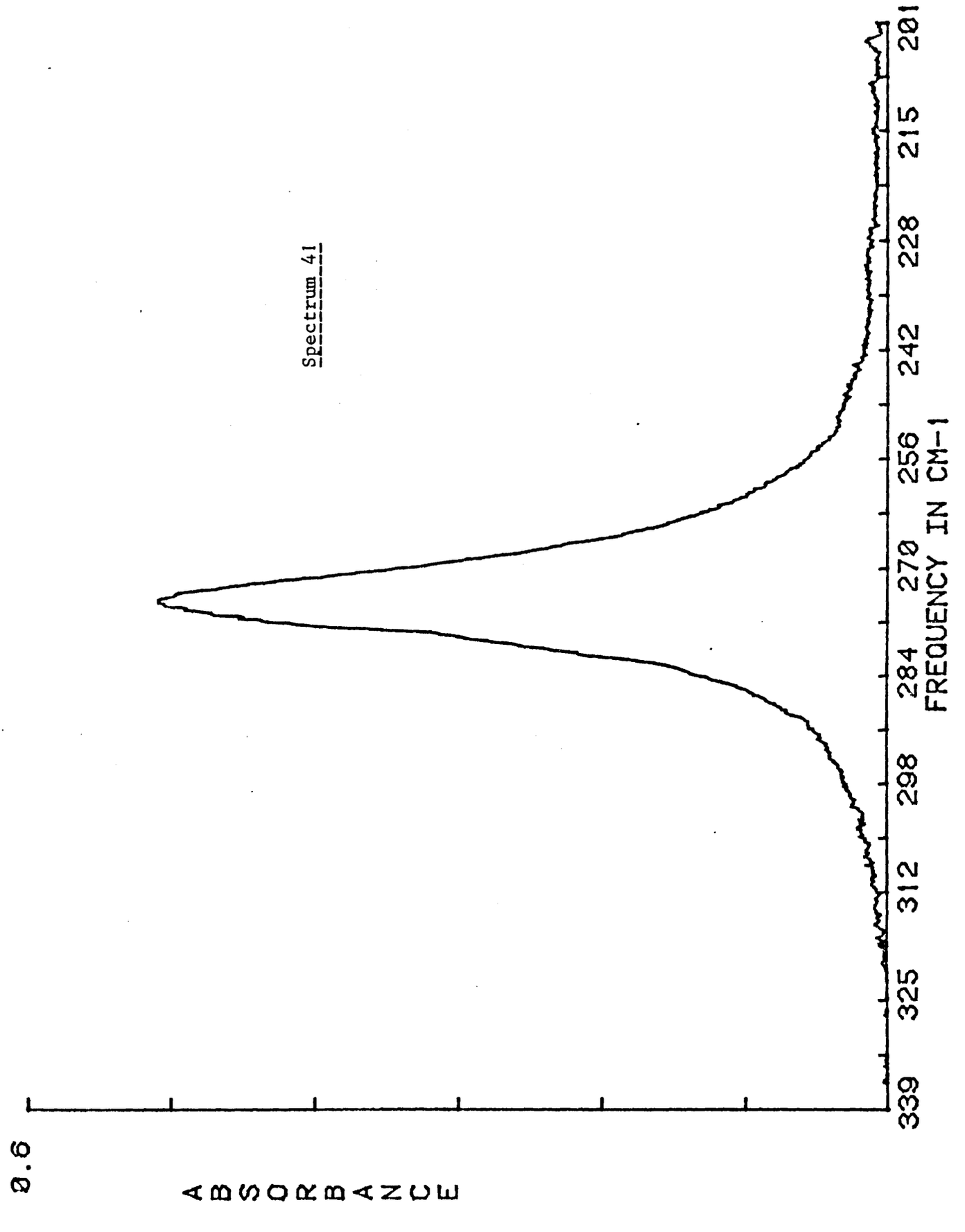
Spectrum 41
0.6
ABSORBANCE
339
325
312
298
284
270
256
242
228
215
201
FREQUENCY IN CM-1

Spectrum 42

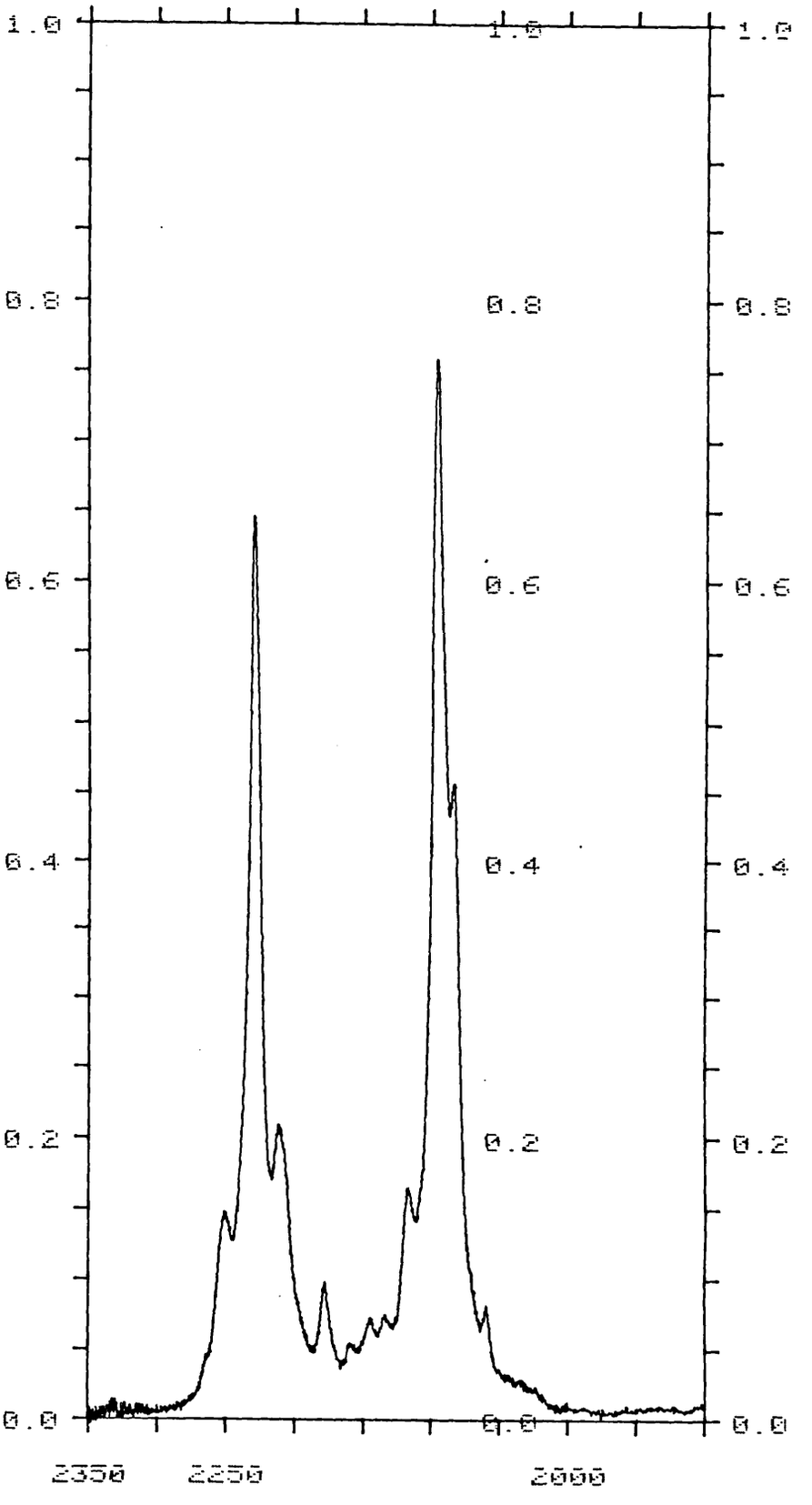

Spectrum 43

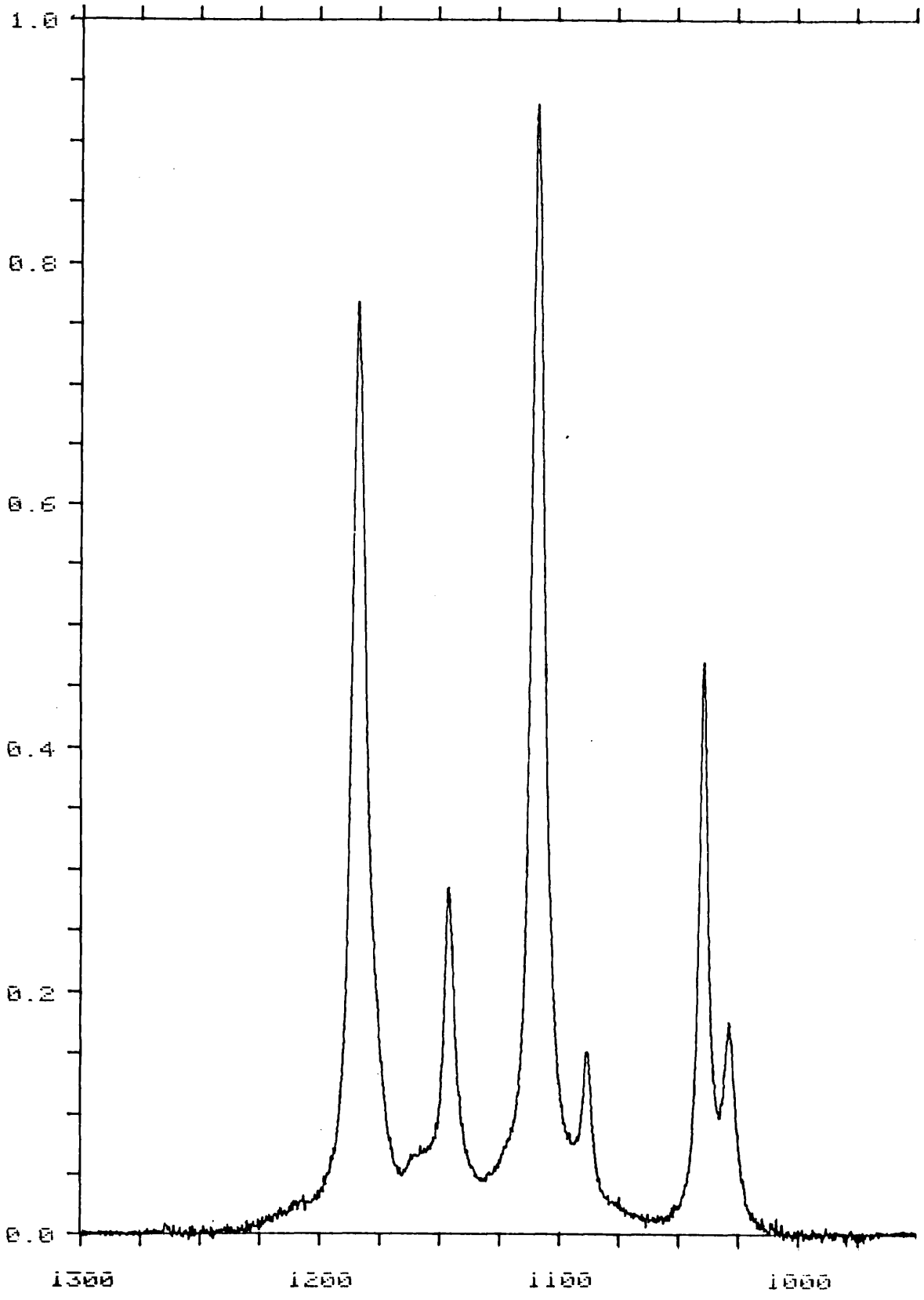

Spectrum 43ctd.

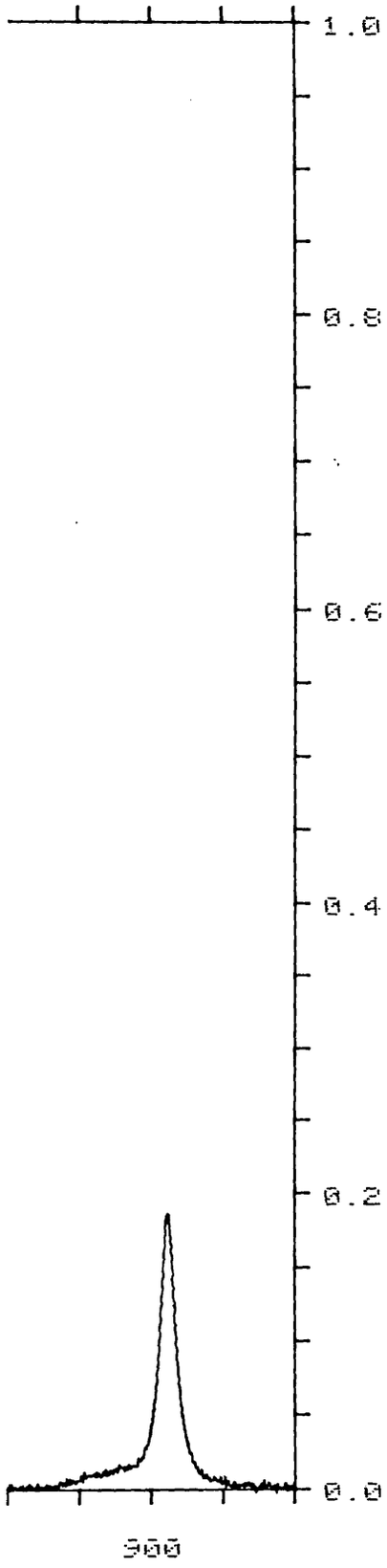

Spectrum 44

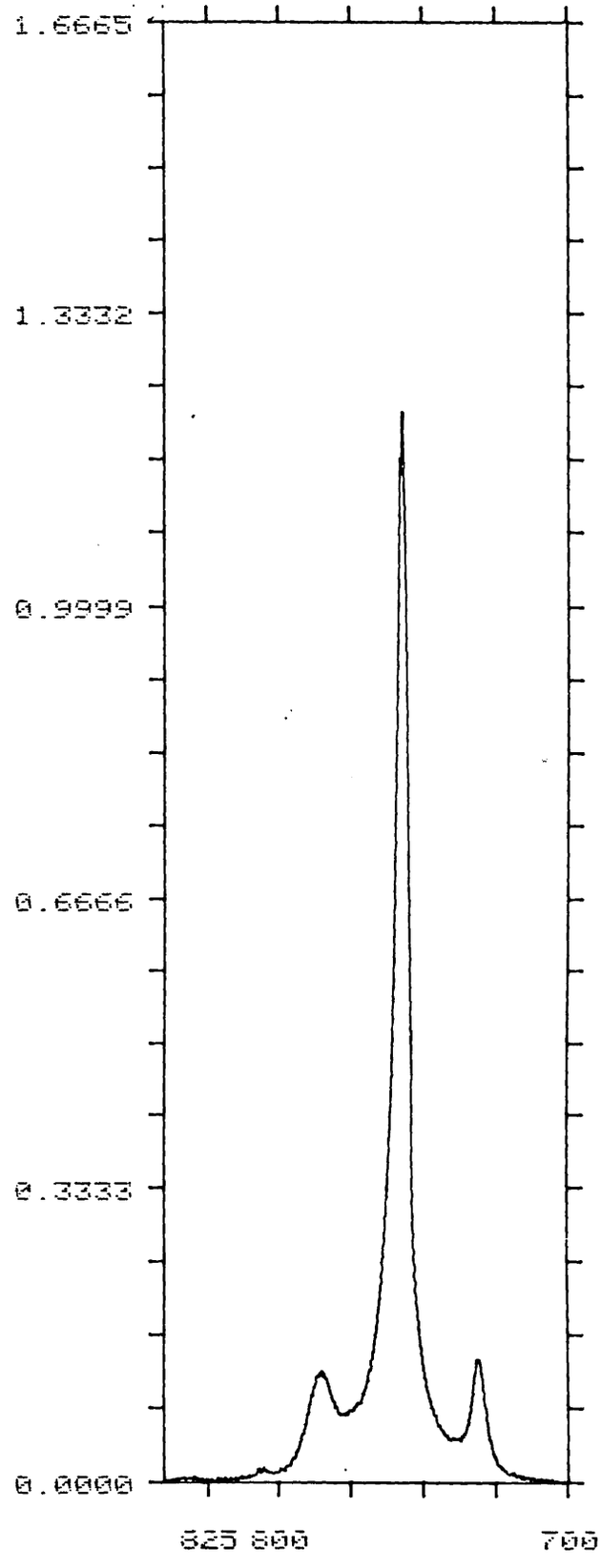

Spectrum 45

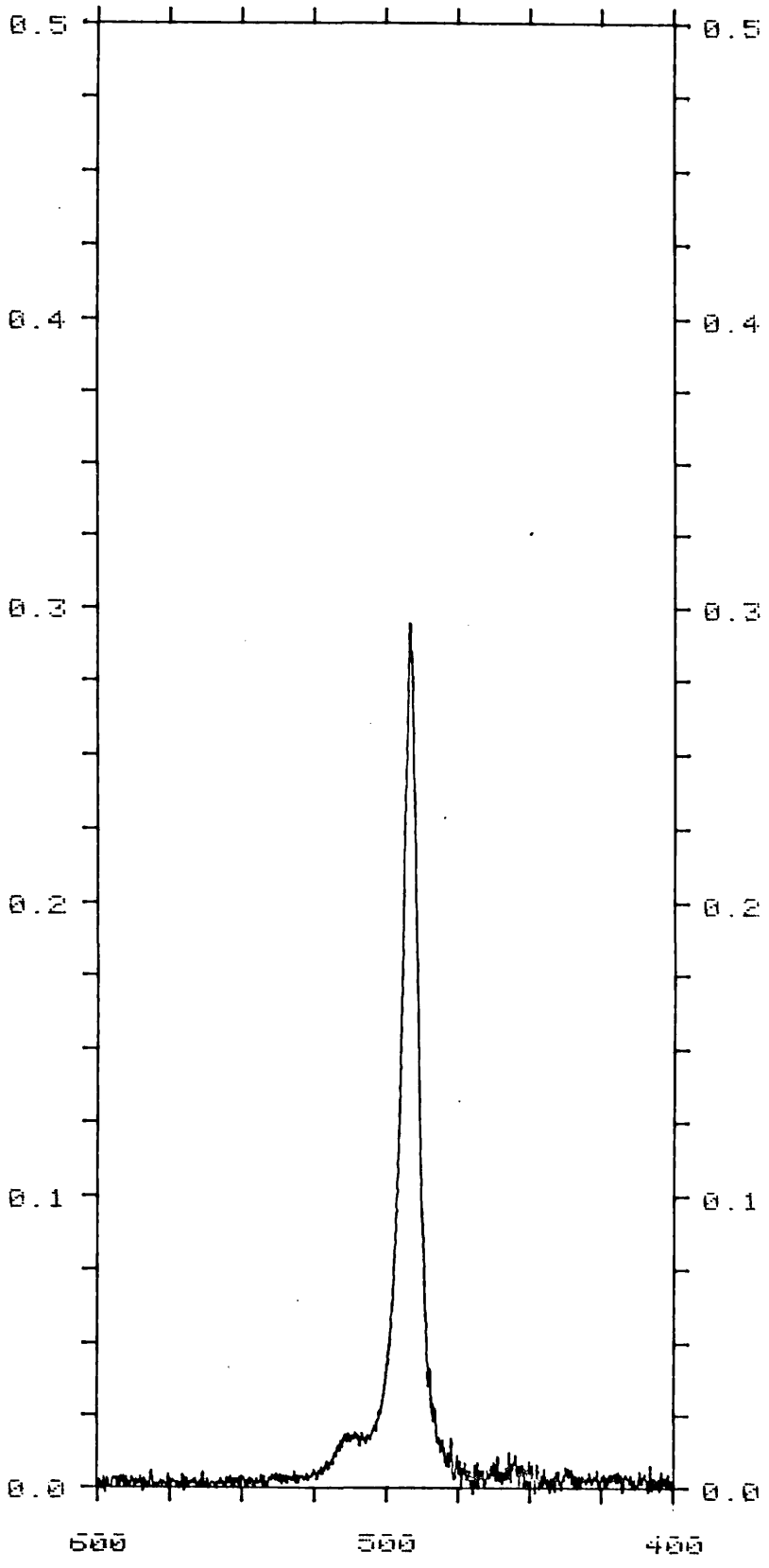

Spectrum 46

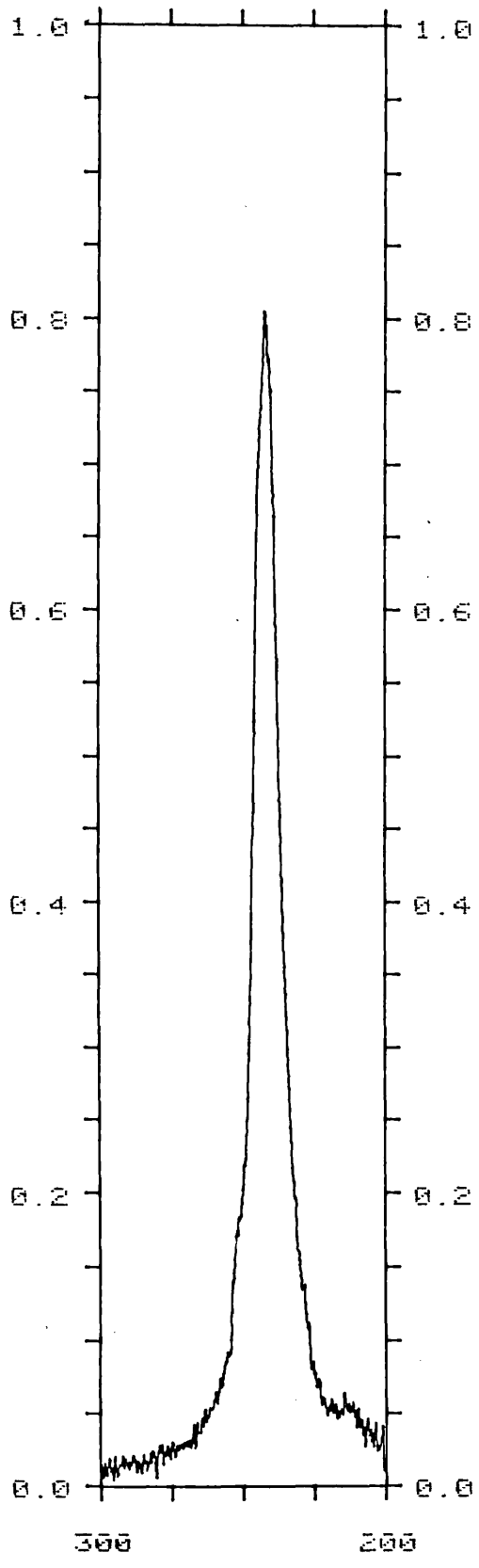

Spectrum 47

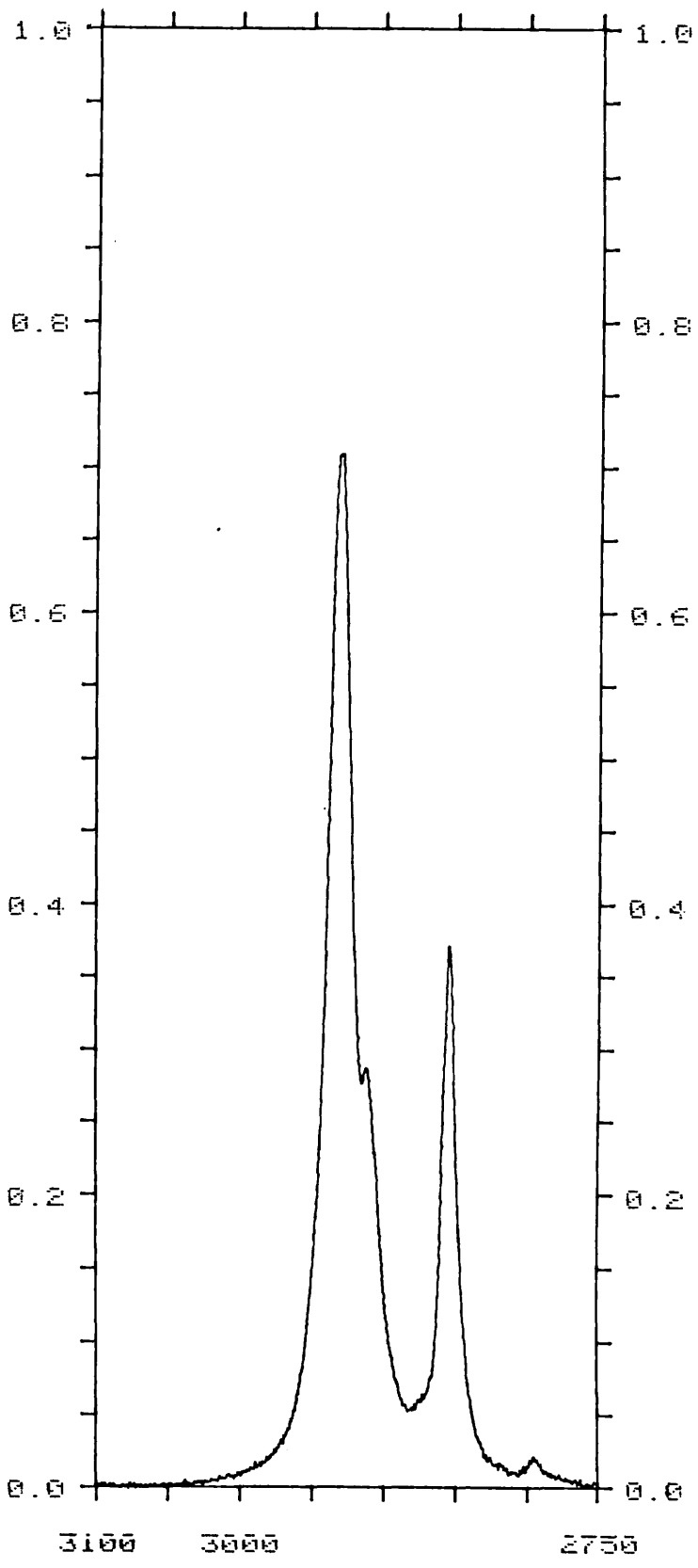

Spectrum 48

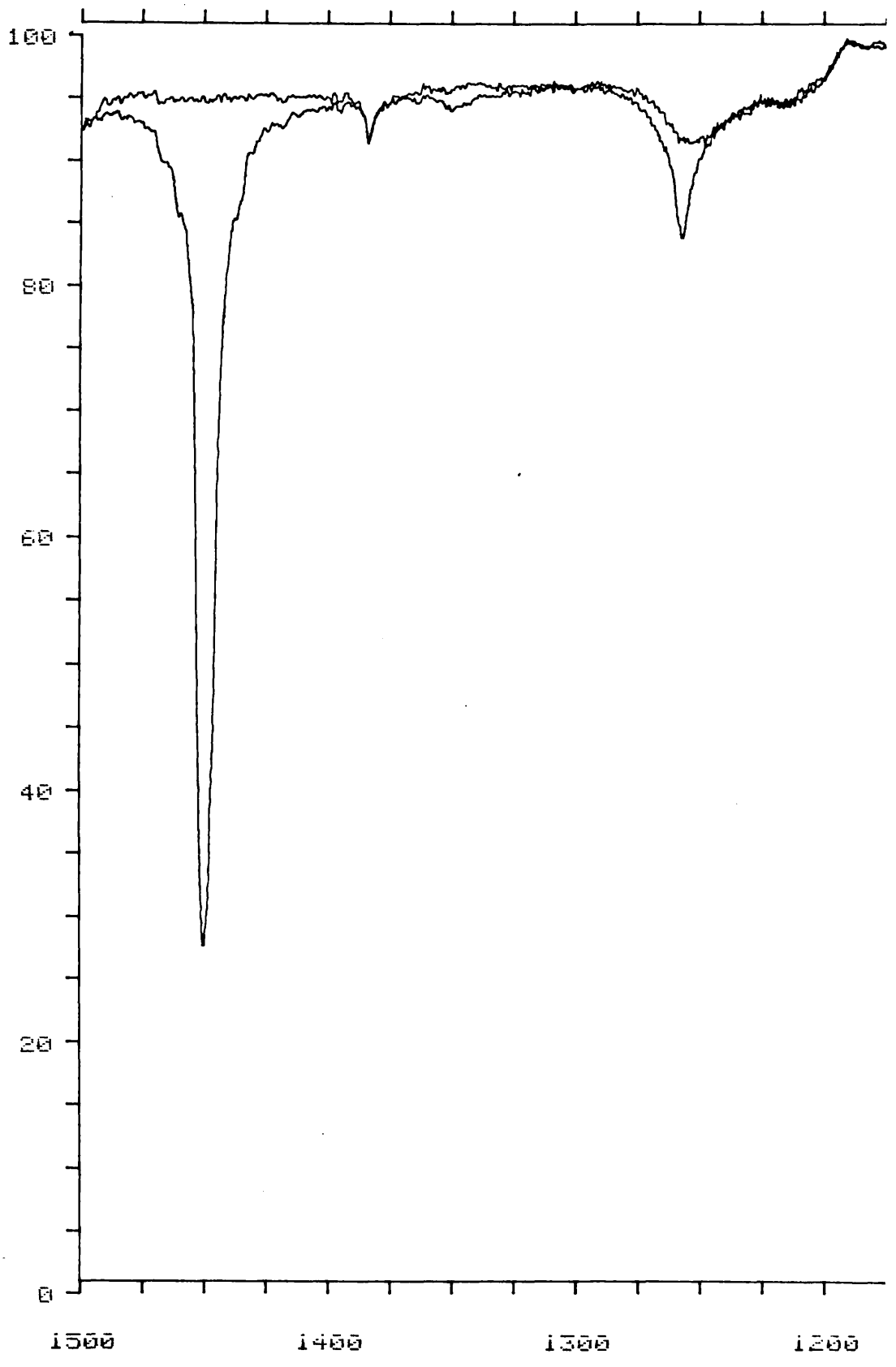

Spectrum 49

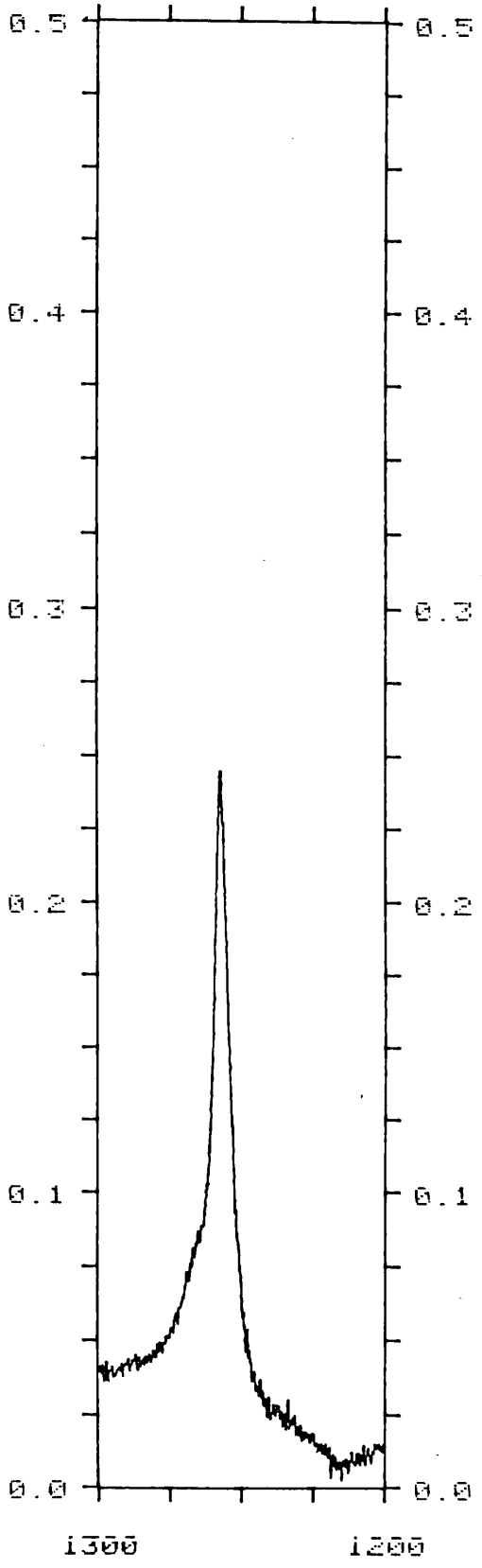

Spectrum 50

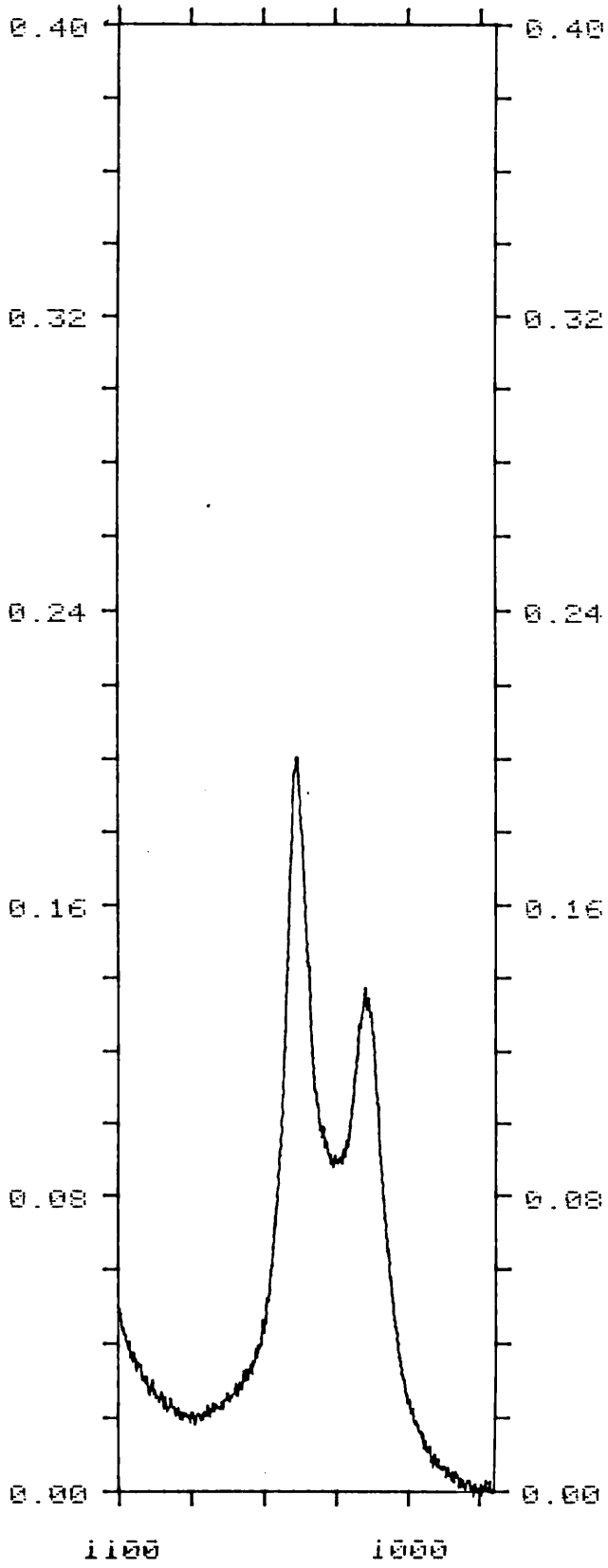

Spectrum 51

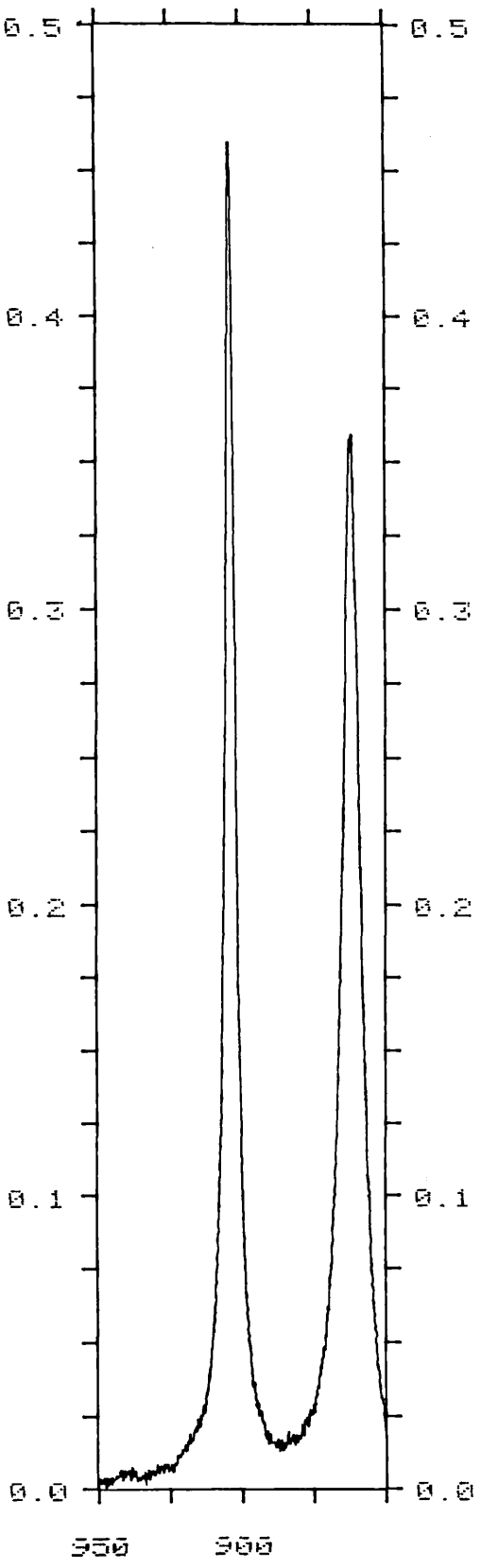

Spectrum 52

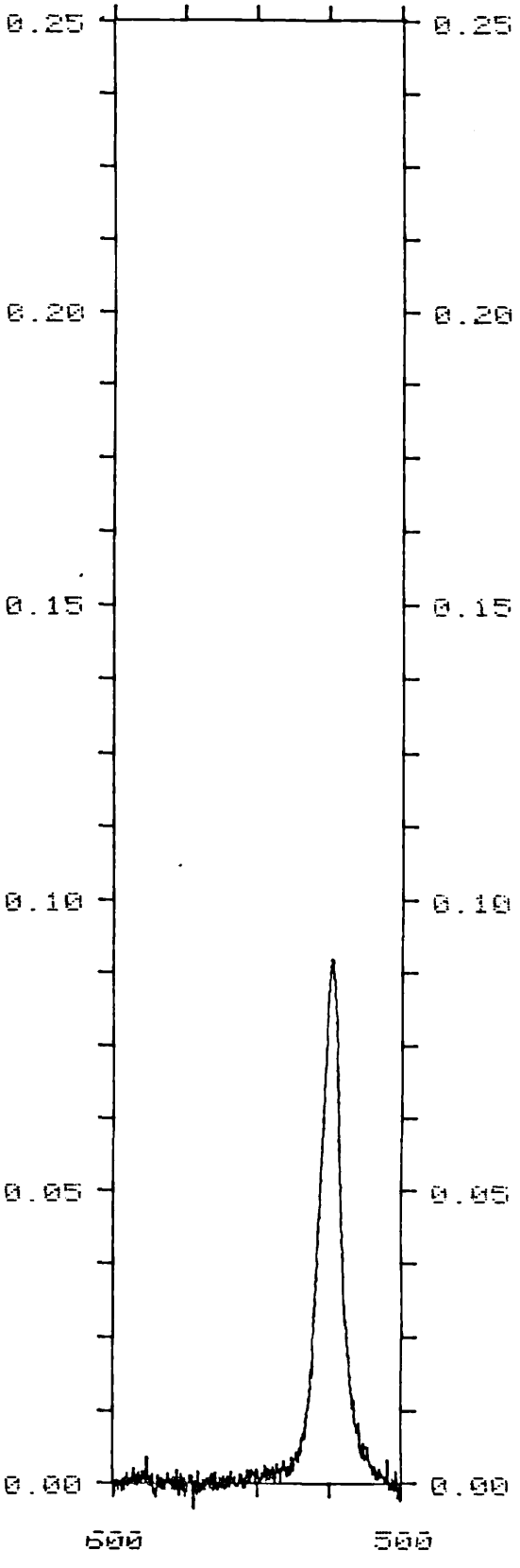

Spectrum 53

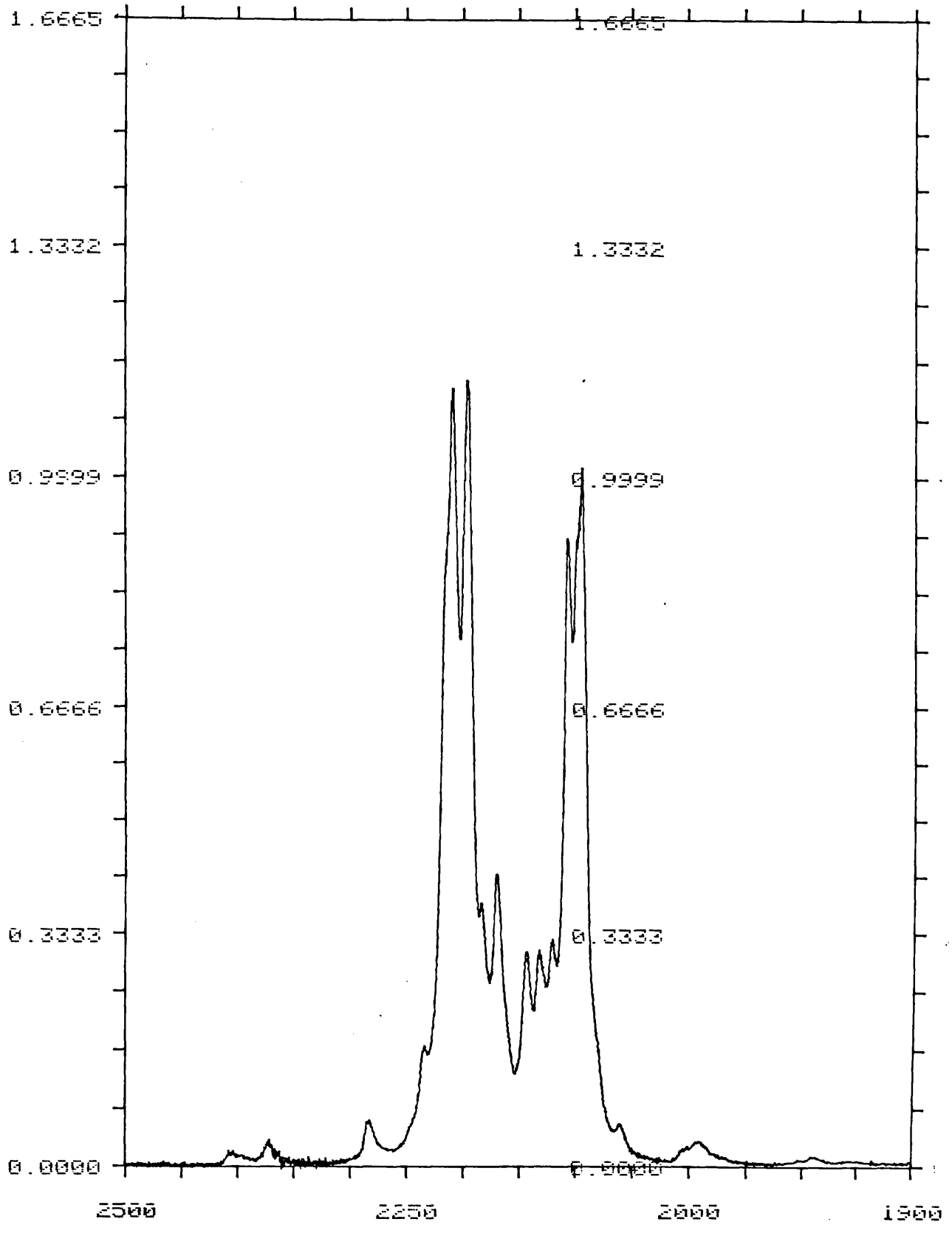

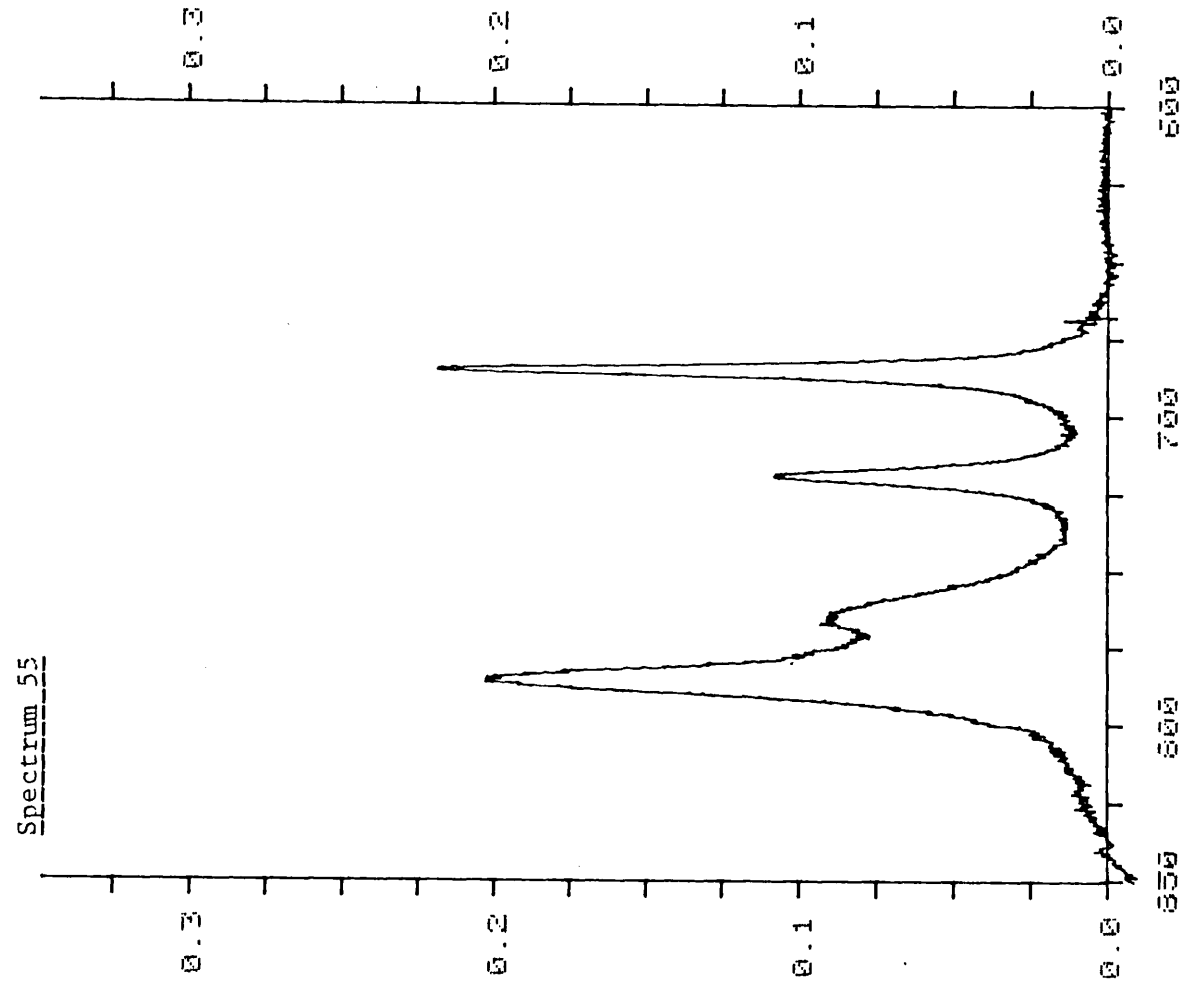
Spectrum 55
0.3
0.2
0.1
0.0
500
700
900
1100

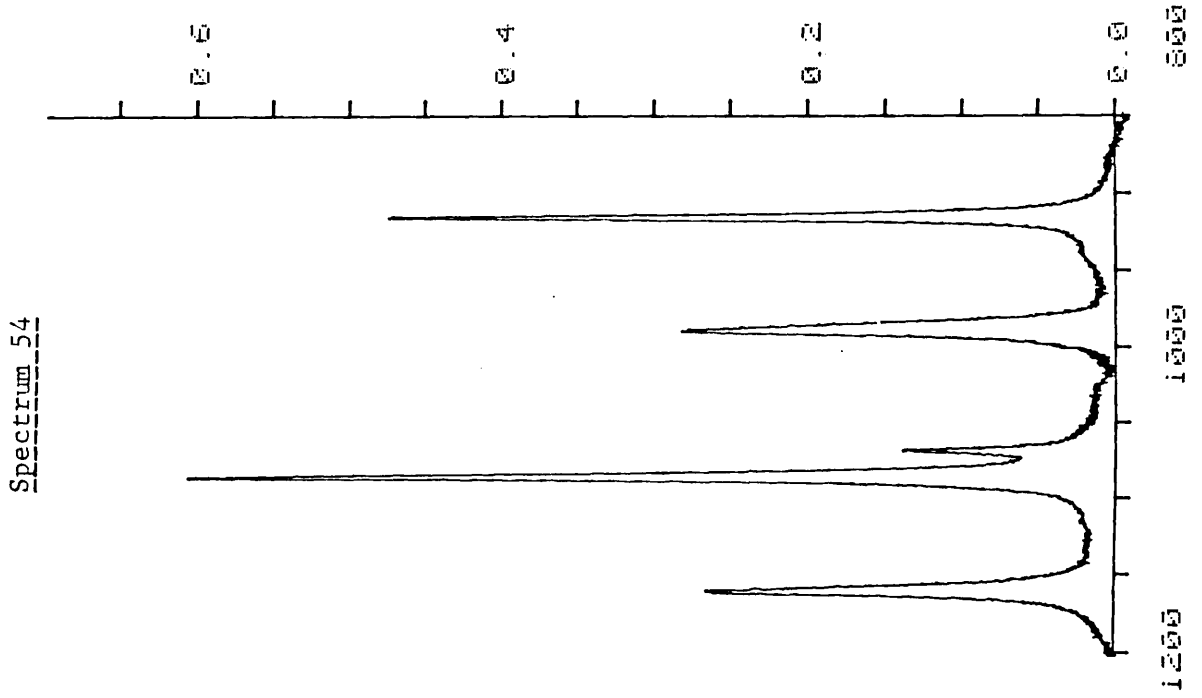
Spectrum 54
0.6
0.4
0.2
0.0
800
1000
1200

Spectrum 56

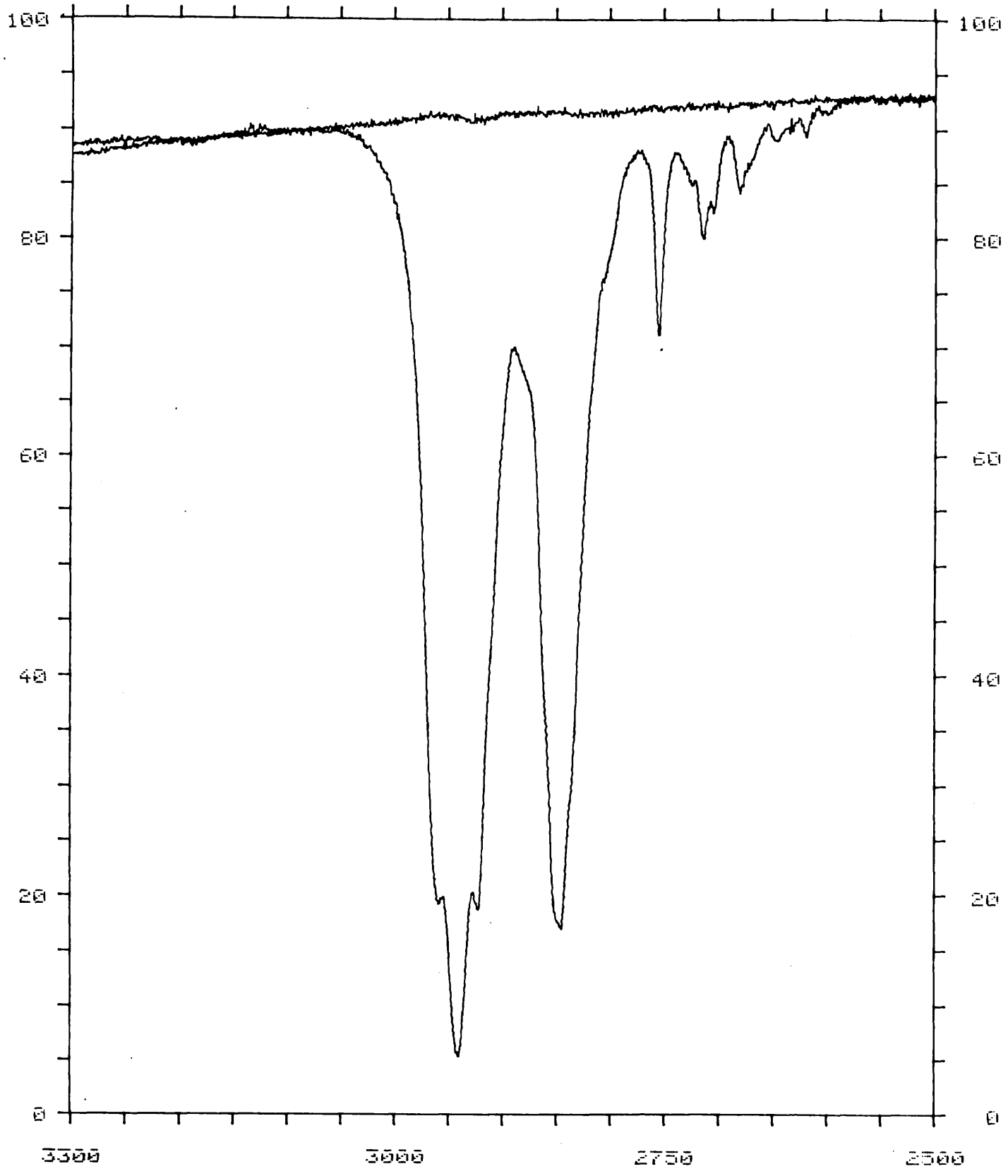

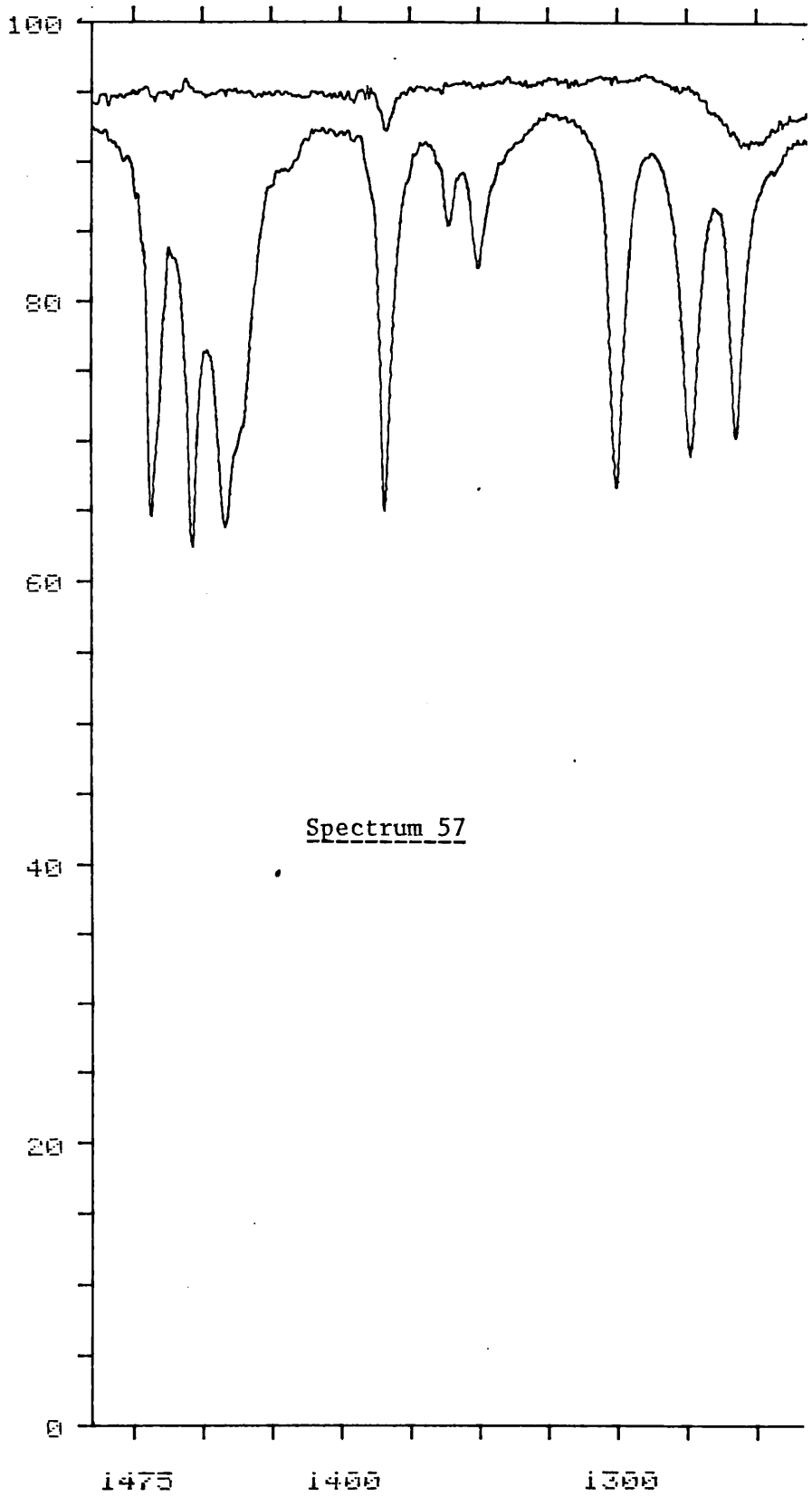

Spectrum 57

Spectrum 57 ctd.

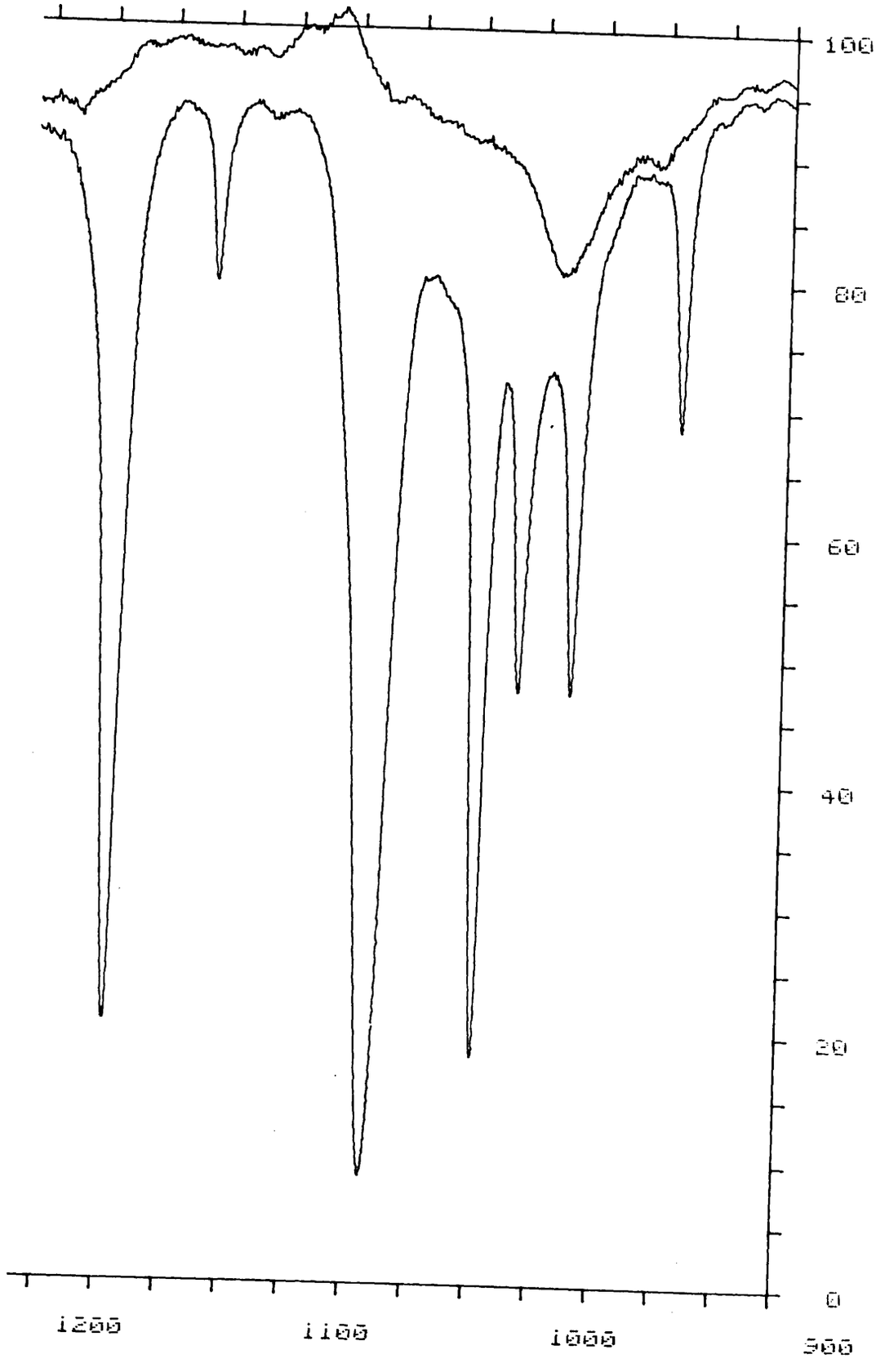

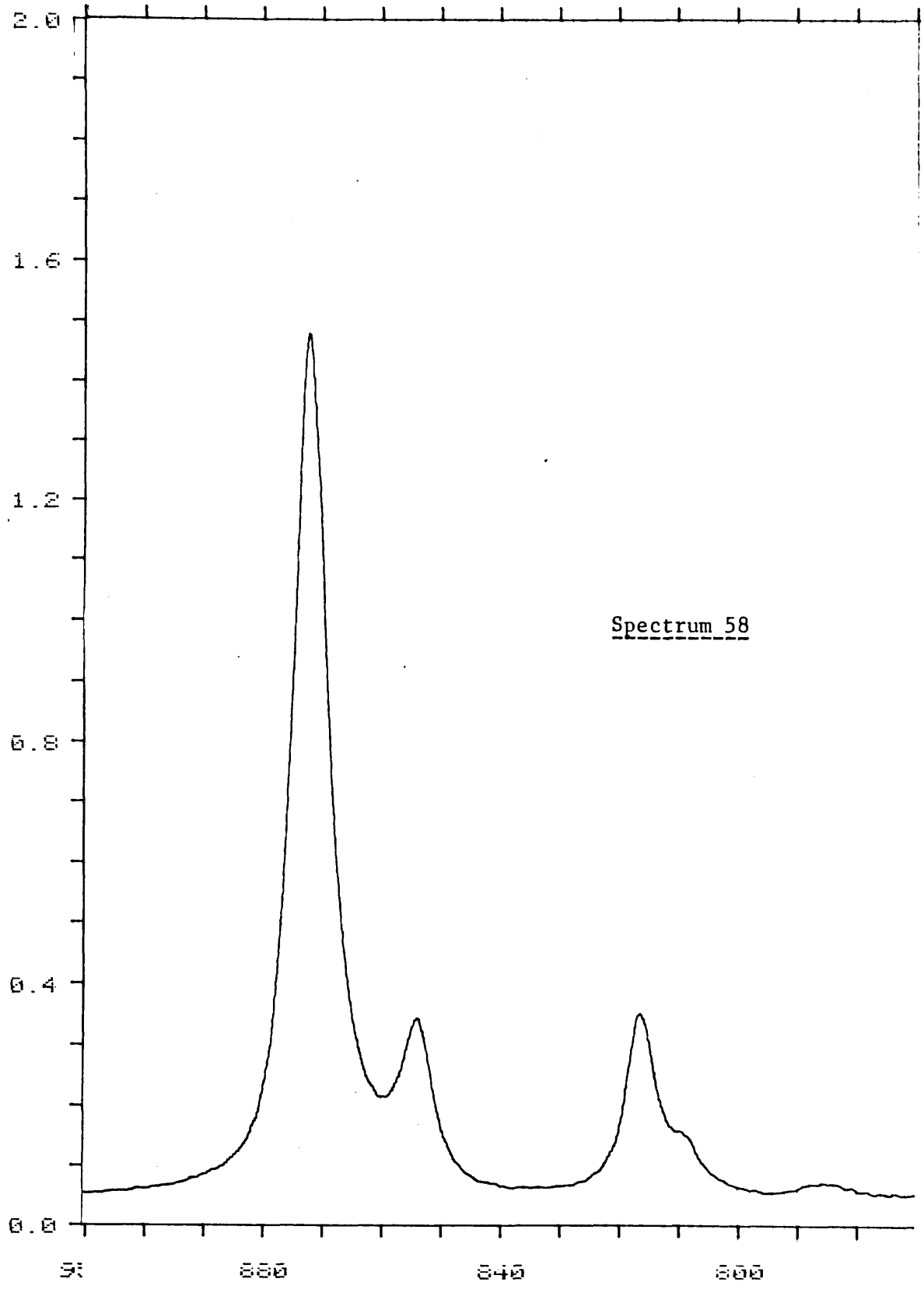
2.0
1.6
1.2
0.8
0.4
0.0
880
840
800
Spectrum 58

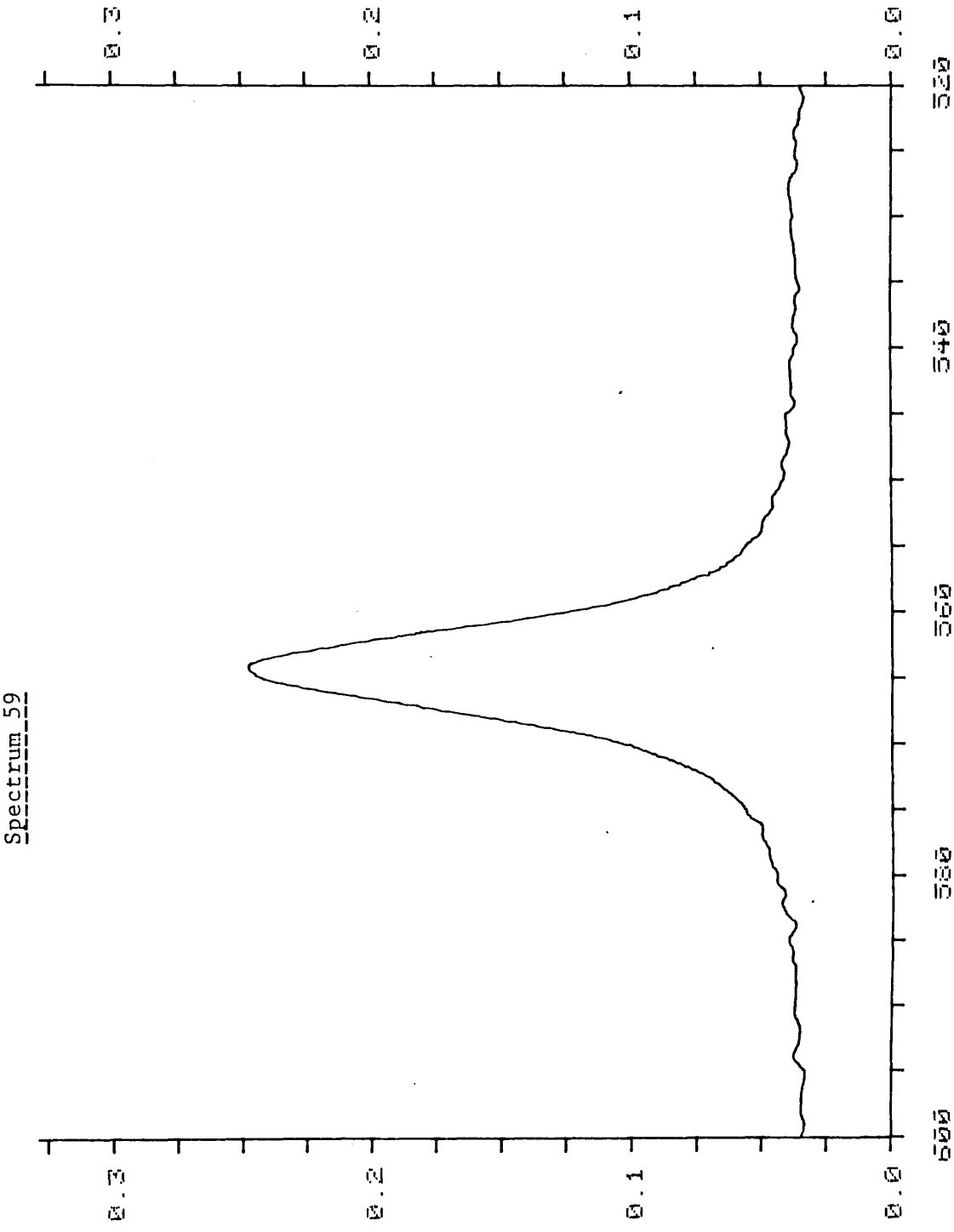
Spectrum 59
0.0
0.1
0.2
0.3
500
520
540
560
580
600
0.0
0.1
0.2
0.3

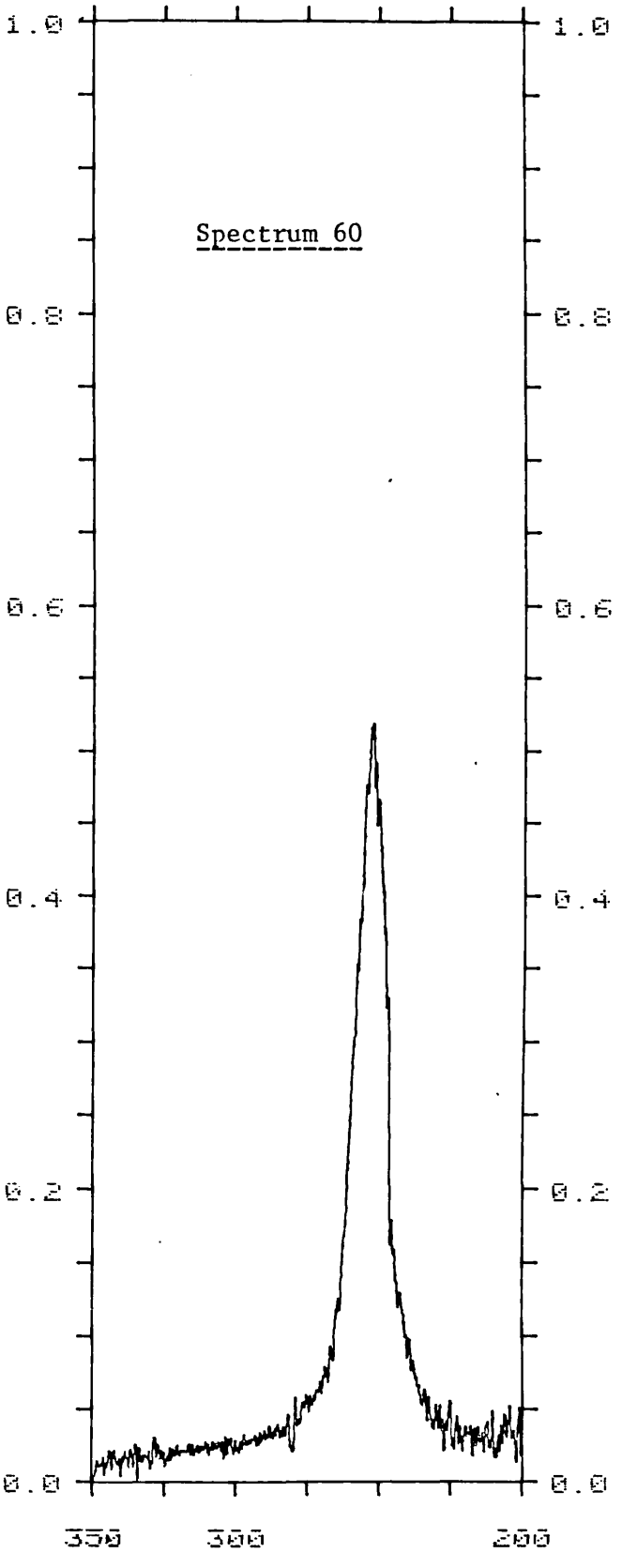
Spectrum 60
1.0
0.8
0.6
0.4
0.2
0.0
350
300
200

Least-squares analysis

Suppose we aim to represent an observable as a function of some parameters p. Then the least squares problem is to adjust the array p so that the sum of the square of the error vectors is a minimum. Let the true and calculated observables be I_{ti} and I_{ci} and define the residual by

$$R = \sum_i (I_{ci} - I_{ti})^2$$

If our initial guess at the parameters produces an array of calculated observables I^o_{ci} then we wish to know the variations Δp which minimises R

$$I_{ci} = I^o_{ci} + \sum_j \left(\frac{\partial I}{\partial p_j}\right) \Delta p_j \equiv I^o_{ci} + \sum_j J_{ij}\, \Delta p_j \qquad (2)$$

$$\therefore \quad R = \sum_i ((I^o_{ci} - I_{ti}) + \sum_j J_{ij}\, \Delta p_j)^2 \qquad (3)$$

$$\frac{\partial R}{\partial \Delta p_j} = 2\sum_i \sum_j (I^o_{ci} - I_{ti} + J_{ij}\Delta p_j) J_{ij} = 0 \qquad (4)$$

Let $I^o_{ti} - I_{ci}$ be written as a vector of 'errors' $\hat{\varepsilon}_i$

The set of such minima equations as above can be put in matrix form

$$\begin{pmatrix} J_{11} & J_{21} & J_{31} & \cdots & J_{i1} \\ J_{12} & J_{22} & & & \\ J_{13} & & & & \\ \vdots & & & & \\ J_{1j} & & & & \end{pmatrix} \begin{pmatrix} \varepsilon_1 \\ \varepsilon_2 \\ \vdots \\ \varepsilon_i \end{pmatrix} = \begin{pmatrix} J_{11} & \cdots & J_{i1} \\ J_{12} & \cdots & J_{i2} \\ & & \\ & & \\ J_{1j} & \cdots & J_{ij} \end{pmatrix} \begin{pmatrix} J_{11} & J_{12} & \cdots & J_{1j} \\ \vdots & & & \\ & & & \\ & & & \\ J_{i1} & & & \end{pmatrix} \begin{pmatrix} \Delta p_1 \\ \Delta p_2 \\ \Delta p_3 \\ \\ \Delta p_j \end{pmatrix}$$

$$J^t \hat{\varepsilon} = (J^t J)\hat{\Delta p} \qquad (5)$$

If all observables are not of equal reliability it may be wished to weight the results in some manner. This can be achieved at the stage of equation (4) by multiplying the equation for ϵ_i by weight W_i. In equation (5) this is accommodated by constructing a diagonal matrix W with entries equal to the weights W_i which leads to

$$J^t W \hat{\epsilon} = (J^t W J) \hat{\Delta p} \qquad (5)$$

Provided that the set of linear equations (4) are adequate to determine the Δp (one obvious condition is $j \geq i$) then the determinant of $J^t W J \neq 0$ and the matrix may be inverted to give the optimum Δp as

$$\hat{\Delta p} = (J^t W J)^{-1} J^t W \hat{\epsilon} \equiv C^{-1} J^t W \hat{\epsilon} \qquad (6)$$

In the event that a linear relation (2) is very inadequate the correction (6) will lead to a corrected $\hat{p}$ which may be little improvement - or even worse! Furthermore it is conceivable that due to existence of acceptable alternative ordering of I_{ci} and I_{ti} alternative solutions exist. To converge onto a particular solution, or to overcome oscillations one of two techniques can be employed.

(a) A small fraction (usually 0.1 to 0.5) of Δp can be added to the original p. Imagine a cross section in the solution space as below -

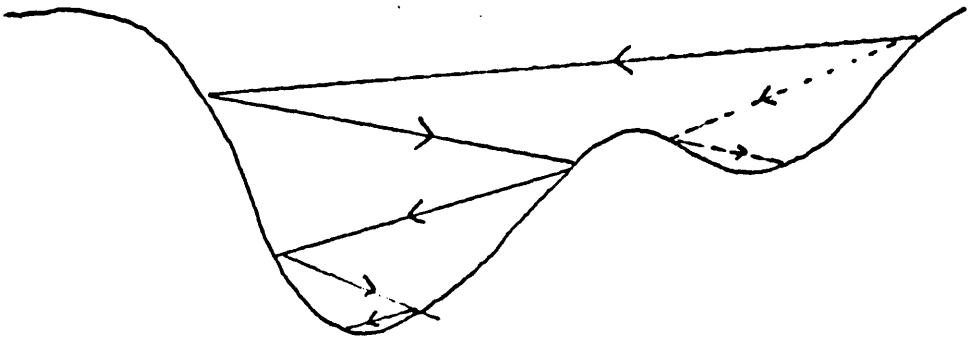

then a typical set of sequential solutions to $I_{c\hat{t}}$ might be as shown by solid line. By taking only half of $\Delta\hat{p}$ convergence of the minimum closer to the original choice of $\hat{p}$ will be more likely.

(b) Addition of aC_{ii} to C ('a' any real constant) before inversion is also reputed to smooth convergence.

ENERGIES CALCULATED USING GAUSSIAN 76

In Section 3.3 it was described how Gaussian 76 was used to calculate the energies for various molecular configurations of 1,4-dioxan, which were subsequently used to derive a set of general valence force constants. In the following pages the raw data is presented in full.

The molecular gometries and corresponding energies are presented on alternate pages. For the former, the value of a representative member of each set of equivalent internal coordinates is given. For the latter, the energy calculated using Gaussian 76 (EN G76) and the energy calculated using the derived force constants (from the least-squares fit to the energies, EN FUNC) are given. These are given for each symmetry species. The "raw" ab initio force constants are then presented.

The following are the values of the internal coordinates corresponding to the minimum of the molecular potential energy, calculated from the Ag data.

E_0 = -0.37154030

CO = 1.43574 A

CC = 1.51752 A

CH^a = 1.08543 A

CH^e = 1.07939 A

H^aCC = 110.060°

H^eCC = 111.968°

H^aCO = 109.406°

H^eCO = 106.529°

COC = 113.572°

OCC = 109.385°

Note: in order to convert the energies to Hartrees add -305 to each figure. This was omitted in the calculations for simplification.

Ag data

CO	CC	CHa	CHe	HaCC	HeCC	HaCO	HeCO	COC	OCC	
1.45	1.54	1.09	1.09	109.47	109.47	109.47	109.47	109.47	109.47	1
1.42	1.54	1.09	1.09	109.47	109.47	109.47	109.47	109.47	109.47	2
1.39	1.54	1.09	1.09	109.47	109.47	109.47	109.47	109.47	109.47	3
1.43632	1.54	1.09	1.09	109.47	109.47	109.47	109.47	109.47	109.47	4
1.43632	1.48	1.09	1.09	109.47	109.47	109.47	109.47	109.47	109.47	5
1.43632	1.51	1.09	1.09	109.47	109.47	109.47	109.47	109.47	109.47	6
1.43632	1.519304	1.06	1.09	109.47	109.47	109.47	109.47	109.47	109.47	7
1.43632	1.519304	1.11	1.09	109.47	109.47	109.47	109.47	109.47	109.47	8
1.43632	1.519304	1.09	1.06	109.47	109.47	109.47	109.47	109.47	109.47	9
1.43632	1.519304	1.09	1.12	109.47	109.47	109.47	109.47	109.47	109.47	10
1.43632	1.519304	1.06	1.12	109.47	109.47	109.47	109.47	109.47	109.47	11
1.43632	1.519304	1.06	1.06	109.47	109.47	109.47	109.47	109.47	109.47	12
1.43632	1.519304	1.084	1.078	109.47	109.47	109.47	109.47	109.47	109.47	13
1.43632	1.519304	1.084	1.078	109.47	109.47	109.47	109.47	106.47	109.47	14
1.43632	1.519304	1.084	1.078	109.47	109.47	109.47	109.47	112.47	109.47	15
1.43632	1.519304	1.084	1.078	109.47	109.47	109.47	109.47	112.9192	109.47	16
1.43632	1.519304	1.084	1.078	109.47	109.47	109.47	109.47	112.9192	106.47	17
1.43632	1.519304	1.084	1.078	109.47	109.47	109.47	109.47	112.9192	112.47	18
1.43632	1.519304	1.084	1.078	109.47	109.47	109.47	109.47	112.9192	109.6242	19
1.41632	1.519304	1.084	1.078	109.47	109.47	109.47	109.47	112.9192	109.6242	20
1.45632	1.519304	1.084	1.078	109.47	109.47	109.47	109.47	112.9192	109.6242	21
1.43194	1.519304	1.084	1.078	109.47	109.47	109.47	109.47	112.9192	109.6242	22
1.43194	1.519304	1.084	1.078	107.878	109.878	109.254	107.615	112.9192	109.6242	23
1.43194	1.519304	1.084	1.078	109.848	111.298	109.905	107.395	112.9192	109.6242	24
1.43194	1.519304	1.084	1.028	109.848	111.298	109.905	107.395	112.9192	109.6242	25
1.43194	1.519304	1.084	1.048	109.848	111.298	109.905	107.395	112.9192	109.6242	26
1.43194	1.519304	1.084	1.108	109.848	111.298	109.905	107.395	112.9192	109.6242	27
1.43194	1.519304	1.084	1.128	109.848	111.298	109.905	107.395	112.9192	109.6242	28
1.43194	1.519304	1.084	1.078	109.848	111.298	109.905	107.395	112.9192	109.6242	29
1.43194	1.519304	1.084	1.078	109.848	111.298	109.905	107.395	112.9192	109.6242	30
1.43194	1.519304	1.114	1.078	109.848	111.298	109.905	107.395	112.9192	109.6242	31
1.43194	1.519304	1.134	1.078	109.848	111.298	109.905	107.395	112.9192	109.6242	32
1.45194	1.519304	1.084	1.078	109.848	111.298	109.905	107.395	112.9192	109.6242	33
1.45194	1.499304	1.084	1.078	109.848	111.298	109.905	107.395	112.9192	109.6242	34
1.41194	1.499304	1.084	1.078	109.848	111.298	109.905	107.395	112.9192	109.6242	35
1.43194	1.519304	1.084	1.078	109.848	111.298	109.905	107.395	112.9192	109.6242	36
1.41194	1.519304	1.084	1.078	109.848	111.298	109.905	107.395	112.9192	109.6242	37

Ag data

```
EN G76= -0.36684083EN FUNC= -0.36694007   ERROR=  0.00009924 K=  1
EN G76= -0.36661045EN FUNC= -0.36650075   ERROR= -0.00010970 K=  2
EN G76= -0.36116217EN FUNC= -0.36129783   ERROR=  0.00013566 K=  3
EN G76= -0.36732535EN FUNC= -0.36733058   ERROR=  0.00000473 K=  4
EN G76= -0.36603087EN FUNC= -0.36609822   ERROR=  0.00006735 K=  5
EN G76= -0.36772225EN FUNC= -0.36770396   ERROR= -0.00001829 K=  6
EN G76= -0.36643348EN FUNC= -0.36645999   ERROR=  0.00002651 K=  7
EN G76= -0.36615225EN FUNC= -0.36610197   ERROR= -0.00005027 K=  8
EN G76= -0.36729996EN FUNC= -0.36717415   ERROR= -0.00012581 K=  9
EN G76= -0.36372120EN FUNC= -0.36354561   ERROR= -0.00017559 K= 10
EN G76= -0.36240248EN FUNC= -0.36229914   ERROR= -0.00010335 K= 11
EN G76= -0.36587319EN FUNC= -0.36574084   ERROR= -0.00013235 K= 12
EN G76= -0.36830137EN FUNC= -0.36823286   ERROR= -0.00006850 K= 13
EN G76= -0.36472333EN FUNC= -0.36490385   ERROR=  0.00018052 K= 14
EN G76= -0.36971053EN FUNC= -0.36975887   ERROR=  0.00004833 K= 15
EN G76= -0.36974788EN FUNC= -0.36983216   ERROR=  0.00008429 K= 16
EN G76= -0.36648742EN FUNC= -0.36647650   ERROR= -0.00001092 K= 17
EN G76= -0.36709535EN FUNC= -0.36695926   ERROR= -0.00013610 K= 18
EN G76= -0.36976583EN FUNC= -0.36983634   ERROR=  0.00007052 K= 19
EN G76= -0.36918247EN FUNC= -0.36916256   ERROR= -0.00001991 K= 20
EN G76= -0.36827354EN FUNC= -0.36839297   ERROR=  0.00011943 K= 21
EN G76= -0.36976583EN FUNC= -0.36986984   ERROR=  0.00010402 K= 22
EN G76= -0.36913783EN FUNC= -0.36926905   ERROR=  0.00013122 K= 23
EN G76= -0.37129757EN FUNC= -0.37125772   ERROR= -0.00003985 K= 24
EN G76= -0.36385338EN FUNC= -0.36409008   ERROR=  0.00023669 K= 25
EN G76= -0.36874316EN FUNC= -0.36858380   ERROR= -0.00015936 K= 26
EN G76= -0.36892924EN FUNC= -0.36905164   ERROR=  0.00012240 K= 27
EN G76= -0.36501117EN FUNC= -0.36486982   ERROR= -0.00014135 K= 28
EN G76= -0.36407114EN FUNC= -0.36428346   ERROR=  0.00021232 K= 29
EN G76= -0.36878791EN FUNC= -0.36862786   ERROR= -0.00016005 K= 30
EN G76= -0.36911916EN FUNC= -0.36922348   ERROR=  0.00010432 K= 31
EN G76= -0.36544275EN FUNC= -0.36527616   ERROR= -0.00016659 K= 32
EN G76= -0.36984114EN FUNC= -0.36992069   ERROR=  0.00007955 K= 33
EN G76= -0.37027039EN FUNC= -0.37018364   ERROR= -0.00008675 K= 34
EN G76= -0.36954253EN FUNC= -0.36940946   ERROR= -0.00013304 K= 35
EN G76= -0.37073676EN FUNC= -0.37078071   ERROR=  0.00004395 K= 36
EN G76= -0.36996023EN FUNC= -0.36990631   ERROR= -0.00005392 K= 37
```

Ag_data

```
EN G76= -0.37037180EN FUNC= -0.37034669   ERROR= -0.00002511 K= 38
EN G76= -0.37042146EN FUNC= -0.37043699   ERROR=  0.00001553 K= 39
EN G76= -0.36955539EN FUNC= -0.36948731   ERROR= -0.00006808 K= 40
EN G76= -0.37013691EN FUNC= -0.37012530   ERROR= -0.00001161 K= 41
EN G76= -0.37114237EN FUNC= -0.37129451   ERROR=  0.00015214 K= 42
EN G76= -0.37106721EN FUNC= -0.37102073   ERROR= -0.00004648 K= 43
EN G76= -0.36994062EN FUNC= -0.36994561   ERROR=  0.00000499 K= 44
EN G76= -0.37076866EN FUNC= -0.37076696   ERROR= -0.00000170 K= 45
EN G76= -0.37134888EN FUNC= -0.37130496   ERROR= -0.00004393 K= 46
EN G76= -0.36800924EN FUNC= -0.36804017   ERROR=  0.00003093 K= 47
EN G76= -0.37020463EN FUNC= -0.37016633   ERROR= -0.00003830 K= 48
EN G76= -0.37038441EN FUNC= -0.37032642   ERROR= -0.00005799 K= 49
EN G76= -0.36924605EN FUNC= -0.36921624   ERROR= -0.00002981 K= 50
EN G76= -0.36958676EN FUNC= -0.36963394   ERROR=  0.00004718 K= 51
EN G76= -0.36942887EN FUNC= -0.36941284   ERROR= -0.00001603 K= 52
EN G76= -0.36847570EN FUNC= -0.36845401   ERROR= -0.00002169 K= 53
EN G76= -0.36978696EN FUNC= -0.36975551   ERROR= -0.00003145 K= 54
EN G76= -0.36824157EN FUNC= -0.36826044   ERROR=  0.00001886 K= 55
EN G76= -0.36919142EN FUNC= -0.36920131   ERROR=  0.00000989 K= 56

EN G76= -0.36958676EN FUNC= -0.36963394   ERROR=  0.00004718 K= 57
EN G76= -0.36910673EN FUNC= -0.36908853   ERROR= -0.00001820 K= 58
EN G76= -0.36972018EN FUNC= -0.36973307   ERROR=  0.00001289 K= 59
EN G76= -0.37085225EN FUNC= -0.37090607   ERROR=  0.00005382 K= 60
EN G76= -0.37113122EN FUNC= -0.37106804   ERROR= -0.00006317 K= 61
EN G76= -0.36988384EN FUNC= -0.36988624   ERROR=  0.00000240 K= 62
EN G76= -0.36952277EN FUNC= -0.36954367   ERROR=  0.00002091 K= 63
EN G76= -0.37047784EN FUNC= -0.37047610   ERROR= -0.00000173 K= 64
EN G76= -0.36929061EN FUNC= -0.36925388   ERROR= -0.00003674 K= 65
EN G76= -0.37052680EN FUNC= -0.37060581   ERROR=  0.00007700 K= 66
EN G76= -0.36919581EN FUNC= -0.36921019   ERROR=  0.00001438 K= 67
EN G76= -0.36958965EN FUNC= -0.36956496   ERROR= -0.00002469 K= 68
EN G76= -0.37030559EN FUNC= -0.37030802   ERROR=  0.00000243 K= 69
EN G76= -0.37051038EN FUNC= -0.37050269   ERROR= -0.00000768 K= 70
EN G76= -0.37138092EN FUNC= -0.37134118   ERROR= -0.00003974 K= 71
EN G76= -0.37031540EN FUNC= -0.37029366   ERROR= -0.00002182 K= 72
EN G76= -0.36990752EN FUNC= -0.36992961   ERROR=  0.00002208 K= 73
EN G76= -0.37000977EN FUNC= -0.36992420   ERROR= -0.00008557 K= 74
```

Ag data

CO	CC	CHa	CHe	HaCC	HeCC	HaCO	HeCO	COC	OCC ,	
1.45194	1.519304	1.084	1.078	109.848	111.298	109.905	107.395	113.9192	109.6242	38
1.45194	1.519304	1.084	1.078	109.848	111.298	109.905	107.395	111.9197	109.6242	39
1.41194	1.519304	1.084	1.078	109.848	111.298	109.905	107.395	111.9197	109.6242	40
1.41194	1.519304	1.084	1.078	109.848	111.298	109.905	107.395	113.9197	109.6242	41
1.43194	1.519304	1.084	1.078	109.848	111.298	109.905	107.395	113.9197	109.6242	42
1.43194	1.519304	1.084	1.078	109.848	111.298	109.905	107.395	111.9197	109.6242	43
1.43194	1.519304	1.084	1.078	109.848	111.298	109.905	107.395	109.9197	109.6242	44
1.43194	1.519304	1.084	1.078	109.848	111.298	109.905	107.395	115.9197	109.6242	45
1.4346	1.51628	1.08418	1.07769	109.848	111.298	109.905	107.395	113.50	109.62	46
1.4546	1.51628	1.08418	1.07769	109.848	111.298	109.905	107.395	113.50	111.62	47
1.4546	1.51628	1.08418	1.07769	109.848	111.298	109.905	107.395	113.50	109.62	48
1.4146	1.51628	1.08418	1.07769	109.848	111.298	109.905	107.395	113.50	109.62	49
1.4146	1.51628	1.08418	1.07769	109.848	111.298	109.905	107.395	113.50	107.62	50
1.4146	1.51628	1.08418	1.07769	109.848	111.298	107.905	107.395	113.50	109.62	51
1.4346	1.51628	1.08418	1.07769	109.848	111.298	109.905	107.395	113.50	111.62	52
1.4546	1.51628	1.08418	1.07769	109.848	111.298	111.905	107.395	113.50	109.62	53
1.4146	1.51628	1.08418	1.07769	109.848	111.298	109.905	105.395	113.50	109.62	54
1.4546	1.51628	1.08418	1.07769	109.848	111.298	109.905	109.395	113.50	109.62	55
1.4146	1.51628	1.08418	1.07769	109.848	111.298	111.905	107.395	113.50	109.62	56
1.4146	1.51628	1.08418	1.07769	109.848	111.298	107.905	107.395	113.50	109.62	57
1.4146	1.51628	1.08418	1.07769	109.848	111.298	109.905	109.395	113.50	109.62	58
1.4346	1.51628	1.08418	1.07769	109.848	111.298	109.905	109.395	113.50	109.62	59
1.4346	1.51628	1.08418	1.07769	109.848	111.298	107.905	107.395	113.50	109.62	60
1.4346	1.51628	1.08418	1.07769	109.848	111.298	109.905	105.395	113.50	109.62	61
1.4346	1.51628	1.08418	1.07769	109.848	111.298	111.905	107.395	113.50	109.62	62
1.4146	1.51628	1.08418	1.07769	109.848	109.298	109.905	107.395	113.50	109.62	63
1.4346	1.51628	1.08418	1.07769	109.848	113.298	109.905	107.395	113.50	109.62	64
1.4546	1.51628	1.08418	1.07769	109.848	113.298	109.905	107.395	113.50	109.62	65
1.4346	1.51628	1.08418	1.07769	109.848	109.298	109.905	107.395	113.50	109.62	66
1.4546	1.51628	1.08418	1.07769	111.848	111.298	109.905	107.395	113.50	109.62	67
1.4146	1.51628	1.08418	1.07769	107.848	111.298	109.905	107.395	113.50	109.62	68
1.4346	1.51628	1.08418	1.07769	111.848	111.298	109.905	107.395	113.50	109.62	69
1.4346	1.51628	1.08418	1.07769	107.848	111.298	109.905	107.395	113.50	109.62	70
1.4342	1.51628	1.08418	1.07769	109.736	111.2697	109.421	106.63	113.50	109.193	71
1.4342	1.51628	1.10418	1.07769	109.736	111.2697	109.421	106.63	113.50	109.193	72
1.4342	1.53628	1.10418	1.07769	109.736	111.2697	109.421	106.63	113.50	109.193	73
1.4342	1.53628	1.06418	1.07769	109.736	111.2697	109.421	106.63	113.50	109.193	74

Ag data

```
EN G76= -0.3706603?EN FUNC= -0.37033933   ERROR= -0.00002100 K= 75
EN G76= -0.3698706?EN FUNC= -0.36992608   ERROR=  0.00005547 K= 76
EN G76= -0.36886337EN FUNC= -0.36884364   ERROR= -0.00001973 K= 77
EN G76= -0.3697609?EN FUNC= -0.36980747   ERROR=  0.00004657 K= 78
EN G76= -0.36901250EN FUNC= -0.36909387   ERROR=  0.00008136 K= 79
EN G76= -0.36938430EN FUNC= -0.36941239   ERROR=  0.00002809 K= 80
EN G76= -0.37073103EN FUNC= -0.37074476   ERROR=  0.00001373 K= 81
EN G76= -0.3707335?EN FUNC= -0.37062877   ERROR= -0.00010472 K= 82
EN G76= -0.37055594EN FUNC= -0.37044019   ERROR= -0.00011574 K= 83
EN G76= -0.37012905EN FUNC= -0.37011070   ERROR= -0.00001834 K= 84
EN G76= -0.3694738?EN FUNC= -0.36947657   ERROR=  0.00000274 K= 85
EN G76= -0.36981262EN FUNC= -0.36978909   ERROR= -0.00002353 K= 86
EN G76= -0.36993914EN FUNC= -0.37002050   ERROR=  0.00008136 K= 87
EN G76= -0.3709990?EN FUNC= -0.37096337   ERROR= -0.00003563 K= 88
EN G76= -0.36981216EN FUNC= -0.36970596   ERROR= -0.00010621 K= 89
EN G76= -0.36652005EN FUNC= -0.36653935   ERROR=  0.00001931 K= 90
EN G76= -0.3706139?EN FUNC= -0.3706146?   ERROR= -0.00000434 K= 91
EN G76= -0.37013631EN FUNC= -0.37007058   ERROR= -0.00006573 K= 92
EN G76= -0.36853295EN FUNC= -0.36856282   ERROR=  0.00002987 K= 93
EN G76= -0.3708419?EN FUNC= -0.37083433   ERROR= -0.00000763 K= 94
EN G76= -0.36969913EN FUNC= -0.36971060   ERROR=  0.00001147 K= 95
EN G76= -0.37012603EN FUNC= -0.37008243   ERROR= -0.00004365 K= 96
EN G76= -0.3698969?EN FUNC= -0.36985261   ERROR= -0.00004437 K= 97
EN G76= -0.37024887EN FUNC= -0.37011692   ERROR= -0.00013194 K= 98
EN G76= -0.36965958EN FUNC= -0.36962037   ERROR= -0.00003921 K= 99
EN G76= -0.37051672EN FUNC= -0.37050148   ERROR= -0.00001523 K=100
EN G76= -0.3698706?EN FUNC= -0.36992608   ERROR=  0.00005547 K=101
EN G76= -0.3698657?EN FUNC= -0.37001426   ERROR=  0.00014847 K=102
EN G76= -0.37011568EN FUNC= -0.37019678   ERROR=  0.00008110 K=103
EN G76= -0.37018446EN FUNC= -0.37040510   ERROR=  0.00022064 K=104
EN G76= -0.36991892EN FUNC= -0.36996269   ERROR=  0.00004377 K=105
EN G76= -0.3698486?EN FUNC= -0.36986509   ERROR=  0.00001640 K=106
EN G76= -0.3697609?EN FUNC= -0.36980747   ERROR=  0.00004657 K=107
EN G76= -0.3697994?EN FUNC= -0.36974691   ERROR= -0.00005257 K=108
EN G76= -0.37000611EN FUNC= -0.37002049   ERROR=  0.00001438 K=109
EN G76= -0.3693283?EN FUNC= -0.36971859   ERROR= -0.00010979 K=110
EN G76= -0.37041405EN FUNC= -0.37030660   ERROR= -0.00010745 K=111
EN G76= -0.3699691?EN FUNC= -0.36984552   ERROR= -0.00012362 K=112
EN G76= -0.36999837EN FUNC= -0.36990597   ERROR= -0.00009240 K=113
EN G76= -0.3695219?EN FUNC= -0.3694911?   ERROR= -0.00003075 K=114
EN G76= -0.3703028?EN FUNC= -0.37023548   ERROR= -0.00006735 K=115
```

Ag data

CO	CC	CHa	CHe	HaCC	HeCC	HaCO	HeCO	COC	OCC	
1.4342	1.49628	1.08418	1.07769	109.736	111.2697	109.421	106.63	113.50	109.193	75
1.4342	1.51628	1.10418	1.07769	109.736	111.2697	111.421	106.63	113.50	109.193	76
1.4342	1.51628	1.10418	1.07769	109.736	111.2697	107.421	106.63	113.50	109.193	77
1.4342	1.51628	1.08418	1.09769	109.736	111.2697	109.421	108.63	113.50	109.193	78
1.4342	1.51628	1.08418	1.09769	109.736	111.2697	109.421	104.63	113.50	109.193	79
1.4542	1.51628	1.10418	1.07769	109.736	111.2697	109.421	106.63	113.50	109.193	80
1.4342	1.53628	1.08418	1.07769	109.736	111.2697	109.421	106.63	115.50	109.193	81
1.4342	1.53628	1.08418	1.07769	109.736	111.2697	109.421	108.63	113.50	109.193	82
1.4342	1.53628	1.08418	1.07769	109.736	111.2697	111.421	106.63	113.50	109.193	83
1.4342	1.53628	1.08418	1.07769	109.736	111.2697	109.421	106.63	113.50	111.193	84
1.4142	1.49628	1.08418	1.07769	109.736	111.2697	109.421	106.63	113.50	109.193	85
1.4142	1.53628	1.08418	1.07769	109.736	111.2697	109.421	106.63	113.50	109.193	86
1.4542	1.53628	1.08418	1.07769	109.736	111.2697	109.421	106.63	113.50	109.193	87
1.4342	1.53628	1.08418	1.07769	109.736	111.2697	109.421	106.63	113.50	109.193	88
1.4342	1.55628	1.08418	1.07769	109.736	111.2697	109.421	106.63	113.50	109.193	89
1.4342	1.51628	1.08418	1.07769	105.736	111.2697	109.421	106.63	113.5	109.193	90
1.4342	1.51628	1.08418	1.07769	109.736	114.2697	109.421	106.63	113.5	109.193	91
1.4342	1.51628	1.08418	1.07769	109.736	111.2697	109.421	104.63	113.5	109.193	92
1.4342	1.51628	1.08418	1.07769	109.736	111.2697	113.421	106.63	113.5	109.193	93
1.43474	1.52318	1.06205	1.07977	108.8174	111.7393	110.5552	106.7277	112.3297	110.0470	94
1.4342	1.51628	1.08418	1.07769	109.736	111.2697	111.421	108.63	113.50	109.193	95
1.4342	1.51628	1.08418	1.07769	109.736	113.2697	111.421	106.63	113.50	109.193	96
1.4342	1.51628	1.08418	1.07769	109.736	113.2697	109.421	108.63	113.50	109.193	97
1.4342	1.51628	1.08418	1.07769	111.736	113.2697	109.421	106.63	113.50	109.193	98
1.4542	1.51628	1.08418	1.07769	109.736	111.2697	109.421	108.63	113.50	109.193	99
1.4342	1.53628	1.08418	1.07769	111.736	111.2697	109.421	106.63	113.50	109.193	100
1.4342	1.51628	1.10418	1.07769	109.736	111.2697	111.421	106.63	113.50	109.193	101
1.4342	1.51628	1.10418	1.07769	109.736	111.2697	109.421	108.63	113.50	109.193	102
1.4342	1.51628	1.08418	1.09769	111.736	111.2697	109.421	106.63	113.50	109.193	103
1.4342	1.51628	1.08418	1.09769	109.736	113.2697	109.421	106.63	113.50	109.193	104
1.4342	1.51628	1.08418	1.09769	109.736	111.2697	111.421	106.63	113.50	109.193	105
1.4342	1.51628	1.08418	1.07769	111.736	111.2697	109.421	108.63	113.50	109.193	106
1.4342	1.51628	1.08418	1.09769	109.736	111.2697	109.421	108.63	113.50	109.193	107
1.4342	1.51628	1.08418	1.07769	111.736	111.2697	111.421	106.63	113.50	109.193	108
1.4342	1.51628	1.10418	1.07769	111.736	111.2697	109.421	106.63	113.50	109.193	108
1.4542	1.51628	1.08418	1.07769	109.736	111.2697	111.421	106.63	113.50	109.193	110
1.4542	1.51628	1.08418	1.07769	109.736	113.2697	109.421	106.63	113.50	109.193	111
1.4542	1.51628	1.08418	1.07769	109.736	111.2697	109.421	106.63	115.50	109.193	112
1.4342	1.51628	1.08418	1.07769	109.736	111.2697	109.421	106.63	115.50	111.193	113
1.4542	1.51628	1.08418	1.07769	109.736	111.2697	109.421	106.63	113.50	111.193	114
1.4542	1.51628	1.08418	1.07769	111.736	111.2697	109.421	106.63	113.50	109.193	115

Ag data

CO	CC	CHa	CHe	HaCC	HeCC	HaCO	HeCO	COC	OCC	
-										
1.4342	1.51628	1.10418	1.07769	109.736	111.2697	109.421	106.63	115.50	109.193	116
1.4342	1.51628	1.08418	1.09769	109.736	111.2697	109.421	106.63	115.50	109.193	117
1.4342	1.51628	1.10418	1.07769	109.736	111.2697	109.421	106.63	113.50	111.193	118
1.4342	1.51628	1.08418	1.09769	109.736	111.2697	109.421	106.63	113.50	111.193	119
1.4342	1.51628	1.08418	1.07769	111.736	111.2697	109.421	106.63	115.50	109.193	120
1.4342	1.51628	1.08418	1.07769	109.736	113.2697	109.421	106.63	115.50	109.193	121
1.4342	1.51628	1.08418	1.07769	109.736	111.2697	111.421	106.63	115.50	109.193	122
1.4342	1.51628	1.08418	1.07769	109.736	111.2697	109.421	108.63	115.50	109.193	123
1.4342	1.51628	1.08418	1.07769	111.736	111.2697	109.421	106.63	113.50	111.193	124
1.4342	1.51628	1.08418	1.07769	109.736	113.2697	109.421	106.63	113.50	111.193	125
1.4342	1.51628	1.08418	1.07769	109.736	111.2697	111.421	106.63	113.50	111.193	126
1.4342	1.51628	1.08418	1.07769	109.736	111.2697	109.421	108.63	113.50	111.193	127
1.4642	1.51628	1.08418	1.10769	109.736	111.2697	109.421	106.63	113.50	109.193	128
1.4342	1.54628	1.08418	1.10769	109.736	111.2697	109.421	106.63	113.50	109.193	129
1.4642	1.51628	1.11418	1.07769	109.736	111.2697	109.421	106.63	113.50	109.193	130
1.4342	1.54628	1.11418	1.07769	109.736	111.2697	109.421	106.63	113.50	109.193	131

Ag data

```
EN G76= -0.37001769EN FUNC= -0.37006832   ERROR=  0.00005113 K=116
EN G76= -0.36993815EN FUNC= -0.36998223   ERROR=  0.00004408 K=117

EN G76= -0.36970174EN FUNC= -0.36985110   ERROR=  0.00014936 K=118
EN G76= -0.36957393EN FUNC= -0.36974332   ERROR=  0.00016938 K=119
EN G76= -0.37079531EN FUNC= -0.37071126   ERROR= -0.00008456 K=120
EN G76= -0.37104403EN FUNC= -0.37090077   ERROR= -0.00014325 K=121
EN G76= -0.37056987EN FUNC= -0.37051116   ERROR= -0.00005871 K=122
EN G76= -0.37044523EN FUNC= -0.37046055   ERROR=  0.00001530 K=123
EN G76= -0.36952036EN FUNC= -0.36959594   ERROR=  0.00007559 K=124
EN G76= -0.36951403EN FUNC= -0.36967946   ERROR=  0.00016538 K=125
EN G76= -0.36914657EN FUNC= -0.36914145   ERROR= -0.00000513 K=126
EN G76= -0.36935618EN FUNC= -0.36938363   ERROR=  0.00002745 K=127
EN G76= -0.36693542EN FUNC= -0.36697852   ERROR=  0.00004310 K=128
EN G76= -0.36804303EN FUNC= -0.36820179   ERROR=  0.00015876 K=129
EN G76= -0.36687386EN FUNC= -0.36685221   ERROR= -0.00002165 K=130
EN G76= -0.36813899EN FUNC= -0.36812694   ERROR= -0.00001206 K=131
```

Au data

CO	CC	CHa	CHe	HaCC	HeCC	HaCO	HeCO	COC	OCC	
1.4342	1.51628	1.08418	1.07769	109.736	111.2697	109.421	106.63	113.50	109.193	1
1.4342	1.51628	1.10418	1.09769	109.736	111.2697	109.421	106.63	113.50	109.193	2
1.4342	1.51628	1.08418	1.09769	109.736	111.2697	109.421	106.63	113.50	109.193	3
1.4342	1.51628	1.08481	1.07769	109.736	111.2697	109.421	106.63	113.50	109.193	4
1.4342	1.51628	1.10418	1.05769	109.736	111.2697	109.421	106.63	113.50	109.193	5
1.4342	1.51628	1.03418	1.07769	109.736	111.2697	111.421	108.63	113.50	109.193	6
1.4342	1.51628	1.08418	1.07769	109.736	111.2697	109.421	108.63	113.50	109.193	7
1.4342	1.51628	1.08418	1.07769	109.736	111.2697	107.421	106.63	113.50	109.193	8
1.4342	1.51628	1.08418	1.07769	109.736	111.2697	111.421	104.63	113.50	109.193	9
1.4342	1.51628	1.08418	1.07769	107.736	111.2697	109.421	106.63	113.50	109.193	10
1.4342	1.51628	1.08418	1.07769	111.736	113.2697	109.421	106.63	113.50	109.193	11
1.4342	1.51628	1.08418	1.07769	109.736	113.2697	109.421	106.63	113.50	109.193	12
1.4342	1.51628	1.08418	1.07769	111.736	109.2697	109.421	106.63	113.50	109.193	13
1.4442	1.51628	1.08418	1.07769	109.736	111.2697	109.421	106.63	113.50	109.193	14
1.4542	1.51628	1.08418	1.07769	109.736	111.2697	109.421	106.63	113.50	109.193	15
1.4642	1.51628	1.08418	1.07769	109.736	111.2697	109.421	106.63	113.50	109.193	16
1.4542	1.51628	1.08418	1.07769	111.736	111.2697	109.421	106.63	113.50	109.193	17
1.4542	1.51628	1.08418	1.07769	107.736	111.2697	109.421	106.63	113.50	109.193	18
1.4542	1.51628	1.08418	1.07769	109.736	113.2697	109.421	106.63	113.50	109.193	19
1.4542	1.51628	1.08418	1.07769	109.736	109.2697	109.421	106.63	113.50	109.193	20
1.4542	1.51628	1.08418	1.07769	109.736	109.2697	111.421	106.63	113.500	109.193	21
1.4542	1.51628	1.08418	1.07769	109.736	111.2697	107.421	106.63	113.50	109.193	22
1.4542	1.51628	1.08418	1.07769	109.736	111.2697	109.421	108.63	113.50	109.193	23
1.4542	1.51628	1.08418	1.07769	109.736	111.2697	109.421	104.63	113.50	109.193	24
1.4342	1.52628	1.08418	1.07769	109.736	111.2697	109.421	106.63	113.50	109.193	25
1.4342	1.53628	1.08418	1.07769	109.736	111.2697	109.421	106.63	113.50	109.193	26
1.4342	1.54628	1.08418	1.07769	109.736	111.2697	109.421	106.63	113.50	109.193	27
1.4342	1.53628	1.10418	1.07769	109.736	111.2697	109.421	106.63	113.50	109.193	28
1.4342	1.53628	1.08413	1.09769	109.736	111.2697	109.421	106.63	113.50	109.193	29
1.4542	1.51628	1.10418	1.07769	109.736	111.2697	109.421	106.63	113.50	109.193	30
1.4342	1.53628	1.08418	1.07769	111.736	111.2697	109.421	106.63	113.50	109.193	31
1.4342	1.53628	1.08413	1.07769	109.736	113.2697	109.421	106.63	113.50	109.193	32
1.4342	1.53628	1.08418	1.07769	109.736	111.2697	111.421	106.63	113.50	109.193	33
1.4342	1.53628	1.08418	1.07769	109.736	111.2697	109.421	108.63	113.50	109.193	34
1.4342	1.51628	1.10418	1.07769	109.736	111.2697	111.421	106.63	113.50	109.193	35
1.4342	1.51628	1.10418	1.07769	109.736	111.2697	109.421	108.63	113.50	109.193	36
1.4342	1.51628	1.10418	1.07769	109.736	113.2697	109.421	106.63	113.50	109.193	37
1.4342	1.51628	1.10418	1.07769	111.736	111.2697	109.421	106.63	113.50	109.193	38
1.4342	1.51628	1.08418	1.09769	109.736	111.2697	109.421	108.63	113.50	109.193	39
1.4342	1.51628	1.08418	1.09769	109.736	113.2697	109.421	106.63	113.50	109.193	40

Au data

```
EN G76= -0.37138092EN FUNC= -0.37132312   ERROR= -0.00005780 K=  1
EN G76= -0.36923034EN FUNC= -0.36918056   ERROR= -0.00004978 K=  2
EN G76= -0.37028798EN FUNC= -0.37026194   ERROR= -0.00002604 K=  3
EN G76= -0.37034513EN FUNC= -0.37032947   ERROR= -0.00001566 K=  4
EN G76= -0.36927445EN FUNC= -0.36922464   ERROR= -0.00004981 K=  5

EN G76= -0.36893529EN FUNC= -0.36892712   ERROR= -0.00000817 K=  6
EN G76= -0.37052362EN FUNC= -0.37045512   ERROR= -0.00006850 K=  7
EN G76= -0.37042102EN FUNC= -0.37042312   ERROR=  0.00000210 K=  8
EN G76= -0.37019140EN FUNC= -0.37018312   ERROR= -0.00000828 K=  9
EN G76= -0.37047270EN FUNC= -0.37045112   ERROR= -0.00002158 K= 10
EN G76= -0.36895692EN FUNC= -0.36890112   ERROR= -0.00005580 K= 11
EN G76= -0.37057497EN FUNC= -0.37048112   ERROR= -0.00009385 K= 12
EN G76= -0.37037597EN FUNC= -0.37031712   ERROR= -0.00005885 K= 13
EN G76= -0.37112809EN FUNC= -0.37106882   ERROR= -0.00005926 K= 14
EN G76= -0.37036954EN FUNC= -0.37030594   ERROR= -0.00006360 K= 15
EN G76= -0.36910126EN FUNC= -0.36903446   ERROR= -0.00006679 K= 16
EN G76= -0.36958743EN FUNC= -0.36956010   ERROR= -0.00002733 K= 17
EN G76= -0.36933558EN FUNC= -0.36930778   ERROR= -0.00002780 K= 18
EN G76= -0.36909235EN FUNC= -0.36913394   ERROR=  0.00004159 K= 19
EN G76= -0.36972737EN FUNC= -0.36979394   ERROR=  0.00006657 K= 20
EN G76= -0.36965761EN FUNC= -0.36958994   ERROR= -0.00006767 K= 21
EN G76= -0.36946952EN FUNC= -0.36940594   ERROR= -0.00006358 K= 22
EN G76= -0.36931494EN FUNC= -0.36924074   ERROR= -0.00007420 K= 23
EN G76= -0.36970922EN FUNC= -0.36963514   ERROR= -0.00007408 K= 24
EN G76= -0.37126896EN FUNC= -0.37121496   ERROR= -0.00005401 K= 25
EN G76= -0.37093834EN FUNC= -0.37089048   ERROR= -0.00004786 K= 26
EN G76= -0.37038420EN FUNC= -0.37034968   ERROR= -0.00003452 K= 27
EN G76= -0.36984750EN FUNC= -0.36980298   ERROR= -0.00004452 K= 28
EN G76= -0.36980676EN FUNC= -0.36976746   ERROR= -0.00003930 K= 29
EN G76= -0.36922802EN FUNC= -0.36918448   ERROR= -0.00004354 K= 30
EN G76= -0.36997674EN FUNC= -0.36993608   ERROR= -0.00004066 K= 31
EN G76= -0.37016013EN FUNC= -0.37011928   ERROR= -0.00004085 K= 32
EN G76= -0.37014436EN FUNC= -0.37010328   ERROR= -0.00004110 K= 33
EN G76= -0.37020122EN FUNC= -0.37016208   ERROR= -0.00003914 K= 34
EN G76= -0.36941554EN FUNC= -0.36937378   ERROR= -0.00004176 K= 35
EN G76= -0.36959306EN FUNC= -0.36955298   ERROR= -0.00004008 K= 36
EN G76= -0.36965977EN FUNC= -0.36961818   ERROR= -0.00004159 K= 37
EN G76= -0.36940133EN FUNC= -0.36935970   ERROR= -0.00004163 K= 38
EN G76= -0.36946613EN FUNC= -0.36942330   ERROR= -0.00004283 K= 39
EN G76= -0.36947617EN FUNC= -0.36943514   ERROR= -0.00004103 K= 40
```

Au data

CO	CC	CHa	CHe	HaCC	HeCC	HaCO	HeCO	COC	OCC	
1.4342	1.51628	1.08418	1.09769	111.736	111.2697	109.421	106.63	113.50	109.193	41
1.4342	1.51628	1.08418	1.09769	109.736	111.2697	111.421	106.63	113.50	109.193	42
1.4342	1.51628	1.08418	1.07769	109.736	113.2697	109.421	108.63	113.50	109.193	43
1.4342	1.51628	1.08418	1.07769	111.736	111.2697	109.421	108.63	113.50	109.193	44
1.4342	1.51628	1.08418	1.07769	109.736	113.2697	111.421	106.63	113.50	109.193	45
1.4342	1.51628	1.08418	1.07769	111.736	111.2697	111.421	106.63	113.50	109.193	46
1.4542	1.53628	1.08418	1.07769	109.736	111.2697	109.421	106.63	113.50	109.193	47

```
EN G76= -0.36949592EN FUNC= -0.36945434   ERROR= -0.00004158 K= 41
EN G76= -0.36941581EN FUNC= -0.36937474   ERROR= -0.00004107 K= 42
EN G76= -0.36895134EN FUNC= -0.36890912   ERROR= -0.00004222 K= 43
EN G76= -0.36894928EN FUNC= -0.36890312   ERROR= -0.00004616 K= 44
EN G76= -0.36896889EN FUNC= -0.36888512   ERROR= -0.00008377 K= 45
EN G76= -0.36871892EN FUNC= -0.36868312   ERROR= -0.00003580 K= 46
EN G76= -0.36988821EN FUNC= -0.36984518   ERROR= -0.00004303 K= 47
```

Bu data

CO	CC	CHa	CHe	HaCC	HeCC	HaCO	HeCO	'COC	OCC	
1.4342	1.51628	1.08418	1.07769	109.736	111.2697	109.421	106.63	113.50	109.193	1
1.4342	1.51628	1.10418	1.09769	109.736	111.2697	109.421	106.63	113.50	109.193	2
1.4342	1.51628	1.08418	1.09769	109.736	111.2697	109.421	106.63	113.50	109.193	3
1.4342	1.51628	1.06418	1.07769	109.736	111.2697	109.421	106.63	113.50	109.193	4
1.4342	1.51628	1.10418	1.05769	109.736	111.2697	109.421	106.63	113.50	109.193	5
1.4342	1.51628	1.08418	1.07769	109.736	111.2697	111.421	108.63	113.50	109.193	6
1.4342	1.51628	1.08418	1.07769	109.736	111.2697	111.421	104.63	113.50	109.193	7
1.4342	1.51628	1.08418	1.07769	109.736	111.2697	109.421	108.63	113.50	109.193	8
1.4342	1.51628	1.08418	1.07769	109.736	111.2697	107.421	106.63	113.50	109.193	9
1.4342	1.51628	1.08418	1.07769	111.736	113.2697	109.421	106.63	113.50	109.193	10
1.4342	1.51628	1.08418	1.07769	107.736	111.2697	109.421	106.63	113.50	109.193	11
1.4342	1.51628	1.08418	1.07769	109.736	113.2697	109.421	106.63	113.50	109.193	12
1.4342	1.51628	1.08418	1.07769	111.736	109.2697	109.421	106.63	113.50	109.193	13
1.4442	1.51628	1.08418	1.07769	109.736	111.2697	109.421	106.63	113.50	109.193	14
1.4542	1.51628	1.08418	1.07769	109.736	111.2697	109.421	106.63	113.50	109.193	15
1.4642	1.51628	1.08418	1.07769	109.736	111.2697	109.421	106.63	113.50	109.193	16
1.4542	1.51628	1.08418	1.07769	111.736	111.2697	109.421	106.63	113.50	109.193	17
1.4542	1.51628	1.08418	1.07769	107.736	111.2697	109.421	106.63	113.50	109.193	18
1.4542	1.51628	1.08418	1.07769	109.736	113.2697	109.421	106.63	113.50	109.193	19
1.4542	1.51628	1.08418	1.07769	109.736	109.2697	109.421	106.63	113.50	109.193	20
1.4542	1.51628	1.08418	1.07769	109.736	111.2697	111.421	106.63	113.50	109.193	21
1.4542	1.51628	1.08418	1.07769	109.736	111.2697	107.421	106.63	113.50	109.193	22
1.4542	1.51628	1.08418	1.07769	109.736	111.2697	109.421	108.63	113.50	109.193	23
1.4542	1.51628	1.08418	1.07769	109.736	111.2697	109.421	104.63	113.50	109.193	24
1.4542	1.51628	1.10418	1.07769	109.736	111.2697	109.421	106.63	113.50	109.193	25
1.4542	1.51628	1.06418	1.07769	109.736	111.2697	109.421	106.63	113.50	109.193	26
1.4542	1.51628	1.08418	1.09769	109.736	111.2697	109.421	106.63	113.50	109.193	27
1.4542	1.51628	1.08418	1.05769	109.736	111.2697	109.421	106.63	113.50	109.193	28
1.4342	1.51628	1.08418	1.07769	111.736	111.2697	111.421	106.63	113.50	109.193	29
1.4342	1.51628	1.08418	1.07769	111.736	111.2697	107.421	106.63	113.50	109.193	30
1.4342	1.51628	1.08418	1.07769	109.736	113.2697	109.421	108.63	113.50	109.193	31
1.4342	1.51628	1.08418	1.07769	109.736	113.2697	109.421	104.63	113.50	109.193	32
1.4342	1.51628	1.08418	1.07769	111.736	111.2697	109.421	108.63	113.50	109.193	33
1.4342	1.51628	1.08418	1.07769	111.736	111.2697	109.421	104.63	113.50	109.193	34
1.4342	1.51628	1.08418	1.07769	109.736	113.2697	111.421	106.63	113.50	109.193	35
1.4342	1.51628	1.08418	1.07769	109.736	113.2697	107.421	106.63	113.50	109.193	36
1.4342	1.51628	1.08418	1.07769	109.736	111.2697	109.421	106.63	115.50	109.193	
1.4342	1.51628	1.08418	1.07769	109.736	111.2697	109.421	106.63	114.50	109.196	37
1.4342	1.51628	1.08418	1.07769	109.736	111.2697	109.421	106.63	116.50	109.193	38
1.4542	1.51628	1.08418	1.07769	109.736	111.2697	109.421	106.63	115.50	109.193	39

Bu data

```
EN G76= -0.37138092EN FUNC= -0.37133693   ERROR= -0.00004399 K=  1
EN G76= -0.36923632EN FUNC= -0.36922031   ERROR= -0.00001601 K=  2
EN G76= -0.37029030EN FUNC= -0.37026197   ERROR= -0.00002833 K=  3
EN G76= -0.37033688EN FUNC= -0.37030547   ERROR= -0.00003141 K=  4
EN G76= -0.36925674EN FUNC= -0.36924071   ERROR= -0.00001603 K=  5
EN G76= -0.36889809EN FUNC= -0.36895093   ERROR=  0.00005284 K=  6
EN G76= -0.37022551EN FUNC= -0.37027893   ERROR=  0.00005342 K=  7
EN G76= -0.37048758EN FUNC= -0.37045893   ERROR= -0.00002865 K=  8
EN G76= -0.37045551EN FUNC= -0.37049293   ERROR=  0.00003742 K=  9
EN G76= -0.36896867EN FUNC= -0.36891493   ERROR= -0.00005374 K= 10
EN G76= -0.37060603EN FUNC= -0.37056493   ERROR= -0.00004110 K= 11
EN G76= -0.37054439EN FUNC= -0.37048693   ERROR= -0.00005746 K= 12
EN G76= -0.37056953EN FUNC= -0.37051493   ERROR= -0.00005460 K= 13
EN G76= -0.37110586EN FUNC= -0.37106543   ERROR= -0.00004043 K= 14
EN G76= -0.37027453EN FUNC= -0.37025095   ERROR= -0.00002358 K= 15
EN G76= -0.36888810EN FUNC= -0.36889348   ERROR=  0.00000537 K= 16
EN G76= -0.36944312EN FUNC= -0.36942295   ERROR= -0.00002017 K= 17
EN G76= -0.36955544EN FUNC= -0.36953495   ERROR= -0.00002049 K= 18
EN G76= -0.36901971EN FUNC= -0.36907255   ERROR=  0.00005284 K= 19
EN G76= -0.36967658EN FUNC= -0.36972935   ERROR=  0.00005277 K= 20
EN G76= -0.36937074EN FUNC= -0.36933895   ERROR= -0.00003179 K= 21
EN G76= -0.36950711EN FUNC= -0.36947495   ERROR= -0.00003216 K= 22
EN G76= -0.36902270EN FUNC= -0.36901415   ERROR= -0.00000855 K= 23
EN G76= -0.36974047EN FUNC= -0.36973175   ERROR= -0.00000872 K= 24
EN G76= -0.36913447EN FUNC= -0.36912349   ERROR= -0.00001098 K= 25
EN G76= -0.36932799EN FUNC= -0.36931549   ERROR= -0.00001251 K= 26
EN G76= -0.36915093EN FUNC= -0.36914247   ERROR= -0.00000846 K= 27
EN G76= -0.36921826EN FUNC= -0.36920951   ERROR= -0.00000875 K= 28
EN G76= -0.36889344EN FUNC= -0.36894093   ERROR=  0.00004249 K= 29
EN G76= -0.37045639EN FUNC= -0.37050093   ERROR=  0.00004454 K= 30
EN G76= -0.36890140EN FUNC= -0.36886093   ERROR= -0.00004046 K= 31
EN G76= -0.37039477EN FUNC= -0.37035693   ERROR= -0.00003784 K= 32
EN G76= -0.36903583EN FUNC= -0.36901093   ERROR= -0.00002490 K= 33
EN G76= -0.37038926EN FUNC= -0.37036293   ERROR= -0.00002633 K= 34
EN G76= -0.36893774EN FUNC= -0.36896293   ERROR=  0.00002519 K= 35
EN G76= -0.37029998EN FUNC= -0.37032293   ERROR=  0.00002295 K= 36
EN G76= -0.37087907EN FUNC= -0.37084693   ERROR= -0.00003274 K= 37
EN G76= -0.37125781EN FUNC= -0.37123627   ERROR= -0.00002155 K= 38
EN G76= -0.37024801EN FUNC= -0.37023443   ERROR= -0.00001358 K= 39
EN G76= -0.36924641EN FUNC= -0.36922695   ERROR= -0.00001946 K= 40
```

Bu data

```
EN G76= -0.36958032EN FUNC= -0.36954043   ERROR= -0.00003989 K= 41
EN G76= -0.36961497EN FUNC= -0.36959347   ERROR= -0.00002150 K= 42
EN G76= -0.36941433EN FUNC= -0.36942331   ERROR=  0.00000898 K= 43
EN G76= -0.36952665EN FUNC= -0.36950627   ERROR= -0.00002038 K= 44
EN G76= -0.36962782EN FUNC= -0.36965397   ERROR=  0.00002615 K= 45
EN G76= -0.36946653EN FUNC= -0.36944477   ERROR= -0.00002176 K= 46
EN G76= -0.36946487EN FUNC= -0.36947317   ERROR=  0.00000830 K= 47
EN G76= -0.36942295EN FUNC= -0.36936877   ERROR= -0.00005418 K= 48
EN G76= -0.36932500EN FUNC= -0.36930547   ERROR= -0.00001953 K= 49
EN G76= -0.36976803EN FUNC= -0.36974437   ERROR= -0.00002366 K= 50
EN G76= -0.37001028EN FUNC= -0.36999093   ERROR= -0.00001935 K= 51
EN G76= -0.37006149EN FUNC= -0.36999693   ERROR= -0.00006456 K= 52
EN G76= -0.36994150EN FUNC= -0.36996293   ERROR=  0.00002135 K= 53
EN G76= -0.36984621EN FUNC= -0.36982493   ERROR= -0.00002128 K= 54
EN G76= -0.37104443EN FUNC= -0.37099993   ERROR= -0.00004450 K= 55
EN G76= -0.37003629EN FUNC= -0.36998893   ERROR= -0.00004736 K= 56
EN G76= -0.36834993EN FUNC= -0.36830393   ERROR= -0.00004600 K= 57
EN G76= -0.36825968EN FUNC= -0.36825293   ERROR= -0.00000675 K= 58
EN G76= -0.36826537EN FUNC= -0.36828093   ERROR=  0.00001556 K= 59
EN G76= -0.36825968EN FUNC= -0.36825293   ERROR= -0.00000675 K= 60
EN G76= -0.36902530EN FUNC= -0.36903467   ERROR=  0.00000937 K= 61
EN G76= -0.36908813EN FUNC= -0.36907997   ERROR= -0.00000816 K= 62
EN G76= -0.36831362EN FUNC= -0.36833335   ERROR=  0.00001973 K= 63
EN G76= -0.36825968EN FUNC= -0.36825293   ERROR= -0.00000675 K= 64
EN G76= -0.36864439EN FUNC= -0.36860693   ERROR= -0.00003796 K= 65
EN G76= -0.36826537EN FUNC= -0.36828093   ERROR=  0.00001556 K= 66
```

Bu data

CO	CC	CHa	CHe	HaCC	HeCC	HaCO	HeCO	COC	OCC	
1.4342	1.51628	1.10418	1.07769	111.736	111.2697	109.421	106.63	113.50	109.193	40
1.4342	1.51628	1.10418	1.07769	109.736	113.2697	109.421	106.63	113.50	109.193	41
1.4342	1.51628	1.10418	1.07769	109.736	111.2697	111.421	106.63	113.50	109.193	42
1.4342	1.51628	1.10418	1.07769	109.736	111.2697	109.421	108.63	113.50	109.193	43
1.4342	1.51628	1.08418	1.09769	111.736	111.2697	109.421	106.63	113.50	109.193	44
1.4342	1.51628	1.08418	1.09769	109.736	113.2697	109.421	106.63	113.50	109.193	45
1.4342	1.51628	1.08418	1.09769	109.736	111.2697	111.421	106.63	113.50	109.193	46
1.4342	1.51628	1.08418	1.09769	109.736	111.2697	109.421	108.63	113.50	109.193	47
1.4342	1.51628	1.10418	1.07769	109.736	111.2697	109.421	106.63	115.50	109.193	48
1.4342	1.51628	1.08418	1.09769	109.736	111.2697	109.421	106.63	115.50	109.193	49
1.4342	1.51628	1.08418	1.07769	111.736	111.2697	109.421	106.63	115.50	109.193	50
1.4342	1.51628	1.08418	1.07769	109.736	113.2697	109.421	106.63	115.50	109.193	51
1.4342	1.51628	1.08418	1.07769	109.736	111.2697	111.421	106.63	115.50	109.193	52
1.4342	1.51628	1.08418	1.07769	109.736	111.2697	109.421	108.63	115.50	109.193	53
1.4342	1.51628	1.08418	1.07769	109.736	111.2697	109.421	106.63	113.50	110.193	54
1.4342	1.51628	1.08418	1.07769	109.736	111.2697	109.421	106.63	113.50	111.193	55
1.4342	1.51628	1.08418	1.07769	109.736	111.2697	109.421	106.63	113.50	112.193	56
1.4342	1.51628	1.08418	1.07769	111.736	111.2697	109.421	106.63	113.50	111.193	57
1.4342	1.51628	1.08418	1.07769	109.736	111.2697	111.421	106.63	113.50	111.193	58
1.4342	1.51628	1.08418	1.07769	111.736	111.2697	109.421	106.63	113.50	111.193	59
1.4342	1.51628	1.10418	1.07769	109.736	111.2697	109.421	106.63	113.50	111.193	60
1.4342	1.51628	1.08418	1.09769	109.736	111.2697	109.421	106.63	113.50	111.193	61
1.4542	1.51628	1.08418	1.07769	109.736	111.2697	109.421	106.63	113.50	111.193	62
1.4342	1.51628	1.08418	1.07769	111.736	111.2697	109.421	106.63	113.50	111.193	63
1.4342	1.51628	1.08418	1.07769	109.736	113.2697	109.421	106.63	113.50	111.193	64
1.4342	1.51628	1.08418	1.07769	109.736	111.2697	111.421	106.63	113.50	111.193	65
1.4342	1.51628	1.08418	1.07769	109.736	111.2697	109.421	108.63	113.50	111.193	66

Bg_data

CO	CC	CHa	CHe	HaCC	HeCC	HaCO	HeCO	COC	OCC	
1.4342	1.51628	1.08418	1.07769	109.736	111.2697	109.421	106.63	113.50	109.193	1
1.4442	1.51628	1.08418	1.07769	109.736	111.2697	109.421	106.63	113.50	109.193	2
1.4542	1.51628	1.08418	1.07769	109.736	111.2697	109.421	106.63	113.50	109.193	3
1.4342	1.51628	1.08418	1.07769	109.736	111.2697	109.421	106.63	113.50	111.193	4
1.4342	1.51628	1.08418	1.07769	109.736	111.2697	109.421	106.63	113.50	112.193	5
1.4542	1.51628	1.08418	1.07769	109.736	111.2697	109.421	106.63	113.50	111.193	6
1.4542	1.51628	1.08418	1.07769	109.736	111.2697	109.421	106.63	113.50	112.193	7

```
EN G76= -0.37138092EN FUNC= -0.37138092   ERROR=  0.00000000 K=  1
EN G76= -0.37112847EN FUNC= -0.37112870   ERROR=  0.00000022 K=  2
EN G76= -0.37037237EN FUNC= -0.37037203   ERROR= -0.00000083 K=  3
EN G76= -0.37011947EN FUNC= -0.37010772   ERROR= -0.00001175 K=  4
EN G76= -0.36853429EN FUNC= -0.36851622   ERROR= -0.00001807 K=  5
EN G76= -0.36853275EN FUNC= -0.36858803   ERROR=  0.00000528 K=  6
EN G76= -0.36672867EN FUNC= -0.36674113   ERROR=  0.00001247 K=  7
```

TABLE .

Ag. SYMMETRIZED FORCE CONSTANTS.*

	CO	CC	CH^a	CH^e	H^aCC	H^eCC	H^aCO	H^eCO	COC	OCC
CO	577	36.3	8.9	0.0	-5.0	10.2	36.7	41.9	56.0	24.9
CC		479	-5.3	-8.5	28.2	-19.9	7.6	-36.3	-14.0	12.8
CH^a			565	11.3	-3.0	-42.7	-14.1	-32.4	-8.9	-34.4
CH^e				591	-17.0	-18.6	-11.0	1.3	13.8	16.4
H^aCC					103.3	45.0	45.5	36.0	2.4	32.0
H^eCC						84.1	38.0	47.7	3.8	37.5
H^aCO							104.1	35.1	4.7	45.9
H^eCO								104.1	4.2	31.7
COC									69.7	27.5
OCC										113.1

TABLE ___.

Au SYMMETRIZED FORCE CONSTANTS.*

	CO	CC	CH^a	CH^e	H^aCC	H^eCC	H^aCO	H^eCO
CO	554	10.8	19.6	6.2	-15.4	40.3	0	24.8
CC		472	10.8	23.8	14.2	-12.2	-19.9	-24.8
CH^a			577	6.0	3.9	-23.9	-1.3	-19.7
CH^e				578	-7.9	-1.9	-1.7	-3.7
H^aCC					94.9	38.6	48.8	38.0
H^eCC						92.2	39.1	39.1
H^aCO							103.6	36.3
H^eCO								100.5

TABLE .

Bu SYMMETRIZED FORCE CONSTANTS.*

	CO	CH^a	CH^e	H^aCC	H^eCC	H^aCO	H^eCO	COC	OCC
CO	592	26.2	9.1	6.8	40.1	8.5	45.1	82.2	85.3
CH^a		562	2.8	-8.5	-16.8	4.8	-9.9	1.5	-8.2
CH^e			585	-19.9	-4.0	-6.9	-1.9	4.3	-17.6
H^aCC				84.0	43.7	43.7	38.0	5.8	45.6
H^eCC					93.1	38.2	42.1	3.3	25.3
H^aCO						101.7	38.3	2.8	42.0
H^eCO							101.6	10.2	35.7
COC								85.2	0
OCC									110.9

Note: Bg CO is 550; Bg OCC is 104.7

* Units are Nm^{-1}, $Nm^{-1}(rad)^{-1}$ and $Nm^{-1}(rad)^{-2}$ as appropriate

Fortran Program for the Calculation of APTs from Experimental Intensities.

In the pages that follow the program ZSIGN is listed. This was used to investigate the sign choices for the experimental dp/dQ and to calculate the experimental APTs, as was described in Section 4.1.

```
      PROGRAM ZSIGN
      DIMENSION NNPRNT(30),NNTOT(30)
      DIMENSION NROW(50),NCOLM(50),DPDQ(3,100),WT(100)
      dimension znewdpdq(3,70)
      DIMENSION BEER(70,70),XBEER(70,70),XBEERX(70,70)
      DIMENSION AA(70,70)
      DIMENSION EXPT(50),IP(13000,8),NAME(8),NSGN(50),BT(75,75)
      DIMENSION AM(20),G(75,75),FREQ(75),XLTR(75,75),ZLINV(75,75)
      DIMENSION BIGPERM(50)
      DIMENSION ZB(75,75),DEXPT(50)
      DIMENSION APX(3,75),PX(3,75)
      dimension xfreq(50)
      DIMENSION B(75,75),XL(75,75)
      DIMENSION PQ(3,75)
      DIMENSION BANDINT(50)
      DIMENSION F(75,75)
      DIMENSION DNOBAND(50)
      DIMENSION DDEXPT(50)
      CHARACTER*30 LABEL
C
C     INPUT BAND INTENSITY (Km mol-1)
C
C
C     INPUT NO OF BANDS , NO OF INTERNAL COORDINATES , NO OF ENTRIES IN
C                                                                PQ MATRIX
      READ(65,*)NBANDS,NR,NCPTS
C
C     INPUT DIRECTION OF DIPOLE CHANGE (X=1,Y=2,Z=3)
C     INPUT NO OF NORMAL COORDINATE , SIGN OF CPT , EXPT BAND INTENSITY
C     INPUT FRACTION OF INTENSITY TO THIS CPT
C
      DO 2 I=1,NCPTS
      READ(65,*)NROW(I),NCOLM(I),NSGN(I),EXPT(I),WT(I)
      WRITE(82,*)NROW(I),NCOLM(I),NSGN(I),EXPT(I),WT(I)
    2 CONTINUE
      DO 4 I=1,NCPTS
      K=NROW(I)
      J=NCOLM(I)
      DPDQ(K,J)=0.03203*((EXPT(I)*WT(I))**0.5)
      DPDQ(K,J)=DPDQ(K,J)*NSGN(I)
      WRITE(82,*)K,J,EXPT(I),DPDQ(K,J)
    4 CONTINUE
C
C     DPDQ IS PQ MATRIX
C
C
C     GENERATE SIGN PERMUTATION MATRIX FOR DPDQ
C     INPUT NO OF DPDQ TO BE VARIED
C
      READ(65,*)NCOL
      K=1
      DO 10 M=1,NCOL
      NCOL1=2**M
      NCOL2=(2**(M+1))-1
      DO 6 J=1,M
      DO 6 I=NCOL1,NCOL2
      L=I/2
      IF(J.EQ.M)GO TO 8
      IP(I,J)=IP(L,J)
      GO TO 6
    8 IP(I,J)=K
```

```
      K=-K
    6 CONTINUE
   10 CONTINUE
C
C     INPUT WHICH DPDQ ARE BEING VARIED
C
      READ(65,*)(NAME(I),I=1,NCOL)
C
C     INPUT SIGNS OF REST OF DPDQ
C
C
C     INPUT MATRICES FROM FOR055.DAT , DERIVED FROM NORMAL
C                                          COORDINATE CALC
      READ(55,111)LABEL
      READ(55,*)NR,NOAT                    FOR DEUT CPD
      NQ=3*NOAT
      LESSNQ=NQ-6
      READ(55,111)LABEL
      WRITE(6,111)LABEL
      READ(55,109)((BT(I,J),J=1,NR),I=1,NQ)
      READ(55,111)LABEL
      WRITE(6,111)LABEL
      READ(55,109)(AM(I),I=1,NOAT)
      READ(55,111)LABEL
      WRITE(6,111)LABEL
      READ(55,109)((G(I,J),J=1,NR),I=1,NR)
      READ(55,111)LABEL
      READ(55,109)((F(I,J),J=1,NR),I=1,NR)
      READ(55,111)LABEL
      DO 88 I=1,NQ
      READ(55,*)V
      FREQ(I)=V
   88 CONTINUE
      DO 90 I=1,LESSNQ
      XFREQ(I)=(FREQ(I)/1302.9)**2
   90 CONTINUE
      READ(55,*)((XLTR(I,J),J=1,NR),I=1,LESSNQ)

C
C    INPUT L-1 AND B FOR DO CPD FROM FOR070.DAT
C
      NQ=3*NOAT
      LESSNQ=NQ-6
      READ(70,109)((ZB(I,J),J=1,NQ),I=1,NR)
      READ(70,109)((ZLINV(I,J),J=1,NR),I=1,LESSNQ)
   13 DO 15 I=1,NCPTS
      BIGPERM(I)=1
   15 CONTINUE
C     INSERT PERM MATRIX INTO BIGPERM , ROW AT A TIME
C     FORM LOOP FOR DETERMINATION OF PX
C
C

      DO 144 IX=NCOL1,NCOL2
      DO 16 I=1,NCOL
      IPICK=NAME(I)
      BIGPERM(IPICK)=IP(IX,I)
   16 CONTINUE
C
C     CREATE DPDQ FOR THIS LOOP
C
```

```
      DO 18 I=1,NCPTS
      K=NROW(I)
      J=NCOLM(I)
      ZNEWDPDQ(K,J)=DPDQ(K,J)*BIGPERM(I)
   18 CONTINUE
C
C     ZNEWDPDQ IS PQ MATRIX WITH APPROPRIATE SIGNS
C
C
C     NOW CALCULATE PX = PQ*L-1*B FOR DO COMPOUND
C
  109 FORMAT(6F12.8)
      IF(IX.GT.NCOL1)GO TO 941
  941 CONTINUE
      DO 20 I=1,3
      DO 20 J=1,NR
      APX(I,J)=0.0
      DO 20 K=1,LESSNQ
      APX(I,J)=APX(I,J)+znewdpdq(I,K)*ZLINV(K,J)



   20 CONTINUE

      DO 22 I=1,3
      DO 22 J=1,NQ
      PX(I,J)=0.0
      DO 22 K=1,NR
      PX(I,J)=PX(I,J)+APX(I,K)*ZB(K,J)
   22 CONTINUE
  333 FORMAT(' PX')
C
C    WE NOW HAVE PX FOR THIS SIGN CHOICE
C    USE THIS PX TO CALC INTENSITIES FOR DEUT CPD , PQ=PX.A.L
C
C
C
C
  111 FORMAT(A30)
  100 IF(IX.GT.NCOL1)GO TO 572
  110 FORMAT(3F10.5)
C     FORM B
      DO 500 I=1,NR
      DO 500 J=1,NQ
      B(I,J)=BT(J,I)
  500 CONTINUE
C
C     FORM (M-1)BT
C
      DO 510 I=1,NQ
      DO 510 J=1,NR
      K=1+(I-1)/3
      BT(I,J)=BT(I,J)/AM(K)
  510 CONTINUE
      DO 811 I=1,NQ
      DO 811 J=1,NR
      DO 811 K=1,NR
      BEER(I,J)=BEER(I,J)+BT(I,K)*F(K,J)
  811 CONTINUE
      DO 812 I=1,NQ
      DO 812 J=1,LESSNQ
```

```
      DO 812 K=1,NR
      XBEER(I,J)=XBEER(I,J)+BEER(I,K)*XLTR(J,K)
  812 CONTINUE
      DO 813 I=1,NQ
      DO 813 J=1,LESSNQ
      XBEERX(I,J)=XBEER(I,J)/XFREQ(J)
  813 CONTINUE
C
C     XBEERX IS AL
C
C
C     PREMULTIPLY BY B SHOULD GIVE L
C
      DO 814 I=1,NR
      DO 814 J=1,LESSNQ
      DO 814 K=1,NQ
      AA(I,J)=AA(I,J)+B(I,K)*XBEERX(K,J)
  814 CONTINUE
C     FORM L MATRIX
C
      DO 515 I=1,NR
      DO 515 J=1,LESSNQ
      XL(I,J)=XLTR(J,I)
  515 CONTINUE
      DO 921 I=1,NR
      DO 921 J=1,LESSNQ
      AA(I,J)=AA(I,J)-XL(I,J)
  921 CONTINUE
      WRITE(96,109)((AA(I,J),J=1,LESSNQ),I=1,NR)
C
C     FOR096.DAT SHOULD CONSIST OF ZEROS
C
  572 CONTINUE
      DO 620 I=1,3
      DO 620 J=1,LESSNQ
      PQ(I,J)=0.0
      DO 620 K=1,NQ
      PQ(I,J)=PQ(I,J)+PX(I,K)*XBEERX(K,J)
      IF(IX.GT.NCOL1)GO TO 620
  620 CONTINUE
C

C     DP/DQ(EU**.5) = .03203[A(I)(KmMOL**-1)/DEGEN(I)]**.5
C     MUST FIND SUM OF CPTS**2
C
      WRITE(96,109)((PQ(I,J),J=1,LESSNQ),I=1,3)
      DO 700 J=1,LESSNQ
      DO 700 I=1,3
      PQ(I,J)=PQ(I,J)**2
  700 CONTINUE
      DO 710 J=1,LESSNQ
      BANDINT(J)=0.0
      DO 710 I=1,3
      BANDINT(J)=PQ(I,J)+BANDINT(J)
  710 CONTINUE
      DO 720 J=1,LESSNQ
      BANDINT(J)=BANDINT(J)/(0.03203**2)
  720 CONTINUE
C
C     BANDINT(I) IS I'TH DEUT CALC INTENSITY
C
```

```
C
C      CALCULATE FIT PARAMETER
C      READ EXPT DEUTERATED INTENSITIES FROM FOR070
C
       if(ix.gt.ncol1)go to 885
       DO 84 I=1,NBANDS
       READ(75,*)DNOBAND(I),DEXPT(I)
    84 CONTINUE
       DO 885 I=1,NBANDS
       NUMB=DNOBAND(I)
       DDEXPT(NUMB)=DEXPT(I)
   885 CONTINUE
       TOT=0.0
       IF(IX.GT.NCOL1)GO TO 907
C
C      INPUT NO OF BANDS TO BE LISTED
C      INPUT NO OF BANDS CONTRIBUTING TO FIT FACTOR
C
       READ(65,*)NPRNT,NTOT
C
C      INPUT BANDS TO BE PRINTED
C      INPUT BANDS FOR FIT FACTOR
C
       READ(65,*)(NNPRNT(I),I=1,NPRNT)
       READ(65,*)(NNTOT(I),I=1,NTOT)
   907 DO 890 I=1,NPRNT
       J=NNPRNT(I)
       WRITE(80,*)J,DDEXPT(J),BANDINT(J)
       WRITE(6,*)J,DDEXPT(J),BANDINT(J)
   890 CONTINUE
       DO 900 I=1,NTOT
       K=NNTOT(I)
       TOT=TOT+(((DDEXPT(K)-BANDINT(K))**2)/(DDEXPT(K)**2))**.5
   900 CONTINUE
       TOT=TOT/NTOT
C
C      TOT IS FIT FACTOR FOR THE SIGN CHOICE IN THE IX'TH ROW OF
C                                                      MATRIX IP
       WRITE(80,114)TOT,(IP(IX,I),I=1,NCOL)
       WRITE(6,114)TOT,(IP(IX,I),I=1,NCOL)
       WRITE(81,109)((PX(I,J),J=1,NQ),I=1,3)
       WRITE(81,906)
   906 FORMAT('.....')
C
C      PX IS PRINTED IN FOR081.DAT
C
   114 FORMAT(F12.6,21I3)
C
C      FORM NEXT PERMUTATION OF DPDQ
   144 CONTINUE
   930 STOP
       END
```

DIOXAN L MATRICES

The following tables show the L matrices used in the dioxan intensity analyses. The internal coordinates are defined as follows:

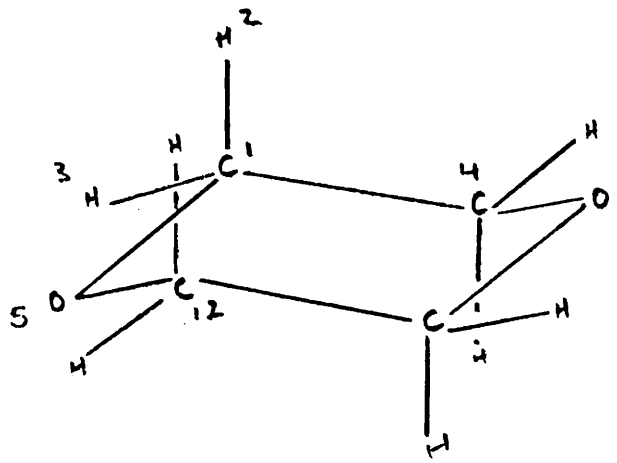

$CH^e \equiv 1\text{-}3$	$H^eCC \equiv \hat{3}14$
$CH^a \equiv 1\text{-}2$	$H^eCO \equiv \hat{3}15$
$CC \equiv 1\text{-}4$	$H^aCC \equiv \hat{2}14$
$CO \equiv 1\text{-}5$	$H^aCO \equiv \hat{2}15$
	$OCC \equiv \hat{4}15$
	$COC \equiv \hat{1}512$

r and R below are the lengths of the appropriate bands that form the angle.

A_u Vibrations - Field A.

	2973	2861	1480	1348	1227	1112	1035	868	185
ΔCH_e	.487	-.180	.003	-.007	-.005	.005	.007	-.007	0
ΔCH_a	-.192	-.482	.013	-.007	0	-.005	-.014	-.005	0
ΔCC	-.020	.043	.023	-.178	-.034	.159	-.090	-.119	-.007
ΔCO	-.006	.019	.014	.044	-.034	-.140	.027	-.136	-.005
$(rR)^{\frac{1}{2}}\Delta HCH$	-.024	.069	.705	-.156	-.030	-.007	.145	-.057	.017
$(rR)^{\frac{1}{2}}\Delta H^eCC$	-.042	-.063	-.228	.305	.385	.165	.217	-.183	.018
$(rR)^{\frac{1}{2}}\Delta H^eCO$	-.053	-.027	-.293	-.240	-.473	.043	.125	.065	.015
$(rR)^{\frac{1}{2}}\Delta H^aCC$	.088	.040	-.033	.478	-.189	-.058	-.432	-.025	.007
$(rR)^{\frac{1}{2}}\Delta H^aCO$	.049	.020	-.231	-.430	.295	-.152	-.166	.093	.008
$(rR)^{\frac{1}{2}}\Delta OCC$	-.018	-.058	-.044	.073	.027	.012	.107	.136	-.079

Bu Vibrations - Field A.

	2975	2856	1457	1376	1304	1042	891	612	273
ΔCH^e	-.492	.163	-.003	.007	0	.015	0	-.002	0
ΔCH^a	.175	.489	-.011	-.007	-.008	0	-.006	-.001	0
ΔCO	.008	-.020	-.025	.042	-.082	.058	-.124	.044	-.006
$(rR)^{\frac{1}{2}}\Delta HCH$	.027	-.065	-.722	-.041	.069	.134	.012	-.001	.011
$(rR)^{\frac{1}{2}}\Delta H^eCC$	.057	.005	.162	.360	-.459	.175	.197	.031	.018
$(rR)^{\frac{1}{2}}\Delta H^eCO$	.049	.033	.291	-.161	.483	.228	-.031	.032	.014
$(rR)^{\frac{1}{2}}\Delta H^aCC$	-.020	.015	.164	.418	.097	-.277	-.255	-.154	.001
$(rR)^{\frac{1}{2}}\Delta H^aCO$	-.056	-.023	.181	-.545	-.244	-.060	.013	-.100	-.005
$(rR)^{\frac{1}{2}}\Delta OCC$	-.070	.053	.049	-.034	.044	-.253	.076	.225	-.473
$r\Delta COC$	.091	.008	.006	.041	.123	.193	.177	-.247	-.124

Au Vibrations - Field B.

	2970	2864	1487	1399	1264	1120	1079	833	169
ΔCH^e	.485	-.183	-.003	.009	.003	.002	.004	.007	0
ΔCH^a	-.195	-.479	-.019	.012	-.001	.007	-.015	0	0
ΔCC	-.018	.045	-.085	.148	-.074	-.093	-.093	.170	.009
ΔCO	-.007	.020	.014	.020	.078	.185	-.010	.030	.009
$(rR)^{\frac{1}{2}}\Delta HCH$	-.023	.073	-.659	.125	.157	.073	.253	.027	-.017
$(rR)^{\frac{1}{2}}\Delta H^eCC$	-.041	-.067	.192	-.491	-.154	.086	.082	.290	-.123
$(rR)^{\frac{1}{2}}\Delta H^eCO$	-.054	-.027	.351	.441	.143	-.194	.105	.045	-.012
$(rR)^{\frac{1}{2}}\Delta H^aCC$	.086	.040	.083	-.215	.365	.007	-.495	-.153	-.010
$(rR)^{\frac{1}{2}}\Delta H^aCO$	.050	.021	.079	.203	-.550	.072	-.082	-.145	-.013
$(rR)^{\frac{1}{2}}\Delta OCC$	-.019	-.061	.071	-.096	.005	-.063	.118	-.076	.077

Bu Vibrations - Field B.

	2976	2854	1453	1381	1302	1036	804	642	294
ΔCH^e	.491	.169	.003	-.001	.012	-.014	-.002	.002	0
ΔCH^a	-.181	.486	-.009	-.005	-.010	.001	-.002	.002	0
ΔCO	-.007	-.019	-.055	.038	-.006	-.006	-.154	.041	0
$(rR)^{\frac{1}{2}}\Delta HCH$	-.024	-.062	-.428	-.563	.067	-.178	-.098	-.021	-.023
$(rR)^{\frac{1}{2}}\Delta H^eCC$	-.055	.005	-.253	.534	.146	-.238	-.027	-.080	-.025
$(rR)^{\frac{1}{2}}\Delta H^eCO$	-.055	.031	.593	-.156	.105	-.006	-.041	-.061	-.014
$(rR)^{\frac{1}{2}}\Delta H^aCC$	.020	.014	.014	.191	.314	.391	.004	.297	-.167
$(rR)^{\frac{1}{2}}\Delta H^aCO$	.056	-.023	.136	.072	-.595	-.102	.118	.056	.005
$(rR)^{\frac{1}{2}}\Delta OCC$	.071	.051	.007	.017	-.063	.249	.068	-.221	.090
$r\Delta COC$	-.096	.006	.091	-.055	.165	-.266	.177	.108	.094